



NATIONAL TECHNICAL UNIVERSITY OF ATHENS

SCHOOL OF CIVIL ENGINEERING

**BIOLOGICAL PHOSPHORUS REMOVAL COUPLED
WITH NITRITATION-DENITRITATION FOR LOW
CARBON/NITROGEN WASTEWATER TREATMENT
SYSTEMS**

DOCTORAL THESIS

DIMITRIS A. ANDREADAKIS

Chemical Engineer University of Patras, M.Sc.-NTUA

SUPERVISOR:

CONSTANTINOS NOUTSOPOULOS

Associate Professor, NTUA

ATHENS, June 2022



NATIONAL TECHNICAL UNIVERSITY OF ATHENS

SCHOOL OF CIVIL ENGINEERING

**BIOLOGICAL PHOSPHORUS REMOVAL COUPLED WITH
NITRITATION-DENITRITATION FOR LOW
CARBON/NITROGEN WASTEWATER TREATMENT
SYSTEMS**

DOCTORAL THESIS

DIMITRIS A. ANDREADAKIS

Chemical Engineer University of Patras, M.Sc.-NTUA

ADVISORY COMMITTEE

1. Constantinos Noutsopoulos, Associate Professor NTUA (Supervisor)
2. Daniel Mamais, Professor NTUA
3. Simos Malamis, Associate Professor NTUA

EXAMINATION COMMITTEE

1. Constantinos Noutsopoulos, Associate Professor NTUA (Supervisor)
2. Daniel Mamais, Professor NTUA
3. Simos Malamis, Associate Professor NTUA
4. Gerasimos Lyberatos, Professor NTUA
5. Vassilios Tsihrintzis, Professor NTUA
6. Paraschos Melidis, Professor DUTH
7. Athanasios Stasinakis, Associate Professor University of Aegean

ATHENS, June 2022



ΕΘΝΙΚΟ ΜΕΤΣΟΒΙΟ ΠΟΛΥΤΕΧΝΕΙΟ

ΣΧΟΛΗ ΠΟΛΙΤΙΚΩΝ ΜΗΧΑΝΙΚΩΝ

**ΒΙΟΛΟΓΙΚΗ ΑΠΟΜΑΚΡΥΝΣΗ ΦΩΣΦΟΡΟΥ ΜΕ
ΠΑΡΑΛΛΗΛΗ ΝΙΤΡΩΔΟΠΟΙΗΣΗ-
ΑΠΟΝΙΤΡΩΔΟΠΟΙΗΣΗ ΣΕ ΣΥΣΤΗΜΑΤΑ
ΕΠΕΞΕΡΓΑΣΙΑΣ ΥΓΡΩΝ ΑΠΟΒΛΗΤΩΝ ΜΕ ΧΑΜΗΛΟ
ΛΟΓΟ ΑΝΘΡΑΚΑ ΠΡΟΣ ΑΖΩΤΟ**

ΔΙΔΑΚΤΟΡΙΚΗ ΔΙΑΤΡΙΒΗ

ΔΗΜΗΤΡΗ Α. ΑΝΔΡΕΑΔΑΚΗ

Διπλωματούχου Χημικού Μηχανικού Πανεπιστημίου Πατρών, Μ.Δ.Ε.-ΕΜΠ

ΣΥΜΒΟΥΛΕΥΤΙΚΗ ΕΠΙΤΡΟΠΗ

1. Κωνσταντίνος Νουτσόπουλος, Αναπληρωτής Καθηγητής ΕΜΠ (Επιβλέπων)
2. Δανιήλ Μαμάης, Καθηγητή, ΕΜΠ
3. Συμεών Μαλαμής, Αναπληρωτής Καθηγητής ΕΜΠ

ΕΞΕΤΑΣΤΙΚΗ ΕΠΙΤΡΟΠΗ

1. Κωνσταντίνος Νουτσόπουλος, Αναπληρωτής Καθηγητής ΕΜΠ (Επιβλέπων)
2. Δανιήλ Μαμάης, Καθηγητής ΕΜΠ
3. Συμεών Μαλαμής, Αναπληρωτής Καθηγητής ΕΜΠ
4. Γεράσιμος Λυμπεράτος, Καθηγητής ΕΜΠ
5. Βασίλειος Τσιχριντζής, Καθηγητής ΕΜΠ
6. Παράσχος Μελίδης, Καθηγητής ΔΠΘ
7. Αθανάσιος Στασινάκης, Αναπληρωτής Καθηγητής Πανεπιστημίου Αιγαίου

ΑΘΗΝΑ, Ιούνιος 2022

Acknowledgements

Before all, I feel the need to express my deepest gratitude to my advisor, associate Prof. Costas Noutsopoulos, for entrusting and providing me with the opportunity to carry out this work, as well as for his valuable guidance and support over the past years. I would also like to thank the head of the Sanitary Engineering Laboratory, Prof. Daniel Mamais, and associate Prof. Simos Malamis, for their valuable contribution as members of my thesis advisory committee. It has been a privilege to work alongside these people and I look forward to possible future collaborations.

I would like to thank the members of the examination committee, Prof. Gerasimos Lyberatos, Prof. Vasileios Tsihrintzis, Prof. Paraschos Melidis and associate Prof. Athanasios Stasinakis for their interesting questions and valuable comments during my examination, and also for their encouraging words.

A special thanks to Marianna Gioldasi for training me in the analytical methods I required for my research, her constant availability and assistance, as well as her pleasant company throughout the countless hours spent in the laboratory. I would also like to thank Nikos Kouris for his invaluable assistance over the years, as well as my colleague and friend, Gerasimos Fragiskatos, for our cooperation and vibrant discussions during the early steps of my research.

In addition, I would like to thank the students who assisted me in the laboratory throughout my research. In particular: Kyriaki Argyropoulou, Theodora Misirli, Eva Themeli, Peri Dimoka, Maria Kalli, Eleni Siamani, Asimina Koukoura, Ourania Kalopisi Lontou and Vera Charalampous. Their contribution is very much appreciated and I hold fond memories of our collaborations.

On a personal note, I would like to thank my family and friends (they know who they are) for their constant support, and especially for their patience and understanding during difficult times. If I was to accurately express my sincere appreciation to each individual, I fear it would double the volume of this issue.

Abstract

The side-treatment of reject water has emerged an attractive option over the past years due to its potential for relieving nutrient loading of the main-stream processes, while removing nitrogen at a reduced cost. This is achieved by the suppression of Nitrite Oxidizing Bacteria (NOB) due to the high Free Ammonia (FA) concentrations that characterize reject waters and the implementation of the nitrification/denitrification pathway, which compared to conventional nitrification/denitrification, has a lower demand in oxygen and carbon. While these conditions are beneficial for nitrogen removal, this is not the case for enhanced biological phosphorus removal (EBPR), as polyphosphate accumulating organisms (PAOs) have been reported to be severely inhibited by nitrite accumulations. More specifically, free nitrous acid (FNA), which is the protonated form of nitrite, has been revealed to be the actual inhibitor of PAOs, meaning that the severity to which PAOs are inhibited by nitrite increases significantly at lower pH. The degree to which PAOs have been reported to be inhibited by FNA itself varies in the literature, as does the tolerance of each respiration pathway (aerobic/anoxic), with contradictory conclusions. In addition, it has recently come to light that FA is also an inhibitor of PAOs, although research on this matter is rather limited as of this point. Regardless, the conditions of nitrification/denitrification appear to be hostile for PAOs and the application of EBPR, raising the question if the coupling of these processes is feasible.

The goal of this dissertation is to provide an answer to this question. To this end, the following objectives were established: First was an extensive assessment of the inhibitory effect of FNA on PAOs, both under aerobic and anoxic conditions, with consideration to biomass acclimation to the inhibitor. This aims to settle disputes in the literature but also determine the mode of inhibition which has yet to be established. Second was to determine the effect of FA on PAOs along with its respective mode of inhibition, for which little information is available. Third was to assess the combined effect of FNA and FA on PAOs and develop a unified inhibition model. Fourth was the assessment of the effect of FNA and FA on the main antagonistic microbial group towards PAOs, namely glycogen accumulating organisms (GAOs). This assessment is of value, as a possible higher tolerance of GAOs to these inhibitors could indicate that PAOs face the danger of washing out even in relatively mild inhibitory conditions. Fifth was to develop strategies for the proliferation of PAOs and the suppression of GAOs under inhibitory conditions, and sixth was to optimize conditions for the prevalence of PAOs in high nitrogen loading systems and assess the limits of EBPR under these conditions, ultimately completing the aim of this work.

In order to investigate the effects of FNA and FA on PAOs and GAOs, a laboratory-scale sequencing batch reactor (SBR) was set-up in the Sanitary Engineering Laboratory of the School of Civil Engineering, NTUA for their cultivation. The SBR operated from September 2017 to April 2021 with several resets and intermediate breaks, depending on the investigation phase. The SBR's configuration was altered for each experimental period based on the specific goals of that phase but was generally based on the alternation of an anaerobic phase, at the start of which feed would enter via pump, an aerobic phase, achieved via air pump and an anoxic phase. While these phases were automated, settling and decanting was carried out manually, once per day.

Feed consisted of synthetic wastewater, that was prepared on a daily basis, the composition of which was specific to each investigation. During each experimental period, once the reactor had displayed a steady performance, a series of ex-situ batch experiments were conducted on sludge retrieved from the SBR. The effect of FNA and FA on PAOs was determined based on their effect on the aerobic and anoxic phosphorus uptake rate (PUR) of the biomass. In the case of GAOs, the effect of FNA and FA was evaluated based on their effect on the maximum growth rate of the biomass. This required the development of a very highly GAO-enriched biomass (>90% of the total microbial population). In addition to the ex-situ experiments, a series of strategies, based on the choice of substrate and the SBR configuration, for the promotion of PAOs over GAOs, were evaluated in-situ.

The investigation regarding the effect of FNA on PAOs revealed that both aerobic and anoxic PUR are significantly inhibited by FNA and to the same degree (meaning that FNA affects PAOs regardless of the respiration pathway). For an acclimated biomass, FNA was found to inhibit PUR by 50% at the concentration of 1.5 $\mu\text{g N/L}$ and by 100% at a concentration just over 13 $\mu\text{g N/L}$. PUR inhibition by FNA was determined to be best described by a non-competitive inhibition model with an inhibition constant of $K_{\text{IFNA}}=1.5 \mu\text{g N/L}$.

The investigation regarding the effect of FA on PAOs concluded that FA is also a strong inhibitor of PAOs, with PUR being inhibited by more than 90% at the FA concentration of 30 mg N/L. Similarly to the case of FNA, FA appeared to inhibit the aerobic and anoxic pathway to the same degree. PUR inhibition by FA was determined to be best described by an uncompetitive inhibition model with a K_{IFA} in the range of 8-10 mg N/L. In the case of anoxic PUR inhibition, the inhibition model proposed by Levenspiel gave the most satisfactory fit with the experimental data.

The simultaneous presence of FA and FNA has a much more adverse effect on PUR compared to when PAOs were exposed to a single inhibitor. An enzymatic inhibition model was developed to describe simultaneous inhibition of PUR by FNA and FA, based on the separate inhibition models that were established. The combined inhibition model gave very satisfactory predictions when FNA and FA were assumed to be capable of binding to the same enzyme-substrate complex, and less accurate predictions when FNA and FA were assumed to be incapable of binding to the same complex. This inhibition model may be used to predict the performance of PAOs throughout a specific set of conditions (NH_4 & NO_2 concentrations, pH and temperature) but also determine an optimum variation of pH for PUR throughout the processes of nitrification and denitrification.

The investigation regarding the effect of FNA on GAOs revealed that GAOs are also inhibited by FNA, although generally to a lesser extent than PAOs. Interestingly, the effect of FNA on the growth of GAOs appears to be pH dependant, with FNA affecting GAOs significantly more at higher pH values (At pH=7, GAO growth was inhibited by 50% at the FNA concentration of 10 $\mu\text{g N/L}$, while at the pH of 8, the same degree of inhibition was observed at the concentration of 3 $\mu\text{g N/L}$). In comparison to PAOs, GAOs appear to have a significantly higher tolerance to FNA at low pH, while at relatively high pH (8), the tolerance of the two microbial groups to FNA are similar. However, the investigation on the effect of FA on GAOs revealed that GAOs were not affected by the inhibitor, up to a concentration of 16.3 mg N/L, which was the highest FA concentration studied. It may therefore be concluded that the prevailing conditions in high

nitrogen loading systems may provide a significant advantage to GAOs, endangering the sustainability of PAOs.

A series of feeding strategies that were examined revealed that strategies that have been applied successfully for the suppression of GAOs and the proliferation of PAOs, may not hold up under the inhibitory conditions of nitrification/denitrification systems. However, one strategy that proved most successful was the promotion of PAOs via the denitrification pathway, using propionate as the sole carbon source. The strategy relies on the fact that all known GAOs appear incapable of reducing nitrite with propionate and is achieved by providing PAOs priority in the utilization of nitrite over common heterotrophs. At a volumetric nitrogen loading rate (vNLR) of 0.1 kg N/m³ d, this strategy achieved a highly PAO-enriched biomass (approximately 50% of the total microbial community), in which the population of GAOs was significantly low. The biomass displayed a steady capacity for excellent P-removal both under aerobic and anoxic conditions, performing at an average PUR of 25 and 10 mg P/g VSS h under aerobic and anoxic conditions, respectively. However, a downside of this strategy is that due to the relatively slow denitrification rates of PAOs, its application may require greater anoxic retention times, limiting the potential for treatment of high vNLRs. In a second stage of operation, the increase of the vNLR from 0.1 to 0.15 kg N/m³ d, resulted in the biomass performing at half its former capacity.

Based on the combined inhibition model, a series of mathematical simulations were performed in order to evaluate the potential for EBPR alongside nitrification/denitrification in high nitrogen loading systems. The theoretical configuration that was examined was optimized with regard to appropriate alteration of aerobic and anoxic conditions, as to prevent nitrite accumulation and retain a relatively high pH at relatively high values, providing PAOs with an exclusive denitrification period (as to employ the GAO suppression strategy) after the rapid removal of a significant nitrite portion by common heterotrophs which may be achieved by providing a regulated carbon dose, and the quality of the treated effluent. The viability of EBPR was evaluated for several vNLRs up to 0.3 kg N/m³ d, considering the overall inhibition of PAOs, the adequacy of the GAO suppression strategy, the necessity for pH control as to minimize PAO inhibition and the effective achievement of NOB shunt. Based on the results of the simulations and their evaluation, it was concluded that a vNLR of 0.2 kg N/m³ d could allow sufficient and relatively safe EBPR without the need for pH manipulation. Higher vNLR's, may allow EBPR with some pH control which is costly, while vNLR's above 0.3 kg N/m³ d likely forbid the application of EBPR, as the inhibitory conditions alone would severely compromise the sustainability of PAOs.

In conclusion, the side-stream treatment of reject water with EBPR alongside nitrification/denitrification is feasible, although its application faces certain challenges and requires a series of prerequisites. For one, the GAO-suppression strategy demands the supply of propionate, which would likely need to be provided via fermentation of primary sludge under specific conditions. In general, the implementation of this treatment should only be considered when EBPR in the main treatment facilities is challenged due to a low carbon content of the wastewater. In this case, the simultaneous removal of nitrogen and phosphorus with the same carbon source in order to minimize the demand for external carbon, is a viable option. Otherwise, the limitations of operating at a low vNLR, such as the need for greater reactor volumes, may outweigh the benefits of this approach.

ΒΙΟΛΟΓΙΚΗ ΑΠΟΜΑΚΡΥΝΣΗ ΦΩΣΦΟΡΟΥ ΜΕ ΠΑΡΑΛΛΗΛΗ ΝΙΤΡΩΔΟΠΟΙΗΣΗ- ΑΠΟΝΙΤΡΩΔΟΠΟΙΗΣΗ ΣΕ ΣΥΣΤΗΜΑΤΑ ΕΠΕΞΕΡΓΑΣΙΑΣ ΥΓΡΩΝΑΠΟΒΛΗΤΩΝ ΜΕ ΧΑΜΗΛΟ ΛΟΓΟ ΑΝΘΡΑΚΑ ΠΡΟΣ ΑΖΩΤΟ

Εκτεταμένη περίληψη

1. Εισαγωγή

Η αποτελεσματική επεξεργασία των αστικών λυμάτων πριν την διάθεσή τους στους υδάτινους αποδέκτες αποτελεί απαραίτητη προϋπόθεση για την διασφάλιση της καλής ποιότητας των υδάτων. Η βιολογική επεξεργασία στις εγκαταστάσεις επεξεργασίας λυμάτων (ΕΕΛ) στοχεύει πρωτίστως στην απομάκρυνση του βιοαποδομήσιμου οργανικού φορτίου των λυμάτων, του οποίου η διάθεση μπορεί να προκαλέσει προβλήματα αποξυγόνωσης στον αποδέκτη, αλλά και στην απομάκρυνση θρεπτικών (αζώτου και φωσφόρου), των οποίων η ανεξέλεγκτη διάθεση μπορεί να οδηγήσει σε φαινόμενα ευτροφισμού.

Η βιολογική απομάκρυνση του αζώτου επιτυγχάνεται κατά κανόνα μέσω των διεργασιών νιτροποίησης και απονιτροποίησης. Κατά την νιτροποίηση, μια κατηγορία αυτοτροφικών μικροοργανισμών, γνωστή ως AOB (Ammonium Oxidizing Bacteria), οξειδώνει αρχικά το αμμωνιακό άζωτο, το οποίο αποτελεί την σημαντικότερη μορφή αζώτου στα ανεπεξέργαστα λύματα, προς νιτρώδες άζωτο (νιτρωδοποίηση). Στη συνέχεια, μια δεύτερη κατηγορία αυτότροφων βακτηρίων, γνωστή ως NOB (Nitrite Oxidizing Bacteria), οξειδώνει το παραγόμενο νιτρώδες άζωτο προς νιτρικό άζωτο (νιτρικοποίηση). Οι δύο αυτές επιμέρους διεργασίες συνθέτουν την διαδικασία της νιτροποίησης, η οποία απαιτεί την παροχή οξυγόνου. Στην συνέχεια, απουσία οξυγόνου, ετεροτροφικοί-οργανοτροφικοί μικροοργανισμοί αξιοποιούν τα νιτρικά ως αποδέκτη ηλεκτρονίων για την οξείδωση και απομάκρυνση του οργανικού φορτίου, με την παράλληλη αναγωγή και απομάκρυνση του αζώτου (απονιτροποίηση).

Η βιολογική απομάκρυνση του φωσφόρου επιτυγχάνεται με την επιλογή μιας συγκεκριμένης κατηγορίας μικροοργανισμών, τα οποία είναι γνωστά ως πολυφωσφορικά βακτήρια (Polyphosphate Accumulating Organisms – PAOs). Όπως υποδηλώνει η ονομασία τους, τα πολυφωσφορικά βακτήρια συνθέτουν υψηλές ποσότητες ενδοκυτταρικά αποθηκευμένων πολυφωσφορικών αλυσίδων, τις οποίες υδρολύουν κάτω από αναερόβιες συνθήκες για την παραγωγή ενέργειας. Η ενέργεια αυτή αξιοποιείται για την συντήρηση των κυττάρων, αλλά και για την δέσμευση διαλυτών οργανικών ενώσεων από τα λύματα και την αποθήκευσή τους ενδοκυτταρικά ως πολυμερή. Στην συνέχεια, παρουσία αποδέκτη ηλεκτρονίων, τα πολυφωσφορικά διασπούν τα αποθηκευμένα μακρομόρια και χρησιμοποιούν την παραγόμενη ενέργεια για κυτταρική σύνθεση και την αναπλήρωση των πολυφωσφορικών τους αλυσίδων, απομακρύνοντας παράλληλα φώσφορο από τα λύματα. Έτσι, με την διάταξη μιας αναερόβιας δεξαμενής ανάντη των βιολογικών δεξαμενών, δίνεται προτεραιότητα στη δέσμευση του διαλυτού οργανικού άνθρακα από τα PAOs, με αποτέλεσμα τον εμπλουτισμό της

ιλύος με αυτά. Η βιολογική απομάκρυνση φωσφόρου επιτυγχάνεται τελικά με την απομάκρυνση της περίσσειας εμπλουτισμένης ιλύος.

Η τελική διάθεση της περίσσειας ιλύος προϋποθέτει μια σειρά από επιμέρους επεξεργασίες με στόχο την σταθεροποίησή της και την μείωση του υδάτινου περιεχόμενου της. Κατά τα έργα της ιλύος, παράγονται στραγγίδια τα οποία χαρακτηρίζονται από υψηλές συγκεντρώσεις αζώτου και φωσφόρου, καθώς επίσης και από έναν σχετικά χαμηλό λόγο άνθρακα προς άζωτο (C:N). Τυπικά, αυτά τα ρεύματα ανακυκλοφορούνται στην κύρια ροή επεξεργασίας, αυξάνοντας την φόρτιση της βιολογικής βαθμίδας. Τα τελευταία χρόνια, η χωριστή επεξεργασία αυτών των ρευμάτων πριν την ανακυκλοφορία τους μελετάται ευρέως ως μία πολύ υποσχόμενη πρακτική. Λόγω της υψηλής συγκέντρωσης αμμωνιακού αζώτου που χαρακτηρίζει τα στραγγίδια αφυδάτωσης (ως αποτέλεσμα της αναερόβιας χώνευσης) καθώς και του υψηλού pH), τα στραγγίδια περιέχουν υψηλές συγκεντρώσεις ελεύθερης αμμωνίας (Free Ammonia – FA), η οποία είναι γνωστή για την αναχαιτιστική της επίδραση σε μια σειρά από μικροβιακές δραστηριότητες. Ανάμεσα στους μικροοργανισμούς που αναχαιτίζονται από την ελεύθερη αμμωνία είναι και οι υπεύθυνοι για την διεργασία της νιτροποίησης. Ωστόσο, η ελεύθερη αμμωνία αναχαιτίζει τα NOB σε πολύ μεγαλύτερο βαθμό από τα AOB, καθιστώντας εφικτή την παράκαμψη της νιτροποίησης. Υπό ανοξικές συνθήκες, τα νιτρώδη μπορούν να αναχθούν με την ίδια ευκολία από τους ετεροτροφικούς μικροοργανισμούς και μάλιστα με μικρότερη κατανάλωση οργανικού άνθρακα. Παράλληλα, με την ακύρωση του δεύτερου σταδίου της νιτροποίησης, η ζήτηση οξυγόνου μειώνεται σημαντικά (περίπου κατά 25%), μειώνοντας την απαίτηση σε αερισμό και κατά προέκταση το κόστος της επεξεργασίας.

Παρόλο που η απονιτροποίηση απαιτεί λιγότερο οργανικό άνθρακα συγκριτικά με την πλήρη απονιτροποίηση (περίπου κατά 40%), ο χαμηλός λόγος C:N που χαρακτηρίζει τα στραγγίδια, καθώς και η χαμηλή περιεκτικότητά τους σε εύκολα βιοδιασπάσιμο οργανικό άνθρακα, καθιστά απαραίτητη την προσθήκη μιας εξωτερικής πηγής διαλυτού οργανικού άνθρακα. Το γεγονός αυτό σε συνδυασμό με την απαίτηση για απομάκρυνση της σημαντικής ποσότητας φωσφόρου των στραγγιδίων, καθιστούν την εφαρμογή της βιολογικής απομάκρυνσης φωσφόρου παράλληλα με την απομάκρυνση του αζώτου μέσω νιτροποίησης/απονιτροποίησης ως θεμιτή επιλογή, καθώς άζωτο και φώσφορος μπορούν να απομακρυνθούν χρησιμοποιώντας την ίδια πηγή οργανικού άνθρακα.

Ωστόσο, οι συνθήκες που χαρακτηρίζουν τα συστήματα νιτροποίησης /απονιτροποίησης, ενδέχεται να μην επιτρέπουν την βιολογική απομάκρυνση φωσφόρου, καθώς υπάρχουν αναφορές ότι τα νιτρώδη αναχαιτίζουν τις δραστηριότητες των πολυφωσφορικών βακτηρίων. Συγκεκριμένα, το ελεύθερο νιτρώδες οξύ (Free Nitrous Acid – FNA), το οποίο αποτελεί την πρωτονωμένη μορφή του νιτρώδους αζώτου, η παρουσία του οποίου ενοείται σε χαμηλά pH, αναχαιτίζει σε σημαντικό βαθμό τις λειτουργίες των PAOs (Zhou et al., 2007). Ο αναφερόμενος βαθμός στον οποίο αναχαιτίζονται τα PAOs ποικίλει στην βιβλιογραφία και μπορεί να διαφέρει ως προς τον εγκλιματισμό στο FNA καθώς και την οδό που επηρεάζεται (αερόβια/ανοξική). Σε όλες τις περιπτώσεις, η συσσώρευση νιτρωδών που αναμένεται με βάση τις συγκεντρώσεις των αμμωνιακών που απαιτούνται για την αναχαιτίση των NOB, πιθανότατα θα αναστέλλουν σοβαρά τη δραστηριότητα των PAOs και ενδέχεται να απαγορεύουν την εφαρμογή της βιολογικής απομάκρυνσης φωσφόρου σε αυτές τις συνθήκες. Επιπροσθέτως, υπάρχουν πρόσφατες αναφορές ότι το FA επίσης αναχαιτίζει τα PAOs (Yang et al., 2018), αν και η σχετική έρευνα είναι πολύ περιορισμένη μέχρι στιγμής. Ενώ το FA ενοείται σε υψηλό pH, το ποσοστό των νιτρωδών στην μορφή του FNA αυξάνεται αντίθετα με το pH. Κατά τη νιτροποίηση, η μετατροπή του αμμωνιακού αζώτου σε νιτρώδες άζωτο συνοδεύεται με μια βιοχημική πτώση του pH, αυξάνοντας

έτσι σημαντικά την συγκέντρωση του FNA κατά την διάρκεια της διαδικασίας. Οι συνθήκες για τα PAOs βελτιώνονται κατά την απονιτροδοποίηση καθώς απομακρύνονται νιτρώδη, ενώ υπάρχει βιοχημική αύξηση του pH. Ωστόσο, η συνδυασμένη επίδραση του FA και του FNA στα PAOs κατά την διάρκεια της αερόβιας φάσης μπορεί να μην επιτρέπει τη βιωσιμότητά τους σε ένα τέτοιο σύστημα. Η κατάσταση για τα PAOs γίνεται ακόμη πιο ζοφερή αν αναλογιστεί κανείς τον ανταγωνισμό τους με μια άλλη ανταγωνιστική μικροβιακή κοινότητα, γνωστή ως GAOs (Glycogen Accumulating Organisms). Ομοίως με τα PAOs, τα GAOs μπορούν να προσλαμβάνουν διαλυτό άνθρακα υπό αναερόβιες συνθήκες χωρίς να συμβάλλουν στην απομάκρυνση του φωσφόρου, καθώς η απαιτούμενη ενέργεια στην περίπτωση τους παρέχεται μέσω της γλυκόλυσης. Επομένως, σε συνθήκες υψηλών συσσωρεύσεων αμμωνιακού και νιτρώδους αζώτου, η επίδραση των FNA και FA στα GAOs είναι επίσης σημαντική, καθώς μια υψηλότερη ανοχή σε αυτές τις ουσίες θα είχε ως αποτέλεσμα την πιθανή επικράτησή τους έναντι των PAOs και την αποτυχία του βιολογικής απομάκρυνσης φωσφόρου.

Λαμβάνοντας υπόψη τα παραπάνω, είναι σαφές ότι η επιτυχής εφαρμογή της βιολογικής απομάκρυνσης φωσφόρου σε συστήματα νιτροδοποίησης/απονιτροδοποίησης, για την αποτελεσματική επεξεργασία στραγγιδίων, αντιμετωπίζει σημαντικές προκλήσεις. Η φόρτιση αζώτου και το pH είναι παράμετροι ιδιαίτερης σημασίας, με τις συγκεντρώσεις των FNA και FA να επηρεάζουν όχι μόνο την επιθυμητή αναχαίτιση των NOB, αλλά και τον ανταγωνισμό μεταξύ των PAOs και GAOs κατά τις διεργασίες νιτροδοποίησης και απονιτροδοποίησης σε διαφορετικό βαθμό, με ενδεχόμενες αρνητικές συνέπειες στην απόδοση. ή ακόμη και την βιωσιμότητα της βιολογικής απομάκρυνσης φωσφόρου σε αυτές τις συνθήκες.

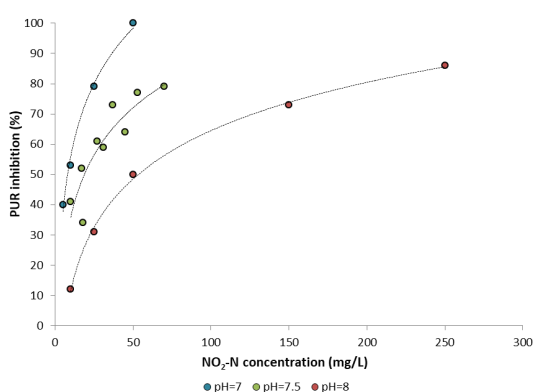
2. Ερευνητικοί στόχοι

Με βάση την ανάλυση της διεθνούς βιβλιογραφίας και τα ερευνητικά κενά που επισημάνθηκαν σε αυτήν καθορίστηκε το αντικείμενο της διδακτορικής διατριβής το οποίο είναι η διερεύνηση της δυνατότητας επίτευξης βιολογικής απομάκρυνσης φωσφόρου σε συστήματα επεξεργασίας υγρών αποβλήτων με χαμηλό λόγο άνθρακα προς άζωτο μέσω νιτροδοποίησης – απονιτροδοποίησης. Προκειμένου να επιτευχθεί ο στόχος αυτός κρίθηκε σκόπιμο να απαντηθούν μία σειρά από ερευνητικά ερωτήματα μέσω των ακόλουθων διερευνήσεων:

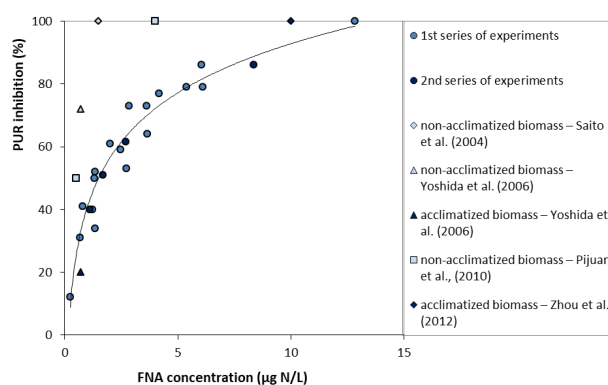
- ⇒ διερεύνηση της αναχαιτιστικής δράσης του ελεύθερου νιτρώδους οξέος και της ελεύθερης αμμωνίας στην δραστηριότητα των πολυφωσφορικών βακτηρίων σε αερόβιες και ανοξικές συνθήκες καθώς και η ανάπτυξη των σχετικών μαθηματικών μοντέλων αναχαίτισης,
- ⇒ πειραματική και μαθηματική προσομοίωση της συνδυασμένης επίδρασης του ελεύθερου νιτρώδους οξέος και της ελεύθερης αμμωνίας στη δράση των πολυφωσφορικών βακτηρίων,
- ⇒ διερεύνηση της αναχαιτιστικής δράσης του ελεύθερου νιτρώδους οξέος και της ελεύθερης αμμωνίας στην δραστηριότητα των βακτηρίων συσώρευσης γλυκογόνου καθώς και η ανάπτυξη των σχετικών μαθηματικών μοντέλων αναχαίτισης,
- ⇒ διερεύνηση της επίδρασης του είδους του οργανικού υποστρώματος στον ανταγωνισμό των πολυφωσφορικών βακτηρίων και των βακτηρίων συσώρευσης γλυκογόνου σε συστήματα νιτροδοποίησης – απονιτροδοποίησης,
- ⇒ ανάπτυξη στρατηγικών βελτιστοποίησης της βιολογικής απομάκρυνσης φωσφόρου σε συστήματα νιτροδοποίησης – απονιτροδοποίησης.

3. Διερεύνηση της επίδρασης των νιτρωδών και της ελεύθερης αμμωνίας στην αερόβια και ανοξική δράση των πολυφωσφορικών βακτηρίων

Η διερεύνηση της επίδρασης των νιτρωδών στην ταχύτητα πρόσληψης φωσφόρου σε αερόβιες συνθήκες πραγματοποιήθηκε μέσω πειραμάτων batch σε εγκλιματισμένη και μη-εγκλιματισμένη βιομάζα η οποία καλλιεργήθηκε σε εργαστηριακό αντιδραστήρα SBR. Σύμφωνα με τα πειραματικά αποτελέσματα διαπιστώθηκε ότι με τη μείωση του pH του ανάμικτου υγρού αυξάνεται η αναχαιτίση της διαδικασίας για τις ίδιες συγκεντρώσεις νιτρωδών (Σχήμα 1). Κατά συνέπεια και λαμβάνοντας υπόψη τη χημεία του συστήματος των νιτρωδών διαπιστώνεται ότι η βασική αναχαιτιστική ουσία είναι το ελεύθερο νιτρώδες οξύ (FNA). Όπως φαίνεται αναλυτικά στο Σχήμα 2, μία συγκέντρωση ελεύθερου νιτρώδους οξέος της τάξης των 1,5 $\mu\text{g N/L}$ οδηγεί σε 50% αναχαιτίση του ρυθμού πρόσληψης φωσφόρου σε αερόβιες συνθήκες, ενώ πλήρης αναχαιτίση καταγράφεται για συγκεντρώσεις ελεύθερου νιτρώδους οξέος της τάξης των 13 $\mu\text{g N/L}$.



Σχήμα 1. Επίδραση του νιτρώδους αζώτου στον αερόβιο ρυθμό πρόσληψης φωσφόρου.



Σχήμα 2. Επίδραση του ελεύθερου νιτρώδους αζώτου στον αερόβιο ρυθμό πρόσληψης φωσφόρου και σύγκριση με άλλες έρευνες.

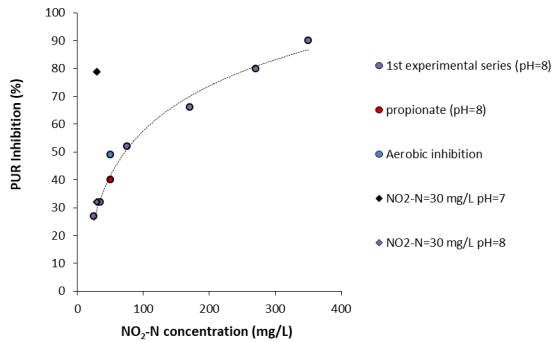
Σύμφωνα με αποτελέσματα στοχευμένων εργαστηριακών πειραμάτων προέκυψε ότι η αναχαιτίση του ρυθμού πρόσληψης φωσφόρου σε αερόβιες συνθήκες λόγω του ελεύθερου νιτρώδους οξέος περιγράφεται ικανοποιητικά από ένα non-competitive μοντέλο, η βέλτιστη μαθηματική περιγραφή του οποίου επιτυγχάνεται από το απλό non-competitive μοντέλο αναχαιτίσης της σχέσης 1.

$$PUR = PUR_{max} \frac{K_{iFNA}}{S_{FNA} + K_{iFNA}} \quad (1)$$

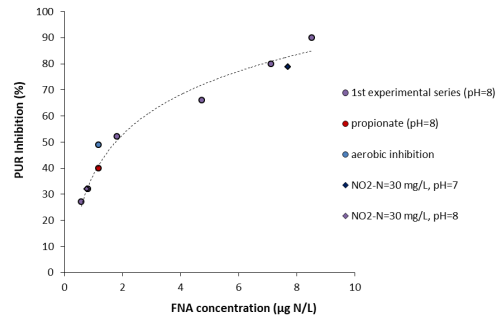
όπου K_{iFNA} είναι η σταθερά αναχαιτίσης η οποία αντιστοιχεί στη συγκέντρωση του ελεύθερου νιτρώδους οξέος για την οποία καταγράφεται 50% αναχαιτίση του ρυθμού πρόσληψης φωσφόρου σε αερόβιες συνθήκες, S_{FNA} είναι η συγκέντρωση του ελεύθερου νιτρώδους οξέος στον αντιδραστήρα και PUR_{max} είναι η μέγιστη ταχύτητα πρόσληψης φωσφόρου σε συνθήκες απουσίας αναχαιτιστικού παράγοντα.

Σε αντιστοιχία με τα ανωτέρω διερευνήθηκε επίσης η αναχαιτιστική δράση των νιτρωδών στην ανοξική δράση των πολυφωσφορικών βακτηρίων και ειδικότερα στην ταχύτητα πρόσληψης φωσφόρου σε ανοξικές συνθήκες. Η διερεύνηση πραγματοποιήθηκε μέσω πειραμάτων batch σε βιομάζα που καλλιεργήθηκε σε αντιδραστήρα SBR. Τα αποτελέσματα των σχετικών πειραμάτων

καταδεικνύουν ότι όπως και στην περίπτωση των αερόβιων συνθηκών, έτσι και στις ανοξικές συνθήκες η αναχαιτιστική ουσία είναι το ελεύθερο νιτρώδες οξύ παρά τα νιτρώδη (Σχήματα 3-4). Βάσει των αποτελεσμάτων, χαμηλές συγκεντρώσεις ελεύθερου νιτρώδους οξέος της τάξης των 1,5 μg N/L μπορεί να οδηγήσουν σε αναχαιτίωση του ρυθμού πρόσληψης φωσφόρου σε ανοξικές συνθήκες κατά 50%, γεγονός που υποδηλώνει ότι η ανοχή των πολυφωσφορικών μικροοργανισμών στην παρουσία του ελεύθερου νιτρώδους οξέος τόσο σε αερόβιες όσο και σε ανοξικές συνθήκες είναι παρόμοια. Τέλος επιβεβαιώθηκε ότι ο μηχανισμός αναχαιτίωσης ακολουθεί το non-competitive μοντέλο και στην περίπτωση των ανοξικών συνθηκών.

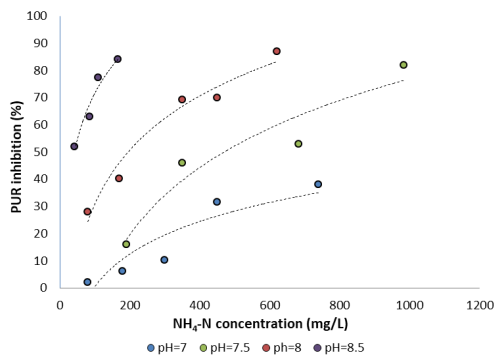


Σχήμα 3. Επίδραση του νιτρώδους αζώτου στον ανοξικό ρυθμό πρόσληψης φωσφόρου.

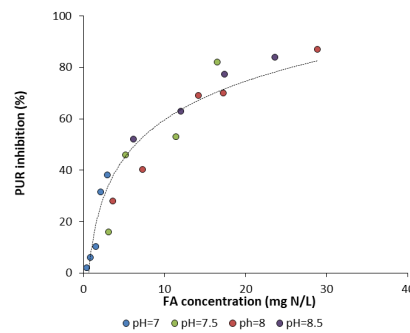


Σχήμα 4. Επίδραση του ελεύθερου νιτρώδους αζώτου στον ανοξικό ρυθμό πρόσληψης φωσφόρου.

Η διερεύνηση της επίδρασης του αμμωνιακού αζώτου στην ταχύτητα πρόσληψης φωσφόρου σε αερόβιες συνθήκες πραγματοποιήθηκε μέσω πειραμάτων batch σε εγκλιματισμένη και μη-εγκλιματισμένη βιομάζα η οποία καλλιεργήθηκε σε εργαστηριακό αντιδραστήρα SBR. Σύμφωνα με τα πειραματικά αποτελέσματα διαπιστώθηκε ότι με την αύξηση του pH του ανάμικτου υγρού αυξάνεται η αναχαιτίωση της διαδικασίας για τις ίδιες συγκεντρώσεις αμμωνιακού αζώτου (Σχήμα 5), γεγονός που υποδηλώνει με σαφήνεια ότι η βασική αναχαιτιστική ουσία της διεργασίας είναι η ελεύθερη αμμωνία. Όπως φαίνεται στο Σχήμα 6 μία συγκέντρωση ελεύθερης αμμωνίας της τάξης των 8 mg N/L οδηγεί σε 50% αναχαιτίωση του ρυθμού πρόσληψης φωσφόρου σε αερόβιες συνθήκες, ενώ πλήρης αναχαιτίωση αναμένεται για συγκεντρώσεις ελεύθερης αμμωνίας της τάξης των 40 mg N/L.



Σχήμα 5. Επίδραση του αμμωνιακού αζώτου στον αερόβιο ρυθμό πρόσληψης φωσφόρου.



Σχήμα 6. Επίδραση της ελεύθερης αμμωνίας στον αερόβιο ρυθμό πρόσληψης φωσφόρου.

Περαιτέρω, από αποτελέσματα στοχευμένων πειραμάτων εύρεσης του μοντέλου αναχαίτισης διαπιστώθηκε ότι η επίδραση της ελεύθερης αμμωνίας στον αερόβιο ρυθμό πρόσληψης φωσφόρου περιγράφεται από ένα un-competitive μοντέλο αναχαίτισης, η βέλτιστη μαθηματική προσομοίωση του οποίου δίνεται από τη σχέση 2.

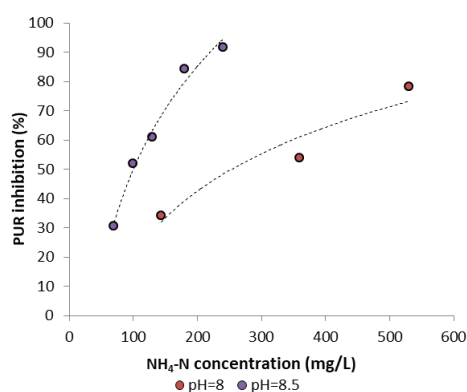
$$PUR = PUR_{max} \frac{S}{S \cdot \left(1 + \frac{S_{FA}}{K_{iFA}}\right) + K_S} \quad (2)$$

όπου K_{iFA} είναι η σταθερά αναχαίτισης, S_{FA} είναι η συγκέντρωση της ελεύθερης αμμωνίας στον αντιδραστήρα, S είναι η συγκέντρωση των φωσφορικών στον αντιδραστήρα, K_S είναι ο συντελεστής ημι-κορεσμού για τα φωσφορικά και PUR_{max} είναι ο μέγιστος ρυθμός πρόσληψης φωσφόρου σε αερόβιες συνθήκες απουσία αναχαίτισιμου παράγοντα.

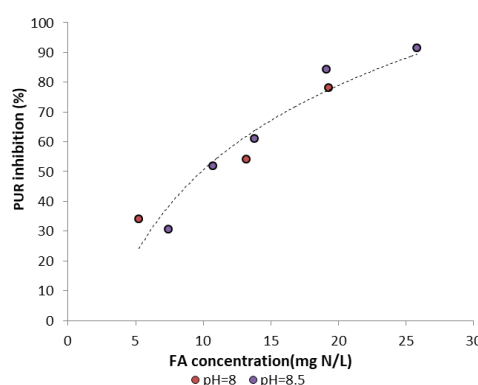
Αντίστοιχα πειράματα εργαστηριακής κλίμακας πραγματοποιήθηκαν για να εκτιμηθεί η επίδραση της ελεύθερης αμμωνίας στην δραστηριότητα των πολυφωσφορικών βακτηρίων σε ανοξικές συνθήκες. Σύμφωνα με τα αποτελέσματα η επίδραση της ελεύθερης αμμωνίας στην ταχύτητα πρόσληψης φωσφόρου σε ανοξικές συνθήκες είναι αντίστοιχη αυτής σε αερόβιες συνθήκες. Ειδικότερα, συγκεντρώσεις ελεύθερης αμμωνίας μεγαλύτερες από 30 mg N/L μπορούν να οδηγήσουν σε πλήρη αναχαίτιση της διαδικασίας (Σχήμα 8). Τέλος διαπιστώθηκε ότι ο μηχανισμός αναχαίτισης των δράσης των πολυφωσφορικών βακτηρίων σε ανοξικές συνθήκες ακολουθεί ένα un-competitive μοντέλο αναχαίτισης, η βέλτιστη περιγραφή του οποίου δίνεται από το απλό μοντέλο αναχαίτισης της Levenspiel που περιγράφεται από τη σχέση 3:

$$PUR = PUR_{max} \left(1 - \frac{S_{FA}}{S_{FA}^*}\right)^n \quad (3)$$

όπου S_{FA}^* είναι η συγκέντρωση της ελεύθερης αμμωνίας στον αντιδραστήρα για την οποία αναχαίτιζεται πλήρως η διεργασία και n είναι μία εμπειρική σταθερά.



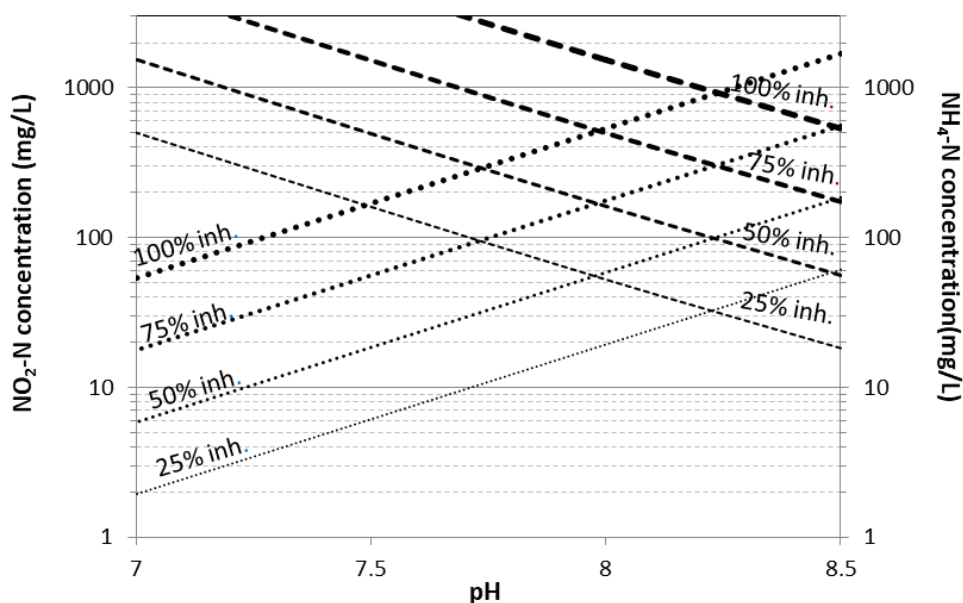
Σχήμα 7. Επίδραση του αμμωνιακού αζώτου στον ανοξικό ρυθμό πρόσληψης φωσφόρου.



Σχήμα 8. Επίδραση της ελεύθερης αμμωνίας στον ανοξικό ρυθμό πρόσληψης φωσφόρου.

Με βάση τα αποτελέσματα όλων των ανωτέρω διερευνήσεων διαπιστώθηκε ότι δράση των πολυφωσφορικών βακτηρίων τόσο σε αερόβιες όσο και σε ανοξικές συνθήκες δύναται να επηρεασθεί σε πολύ σημαντικό βαθμό από την παρουσία ελεύθερου νιτρώδους οξέος και ελεύθερης αμμωνίας και συνεπώς η τιμή του pH μπορεί να καθορίσει τη δυνατότητα επίτευξης βιολογικής απομάκρυνσης

φωσφόρου σε συστήματα νιτροδοποίησης-απονιτροδοποίησης. Σε χαμηλές τιμές του pH ευνοείται η παρουσία του ελεύθερου νιτρώδους οξέος και του αμμωνιακού αζώτου, ενώ σε αυξημένες τιμές του pH ευνοούνται υψηλότερες συγκεντρώσεις νιτρώδων και ελεύθερης αμμωνίας. Με βάση τα επιμέρους μοντέλα αναχαιτίσης κατασκευάστηκε το Σχήμα 9 στο οποίο αποτυπώνεται ο βαθμός αναχαιτίσης ανάλογα με την παρουσία έιαστης αναχαιτιστικής ουσίας. Για παράδειγμα για μία συγκέντρωση αζώτου της τάξης των 200 mg N/L σε συνθήκες ισορροπίας και βέλτιστης τιμής του pH, η βιολογική απομάκρυνση του φωσφόρου αναμένεται να αναχαιτισθεί κατά 50% λόγω παρουσίας ελεύθερου νιτρώδους οξέος και 50% λόγω της παρουσίας της ελεύθερης αμμωνίας. Η μελέτη της συνδυαστικής επίδρασης των δύο ουσιών μελετήθηκε σε επόμενη ενότητα. Ωστόσο, με βάση τα αποτελέσματα αυτά διαπιστώνεται ότι η επίτευξη βιολογικής απομάκρυνσης φωσφόρου σε συστήματα νιτροδοποίησης – απονιτροδοποίησης αποτελεί ένα μάλλον δύσκολο εγχείρημα.



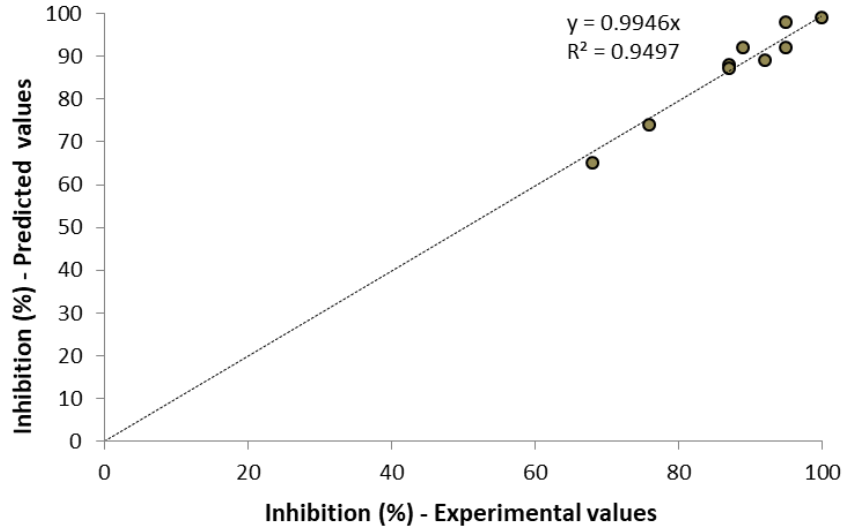
Σχήμα 9. Προβλεπόμενη αναχαιτίση του ρυθμού δέσμευσης φωσφόρου, με βάση την φόρτιση του αζώτου και το pH, από το νιτρώδες άζωτο (•••) και από το αμμωνιακό άζωτο (---), στους 20°C (οι συγκεντρώσεις αζώτου στους άξονες εμφανίζονται σε λογαριθμική κλίμακα).

4. Προσομοίωση της συνδυασμένης επίδρασης του ελεύθερου νιτρώδους οξέος και της ελεύθερης αμμωνίας στη δράση των πολυφωσφορικών βακτηρίων

Προκειμένου να μελετηθεί η επίδραση της ταυτόχρονης παρουσίας ελεύθερου νιτρώδους οξέος και ελεύθερης αμμωνίας στην δράση των πολυφωσφορικών βακτηρίων πραγματοποιήθηκε μία σειρά πειραμάτων εργαστηριακής κλίμακας για μία σειρά συνδυασμών συγκεντρώσεων νιτρώδων (μεταξύ 25-120 mg/L) και αμμωνιακού αζώτου (μεταξύ 110-700 mg/L) σε τιμές pH στο εύρος του 7,3-8,2.

Όπως φαίνεται στο Σχήμα 10 τα πειραματικά αποτελέσματα βρίσκονται σε πολύ ικανοποιητική συμφωνία με τα αποτελέσματα της εφαρμογής της σχέσης 4, η οποία προκύπτει με συνδυασμό των μαθηματικών μοντέλων αναχαιτίσης που προέκυψαν για την κάθε ουσία χωριστά.

$$Inh_{FNA\&FA} = 1 - (1 - Inh_{FNA}) \times (1 - Inh_{FA}) \quad (4)$$



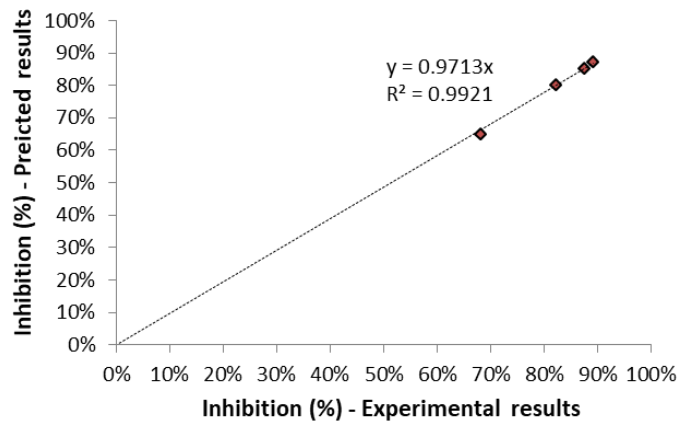
Σχήμα 10. Συσχέτιση των πειραματικών δεδομένων με την προβλεπόμενη αναχαίτιση (μέσω της Σχέσης 4) για την κοινή επίδραση του ελεύθερου νιτρώδους οξέος και της ελεύθερης αμμωνίας στον ρυθμό πρόσληψης φωσφόρου.

Στο πλαίσιο της προσομοίωσης του φαινομένου της συνδυαστικής αναχαίτισης των πολυφωσφορικών βακτηρίων από την ελεύθερη αμμωνία και το ελεύθερο νιτρώδες οξύ αναπτύχθηκαν δύο μαθηματικά μοντέλα βασισμένα σε ενζυμική ανάλυση τα οποία αποτυπώνονται στις σχέσεις 5-6.

$$PUR = \frac{PUR_{max}[S]}{K_s \left(1 + \frac{[S_{FNA}]}{K_{iFNA}}\right) + [S] \left(1 + \frac{[S_{FNA}]}{K_{iFNA}} + \frac{[S_{FA}]}{K_{FA}}\right)} \quad (5)$$

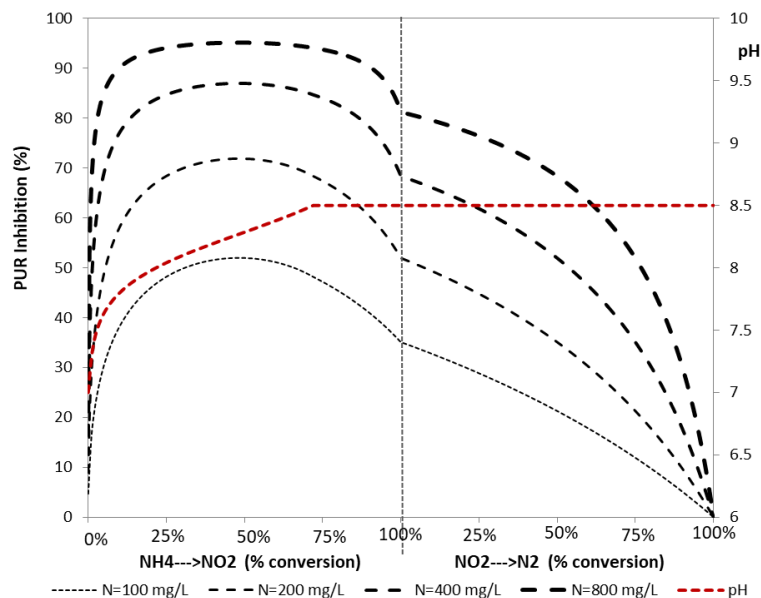
$$PUR = PUR_{max} \times \frac{K_{iFNA}}{S_{FNA} + K_{iFNA}} \times \frac{S}{S \left(1 + \frac{S_{FA}}{K_{iFA}}\right) + K_s} \quad (6)$$

Η βασική διαφοροποίηση των δύο μοντέλων αφορά στην ικανότητα ή μη ενός non-competitive αναχαιτιστικού παράγοντα (ελεύθερο νιτρώδες οξύ) να προσδεθεί στο σύμπλοκο ενζύμου-υποστρώματος στο οποίο έχει ήδη προσδεθεί ένας un-competitive αναχαιτιστικός παράγοντας (ελεύθερη αμμωνία) και αντίστροφα. Από τη σύγκριση των δύο μοντέλων έναντι των μετρημένων τιμών προέκυψε ότι το τροποποιημένο ενζυμικό κινητικό μοντέλο της σχέσης 6 μπορεί να περιγράψει πολύ ικανοποιητικά το φαινόμενο της συνδυαστικής αναχαίτισης της δράσης των πολυφωσφορικών βακτηρίων από το ελεύθερο νιτρώδες οξύ και την ελεύθερη αμμωνία (Σχήμα 11).



Σχήμα 11. Συσχέτιση των πειραματικών δεδομένων με την προβλεπόμενη αναχαίτιση μέσω του τροποποιημένου ενζυμικού μοντέλου (Σχέση 6) για την κοινή επίδραση του ελεύθερου νιτρώδους οξέος και της ελεύθερης αμμωνίας στον ρυθμό πρόσληψης φωσφόρου.

Το τροποποιημένο ενζυμικό μοντέλο (Σχέση 6) μπορεί να αξιοποιηθεί για να προβλέψει την συνολική αναχαίτιση του βαθμού πρόσληψης φωσφόρου για μια σειρά συνθηκών (συγκεντρώσεις αμμωνιακού και νιτρώδους αζώτου, θερμοκρασία και pH), αλλά και για τον προσδιορισμό του βέλτιστου (για τα πολυφωσφορικά) pH ανάλογα με τον καταμερισμό του αζώτου σε αμμωνιακά και νιτρώδη. Με βάση αυτό, το μοντέλο δύναται να προσδιορίσει την βέλτιστη ρύθμιση του pH κατά τις διεργασίες νιτρωδοποίησης και απονιτρωδοποίησης, που οδηγεί στην ελάχιστη συνολική αναχαίτιση. Το σχήμα 12 παρουσιάζει τα αποτελέσματα μιας προσομοίωσης αυτών των διεργασιών για διάφορες συγκεντρώσεις αζώτου. Όπως φαίνεται, η αποτελεσματική ρύθμιση του pH δύναται να δημιουργήσει ένα πλατό στην συνολική αναχαίτιση των πολυφωσφορικών.



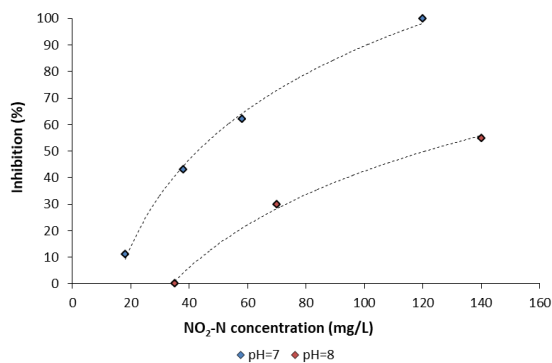
Σχήμα 12. Πρόβλεψη της συνολικής αναχαίτισης του ρυθμού δέσμευσης φωσφόρου κατά τις διεργασίες νιτρωδοποίησης και απονιτρωδοποίησης για διάφορες φορτίσεις αζώτου υπό βέλτιστο pH στους 20°C (η τιμή του 8.5 έχει οριστεί ως την ανώτερη αποδεικτή για το pH).

5. Διερεύνηση της επίδρασης των νιτρωδών και της ελεύθερης αμμωνίας στην δραστηριότητα των βακτηρίων συσσώρευσης γλυκογόνου

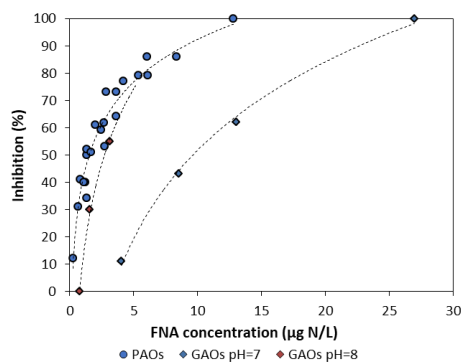
Προκειμένου να διερευνηθεί η επίδραση των νιτρωδών και της ελεύθερης αμμωνίας στην δραστηριότητα των βακτηρίων συσσώρευσης γλυκογόνου που αποτελούν και τους σημαντικότερους ανταγωνιστές των πολυφωσφορικών βακτηρίων, λειτούργησε αντιδραστήρας SBR στον οποίο αναπτύχθηκε βιομάζα η οποία αποτελούταν κατά 90% από *Competibacter spp.*

Στη συνέχεια, η βιομάζα αυτή χρησιμοποιήθηκε σε πειράματα batch μέτρησης της μέγιστης ειδικής ταχύτητας ανάπτυξης των βακτηρίων συσσώρευσης γλυκογόνου για διαφορετικές συγκεντρώσεις νιτρωδών και διαφορετικά pH.

Σύμφωνα με τα αποτελέσματα αυτών των πειραμάτων (Σχήματα 13-14) διαπιστώθηκε ότι το ελεύθερο νιτρώδες οξύ είναι ο κύριος αναχαιτιστικός παράγοντας. Επιπλέον προέκυψε ότι τα βακτήρια συσσώρευσης γλυκογόνου είναι πιο ανθεκτικά στην παρουσία του ελεύθερου νιτρώδους οξέος από τα πολυφωσφορικά βακτήρια σε pH κοντά στο 7 ενώ η ανθεκτικότητά τους μειώνεται σε υψηλότερες τιμές του pH.



Σχήμα 13. Επίδραση του νιτρώδους αζώτου στην ανάπτυξη των GAOs.



Σχήμα 14. Επίδραση του ελεύθερου νιτρώδους αζώτου στην ανάπτυξη των GAOs και σύγκριση με την επίδρασή του στον ρυθμό δέσμευσης φωσφόρου των PAOs.

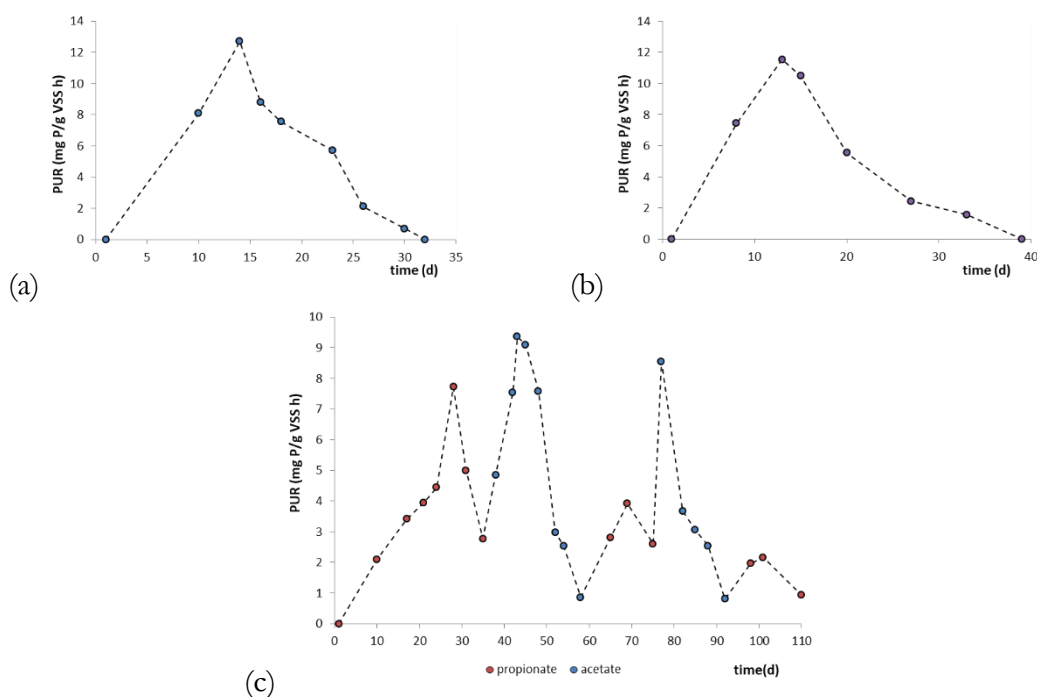
Από την αξιολόγηση εναλλακτικών μοντέλων αναχαιτίσις, η βέλτιστη περιγραφή του φαινομένου αναχαιτίσις της ταχύτητας ανάπτυξης των βακτηρίων συσσώρευσης γλυκογόνου συναρτήσκει της συγκέντρωσης του ελεύθερου νιτρώδους οξέος και του pH δίνεται από την σχέση 7.

$$\mu = \mu_{max} \frac{K_{iFNA}^{10,142 \cdot e^{-0,203 \cdot pH}}}{S_{FNA}^{10,142 \cdot e^{-0,203 \cdot pH}} + K_{iFNA}^{10,142 \cdot e^{-0,203 \cdot pH}}} \quad (7)$$

Τέλος τα αποτελέσματα των πειραμάτων διερεύνησης της επίδρασης της ελεύθερης αμμωνίας στην ταχύτητα ανάπτυξης των βακτηρίων συσσώρευσης γλυκογόνου κατέδειξαν ότι οι μικροοργανισμοί αυτοί είναι πολύ ανθεκτικοί στην παρουσία της ελεύθερης αμμωνίας ακόμα και σε συγκεντρώσεις της τάξης των 16 mg N/L οι οποίες προκαλούν αναχαιτίσις μεγαλύτερη από 50% της δραστηριότητας των πολυφωσφορικών βακτηρίων.

6. Μελέτη της επίδρασης του είδους του οργανικού υποστρώματος στον ανταγωνισμό των πολυφωσφορικών βακτηριών και των βακτηρίων συσσώρευσης γλυκογόνου σε συστήματα νιτρωδοποίησης – απονιτρωδοποίησης

Στο πλαίσιο της διερεύνησης της επίδρασης του ελεύθερου νιτρώδους οξέος στον ανταγωνισμό των PAOs και GAOs, αναπτύχθηκαν 3 διαφορετικές καλλιέργειες για την διερεύνηση της επίδρασης του οργανικού υποστρώματος σε συνθήκες συσσώρευσης νιτρώδους αζώτου. Σε κάθε αντιδραστήρα επικρατούσαν παρόμοιες συνθήκες νιτρωδοποίησης και απονιτρωδοποίησης με το ελεύθερο νιτρώδες οξύ να συσσωρεύεται έως 0,5 μg N/L κατά την αερόβια φάση (με μια μέση τιμή των 0,35 μg N/L, που έχει βρεθεί να αναχαιτίζει τα PAOs κατά περίπου 15%). Τα οργανικά υποστρώματα που εξετάστηκαν ήταν: α) οξικό οξύ, β) μίγμα οξικού και προπιονικού οξέος (50%-50%), και γ) τακτική εναλλαγή ανάμεσα σε προπιονικό και οξικό οξύ. Η ικανότητα της βιομάζας να απομακρύνει φώσφορο παρακολουθούνταν τακτικά κατά την διάρκεια της λειτουργίας και τα προφίλ του ρυθμού απομάκρυνσης με την πάροδο του χρόνου παρουσιάζονται στο Σχήμα 15. Όπως είναι εμφανές, η χρήση οξικού οξέος και του μίγματος οξικού-προπιονικού δεν ωφέλησαν τα PAOs, των οποίων η δραστηριότητα τερματίστηκε μέσα σε μόλις 30-40 μέρες από την εκκίνηση της καλλιέργειας. Η τακτική εναλλαγή μεταξύ οξικού και προπιονικού οξέος από την άλλη επέτρεψε την παρουσία τους για αρκετά μεγαλύτερο διάστημα, καθώς περιορίσε την επικράτηση των GAOs. Ωστόσο, η απομάκρυνση φωσφόρου ήταν αρκετά ασταθής, ενώ με κάθε εναλλαγή τροφής η ανάκαμψη του ρυθμού δέσμευσης ήταν ολοένα και μικρότερη.

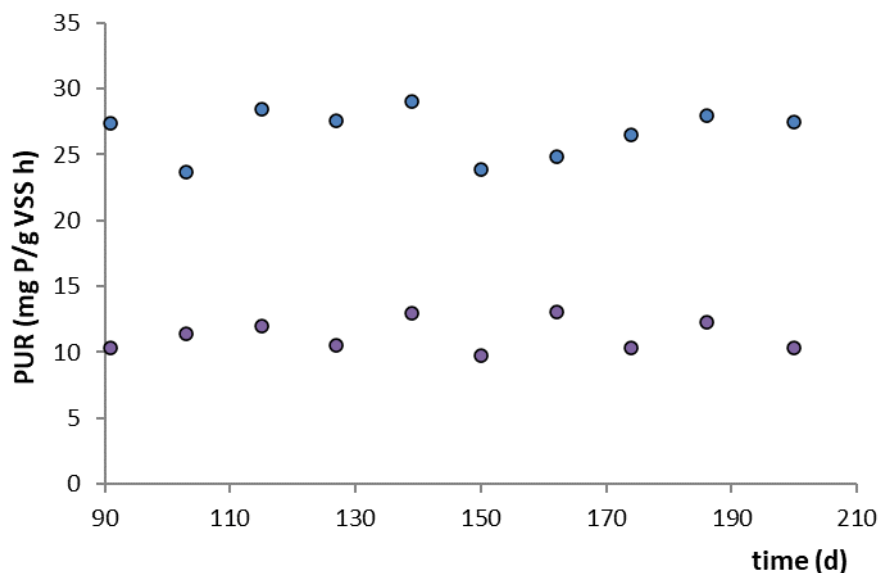


Σχήμα 15. Μεταβολή του ρυθμού απομάκρυνσης φωσφόρου κατά την διάρκεια λειτουργίας των συστημάτων με υπόστρωμα α) οξικό οξύ, β) μίγμα οξικού και προπιονικού οξέος, γ) εναλλαγή οξικού και προπιονικού οξέος.

7. Ανάπτυξη στρατηγικών βελτιστοποίησης της βιολογικής απομάκρυνσης φωσφόρου σε συστήματα νιτρωδοποίησης – απονιτρωδοποίησης.

Ενώ η αποτελεσματική ρύθμιση του pH μπορεί να διευκολύνει την δραστηριότητα των PAOs, η βιωσιμότητά τους σε συνθήκες αναχαίτισης απαιτεί στρατηγικές για την επικράτησή τους απέναντι στις ανταγωνιστικές ομάδες των GAOs. Μια στρατηγική που εφαρμόστηκε και αποδείχθηκε ιδιαίτερα αποτελεσματική ήταν η προαγωγή της ανάπτυξής τους μέσω απονιτρωδοποίησης με υπόστρωμα το προπιονικό οξύ. Η μέθοδος στηρίζεται στην αδυναμία των GAOs να αξιοποιήσουν τα νιτρώδη ως αποδέκτη ηλεκτρονίων όταν το προπιονικό οξύ αποτελεί την μοναδική πηγή άνθρακα. Έτσι, δίνοντας προτεραιότητα νιτρωδοποίησης στα PAOs απέναντι στους κοινούς ετερότροφους, κάτι που επιτυγχάνεται με την μη-προσθήκη οργανικής τροφής κατά την ανοξική φάση, διασφαλίζεται για αυτούς ένας αποκλειστικός χρόνος ανάπτυξης.

Η εφαρμογή αυτής της στρατηγικής σε έναν αντιδραστήρα που λειτουργήσε με φόρτιση αμμωνιακού αζώτου ίση με $0,1 \text{ kg N/m}^3 \text{ d}$, είχε ως αποτέλεσμα την ανάπτυξη μιας σημαντικά εμπλουτισμένης βιομάζας σε PAOs (σε ποσοστό 50% επί των συνολικών μικροοργανισμών), ενώ η παρουσία των GAOs ήταν αμελητέα. Η βιομάζα ανέδειξε σταθερούς και σημαντικά υψηλούς ρυθμούς απομάκρυνσης φωσφόρου, τόσο σε αερόβιες όσο και σε ανοξικές συνθήκες. Ο μέσος μέγιστος αερόβιος ρυθμός απομάκρυνσης φωσφόρου ήταν 25 mg P/gVSS h , ενώ ο αντίστοιχος ανοξικός ρυθμός ήταν 10 mg P/gVSS h (Σχήμα 16), οδηγώντας στο συμπέρασμα ότι η ανοξική απομάκρυνση φωσφόρου πραγματοποιείται στο 40% της ταχύτητας της αντίστοιχης αερόβιας απομάκρυνσης.



Σχήμα 16. Διακύμανση αερόβιου και ανοξικού ρυθμού απομάκρυνσης φωσφόρου κατά την λειτουργία του συστήματος.

Η λειτουργία του αντιδραστήρα σε υψηλότερη φόρτιση αμμωνιακού αζώτου ($0,15 \text{ kg N/m}^3 \text{ d}$), είχε ως αποτέλεσμα την μείωση της απόδοσης της βιομάζας κατά περίπου 50%, λόγω της συσσώρευσης υψηλότερων συγκεντρώσεων FNA που έφταναν $1 \text{ } \mu\text{g N/L}$. Η πτώση αυτή οφείλεται τόσο στον μικρότερο πληθυσμό των πολυφωσφορικών, λόγω αναχαίτισης της ανάπτυξής τους, όσο και στην άμεση αναχαίτιση της λειτουργίας τους. Σε μετέπειτα φάση, εξετάστηκε η βιωσιμότητά τους σε

συνθήκες πολύ υψηλών συγκεντρώσεων FNA (που έφταναν τα 8 $\mu\text{g N/L}$), μέσω της ρύθμισης pH σε χαμηλή τιμή. Σε αυτές τις συνθήκες, η βιολογική απομάκρυνση αστόχησε, ωστόσο οι πληθυσμοί των GAOs στην βιομάζα παρέμεναν πρακτικά ανύπαρκτοι.

Στο πλαίσιο της βελτιστοποίησης, πραγματοποιήθηκε μια σειρά μαθηματικών προσομοιώσεων προκειμένου να αξιολογηθεί η συνδυασμένη βιολογική απομάκρυνση φωσφόρου και νιτροδοποίησης/απονιτροδοποίησης σε συστήματα υψηλής φόρτισης αζώτου. Η θεωρητική διάταξη που εξετάστηκε βελτιστοποιήθηκε όσον αφορά: i) την εναλλαγή των αερόβιων και ανοξικών συνθηκών, ώστε να αποτραπεί η συσσώρευση νιτροδών και να διατηρηθεί το pH σε σχετικά υψηλές τιμές, ii) την παροχή ενός αποκλειστικού χρόνου απονιτροδοποίησης στα PAOs, μετά την απομάκρυνση μιας σημαντικής ποσότητας νιτροδών από τους κοινούς ετερότροφους, μέσω μιας δοσολογημένης προσθήκης οργανικού άνθρακα, στο πλαίσιο της στρατηγικής καταστολής των GAOs και iii) την ποιότητα των επεξεργασμένων λυμάτων. Η βιωσιμότητα της βιολογικής απομάκρυνσης αξιολογήθηκε για φορτίσεις αμμωνιακού αζώτου από 0,1 έως 0,3 $\text{kg N/m}^3 \text{ d}$, έχοντας υπόψη: α) τη συνολική αναχαίτιση των PAOs υπό τις συνθήκες κάθε σεναρίου, τόσο ως προς τη διατήρηση του πληθυσμού τους όσο και ως προς την απόδοσή τους, β) την επάρκεια της στρατηγικής καταστολής των GAOs σε κάθε σενάριο, γ) την αναγκαιότητα για ρύθμιση του pH για την ελαχιστοποίηση της αναχαίτισης των PAOs και δ) την αποτελεσματική καταστολή των NOB. Με βάση τα αποτελέσματα των προσομοιώσεων και την αξιολόγησή τους, συμπεραίνεται ότι μια φόρτιση αζώτου της τάξεως των 0,2 $\text{kg N/m}^3 \text{ d}$ θα μπορούσε να επιτρέψει επαρκή και σχετικά ασφαλή απομάκρυνση φωσφόρου χωρίς την ανάγκη για ρύθμιση του pH. Η λειτουργία σε υψηλότερες φορτίσεις ενδεχομένως να επέτρεπε επαρκή απομάκρυνση φωσφόρου, αν και πιθανότατα θα απαιτούσε κάποια ρύθμιση του pH που είναι δαπανηρή, ενώ είναι αβέβαιο αν θα εξασφαλιζόταν η επικράτηση των PAOs έναντι των GAOs. Συμπερασματικά, η επίτευξη βιολογικής απομάκρυνσης φωσφόρου σε φορτίσεις αζώτου άνω των 0,3 $\text{kg N/m}^3 \text{ d}$ φαίνεται εξαιρετικά απίθανη, καθώς οι συνθήκες αναχαίτισης από μόνες τους θα έβραζαν σε σοβαρό κίνδυνο τη βιωσιμότητα των πολυφωσφορικών βακτηρίων.

8. Συμπεράσματα

Τα κύρια συμπεράσματα της παρούσας διατριβής μπορούν να συνοψισθούν ως εξής:

- ⇒ Το ελεύθερο νιτρώδες οξύ αναχαιτίζει σημαντικά την δραστηριότητα των πολυφωσφορικών βακτηρίων τόσο σε αερόβιες όσο και σε ανοξικές συνθήκες, με τον ρυθμό απομάκρυνσης φωσφόρου να αναχαιτίζεται κατά 50% σε συγκέντρωση 1,5 $\mu\text{g HNO}_2\text{-N/L}$ (10 $\text{mg NO}_2\text{-N/L}$ σε $\text{pH}=7$, 50 $\text{mg NO}_2\text{-N/L}$ σε $\text{pH}=8$, στους 20°C) και κατά 100% σε συγκεντρώσεις της τάξης των 13 $\mu\text{g HNO}_2\text{-N/L}$ (100 $\text{mg NO}_2\text{-N/L}$ σε $\text{pH}=7$, 500 $\text{mg NO}_2\text{-N/L}$ σε $\text{pH}=8$, στους 20°C). Ο μηχανισμός αναχαίτισης περιγράφεται βέλτιστα ως non-competitive για $K_{\text{IFNA}}=1,5 \mu\text{g N/L}$ και είναι ανεξάρτητος του αποδέκτη ηλεκτρονίων.
- ⇒ Η ελεύθερη αμμωνία αποδείχθηκε ότι επίσης αποτελεί σημαντική αναχαιτιστική ουσία για τα PAOs σε αερόβιες και ανοξικές συνθήκες, προκαλώντας 50% αναχαίτιση του ρυθμού απομάκρυνσης φωσφόρου σε συγκεντρώσεις 8-10 $\text{mg NH}_3\text{-N/L}$. Ο μηχανισμός αναχαίτισης περιγράφεται ικανοποιητικά από ένα un-competitive μοντέλο αναχαίτισης, με την ανοξική αναχαίτιση από FA να περιγράφεται καλύτερα από το μοντέλο της Levenspiel.
- ⇒ Ο βαθμός αναχαίτισης των πολυφωσφορικών βακτηρίων είτε από τα νιτρώδη είτε από το αμμωνιακό άζωτο εξαρτάται από το pH που ελέγχει τις αντίστοιχες μορφές του ελεύθερου

νιτρώδους οξέος και της ελεύθερης αμμωνίας. Σε όρους αζώτου, τα νιτρώδη αποτελούν τον ισχυρότερο αναχαιτιστή όταν το pH είναι κάτω από 8,2 περίπου, ενώ τα αμμωνιακά αποκτούν την μεγαλύτερη βαρύτητα όταν το pH υπερβαίνει αυτήν την τιμή.

- ⇒ Η κοινή επίδραση του ελεύθερου νιτρώδους οξέος και της ελεύθερης αμμωνίας μπορεί να περιγραφεί πολύ ικανοποιητικά από το τροποποιημένο ενζυμικό μοντέλο αναχαιτίσης που αναπτύχθηκε στο πλαίσιο της διατριβής. Πρόσθετα, το μοντέλο δύναται να προσδιορίσει την βέλτιστη διακύμανση του pH κατά τις διεργασίες νιτρωδοποίησης και απονιτρωδοποίησης, για την ελαχιστοποίηση της αναχαιτίσης των PAOs.
- ⇒ Το FNA διαπιστώθηκε επίσης ότι αναχαιτίζει τα GAOs, αν και γενικά σε μικρότερο βαθμό από ότι τα PAOs. Η επίδραση του FNA στην ανάπτυξη των GAOs φαίνεται να εξαρτάται από το pH, με τα GAOs να αναχαιτίζονται περισσότερο σε υψηλό pH (50% αναχαιτίση από 10 $\mu\text{g HNO}_2\text{-N/L}$ στο pH του 7 και από 3 $\mu\text{g HNO}_2\text{-N/L}$ στο pH του 8). Σε σύγκριση με τα PAOs, τα GAOs φαίνεται να έχουν σημαντικά υψηλότερη ανοχή στο FNA σε χαμηλό pH (7), ενώ σε σχετικά υψηλό pH (8) η ανθεκτικότητα των δύο μικροβιακών ομάδων μπορεί να θεωρηθεί συγκρίσιμη. Ως εκ τούτου, ένα υψηλό pH μπορεί να ωφελήσει τα PAOs, όχι μόνο μειώνοντας την περιεκτικότητα σε FNA, αλλά και ελαχιστοποιώντας τον ανταγωνισμό των GAOs. Ωστόσο, τα GAOs εμφανίζουν μεγάλη ανοχή στο FA, μένοντας πρακτικά ανεπηρέαστα από μια συγκέντρωση της τάξεως των 16 $\text{mg NH}_3\text{-N/L}$ (συγκέντρωση που, έχει βρεθεί ότι αναστέλλει τα PAOs κατά περίπου 60%). Ως εκ τούτου, οι υψηλές συγκεντρώσεις FA που επικρατούν σε συστήματα υψηλής φόρτισης αζώτου μπορεί να παρέχουν ένα ανταγωνιστικό πλεονέκτημα στα GAOs, ακυρώνοντας το όφελος της λειτουργίας σε υψηλό pH που ευνοεί τα PAO ως προς το FNA. Η επίδραση του FNA στην ανάπτυξη των GAO περιγράφεται ικανοποιητικά από μοντέλο αναχαιτίσης τύπου Hill, με K_{FNA} ίσο με 9,2 και 3 $\mu\text{g N/L}$ για τα pH του 7 και 8 αντίστοιχα, και έναν συντελεστή Hill στην τιμή των 2,45 και 2 για τα pH του 7 και 8 αντίστοιχα.
- ⇒ Η προαγωγή των PAOs μέσω της απονιτρωδοποίησης με τη χρήση προπιονικού οξέος ως μοναδική πηγή άνθρακα, αποδείχθηκε η πιο αποτελεσματική στρατηγική για την καταστολή των GAOs και την επίτευξη σταθερής και αποτελεσματικής απομάκρυνσης φωσφόρου σε συνθήκες αναχαιτίσης. Η στρατηγική βασίζεται στην παροχή της αποκλειστικής αξιοποίησης των νιτρωδών από τα PAOs για ένα διάστημα όπου μόνο αυτά μπορούν να αναπτυχθούν. Καθώς όμως, οι ρυθμοί απονιτρωδοποίησης των PAOs είναι σημαντικά χαμηλότεροι από τους αντίστοιχους των τυπικών ετεροτροφικών μικροοργανισμών, η εφαρμογή αυτής της στρατηγικής προϋποθέτει υψηλότερους ανοξικούς χρόνους παραμονής, περιορίζοντας την επεξεργασία με υψηλές φορτίσεις αζώτου. Μαθηματική προσομοίωση ενός τέτοιου συστήματος έδειξε ότι η βιολογική απομάκρυνση φωσφόρου σε συνθήκες νιτρωδοποίησης/απονιτρωδοποίησης, είναι επιτεύξιμη για φορτίσεις αζώτου έως 0,2 $\text{kg N/m}^3 \text{ d}$ χωρίς την ανάγκη ρύθμισης του pH, ενώ διαφαίνεται αδύνατη για φορτίσεις πάνω από 0,3 $\text{kg N/m}^3 \text{ d}$.
- ⇒ Η εφαρμογή της βιολογικής απομάκρυνσης φωσφόρου σε συστήματα νιτρωδοποίησης/απονιτρωδοποίησης είναι εφικτή, ωστόσο προϋποθέτει ενδεχομένως την διαθεσιμότητα προπιονικού οξέος. Η προμήθεια μπορεί να γίνει μέσω της υδρόλυσης της πρωτοβάθμιας ύλης με λειτουργία που στοχεύει στην μεγιστοποίηση του κλάσματος του προπιονικού επί του συνολικού παραγόμενου διαλυτού άνθρακα. Σε συστήματα επεξεργασίας υγρών αποβλήτων που χαρακτηρίζονται από έναν σχετικά χαμηλό λόγο C:N, η ταυτόχρονη

απομάκρυνση αζώτου και φωσφόρου με την ίδια πηγή άνθρακα είναι θεμιτή. Σε κάθε περίπτωση όμως, η βιολογική απομάκρυνση φωσφόρου σε αυτές τις συνθήκες θα απαιτεί μεγαλύτερους όγκους αντιδραστήρων σε σχέση με τις αντίστοιχες απαιτήσεις για απομάκρυνση αζώτου.

Contents

Chapter 1:	Introduction.....	1
Chapter 2:	Literature review	5
2.1	Phosphorus speciation and sources.....	5
2.2	Phosphorus removal processes	6
2.2.1	Chemical removal	6
2.2.2	Enhanced Biological Phosphorus Removal (EBPR).....	11
2.3	Configurations implementing EBPR.....	14
2.4	Microbial community in EBPR systems	21
2.4.1	PAOs	21
2.4.2	GAOs	25
2.5	Achievement of EBPR in nitrogen removal systems.....	26
2.5.1	Peculiarities of EBPR coupled with nitrification/denitrification for low C/N wastewater treatment systems	26
2.5.2	Factors affecting EBPR in high nitrogen loading systems	29
Chapter 3:	Thesis objectives	40
Chapter 4:	Materials and methods	43
4.1	Experimental set-up.....	43
4.2	Experimental series	50
4.2.1	Experimental investigations regarding the activities of PAOs.....	50
4.2.2	Experimental investigations regarding the activities of GAOs.....	56
4.3	Analytical methods.....	58
4.3.1	Analysis of total and volatile suspended solids (TSS – VSS).....	58
4.3.2	Analysis of phosphorus.....	60
4.3.3	Analysis of ammoniacal nitrogen.....	61
4.3.4	Analysis of nitrate nitrogen and nitrite nitrogen	63
4.3.5	Analysis of COD.....	63
4.3.6	Measurement of DO, pH and temperature	65
4.3.7	Fluorescent In Situ Hybridization (FISH) analysis	65
Chapter 5:	Results and discussion.....	68
5.1	Introduction	68
5.2	Inhibition of PAOs due to free nitrous acid.....	69
5.2.1	Investigating the inhibitory effect of FNA on aerobic PUR.....	69

5.2.2	Investigating the inhibitory effect of FNA on anoxic PUR	90
5.3	Inhibition of PAO activities due to free ammonia.....	110
5.3.1	Investigating the inhibitory effect of FA on aerobic PUR	111
5.3.2	Investigating the inhibitory effect of FA on anoxic PUR.....	117
5.3.3	Investigating the effect of FA on anaerobic PAO activity	122
5.4	Assessment of the combined effect of FNA and FA and validation of the inhibition models.....	126
5.4.1	Experimental assessment of the combined effect of FNA and FA on aerobic PUR 127	
5.4.2	Validation of the inhibition models	131
5.4.3	Implications for full-scale applications according to the unified inhibition model 137	
5.5	Assessing the inhibitory effect of FNA and FA on GAO activity	142
5.5.1	Performance of the experimental system.....	142
5.5.2	Experimental assessment of the effect of FNA on GAO activity	145
5.5.3	Mathematical modelling of the inhibitory effect of FNA on GAO activity	149
5.5.4	Experimental assessment of the effect of FA on GAO activity.....	152
5.5.5	Investigating the effect of FA on the anaerobic activity of GAOs.....	153
5.6	Evaluating alternative operational strategies for promoting EBPR.....	155
5.6.1	Investigating the role of the carbon source in the PAO-GAO competition.....	155
5.6.2	Evaluating the influence of nitrite in the PAO-GAO competition.....	167
5.6.3	Optimizing EBPR via the selection of PAOs through the denitrification pathway with propionate as the sole carbon source.....	171
5.7	Optimizing EBPR in low C/N systems with nitrogen removal via nitrite.....	183
5.7.1	Simulation of an optimized system for EBPR.....	186
Chapter 6:	Conclusions and recommendations	194
6.1	Main conclusions.....	194
6.2	Recommendations for future research.....	199
References	201

List of Tables

Table 2.1. Results from the qualitative characterization of several reject water sources – physicochemical characteristics, organic carbon and solids (average values \pm standard deviation) (adapted from Noutsopoulos et al., 2018).	29
Table 2.2. Results from the qualitative characterization of several reject water sources –nitrogen and phosphorus (average values \pm standard deviation) (adapted from Noutsopoulos et al., 2018).	29
Table 5.1. Nitrite concentrations examined at each pH	77
Table 5.2. Comparison of studies on the effect of FNA on aerobic PUR	81
Table 5.3. Statistic indices for the FNA inhibition models examined for aerobic PUR.....	90
Table 5.4. Statistic indices for the FNA inhibition models examined for anoxic PUR.....	109
Table 5.5. Ammonium concentrations examined at each pH	111
Table 5.6. Statistic indices for the FA inhibition models examined	116
Table 5.7. Ammonium concentrations examined at each pH	117
Table 5.8. Conditions for batch experiments.....	128
Table 5.9. Conditions of batch experiments for acclimatized biomass.....	131
Table 5.10. Initial concentrations of main parameters in each reactor.....	145
Table 5.11. Statistic indices for the FNA inhibition models examined	151
Table 5.12. COD uptake rates of all reactors	155
Table 5.13. Comparison of anaerobic acetate and propionate uptake rates by PAOs and GAOs	156
Table 5.14. Determined metabolic rates of PAOs.....	178

Table of Figures

Figure 2.1. Speciation of orthophosphate ions expressed as mole fraction of total P in solution as a function of pH (Figure adapted from Hinsinger, 2001).....	6
Figure 2.2. Schematic diagram of chemical precipitation applied during primary and secondary treatment (adapted from Morse et al., 1998).	7
Figure 2.3. Alum and ferrous phosphate concentrations in equilibrium with soluble phosphate (adapted from Metcalf & Eddy, 2003).....	9
Figure 2.4. Required Al/P and Fe/P ratios for different concentrations of soluble phosphorus in the treated effluent (Adapted from Sedlak, 1991).	10
Figure 2.5. Schematic representations of the anaerobic/oxic system (a) and the anaerobic/anoxic/oxic system (b) (Figure adapted from Henze et al., 2008).....	13
Figure 2.6. Schematic of Phoredox (A/O) configuration for EBPR (Figure adapted from Henze et al., 2008).....	15
Figure 2.7. Schematic of the 3-stage Bardenpho configuration (A ² O) for EBPR (Figure adapted from Henze et al., 2008).	16
Figure 2.8: Schematic of the 5-stage Bardenpho configuration for EBPR (Figure adapted from Henze et al., 2008).	16

Figure 2.9. Schematic of the Johannesburg (JHB) configuration for EBPR (Figure adapted from Henze et al., 2008).	17
Figure 2.10: Schematic of the UCT configuration for EBPR (Figure adapted from Henze et al., 2008).	18
Figure 2.11. Schematic of the modified UCT configuration for EBPR (Figure adapted from Henze et al., 2008).	18
Figure 2.12. Schematic of the BCFS configuration for EBPR (Figure adapted from Henze et al., 2008).	19
Figure 2.13. Schematic of the PhoStrip configuration for EBPR (Figure adapted from Henze et al., 2008).	20
Figure 2.14. Anaerobic conversion of VFAs to PHAs (Figure adapted from Mino et al., 1998).	22
Figure 2.15. Anaerobic and aerobic metabolism of PAOs (Figure adapted from Tarayre et al., 2016)	23
Figure 2.16. Schematic diagram of the metabolism of GAOs under anaerobic and aerobic conditions (Figure adapted from Dai et al., 2008).	26
Figure 2.17. Layout of the sampled reject water (RW) according to source include: primary sludge thickening unit (PST-RW), wastage sludge mechanical thickening unit (WST-RW), dewatering unit following conventional anaerobic digestion (SD-CON-RW), dewatering unit following thermal hydrolysis – anaerobic digestion process (SD-HYD-RW) and drying sludge unit (DS-RW) (Figure adapted from Noutsopoulos et al., 2018).	28
Figure 2.18. Arrhenius temperature dependency of maximum growth rate of AOB and NOB, as determined by several authors (Figure adapted from Chaïm De Mulder, 2016).	34
Figure 2.19. Combined temperature and pH effects on the maximum substrate uptake rates of <i>Accumulibacter</i> , <i>Competibacter</i> and Alphaproteobacteria-GAO for (a) acetate and (b) propionate. Black solid line: <i>Accumulibacter</i> , grey solid lines: <i>Competibacter</i> , and, black dotted lines: Alphaproteobacteria-GAO. Maximum substrate uptake rates of <i>Accumulibacter</i> are insensitive to pH changes. Figure adapted from Lopez-Vazquez et al., (2009).	35
Figure 2.20. Minimum aerobic solid retention times of PAOs (Figure adapted from Lopez-Vazquez et al.,(2009).	36
Figure 2.21. FA concentration at different NH ₄ -N and pH values at 20°C.	37
Figure 2.22. FNA concentration with respect to nitrite and pH values at 20°C.	38
Figure 4.1. Experimental setup.	43
Figure 4.2. Typical ex situ batch experiment for determining aerobic PUR	51
Figure 4.3. Typical ex situ batch experiment for determining aerobic and anoxic PUR	51
Figure 4.4. Samples during the aeration phase of a typical experiment investigating aerobic PUR.	52
Figure 4.5. Samples during the anoxic phase of a typical experiment investigating anoxic PUR. At this instance, ice packs have been applied to the reactors to keep temperature within the desired range.	53
Figure 4.6. Phosphorus removal and determination of PURs of a typical batch experiment	54
Figure 4.7. Different types of inhibition using the modified direct linear plot method	55
Figure 4.8. Variation of VSS in typical batch experiment.	57
Figure 4.9. Appliances for TSS and VSS analysis. (a): precision scale, (b): dryer, (c): evaporation oven, d): combustion oven	59

Figure 4.10. Samples prepared for spectral analysis for the determination of orthophosphates	61
Figure 4.11. BUCHI K-314 distillation apparatus	62
Figure 4.12. Samples prepared for spectral analysis for the determination of ammoniacal nitrogen.	62
Figure 4.13. HACK vials for COD analysis.	64
Figure 4.14. COD digester.	64
Figure 4.15. Portable pH meter 3110 manufactured by WTW.	65
Figure 4.16. Multi 3510 portable oxygen meter, manufactured by WTW.	65
Figure 5.1. Typical variation of PO ₄ -P and COD concentrations in the SBR during the anaerobic phase of the first daily cycle.	72
Figure 5.2. Typical variation of PO ₄ -P and COD in the SBR during the anaerobic and aerobic phase of the first daily cycle.	73
Figure 5.3. Typical variation of PO ₄ -P and pH in the SBR during the aerobic phase of the first daily cycle	74
Figure 5.4. Phosphorus removal in a typical ex-situ batch experiment.	74
Figure 5.5. Typical variation of NH ₄ -N and NO _x -N in the SBR during the aerobic phase of the first daily cycle.	75
Figure 5.6. Typical variation of PO ₄ -P, COD and NO _x -N in the SBR during the anoxic phase of the first daily cycle.	76
Figure 5.7. In situ identification of PAOs using Cy-3 labelled PAOMIX (PAOs depicted in red in a and c, all microorganisms stained with DAPI presented in blue in b and d).	77
Figure 5.8. P-removal and determination of PURs for typical batch experiment (NO ₂ -N=10mg/L, pH=7)	78
Figure 5.9. The inhibitory effect of nitrite on aerobic PUR.	79
Figure 5.10. The inhibitory effect of FNA on aerobic PUR.	80
Figure 5.11. Typical variation of NO ₂ -N and NO _x -N in the SBR during the aerobic phase of the first daily cycle	82
Figure 5.12. Typical variation of FNA and pH in the SBR during the aerobic phase of the first daily cycle	82
Figure 5.13. Experimental results on the effect of FNA for the first and second series of experiments.	83
Figure 5.14. Comparison of studies on the effect of FNA on aerobic PUR.	84
Figure 5.15. Variation of PUR throughout operation.	85
Figure 5.16. Diminishment of overall K _{fFNA} over time.	86
Figure 5.17. Phosphorus removal under the effect of 35 mg NO ₂ -N/L and after its removal..	88
Figure 5.18. Comparison of experimental and predicted results regarding the inhibitive effect of FNA on aerobic PUR.	90
Figure 5.19. Variation of PO ₄ -P and NO ₂ -N during the ex-situ batch experiment	93
Figure 5.20. Typical variation of PO ₄ -P and COD in the SBR during the first daily cycle.	95
Figure 5.21. Typical variation of PO ₄ -P and pH in the SBR during the aerobic phase of the first daily cycle.	95
Figure 5.22. Typical variation of ammonium, nitrite and nitrate in the SBR during the first daily cycle.	96
Figure 5.23. Typical variation of FNA and pH in the SBR during the aerobic phase of the first daily cycle.	97

Figure 5.24. Phosphorus removal under anoxic and aerobic conditions of the typical ex-situ batch experiment.....	97
Figure 5.25. Variation of anoxic and aerobic PUR throughout operation.	98
Figure 5.26. In situ identification of PAOs using Cy-3 labelled PAOMIX (PAOs depicted in, all microorganisms stained with DAPI presented in blue).	99
Figure 5.27. PURs for a typical batch experiment ($\text{NO}_2\text{-N}=170$ mg/L, pH=8)	101
Figure 5.28. Denitrification in the typical batch experiment ($\text{NO}_2\text{-N}=170$ mg/L, pH=8).	101
Figure 5.29. Variation of phosphorus during the typical experiment.	102
Figure 5.30. Variation of nitrite during the typical experiment.	102
Figure 5.31. Determination of PURs for the ex-situ experiment.	104
Figure 5.32. Determination of the denitrification rates for the ex-situ experiment.	104
Figure 5.33. Effect of nitrite on anoxic PUR.....	105
Figure 5.34. Effect of FNA on anoxic PUR.	106
Figure 5.35. Comparison of anoxic PUR inhibition with aerobic PUR inhibition.	107
Figure 5.36. Comparison of modified anoxic PUR inhibition with aerobic PUR inhibition. ...	108
Figure 5.37. Comparison of experimental and predicted results regarding the inhibitive effect of FNA on anoxic PUR.....	110
Figure 5.38. Phosphorus variation for typical batch experiment ($\text{NH}_4\text{-N}=85$ mg/L, pH=8.5)	112
Figure 5.39. Aerobic PURs for typical batch experiment ($\text{NH}_4\text{-N}=85$ mg/L, pH=8.5)	113
Figure 5.40. The effect of ammonium nitrogen on aerobic PUR inhibition for the pH of 7, 7.5, 8 and pH=8.5.	113
Figure 5.41. The effect of FA on aerobic PUR inhibition for the pH of 7, 7.5, 8 and 8.5.	114
Figure 5.42. Comparison of experimental and predicted results regarding the inhibitive effect of FA on aerobic PUR.	117
Figure 5.43. Phosphorus variations for typical batch experiment ($\text{NH}_4\text{-N}=100$ mg/L, pH=8.5)	118
Figure 5.44. PURs for typical batch experiment ($\text{NH}_4\text{-N}=100$ mg/L, pH=8.5).....	119
Figure 5.45. The effect of ammonium on anoxic PUR for pH=8 and pH=8.5.....	119
Figure 5.46. The effect of FA on anoxic PUR for pH=8 and 8.5.	120
Figure 5.47. Comparison of anoxic PUR inhibition with aerobic PUR inhibition by FA.	121
Figure 5.48. Comparison of experimental and predicted results regarding the inhibitive effect of FA on anoxic PUR	122
Figure 5.49. The effect of ammonium on the anaerobic COD uptake of PAOs.....	124
Figure 5.50. The effect of ammonium on the anaerobic P-release of PAOs.....	124
Figure 5.51. Predicted effect of nitrogen loading on aerobic PUR with respect to pH and distribution between nitrite (••) and ammonium (---) nitrogen at $T=20^\circ\text{C}$ (Nitrogen concentrations for both nitrite and ammonium are presented in logarithmical scale).	127
Figure 5.52. Experimental results of typical batch experiment.....	129
Figure 5.53. Determination of PURs for typical batch experiment.....	129
Figure 5.54. Correlation of the experimental and the predicted inhibition values for the simultaneous presence of FNA and FA.	130
Figure 5.55. Comparison of simulated and experimental inhibition for various FNA and FA combinations.	132

Figure 5.56. Comparison of simulated and experimental inhibition for various FNA and FA combinations (empirical vs enzyme kinetic model).....	135
Figure 5.57. Comparison of simulated and experimental inhibition for various FNA and FA combinations	135
Figure 5.58. PUR inhibition under the combined presence of FNA and FA.....	137
Figure 5.59. PAO activity under the combined effect of nitrite and ammonium at the pH of 7 (a), 7.5 (b), 8 (c), 8.2 (e) and 8.5 (d).	139
Figure 5.60. Simulated PUR inhibition during nitrification and denitrification under different ammonium loads at T=20°C and optimum pH.....	140
Figure 5.61. Overall inhibition of PAOs under aerobic and anoxic conditions for various initial NH ₄ -N concentrations at optimum pH.	141
Figure 5.62. Typical variation of COD in the SBR during the first daily cycle.....	144
Figure 5.63. In situ identification of GAOs using Cy-3 labeled GAOMIX. All microorganisms stained with DAPI presented in blue (column a), GAOs depicted in red (column b), composite images in purple (column c).	144
Figure 5.64. Typical example of VSS evolution in control reactor.....	146
Figure 5.65. Determination of the net growth rates of GAOs in each reactor	147
Figure 5.66. Inhibition of GAO growth with regard to nitrite nitrogen concentration.	147
Figure 5.67. Comparison of the effect of FNA on the aerobic PUR of PAOs and the growth of GAOs.	149
Figure 5.68. Comparison of experimental and simulated values for FNA inhibition in GAOs growth.....	152
Figure 5.69. Comparison of the net growth rates of GAOs under the FA concentration of 1.7 mg NH ₃ -N (pH=7) and under the FA concentration of 16.1 mg NH ₃ -N (pH=8).....	153
Figure 5.70. The effect of ammonium on the COD uptake of GAOs.....	154
Figure 5.71. Variation of aerobic PUR throughout operation.....	158
Figure 5.72. Variation of the anaerobic phosphorus release rate and COD uptake rate throughout operation	158
Figure 5.73. NO ₂ and total NO _x concentrations at the end of the aerobic phase over time.	159
Figure 5.74. Variation of NO ₂ and total NO _x concentrations during the aerobic and anoxic phase of the first daily cycle (day 18).	159
Figure 5.75. Variation of pH and the concentration of FNA during the aerobic phase of the first daily cycle (day 18).	160
Figure 5.76. Variation of aerobic PUR throughout operation	161
Figure 5.77. NO ₂ and total NO _x concentrations at the end of the aerobic phase over time.	162
Figure 5.78. Variation of NO ₂ and total NO _x concentrations during the aerobic and anoxic phase of the first daily cycle (day 20).	162
Figure 5.79. Variation of pH and the concentration of FNA during the aerobic phase of the first daily cycle (day 20).	163
Figure 5.80. Variation of aerobic PUR throughout operation	165
Figure 5.81. NO ₂ and total NO _x concentrations at the end of the aerobic phase over time. ...	166
Figure 5.82. Variation of NO ₂ and total NO _x concentrations during the aerobic and anoxic phase of the first daily cycle (day 21).	166
Figure 5.83. Variation of pH and the concentration of FNA during the aerobic phase of the first daily cycle (day 21).	167

Figure 5.84. Variation of NO ₂ and total NO _x concentrations throughout a typical cycle.	168
Figure 5.85. Variation of pH and the concentration of FNA during the aerobic phase of the first daily cycle.	169
Figure 5.86. Variation of aerobic PUR throughout operation	170
Figure 5.87. Variation of the anaerobic phosphorus release and COD uptake rates throughout operation.	170
Figure 5.88. In situ identification of GAOs using Cy-3 labelled GAOMIX (GAOs depicted in red, all microorganisms stained with DAPI presented in blue) on day 88 of operation.	171
Figure 5.89. Comparison of the SBR's performance with that observed under higher FNA accumulations	171
Figure 5.90. Variation of phosphorus and COD throughout a typical SBR cycle.	175
Figure 5.91. Variation of ammonium, nitrite and nitrate throughout the aerobic and anoxic phase of a typical SBR cycle.	175
Figure 5.92. Variation of DO and pH throughout the aerobic phase of a typical SBR cycle....	176
Figure 5.93. Variation of FNA and the degree of inhibition throughout a typical SBR cycle...	176
Figure 5.94. In situ identification of PAOs using Cy-3 labelled PAOMIX (PAOs depicted in, all microorganisms stained with DAPI presented in blue).	177
Figure 5.95. Variation of phosphorus in the SBR during the first daily cycle.....	179
Figure 5.96. Variation of nitrite in the SBR during the first daily cycle.	179
Figure 5.97. Variation of FNA and the degree of inhibition throughout a typical SBR cycle...	180
Figure 5.98. Variation of phosphorus in the SBR during the first daily cycle.....	181
Figure 5.99. Variation of nitrite and nitrate in the SBR during the first daily cycle.	182
Figure 5.100. Variation of FNA and the degree of inhibition throughout a typical SBR cycle.	182
Figure 5.101. Variations of NH ₄ -N and NO ₂ -N during	185
Figure 5.102. Variation of pH during a typical cycle of the pilot SBR.	185
Figure 5.103. Variation of NH ₄ -N and NO ₂ -N according to the simulation setting	187
Figure 5.104. Variation of pH throughout the cycle for the scenarios of the simulation.....	188
Figure 5.105. PUR inhibition throughout an SBR cycle for each scenario.....	188
Figure 5.106. PUR inhibition during each phase for each scenario	189
Figure 5.107. NOB inhibition during the aeration phases of the scenario	191
Figure 5.108. Overall inhibition of PAOs in regard to vNLR.....	192
Figure 5.109. Overall aerobic inhibition of PAOs in regard to vNLR.....	192
Figure 5.110. Overall anoxic inhibition of PAOs in regard to vNLR.....	193

Chapter 1: Introduction

The present chapter introduces the problem to be addressed in the thesis. It discusses the goals of this work, its methodology and, finally, presents the thesis outline.

Following the industrial revolution, the significant economic development and restructuring of society was accompanied by a major shift in humankind's relationship with the environment. Indeed, for many years, concerns regarding the adverse ecological impact of industrialization took a backseat in the emergence of the modern capitalist economy. The powering of the newly developed industries with the burning of fossil fuels along with the massive throughput of materials, resulted in the increasing pollution of air, water and soil, while also putting a strain on the Earth's natural resource reserves. Furthermore, population growth and urbanization created additional problems, with the generation of significant domestic waste sources, which in the absence of appropriate sanitation, lead to devastating outbreaks of water-borne diseases such as cholera and typhoid. These occurrences necessitated the suitable handling and treatment of domestic wastes and mobilized the development of sewage collection systems and wastewater treatment plants (WWTPs), which in turn lead to the development of a new scientific branch; that of sanitary engineering. In the years since, wastewater treatment has progressed to not only safeguard public health, but also minimize the adverse environmental effects of waste disposal. In the aftermath of the significant ecological crisis that followed the rapid development of industrialization, the emergence of new treatment technologies along with the acquisition of knowledge and experience in the field of wastewater treatment and pollution prevention and management in general, has sparked efforts to eliminate the anthropogenic footprint on the environment. This endeavour is an ongoing, cumulative process for the rectification of past mismanagement and the preservation of the natural state, the Earth and its resources, for future generations.

The treatment of municipal wastewater, prior to its disposal, primarily involves removal of the organic carbon content of the wastewater along with the removal of nutrients (namely, ammonium and phosphorus), while other pollutants of interest include heavy metals, microplastics, as well as certain organic micropollutants (e.g., emerging contaminants). Disposal of heavy organic carbon loads to the aqueous recipient may significantly enhance microbial growth, which in turn may deplete oxygen levels and lead to the death of aquatic fauna. Disposal of significant amounts of nutrients on the other hand, may enhance algal bloom (an occurrence known as eutrophication) which apart from disrupting the natural ecosystem in its own right, may also indirectly affect the availability of oxygen for aqueous life. Carbon removal in WWTPs is typically achieved via aeration of the wastewater, for its consumption by heterotrophic microorganisms for energy and microbial synthesis. The removal of nutrients may be carried out by either biological or physicochemical means. In general, biological removal of nutrients is the preferred method, where applicable, as it limits the treatment cost, both in terms of capital and environment, since it does not require addition of chemicals.

Biological removal of ammonium is typically performed via nitrification followed by denitrification. Under aerobic conditions, an autotrophic microbial group known as ammonium oxidizing bacteria (AOB) oxidizes ammonium to nitrite, which is then further oxidized to nitrate

by another autotrophic group known as nitrite oxidizing bacteria (NOB). The combination of these two biological reactions constitutes the nitrification process. In the absence of oxygen, the produced nitrate may then be utilized by heterotrophic organisms for the oxidation and removal of carbon, reducing nitrate to inert nitrogen gas in the process. Biological removal of phosphorus on the other hand, is achieved by promoting the growth of a specific microbial group known as polyphosphate accumulating organisms (PAOs). PAOs have a capacity for intracellularly storing polyphosphate chains, which may be used as an energy source in the absence of an electron acceptor (e.g., oxygen, nitrate). Under anaerobic conditions, PAOs hydrolyse their stored polyphosphate chains, releasing phosphorus in the process, and use the energy provided to take up soluble carbon and store it as macromolecules known as polyhydroxyalkanoates (PHAs). Once in the presence of an electron acceptor, PAOs oxidize their stored PHAs and replenish their polyphosphate chains, removing phosphorus from solution. Therefore, implementation of an anaerobic tank upstream of the aerobic and anoxic processes provides PAOs with a priority over common heterotrophs in the utilization of carbon, thereby promoting their growth. As PAOs are capable of storing significant amounts of phosphorus, its removal is achieved along with the removal of the excess PAO-enriched sludge. This process is known as the Enhanced Biological Phosphorus Removal (EBPR) method.

Prior to its disposal, the excess sludge that is produced in WWTPs requires a series of treatments aimed to reduce its water content, followed by sludge stabilization processes. Throughout the sludge treatment processes (particularly during dewatering), a series of reject water streams are generated, which possess a high carbon and nutrient content that require treatment. As such, these streams are typically recycled to the inlet of the WWTP. Due to their significantly high nutrient content, the recirculation of these streams to the main WWTP treatment stream may increase nitrogen and phosphorus loading by up to 20%, limiting the treatment capacity of the mainstream facilities. In addition, reject water is generally characterized by a relatively low C:N ratio, which will lower the overall C:N ratio of the influent upon re-entry. As effective denitrification requires the availability of carbon, nitrogen removal may prove insufficient under these circumstances.

In recent years, the side-stream treatment of reject water prior to its recirculation to the mainstream has been gaining popularity, as it may lessen the burden on the overall operation of the WWTP. Due to the high pH that typically characterizes reject water from the sludge treatment processes, a significant percentage of the ammonium content of the reject water is in the form of Free Ammonia (FA), which is a known inhibitor of various microbial processes. Notably, FA inhibits both AOB and NOB, although it affects the growth and performance of NOB to a significantly higher extent than it affects AOB. Therefore, due to the high nitrogen content of the reject water, its treatment in a side-stream Sequencing Batch Reactor (SBR) with an appropriate loading rate, which would allow the presence of high FA concentrations, could forbid the presence of NOB without severely affecting the performance of AOB. With this, the second stage of denitrification is excluded and during aeration, nitrite is not further oxidized to nitrate. Under anoxic conditions, nitrite may then be reduced by common heterotrophs, similarly to nitrate. This short-cut nitrification/denitrification process (nitritation/denitritation) has proven quite beneficial, as nitrogen removal may be achieved at a reduced aeration demand (by approximately 25% compared to full nitrification) and a reduced demand in carbon (by

approximately 40% compared to denitrification). As such, the side-stream treatment of reject water may reduce the overall treatment cost and ensure effective nitrogen removal.

While the effectiveness of the side-stream treatment of reject water has been adequately documented in regard to nitrogen removal, the side-stream removal of phosphorus has presented certain challenges. As mentioned, the recirculation of phosphorus to the WWTP's inlet could severely increase its loading rate, thereby compromising adequate phosphorus removal. Effective EBPR for higher phosphorus loads would require a greater PAO population within the microbial community. This in turn would require a greater availability of soluble carbon in the influent, which may be taken up during the anaerobic phase. Depending on the composition of the wastewater, the available carbon may be insufficient, meaning that an external carbon source could be required to supplement the needs of PAOs. As the side-stream treatment of reject water generally requires the addition of an external carbon source for the denitrification process, the implementation of EBPR alongside nitrification/denitrification is a desirable option, as both nitrogen and phosphorus may be removed by the same carbon source. However, the accumulations of nitrite that occur in such systems have been found to have a significantly adverse effect on PAOs. More specifically, nitrite in the form of Free Nitrous Acid (FNA) has been reported to be a strong inhibitor of PAOs, affecting both their growth and performance. The reported degree of severity for FNA-induced PAO inhibition varies in the literature and may differ in regard to acclimation to FNA as well as the pathway that is affected (aerobic/anoxic). In all cases, the nitrite accumulations that would occur with respect to the ammonium loadings that would be required for NOB shunt and the implementation of short-cut nitrification/denitrification, would likely severely inhibit PAO activity and may possibly forbid the application of EBPR in these conditions. Moreover, it has recently come to light that FA is also an inhibitor of PAOs, although research regarding the extent of its effect is very limited as of this point. While FA is more abundant at high pH, the percentage of nitrite in the form of FNA increases adversely to pH. During nitrification, the conversion of ammonium to nitrite is accompanied by a biochemical drop in pH, thereby significantly increasing the FNA content of the reject water throughout the process. Conditions for PAOs improve during denitrification along with the removal of nitrite, which is accompanied by a biochemical increase of pH. However, the combined effect of FA and FNA on PAOs during the aerobic phase may not allow their sustainability in such a configuration. The situation for PAOs under these conditions becomes even more bleak when considering that they may be outgrown and washed-out by an antagonistic group known as Glycogen Accumulating Organisms (GAOs). Like PAOs, GAOs may also take up soluble carbon under anaerobic conditions but do not contribute to phosphorus removal, as the required energy in their case is provided via glycolysis. Therefore, in conditions of high ammonium and nitrite accumulations, the effect of FNA and FA on GAOs is also of importance, as a higher tolerance to these inhibitors would result in their possible proliferation over PAOs and the failure of EBPR.

Considering the above, it is clear that the successful application of EBPR, coupled with nitrification/denitrification, for the effective side-stream treatment of reject water is challenging at the very least. The matter is a complex one, with nitrogen loading and pH being of significant importance and FNA and FA accumulations affecting not only the desired NOB shunt, but also the PAO/GAO competition throughout the nitrification and denitrification processes to different extents and ultimately the performance, or even feasibility, of EBPR under these conditions. The

focus of the present work is to assess the inhibitory effects of FNA and FA on PAOs, as well as on competitive GAOs, develop strategies for the proliferation of PAOs in these hostile conditions, and to evaluate the potential for effective EBPR with regard to nitrogen loading in the side stream treatment of low C:N reject water streams. The results of this investigation may provide helpful guidelines for the application of side-stream EBPR and also improve the hitherto accumulated knowledge on the microbial processes of WWTPs, as a modest steppingstone in the ongoing effort for environmental preservation.

Following the present introduction (Chapter 1), Chapter 2 presents and discusses the relevant and up to date research that has been reported in the literature, focusing on the general principles of EBPR and wastewater treatment for phosphorus in general, the PAO-GAO competition and factors that affect it, including inhibitors such as FNA and FA, and the particularities of EBPR for the side-stream treatment of reject water. In consideration of the available information on the subject matter, or lack of it, Chapter 3 lists the main objectives and areas of investigation of the present work. These mainly concern the determination of the degree of inhibition by FNA and FA on PAOs and GAOs, strategies for GAO suppression, and optimization of conditions for EBPR with special regard to pH and nitrogen loading. Chapter 4 presents the materials and methods that were utilized in the investigation while the experimental and mathematical modelling results are presented and critically discussed in Chapter 5. Finally, the main conclusions that derive from this discussion are presented in Chapter 6.

Chapter 2: Literature review

2.1 Phosphorus speciation and sources

Phosphorus (P) is a chemical element which is essential for sustaining life, largely through its presence in the form of phosphates (compounds of the phosphate ion, PO_4^{3-}). Phosphates are a component of DNA, RNA and ATP, as well as phospholipids, which are complex compounds that are fundamental for the function of cells. Phosphorus is not found free in nature, but within a wide variety of minerals, usually as phosphates. Its concentration in the Earth's crust is approximately 1 g/kg, which is relatively high (compared to copper for example, which has a concentration of approximately 0.06 g/kg). Phosphorus minerals are mined mainly for their consumption as fertilizers, with other commercial applications including the use of organophosphorus compounds in detergents, pesticides, and nerve agents. Inorganic phosphate rock, which partially consists of apatite (generally as pentacalcium triorthophosphate fluoride (hydroxide)), is the main commercial source of this element. The demand of phosphorus as a fertilizer is due to the fact that low phosphate levels constitute a very serious limitation to plant growth. This is also true for aquatic systems, in which high phosphate levels may boost microbial and plant growth and lead to eutrophication phenomena.

Nowadays, the largest depositions of phosphorus in aquatic ecosystems are mainly due to anthropogenic activities and less to natural processes. The deposition of agricultural phosphorus-rich fertilizers, the disposal of untreated municipal wastewater as well as runoffs of livestock waste are the most important sources of phosphorus release into the aquatic environment. In the case of municipal wastewater, estimated phosphorus loads are at 0.6 kg/kg of human waste/year, 0.3 kg/kg of laundry detergents/year and 0.1 kg/kg of household detergents and other cleaners/year (Sedlak, 1991). Phosphorus in aqueous systems can be distinguished as soluble or insoluble according to its physical form, and as organic or inorganic according to its chemical state. Inorganic phosphorus is almost always in the form of soluble phosphorus, including orthophosphates and polyphosphates (Tarayre et al., 2016; Li et al., 2021). In urban wastewater, it is found mainly in inorganic form as orthophosphate radicals (PO_4^{3-} , HPO_4^{2-} , H_2PO_4^+) and polyphosphate chains, with several reports indicating that over 80% of total phosphorus in wastewater is in inorganic form (Ge et al., 2015; Andrés et al., 2018; Carrillo et al., 2020). The form in which orthophosphates are found is pH dependant as shown in Figure 2.1, with HPO_4^{2-} and H_2PO_4^+ being the most relative species for the typical pH range of wastewaters.

The main sources of phosphorus in wastewater are human secretions and household detergents, with household detergents accounting for approximately 30-50% of the total phosphorus load. Industrial use of phosphorus is quite limited and as such, industrial wastewater contribute little to phosphorus loading. Some notable industrial contributors are the food, textile, fertilizer and detergent industries (Kroiss et al., 2011; Sengupta and Pandit, 2011). In urban wastewater, the phosphorus load per inhabitant usually ranges from 2.5 - 4.0 g/d.

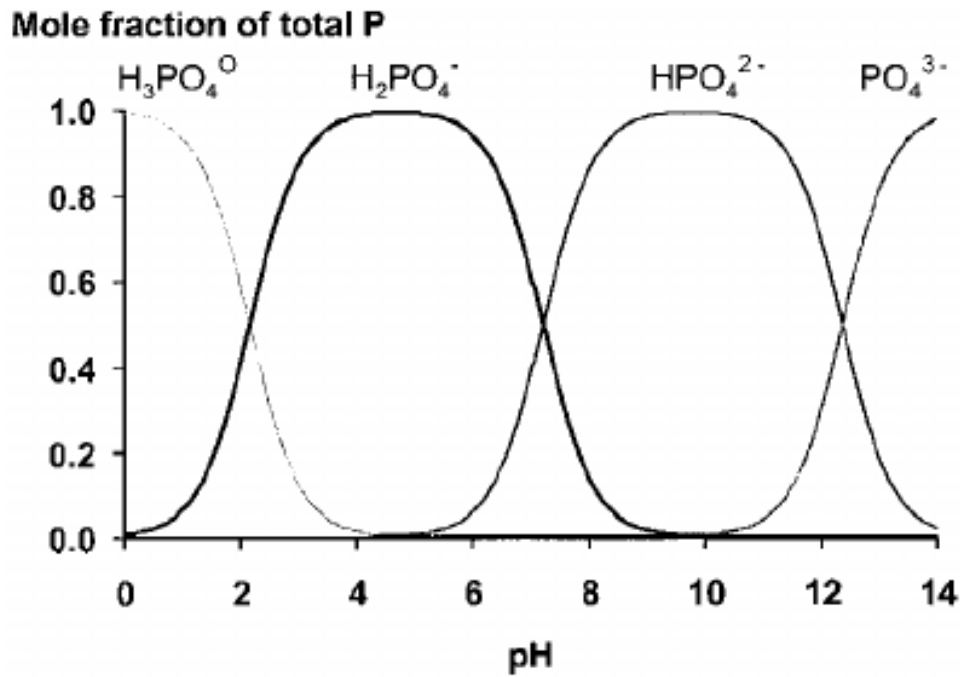


Figure 2.1. Speciation of orthophosphate ions expressed as mole fraction of total P in solution as a function of pH (Figure adapted from Hinsinger, 2001).

2.2 Phosphorus removal processes

2.2.1 Chemical removal

The use of chemical flocculants to remove phosphorus in WWTPs via precipitation began in Switzerland in the 1950s as a solution to the growing problem of eutrophication and is now widely used in many countries around the world (Morse et al., 1998). Chemical precipitation is essentially a physicochemical process, which involves the addition of a flocculant that reacts with the soluble inorganic phosphorus content of the effluent to form solid phosphorus compounds, which precipitate and are removed along with the excess sludge. The most common flocculants are lime ($\text{Ca}(\text{OH})_2$) and alum (Al) and ferrous (Fe) salts which are added in the form of chlorides or sulphates (Morse et al., 1998; Li et al., 2021). The effectiveness of this method depends on the type of flocculant, the pH of the wastewater, as well as mixing conditions (Thistleton et al., 2001). Chemical precipitation is the most commonly used method for phosphorus removal and more than 90% of the phosphorus content of the wastewater can be removed this way (Thistleton et al., 2001).

The addition of chemical flocculants to the wastewater may be carried out at three stages of the overall treatment process and as such, chemical removal of phosphorus is distinguished into removal via pre-precipitation, removal via simultaneous precipitation and removal via post-precipitation. In the pre-precipitation process, chemicals are added to the primary sedimentation tank and the phosphorus precipitate is removed along with the primary sludge. During simultaneous precipitation, chemicals are added to the biological reactor and the sediments are removed along with the secondary sludge. Finally, the post-precipitation method relies on the addition of chemicals after secondary clarification, with the precipitates being removed in a separate sedimentation tank or sand filters (Morse et al., 1998). The degree of phosphorus removal depends on the point at which the chemicals are added, with 70-90% removal achieved

via pre-precipitation, 80-95% removal achieved via simultaneous precipitation, and approximately 95% removal achieved via post-precipitation. The addition of chemical flocculants is preferably done at points of intense mixing conditions to achieve a uniform dispersion throughout the liquid. In the case of pre-precipitation, chemicals may be added to the pumping station or the flow measuring configurations in open channels.

Phosphorus removal by pre-precipitation (Figure 2.2) has the advantage of assisting the settling of suspended solids and may be combined with simultaneous precipitation for a higher degree of removal. However, sewage in the primary treatment stage contains significant amounts of polyphosphates and organic phosphorus that need to be hydrolyzed prior to chemical removal. As such, greater quantities of flocculants are required for effective removal compared to the requirements of secondary or tertiary treatment. The addition of flocculants during biological treatment, in addition to being more economic with chemical usage, has the added advantage of assisting secondary clarification, thereby improving the quality of the treated effluent. One disadvantage of this method is the lack of intense mixing points in the biological reactors for the effective dispersion of the flocculant. When significantly low total phosphorus concentrations (<1 mg/L) are demanded for the treated effluent, it is recommended that secondary precipitation is combined by pre-precipitation or followed by post-precipitation. While significant phosphorus removal may be achieved by post-precipitation, this method is generally not preferred due to the formation of a tertiary sludge (Morse et al., 1998).

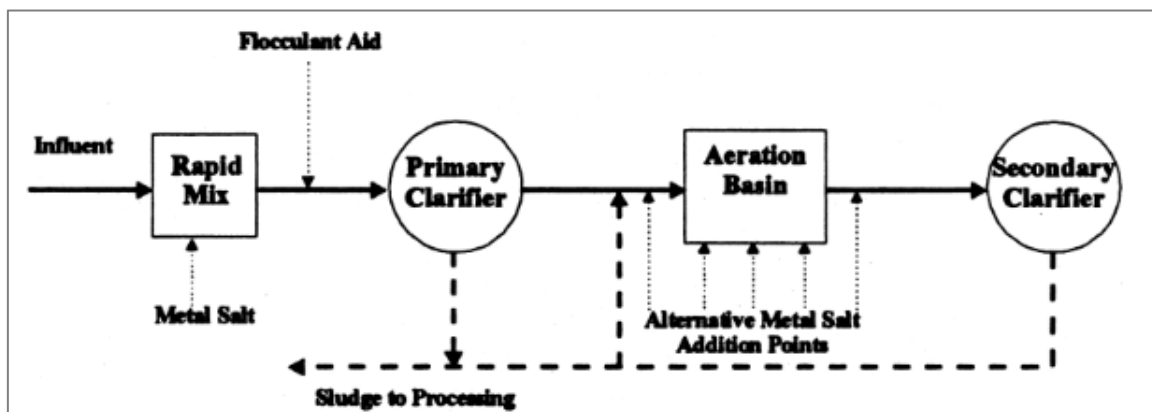
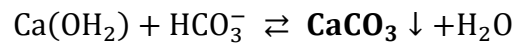


Figure 2.2. Schematic diagram of chemical precipitation applied during primary and secondary treatment (adapted from Morse et al., 1998).

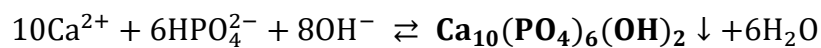
In general, chemical precipitation is a commonly used, cost effective method for phosphorus removal which can be easily applied to existing WWTPs and achieve phosphorus concentrations in treated effluents below 1 mg/L (Morse et al., 1998; Wilfert et al., 2015). However, the associated cost of this method is high compared to biological phosphorus removal, due to large quantities of chemicals that are demanded, while it may also lead to the production of pollutants, such as chloride and sulphate ions. In addition, it also requires the disposal of the chemical sludge that is generated (Altundoğan and Tümen, 2002; Xia et al., 2021). In the case of pre-precipitation, the addition of chemicals may increase primary sludge production by 50-100%, while the addition of flocculants during secondary treatment may increase the excess sludge by 30-40%. As a result, the burden of sludge treatment and disposal processes increases with consequent financial and environmental burden (Johansson, 1994).

Chemical precipitation of phosphorus with calcium hydroxide (slaked lime)

Chemical precipitation with calcium hydroxide was the first applied precipitation method, with which up to 90-95% of phosphorus may be removed. According to this method, $\text{Ca}(\text{OH})_2$ reacts with soluble orthophosphates (HPO_4^{2-}) for the formation of insoluble calcium phosphate compounds, such as hydroxyapatite (Ramasahayam et al., 2014). Calcium hydroxide reacts with the effluent's alkalinity (HCO_3^-) to form calcium carbonate precipitates, respectively, which is removed from solution:



The consumption of alkalinity results in a rise in pH that assists the reaction of the excess calcium ions with orthophosphates according to the following reaction:

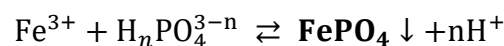
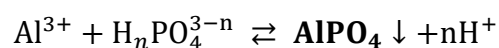


The higher the pH, the lower the solubility of the calcium phosphate compounds and therefore the better the precipitation and removal of phosphorus. In general, in order to achieve high phosphorus removal, the pH must be greater than 10 (Li et al., 2021). Due to the significant increase of pH, the addition of calcium hydroxide is preferably carried out prior to the biological stage, as high pH creates favorable conditions for the nitrification processes.

Calcium hydroxide used to be one of the main chemicals utilized for the removal of phosphorus, but is no longer used to a significant extent. Due to its reaction with the alkalinity of the wastewater, the required chemical dosage is generally independent of the phosphorus content and mainly depends on the alkalinity of the effluent. As such, the required dose is determined to be approximately equal to 1.5 times the alkalinity of the wastewater (as mg CaCO_3/L), which is tantamount to increased treatment costs. In addition, this method results in an increased production of chemical sludge, while there are also problems regarding the handling of chemicals as well as the operation and maintenance of the related distribution equipment (Hruschka, 1980). Also, the effective removal of phosphorus requires significantly high pH values (with the optimum pH value of 11) which may be unsuitable for the subsequent biological processes.

Chemical precipitation with alum and ferrous salts

Chemical precipitation with alum or ferrous flocculants relies on the reaction of the dissolved aluminum and iron ions with orthophosphates for the formation of insoluble phosphorus compounds, as described by the following reactions:



The reactions above are influenced by a number of factors such as the pH and alkalinity of the effluent, as well as the many competing reactions that occur. As such, the required dosage may not be estimated by the stoichiometry of said reactions but is instead determined by scale experiments. Figure 2.3 displays the equilibrium of the insoluble AlPO_4 and FePO_4 compounds with regard to pH. The constant lines indicate the concentration of the residual soluble phosphate (Metcalf and Eddy, 2003). In order to maximize phosphorus removal, the optimum

pH range for the alum and ferrous salts are 6-7 and 5-5.5, respectively. Although it is a simple process that achieves good phosphorus removal, the large influence of pH results in increased operating costs (Li et al., 2021).

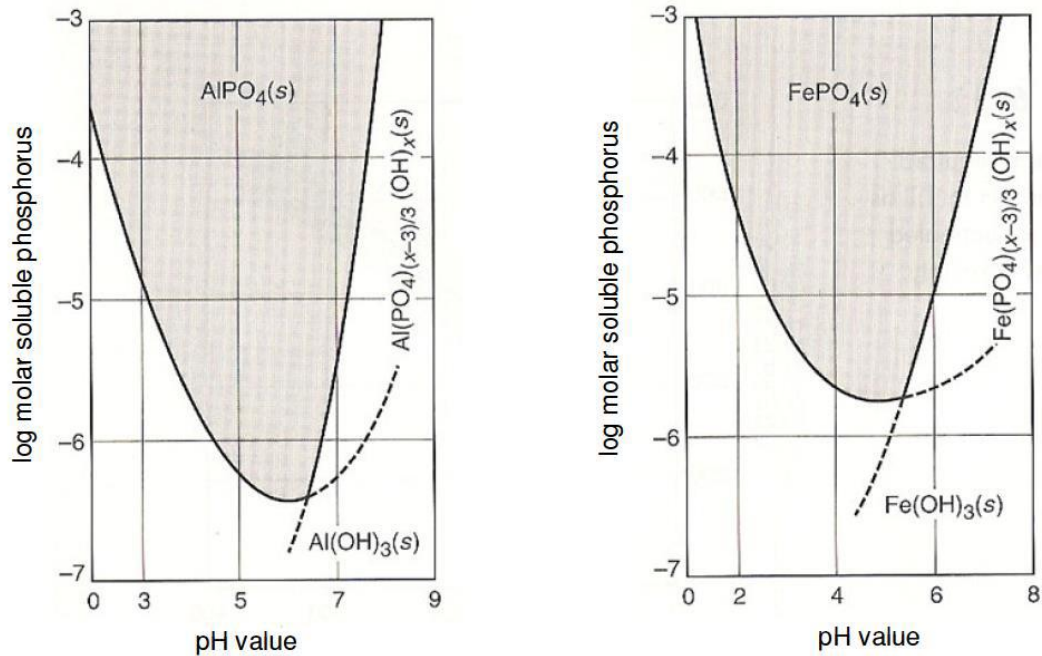


Figure 2.3. Alum and ferrous phosphate concentrations in equilibrium with soluble phosphate (adapted from Metcalf & Eddy, 2003).

In general, the ratio of the amount of flocculant required to the amount of phosphorus to be removed increases as lower phosphorus concentrations in the final effluent are demanded (Figure 2.4). As shown in Figure 2.4, two areas may be distinguished depending on the required concentration of soluble phosphorus in the treated wastewater: the stoichiometric area and the equilibrium area. The stoichiometric region is observed when relatively high phosphorus concentrations are accepted in the treated effluent and phosphorus removal is directly proportional to the amount of the added flocculant. The equilibrium area is observed when low phosphorus concentrations are demanded, where a significantly higher amount of flocculant is required for the necessary removal, an amount that increases exponentially for lower residual phosphorus concentrations.

Ferrous salts are not as effective as alum salts but are relatively inexpensive in comparison and react in a short time. Iron in the form of Fe (II) in particular has significant cost benefits, while in highly oxygenated environments, it can be converted to Fe (III), which forms a strong complex with phosphates (Ramasahayam et al., 2014; Wilfert et al., 2015).

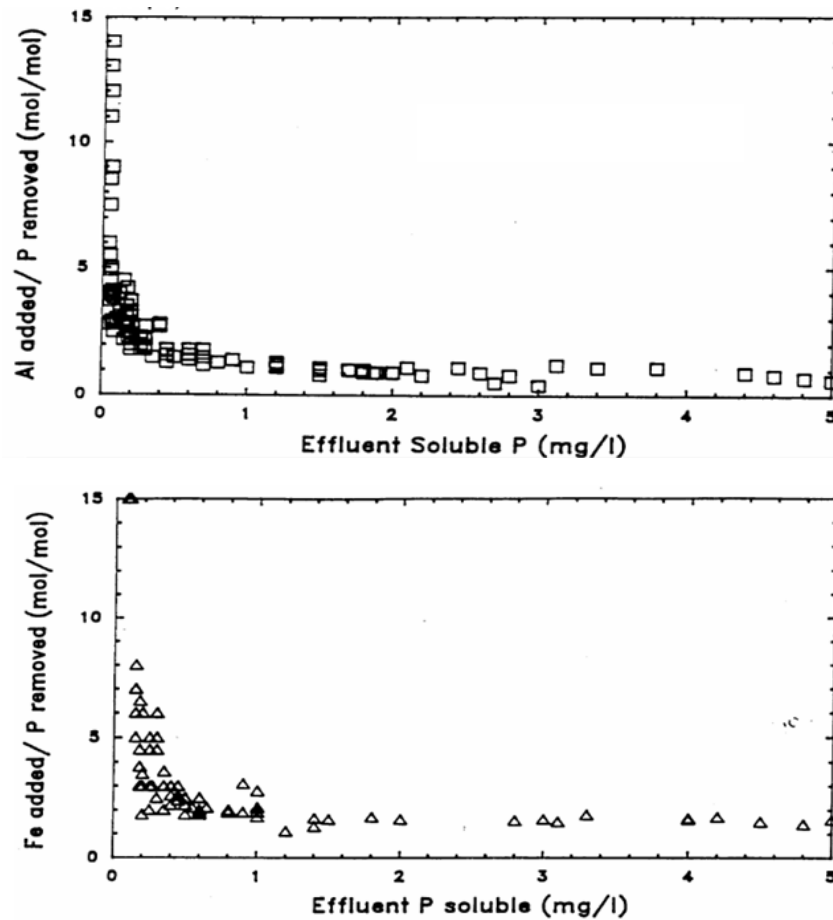


Figure 2.4. Required Al/P and Fe/P ratios for different concentrations of soluble phosphorus in the treated effluent (Adapted from Sedlak, 1991).

Chemical adsorption of phosphorus

Phosphorus removal via chemical adsorption is a method that has been gaining popularity over the past years. The process relies on the transfer of phosphorus from the liquid phase to an adsorbent with which it is removed from solution. The method is a sequence of two processes, a relatively fast, reversible adsorption process and a relatively slow, practically irreversible precipitation process (Arias et al., 2006). The mechanism of adsorption is either mechanical (i.e. Van der Waals) or to a lesser extent chemical. An important benefit of this method is the possibility of phosphorus recovery from the adsorbents via desorption (Ramasahayam et al., 2014).

Various simple materials, industrial by-products or cheap metals, such as quartz, slag, fly ash, activated carbon, etc. can be used as adsorbents (Xia et al., 2021). Extensive research regarding the potency of these materials is being performed and many researchers are working to develop modified adsorbents to improve phosphorus removal efficiency at a reduced cost and successful phosphorus recovery (Ramasahayam et al., 2014 ; Gu et al., 2021).

The use of fly ash in particular has been extensively studied in recent years due to its effectiveness as an adsorbent. Fly ash is a residue resulting from the combustion of coal in power plants. Its abundance and availability make it a cost-effective material for phosphorus removal. Ugurlu (1998) reported very high phosphorus removal (>99.8%) with the use of fly ash, and that

even relatively small amounts of fly ash resulted in significant removal. Arias et al. (2006) studied phosphorus adsorption on quartz particles with ferrous and alum hydroxide coatings. In both cases there was a high adsorption capacity for phosphorus, although the alum oxide particles achieved significantly greater phosphorus removal, providing an excellent material for a pre-adsorption system, which would act as a complementary filtration system for reducing phosphorus levels in wastewater. The use of slag has also been studied and, while having some capacity for phosphorus removal from wastewater, it is not as significant compared to other materials (Ramasahayam et al., 2014).

Adsorbents have the advantages of low cost, simple equipment requirements for their application and reduced sludge production. In addition, the materials used are readily available with a wide range of sources from which they can be obtained. However, to date phosphorus removal via adsorption has not proven very effective, while the cost of replacing the adsorbent is very high. Also, the regeneration process results in the production of an additional wastewater stream that requires treatment (Ugurlu, 1998; Li et al., 2021).

Ion exchange

Phosphorus removal via Ion exchange is a process in which phosphate ions replace flexible ions of a suitable ion exchanger (resin), which contains heavy organic matter, and are thus removed from solution. The immobilized particles of a metal cation form the exchange base, called the exchanger, into which selective phosphate nanoparticles (e.g., iron oxide) are placed (Zhao and Sengupta, 1998). Phosphate ions alternate between the effluent and the exchanger, providing simultaneous removal and recovery of phosphorus (Martin et al., 2009). The exchange capacity of the resin is relatively stable and remains high even after many regenerations (Li et al., 2021).

Several studies have shown that the pH of the solution plays an important role in the removal of phosphates and that a higher pH is beneficial for the removal of phosphorus. However, the presence of certain ions, such as Cl^- , CO_3^{2-} and SO_4^{2-} , negatively affects phosphorus removal (Li et al., 2021). Although the addition of phosphate nanoparticles in the resin theoretically causes the selection of phosphate anions over competing ions, such as sulphate or chloride, in practice, this is not easily achieved due to the relatively low abundance of phosphates in wastewater compared to that of the competing species (Bunce et al., 2018).

Ion exchange systems have the advantage of providing phosphorus recovery through post-processing. While high rates of phosphorus removal have been achieved at a laboratory scale, full-scale application has been limited due to the poor selectivity of phosphorus ions over other ions, pH sensitivity, low efficiency in the neutral pH range, and high operating costs. Additional problems are the high cost of the synthetic resin, the high cost of regeneration, the low regeneration efficiency and the high sensitivity of the resin to organic pollutants. As such, phosphorus removal via ion exchange is considered impractical (Zhao and Sengupta, 1998; Bunce et al., 2018; Li et al., 2021).

2.2.2 Enhanced Biological Phosphorus Removal (EBPR)

EBPR is a method that has been gaining ground in recent years (Nielsen et al., 2019). The method was first described in detail by James Barnard in South Africa in the 1970s (Barnard et al., 1976). The method relies on the selective growth of a particular microbial group that has the

capacity to take up and intracellularly store significant amounts of phosphorus, that are much higher than the typical metabolic requirements (Sperling, 2007). These organisms are known as Polyphosphate Accumulating Organisms (PAOs). While Ordinary Heterotrophic Organisms (OHOs) have a phosphorus content of 2% - 3%, PAOs can absorb phosphorus up to a percentage of 12% (Li et al., 2021).

The first documented research on EBPR was carried out by Levin & Shepiro (1965), who conducted full-scale experiments on activated sludge. They observed an increase in phosphorus when the biomass was subjected to anaerobic conditions and a decrease in phosphorus under aerobic conditions. In fact, the addition of organic substrate (urban wastewater) under anaerobic conditions favoured the following aerobic removal of phosphorus. The aerobic removal of phosphorus was greater than the anaerobic release, resulting in a clear removal of phosphorus from the urban wastewater.

The bacterial community originally thought to be responsible for EBPR was *Acinetobacter*, that include the genus *Tetrasphaera*, which has been observed in some WWTP facilities (Oehmen et al., 2010a). However, further research on the microbiology of these organisms has shown that they do not meet the necessary conditions and this activity is now attributed to Betaproteobacteria and more specifically the genus *Candidatus Accumulibacter phosphatis* (hereafter referenced as *Accumulibacter*) (Mino et al., 1998).

Under anaerobic conditions, PAOs can hydrolyze their intracellular polyphosphate chains, releasing phosphorus in the process and use the energy produced to take up Volatile Fatty Acids (VFAs) and store them intracellularly as polyhydroxyalkanoates (PHAs). Once in the presence of an electron acceptor, PAOs oxidize the stored PHAs, which serve as both the carbon and energy source for the uptake of phosphate and the reformation of their polyphosphate chains. As such, the inclusion of an anaerobic phase in which feed is made available prior to aerobic/anoxic conditions promotes the growth of PAOs since they have priority over OHOs in the utilization of carbon. With this, a PAO-enriched biomass is developed which may absorb a significant amount of phosphorus. Thus, phosphorous removal is achieved via the net removal of the enriched excess sludge.

In typical WWTPs, EBPR is achieved by including an anaerobic reactor at the start of the biological treatment processes. There, the recycled PAO-enriched sludge comes into contact with the influent wastewater which is rich in easily biodegradable organic matter (Carvalho et al., 2014a). The anaerobic hydraulic retention time should be such as to maximize the consumption of organic substrate by the polyphosphate bacteria. This also depends on the composition of the wastewater. If the wastewater contains high concentrations of volatile organic acids, then a short retention time is sufficient because the consumption of VFAs occurs at a very fast rate. However, if the effluent does not contain high concentrations of VFAs, then the required retention time and consequently the required volume of the anaerobic tank should be greater as to allow fermentation in the anaerobic zone and VFA production. In general, a retention time of 1.5 hours is considered sufficient even at temperatures as low as 13.6°C (Randall, 1992). Long anaerobic retention times (over 2.5 hours) should be avoided, as hydrolysis of the intracellular polyphosphate chains of PAOs will occur in order to provide necessary energy for cell maintenance rather than VFA uptake (Henze et al., 2008) have shown that anaerobic phosphorus release and COD removal follow first-order kinetics. It is therefore

recommended that the anaerobic tanks are designed to simulate a piston flow for the achievement of a high Food to Microorganisms (F: M) ratio at the tank inlet. An added bonus of this approach is the prevention of filamentous organism growth which is responsible for bulking problems in WWTPs.

Following the anaerobic uptake of COD, PAOs enter either an aerobic or an anoxic tank, depending on the WWTP's configuration (anaerobic/oxic system – anaerobic/anoxic/oxic system). Once in aerobic conditions, PAOs oxidize their stored PHAs and take up phosphorus for the replenishment of their polyphosphate chains. Some PAOs are also capable of using nitrate or nitrite as an electron acceptors (known as denitrifying polyphosphate accumulating organisms – DPAOs). As such, in anaerobic/anoxic/oxic systems that aim for the biological removal of both phosphorus and nitrogen, phosphorus may be removed via denitrification. PAOs that do not possess the capacity to utilize nitrate, may continue to take up carbon during the anoxic phase and remove phosphorus in the subsequent aerobic phase. Figure 2.5 presents a simplified schematic of the anaerobic/oxic and anaerobic/anoxic/oxic systems (Henze et al., 2008). Due to the presence of nitrate in the recycled sludge, it is common practice to include a secondary anoxic tank for its removal via endogenous respiration in order to ensure proper anaerobic conditions in the anaerobic tank. More detailed EBPR configurations are discussed in section 2.3.

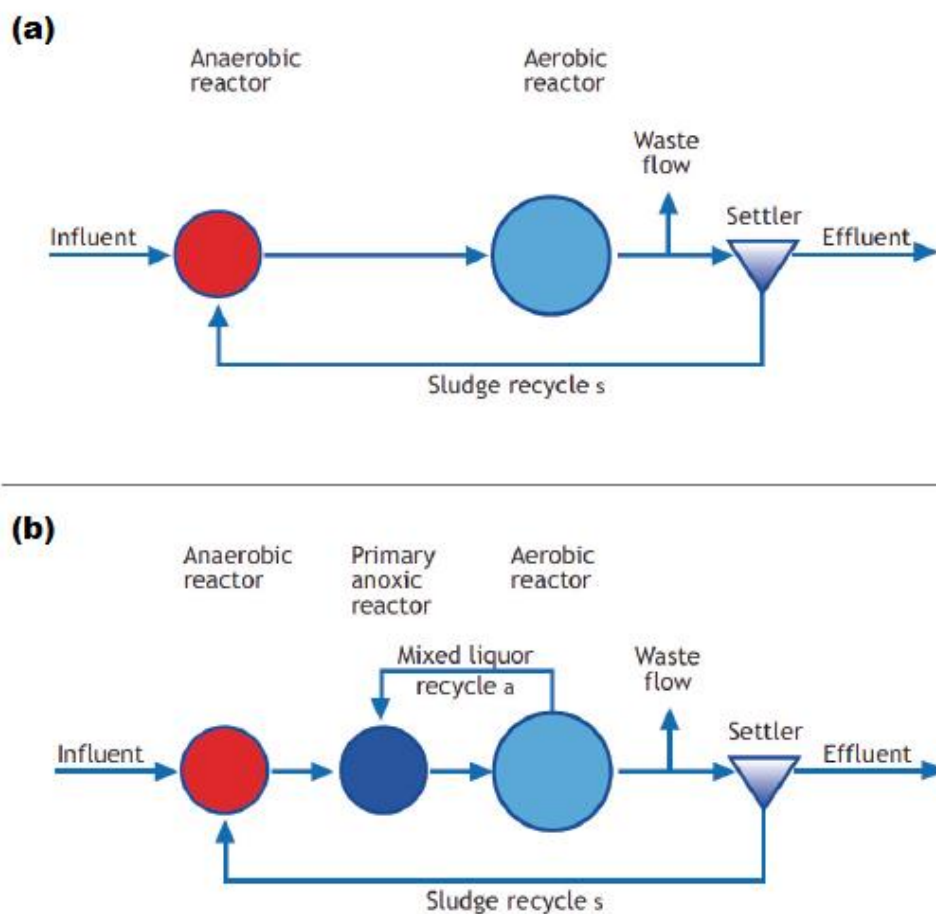


Figure 2.5. Schematic representations of the anaerobic/oxic system (a) and the anaerobic/anoxic/oxic system (b) (Figure adapted from Henze et al., 2008).

When applied correctly, EBPR is an effective, relatively inexpensive and environmentally friendly method, and is considered to be the most sustainable technology in wastewater treatment to meet increasingly stringent nutrient rejection limits (Guerrero et al., 2011; Zeng et al., 2017), with removal rates reaching 80% -90% (Ramasahayam et al., 2014; Xu et al., 2018). Its benefits over chemical phosphorus removal technologies are even more apparent when tertiary treatment is required to meet extremely low effluent limits (Li et al., 2019). Among its advantages are the significantly lower operating costs, the reduced sludge production, the elimination of the salinity problems of the wastewater that occur during the chemical removal of phosphorus and the higher reuse potential of the produced sludge (Blackall et al., 2002). In addition, this method is very popular, as the demand for achieving low phosphorus concentrations in the effluent without the addition of chemicals, and consequently the formation of chemical precipitates, is increasing (Nielsen et al., 2019). The excess sludge obtained by this method is rich in phosphorus that may undergo anaerobic digestion to produce a waste with a high concentration of soluble phosphorus, suitable for use as a fertilizer (Petriglieri et al., 2022). Compared to chemical phosphorus removal, the biological method is a good choice when high levels of phosphorus removal are desired along with phosphorus recovery from wastewater, mainly because phosphorus is a limited, non-renewable, highly useful resource (Acevedo et al., 2017; Nielsen et al., 2019).

However, EBPR is not without problems, as failures and disturbances can occur, even in conditions seemingly ideal for its implementation, while there are fluctuations in its performance (He and McMahon, 2011 ; Bunce et al., 2018). Such cases may lead to the deterioration of the efficiency of the method, causing prolonged periods of insufficient phosphorus removal, and a failure to conform to the corresponding effluent limits. Some examples of the conditions that may disrupt EBPR are heavy rainfall, excessive nitrate recirculation to the anaerobic reactor, or a lack of nutrients (Oehmen et al., 2007). Other factors that have been observed to affect the efficiency and stability of the method are the carbon to phosphorus ratio, the substrate type, the solid residence time (SRT), the hydraulic residence time (HRT), temperature and pH (Li et al., 2019). Also, the existence of another group of microorganisms that compete with PAOs for intracellular storage of organic food, glycogen accumulating organisms (GAOs), is another cause of failure. GAOs metabolize fatty acids or other carbon compounds in a manner similar to PAOs, but do not bind phosphorus, and therefore can cause a reduction in the microbial community of PAOs with consequent reduced phosphorus removal (Bunce et al., 2018).

In general, the main challenge posed by the simultaneous removal of nitrogen and phosphorus via biological methods concerns the adequacy of the carbon source, as PAOs, GAOs and OHOs compete for substrate from municipal wastewater, that is generally considered low in organic content (Kapagiannidis et al., 2013; Wang et al., 2019). Particularly in cases where the wastewater is characterized by a low C/N ratio (where there is an increased carbon demand for denitrification purposes), the addition of an external readily biodegradable carbon source at the anaerobic stage may be required. Since EBPR may be unreliable at times due to periodic disruptions, phosphorus removal during these periods may be supplemented with chemical addition.

2.3 Configurations implementing EBPR

From its humble beginnings in the 1970's, biological nutrient removal has come a long way and is still being optimized to this day. Biological phosphorus removal was pioneered by James L.

Barnard who is recognized for developing the BARDENPHO Process (BARNard DENitrification and PHOSphorus removal), as well as the Phoredox (AO and A²O) system. These processes have since been modified to a variety of extents and applied with various degrees of efficiency. In their work, Henze et al., (2008) gathered and presented the most commonly applied EBPR configurations, which are discussed in this section.

Phoredox or anaerobic/oxic (A/O) system

The A/O system (Figure 2.6) is the simplest configuration for the biological removal of phosphorus. The method relies on the implementation of an anaerobic reactor which receives the influent and the recycled sludge, upstream of an aerobic reactor in which carbon and phosphorus are removed. This configuration does not achieve biological removal of nitrogen via nitrification/denitrification. Instead, the sludge age and aerobic tank are designed and controlled to prevent nitrification. While this configuration has the benefit of being operated at low sludge retention times (as low as 2-3 days), the requirements for nitrogen removal prevent its implementation (Henze et al., 2008). In addition, there have been reports of difficulties in preventing nitrification at temperatures above 20°C, even at sludge ages as low as 3 days (Burke et al., 1986 ; Henze et al., 2008). Consequently, the recirculation of nitrate and nitrite to the anaerobic tank along with the recycled sludge could have an adverse effect on the selective growth of PAOs and EBPR.

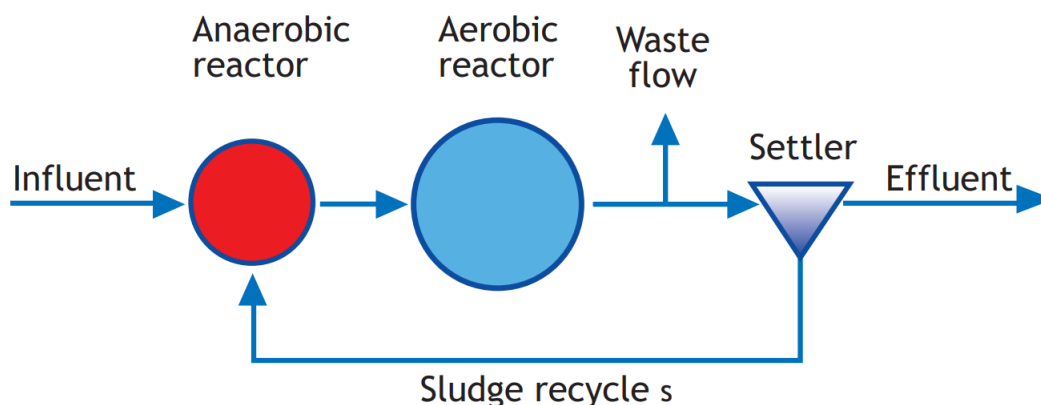


Figure 2.6. Schematic of Phoredox (A/O) configuration for EBPR (Figure adapted from Henze et al., 2008).

Anaerobic/anoxic/oxic (A²O) system

Also known as the 3-stage Bardenpho process, this method is similar to the A/O system, in that it relies on a sequence of anaerobic and aerobic zones for the selective growth of PAOs, where sludge is recycled to the anaerobic tank which receives the carbon-rich influent. The key difference is that this configuration includes an anoxic zone, to which the mixed liquor from the aerobic tank is recycled (Figure 2.7). As such, nitrogen removal via nitrification/denitrification is achieved alongside EBPR. Due to denitrification taking place, nitrate and nitrite concentrations in the sludge that is recycled to the anaerobic tank are relatively low. However, these quantities may be sufficient in adversely affecting EBPR, as the VFA content of the influent may be utilized by OHOs, reducing its availability for PAOs (Henze et al., 2008).

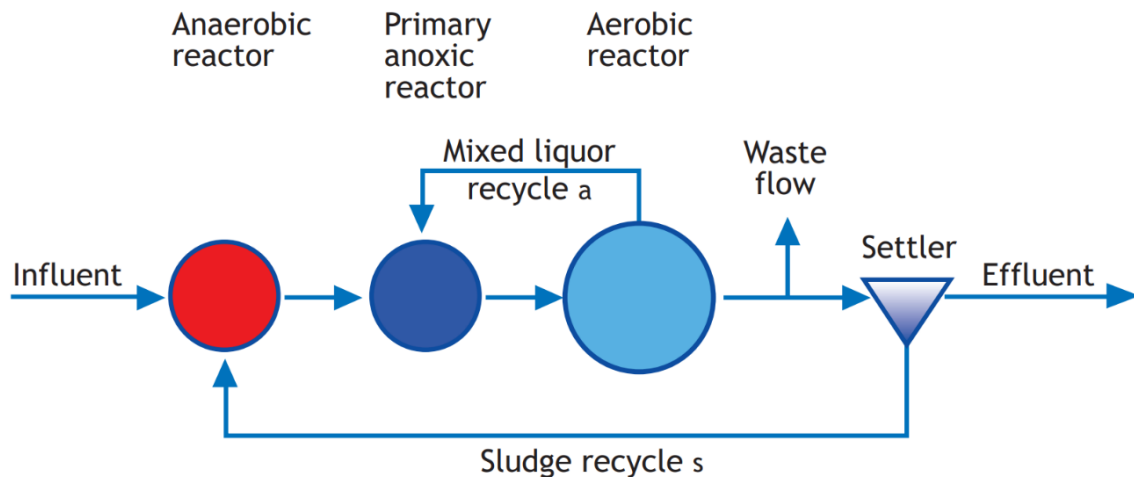


Figure 2.7. Schematic of the 3-stage Bardenpho configuration (A^2O) for EBPR (Figure adapted from Henze et al., 2008).

A modified configuration of the A^2O system is the 5-stage Bardenpho system, also known as the $(A^2O)^2$ system, which includes an additional anoxic tank and a re-aeration reactor (Figure 2.8). This method achieves lower nitrogen concentrations in the treated effluent while also ensuring minimum recirculation of NO_x to the anaerobic tank. As limited biodegradable carbon will remain available in the secondary anoxic reactor, denitrification at this stage will mostly occur via endogenous respiration (which requires an increased reactor volume).

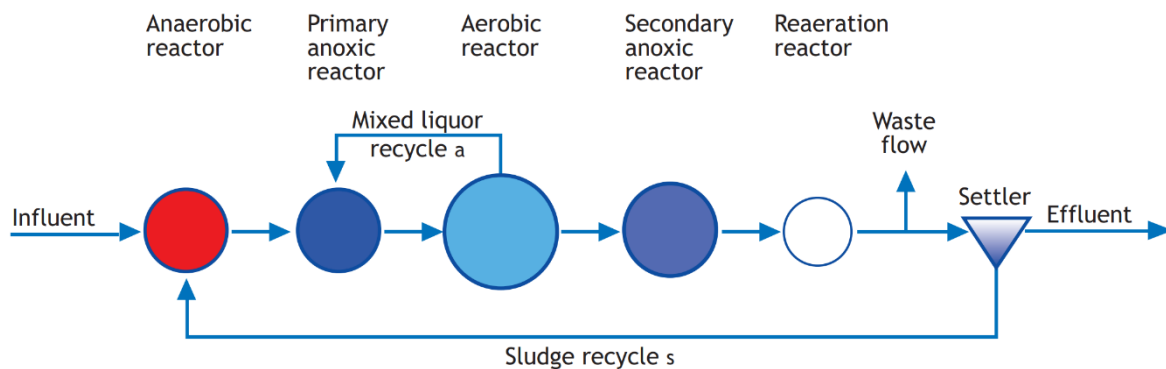


Figure 2.8: Schematic of the 5-stage Bardenpho configuration for EBPR (Figure adapted from Henze et al., 2008).

Johannesburg (JHB) system

The repositioning of the secondary anoxic zone of the 5-stage Bardenpho system from the mainstream flow to the underflow recycle stream (which eliminates the necessity for a re-aeration tank), results in a 4-stage system that has become known as the Johannesburg (JHB) system (Figure 2.9). The repositioning of the secondary anoxic reactor to the underflow stream allows lesser denitrification requirement (and consequently a lower carbon demand), since, contrary to the 5-stage Bardenpho system where nitrate and nitrite need to be removed from the entirety of the effluent, their removal is only required for the recycled stream. This, in addition with the

increased density of the recycled stream, allows decreased reactor volumes for secondary denitrification (Henze et al., 2008). Denitrification in the secondary anoxic zone takes place via endogenous respiration and the effective removal of NO_x is dependent on the endogenous respiration rate, the sludge thickening degree and the retention time. In general, approximately 10 mg/L of nitrate can be removed this way at varying retention times of 0.5–2 hours (Izadi et al., 2020).

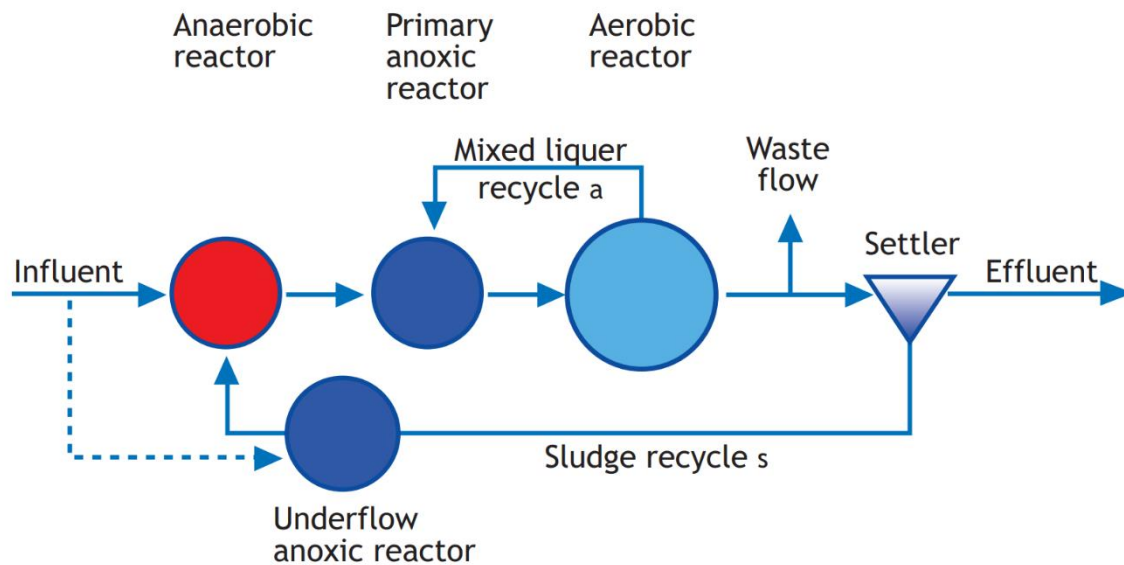


Figure 2.9. Schematic of the Johannesburg (JHB) configuration for EBPR (Figure adapted from Henze et al., 2008).

University of Cape Town (UCT) system

The UCT system is a development of the A^2/O configuration, in which the returned activated sludge (RAS) is recycled to the primary anoxic reactor instead of the anaerobic zone (Figure 2.10). A further recycle draws mixed liquor from the primary anoxic reactor and discharges it to the anaerobic reactor, while mixed liquor is also recycled from the aerobic tank to the anoxic tank. With appropriate internal recirculation of the mixed liquor from the aerobic to the anoxic zone, nitrate concentration in the anoxic reactor can be controlled to be negligible. As such, no nitrate is recycled back to the anaerobic reactor, allowing the maintenance of proper anaerobic conditions in the tank, regardless of the nitrate concentration in the treated effluent. The configuration prevents the consumption of the influent's readily biodegradable COD by OHOs, giving priority for its utilization to PAOs.

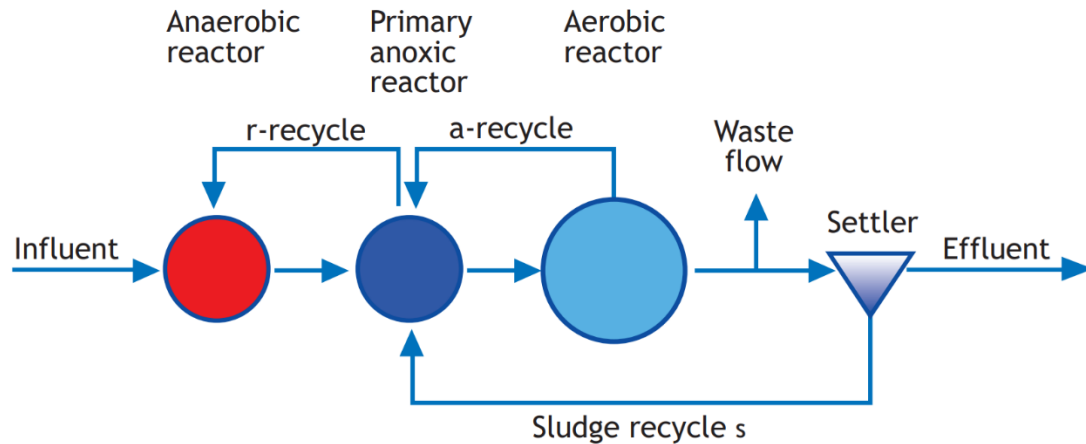


Figure 2.10: Schematic of the UCT configuration for EBPR (Figure adapted from Henze et al., 2008).

Certain variations of the UCT system have been proposed, such as the Virginia Initiative Plant (VIP) (Daigger et al., 1987), which mostly concern the use of multiple series of mixed reactors and operation at specific SRTs. The main modification however that results in what is known as the modified UCT system, is the separation of the anoxic zone into two compartments (Figure 2.11). In this system, the return activated sludge is recycled to the first anoxic compartment while the mixed liquor from the aerobic zone is recycled to the second compartment. The anaerobic zone receives mixed liquor from the first anoxic compartment where the little nitrate that is returned with the sludge is rapidly reduced. As such, the anaerobic zone is protected to a greater extent from the recirculation of nitrate.

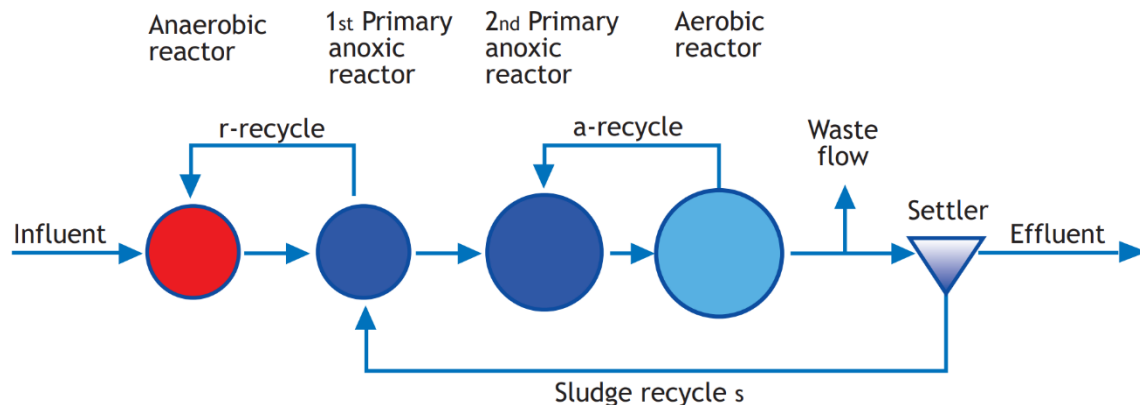


Figure 2.11. Schematic of the modified UCT configuration for EBPR (Figure adapted from Henze et al., 2008).

While the UCT processes achieve good EBPR, a disadvantage of this method is its requirement for large additional internal recycling systems (more so in the case of the modified UTC process) and also large anaerobic reactor volumes (Metcalf and Eddy, 2003).

Biological-chemical phosphorus removal (BCFS system)

The BCFS system is a further adaptation of the modified UCT system that was developed to support EBPR with phosphate stripping and potential recovery in the main line, optimizing the sludge settling properties and the control of nitrogen removal (Henze et al., 2008). In this system, a third recycle is added from the aerobic zone to the first anoxic compartment, in order to maximise denitrification and provide the option of aerating the second anoxic compartment during peak flows (Figure 2.12). Biological phosphorus removal can be supplemented by addition of precipitants to the anaerobic tank where phosphate concentrations are high (though dosing should be performed carefully as PAOs require the availability of phosphate in the subsequent zones). In the BCFS process, a small baffle is placed at the end of a plug flow anaerobic tank. The sludge locally settles back into the anaerobic tank and a clear supernatant can be withdrawn for phosphate precipitation. This way, the accumulation of chemical sludge in the mixed liquor can be prevented, while phosphorus can then be recovered (Barat and van Loosdrecht, 2006 ; Henze et al., 2008).

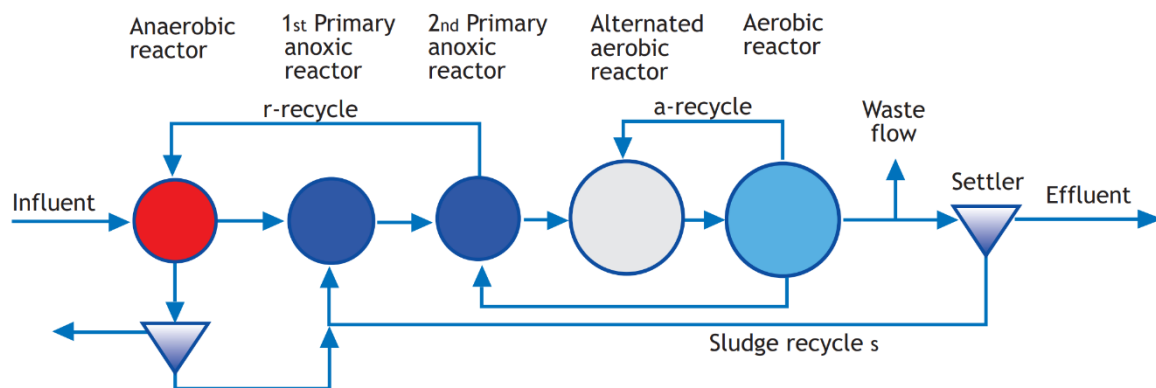


Figure 2.12. Schematic of the BCFS configuration for EBPR (Figure adapted from Henze et al., 2008).

PhoStrip system

The PhoStrip system is a side-stream process that combines chemical and biological removal of phosphorus. The process consists of an aerobic reactor with a clarifier, from which a side-stream of the underflow is driven to an anaerobic stripping tank, where the sludge settles and phosphorus is released (Figure 2.13). The stripped sludge is returned to the aerobic tank while the supernatant undergoes chemical precipitation for the removal of P in a precipitation tank. The supernatant from this tank is then returned to either the influent or the effluent flow (Henze et al., 2008).

While the original PhoStrip system was not designed to remove nitrogen via nitrification/denitrification, it may be modified to include an anoxic tank upstream of the aerobic reactor with internal recycling from the aerobic tank to the anoxic tank.

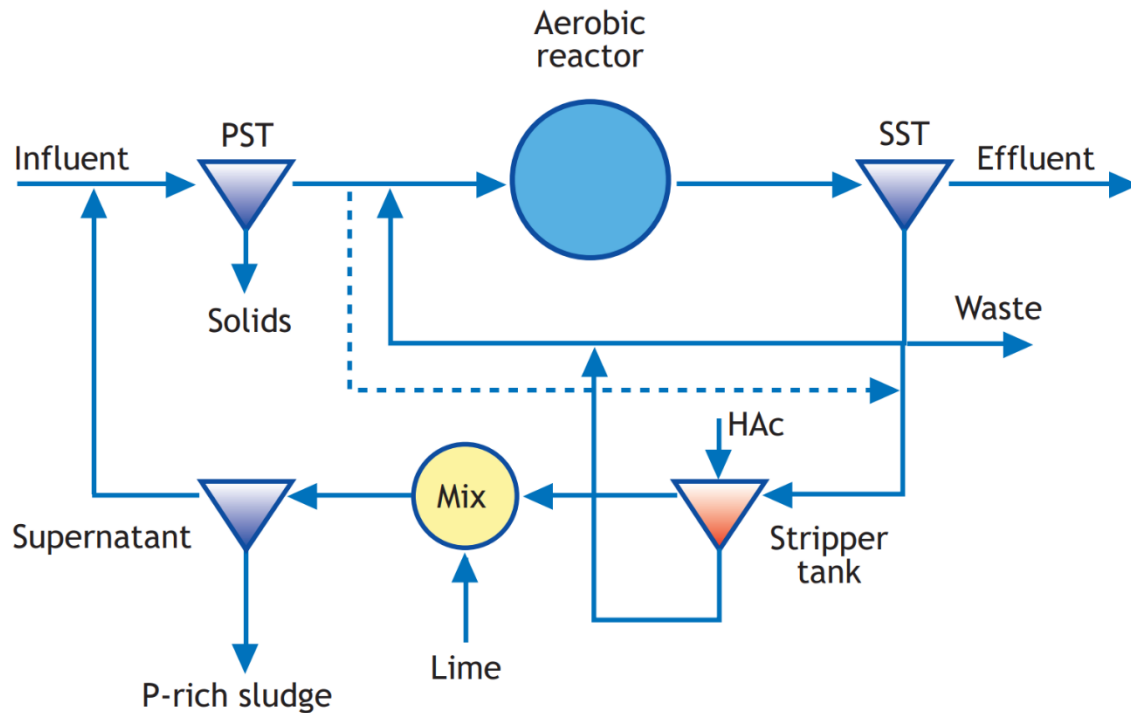


Figure 2.13. Schematic of the PhoStrip configuration for EBPR (Figure adapted from Henze et al., 2008).

EBPR with sequential batch reactor (SBR) systems.

The SBR system is essentially a fill and draw activated sludge system where all biological processes, along with sludge settling and decanting, occur in a single reactor at different timeframes. A typical SBR cycle begins with a filling period, where influent is introduced to the reactor. The application of EBPR requires an initial anaerobic phase under mixing conditions for a duration that is comparable to the anaerobic HRT in continuous flow systems. This is followed by a period of aeration, during which PAOs take up phosphorus. If nitrogen removal is required, the aerobic phase is followed by an anoxic period for the removal of nitrate and nitrite. The sludge is then allowed to settle and the effluent is drawn.

While good EBPR may be achieved with SBR systems, a downside of this configuration may present itself when nitrogen removal is required. This is due to the fact that, unlike conventional continuous flow systems which have the option of placing the anoxic zone upstream of the aerobic zone, due to the nature of the SBR configuration, the anoxic phase may only follow the aerobic phase. As such, the biodegradable COD content of the influent may be significantly reduced during aeration, leaving less available for the needs of denitrification. As such, the addition of an external carbon source may be required for sufficient nitrogen removal. Furthermore, the capacity of PAOs to denitrify becomes of greater importance, as the anoxic phase is the last stage prior to effluent withdrawal. This is because regardless of the performance of PAOs during the aerobic phase, an inability to utilize nitrate and nitrite in the subsequent anoxic phase could lead to the release of phosphorus, which would end up in the effluent. This, in addition to the possible need of an external carbon source for denitrification could prove

extremely problematic. As such, the successful application of EBPR in SBR systems relies heavily on the capacity of PAOs for anoxic P-removal.

A benefit of the SBR system is the possibility for treating influents with a high nitrogen content via the short-cut nitrification/denitrification pathway. This is achieved by NOB inhibition due to high ammonium concentrations (something that may not be applied in continuous flow systems). As such, the SBR configuration is an attractive option for the side-stream treatment of influents with high ammonium concentrations (such as reject water from sludge treatment processes), as nitrogen may be removed at a lower oxygen and carbon demand.

2.4 Microbial community in EBPR systems

2.4.1 PAOs

Polyphosphate accumulating organisms (PAOs) are the microbial group that is responsible for the biological removal of phosphorus. As their name suggests, these microorganisms have the capacity to accumulate significant amounts of polyphosphate chains within their cells. They may be classified as heterotrophic chemosynthetic organisms, i.e. use organic compounds as a carbon source and as an electron donor and receive the necessary energy from chemical reactions.

Unlike most microorganisms, PAOs have the ability to take up simple carbon compounds, without the presence of an external electron acceptor (e.g. oxygen or nitrate/nitrite), and store them intracellularly (Mino et al., 1998; Seviour et al., 2003). Under anaerobic conditions PAOs take up dissolved carbon in the form of volatile fatty acids (VFAs) and store them as polyhydroxyalkanoates (PHAs). The energy for this transfer and conversion as well as for cell maintenance is provided by the hydrolysis of their intracellular polyphosphate chains (Mino et al., 1998). During this reaction, adenosine-tri-phosphate (ATP) is converted to di-phosphate (ADP) and phosphate is released in the liquid phase (Mino et al., 1998 ; Panswad et al., 2003). Although it has been suggested that the organic compounds are transported within the cell via passive diffusion, the predominant view is the active transport with energy offered by the hydrolysis of poly-phosphate chains mentioned above. However, part of the energy is provided via glycolysis (hydrolysis of glycogen). The mechanisms that have been proposed for the hydrolysis of glycogen by PAOs are the Entner-Doudoroff (ED) pathway and the Embden, Meyerhof and Parnas (EMP) pathway (Oehmen et al., 2007), with many references supporting the involvement of both methods (Hesselmann, 2000; Acevedo et al., 2012; Tarayre et al., 2016). It should be noted that the production of ATP via the ED pathway is lower compared to its production through the EMP pathway. However, the determining factor for energy production is the hydrolysis of the polyphosphate chains, making the difference in ATP production between the two pathways of lesser importance (Oehmen et al., 2010).

PHA synthesis requires the production of a reducing agent in the form of Nicotinamide Adenine Dinucleotide (NADH) (Seviour et al., 2003). PAOs mainly use glycolysis for NADH production (Mino et al., 1994). However, when they are low in polyphosphate, glycolysis is used to produce the ATP required for the synthesis of PHAs. It is possible that using the glycolysis pathway to meet ATP needs generates excess NADH, which is used to convert acetyl-CoA and propionyl-CoA to PHAs (Acevedo et al., 2012). Glycolysis was generally considered to be the source of the reducing power, but now there are many references to the Krebs cycle (or TCA cycle) in the role of this source (Comeau et al., 1986; Brdjanovic et al., 1998), while others argue that both

glycolysis and the Krebs cycle (and the glyoxylic acid pathway) are active in the anaerobic metabolism of PAOs (Schuler et al., 2003; He et al., 2011). Zhou et al. (2009) reported that in cases of limited glycogen, PAOs were able to use the Krebs cycle for the production of NADH via increased hydrolysis of polyphosphate chains to compensate for the additional ATP requirements. The involvement of the Krebs cycle depends on the availability of degradable glycogen.

Mino et al. (1998) proposed the following mechanism for the polymerization of the absorbed VFAs (their conversion to PHAs): The hydrolysis of the intracellular polyphosphate chains and stored glycogen provide the energy needed for the uptake of VFAs and their transport within the cell. The compounds are then converted to acetyl-CoA and Propionyl-CoA coenzymes, which are the precursors of PHAs. These conversions are carried out via glycolysis and by the electro-propionate method respectively. Glycolysis, as mentioned above, provides the redox potential, while the electro-propionate method consumes it. However, as some carbon dioxide release is observed, the potential contribution of the TCA cycle cannot be neglected. Further studies have suggested that the TCA cycle (or part of it) definitely contributes to the production of redox potential (Oehmen et al., 2007). Figure 2.14 displays a schematic of the mechanism proposed by Mino et al. (1998).

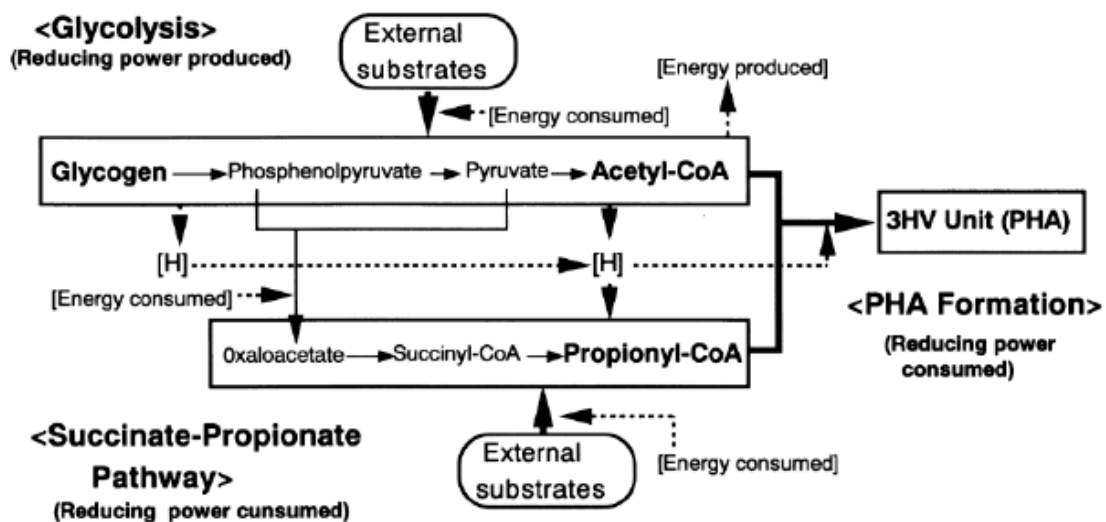


Figure 2.14. Anaerobic conversion of VFAs to PHAs (Figure adapted from Mino et al., 1998).

Under aerobic conditions PAOs oxidize their stored PHAs, which are both the source of carbon and energy for a range of processes, such as cell growth and maintenance, glycogen replenishment, orthophosphate uptake, and polyphosphate chain formation (Mino et al., 1998; Filipe et al., 2001; Lopez-Vazquez et al., 2009b; Pijuan et al., 2009). The mechanism for the aerobic metabolism of PAOs is the Krebs cycle (TCA cycle) (Oehmen et al., 2007).

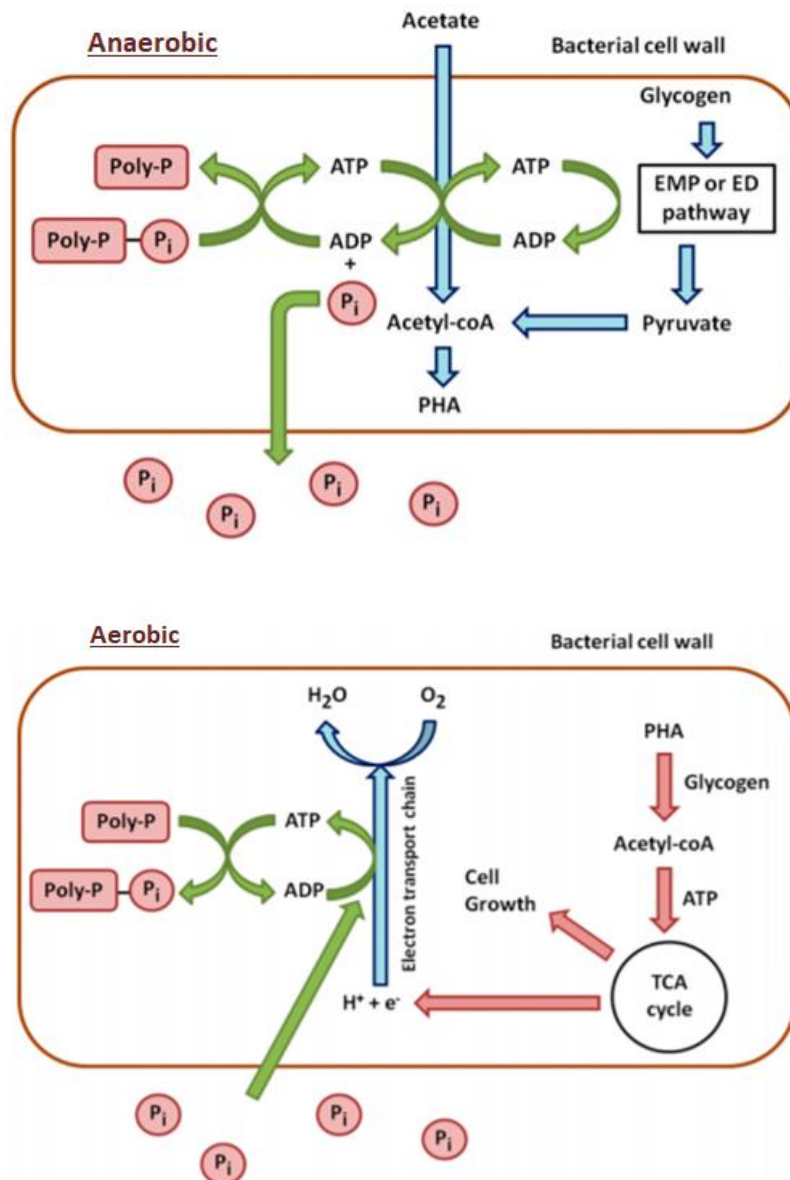


Figure 2.15. Anaerobic and aerobic metabolism of PAOs (Figure adapted from Tarayre et al., 2016)

Some PAOs are also capable of using nitrate or nitrite as electron acceptors, meaning they can remove phosphorus via denitrification. These are commonly referred to as denitrifying polyphosphate accumulating organisms (DPAOs) and their existence has been reported since the late 1980s (Comeau et al., 1987; Gerber et al. 1987). The growth of DPAOs requires the alteration of anaerobic and anoxic conditions, where carbon is made available during the anaerobic phase. In general, PAOs may be classified into three groups according to their affinity for electron acceptors. These are PAOs that may only use oxygen as an electron acceptor, PAOs that may use both oxygen and nitrate, and PAOs that may use oxygen, nitrate and nitrite. The last two groups make up the DPAO community (Hu et al., 2003).

The selective growth of DPAOs can not only reduce oxygen demand in the aerobic zone for PHA oxidation, but also reduce carbon demand since both nitrogen and phosphorus are removed with the same carbon source (Lee and Yun, 2014; Zielińska et al., 2016). According to

Brdjanovic et al. (1998), DPAOs are capable of removing 4-5 g NO₃-N per g of P removed, using their stored PHAs. As such, the presence of DPAOs may reduce aeration and carbon demands, resulting in a reduced overall operation cost (Oehmen et al., 2007).

The selective growth of DPAOs requires their prevalence over common heterotrophic denitrifying bacteria, as the latter display faster denitrification rates. The main factor influencing the emergence of DPAOs has been shown to be the nitrate load in the anoxic reactor, which must surpass the denitrification potential of conventional heterotrophic organisms (Hu et al., 2002).

It is generally accepted that most abundant PAO group in WWTPs is the genus *Candidatus Accumulibacter phosphatis* of the Betaproteobacteria microbial community (Mino et al., 1998; Oehmen et al., 2007; Shen and Zhou, 2016) although this is not always the case (Stokholm-Bjerregaard et al., 2017). This genus is not an individual group but is composed of many individual strains with different morphological and qualitative characteristics. According to analysis of the polyphosphate kinase gene (*ppk1*), which is thought to be primarily responsible for poly-P synthesis in bacteria, the genus can be classified into two main subgroups: *Accumulibacter* type I (PAO I) and *Accumulibacter* type II (PAO II), each of which is further subdivided into individual strains (Flowers et al., 2009). In terms of morphology, PAO I have been observed to possess a bar-shaped cell, while PAO II have a granular form (Carvalho et al., 2007; Oehmen et al., 2010b; Zeng et al., 2016b).

A significant difference between the two main PAO groups is their ability to utilize nitrite and nitrate as an electron acceptor. Guisasola et al. (2009) developed a PAO-enriched biomass at a laboratory scale that was capable of removing phosphorus via nitrite and examined their capacity to reduce nitrate. The authors reported that the biomass could not reduce nitrate, even after a period of acclimatization. Also, Carvalho et al. (2007) developed two separate PAO cultures with acetic acid as the carbon source for one group and propionic acid for the other and observed that only the latter could use nitrate as an electron acceptor. These findings support the hypothesis of the existence of two different types of PAOs and have been validated by the postgenomic analysis by Martín et al. (2006), which showed that the PAO II type does not possess the necessary enzyme for reducing nitrate in contrast to PAO I, while both types have the ability to reduce nitrite. Therefore, the PAO I type can utilize oxygen, nitrite and nitrate, while PAO type II may only utilize oxygen and nitrite (Oehmen et al., 2010). In contrast with this, Rubio-Rincón et al. (2017) argued that neither type of PAOs has the potential to reduce nitrate. The authors suggested that nitrate is first reduced to nitrite by another microbial group, known as Glycogen Accumulating Organisms (GAOs) and that the produced nitrite may then be utilized by PAOs for the removal of phosphorus.

Acevedo et al., (2012) reported that the PAO II type has a greater ability to adapt to changes in polyphosphate storage conditions, possibly because they are able to use different metabolic pathways, while PAO I cannot use the glycolysis pathway and the Krebs cycle as effectively. As such, under low phosphorus conditions the PAO I type which does not have the corresponding flexibility is disadvantaged and gradually eliminated. In general, there are many reports that claim that not all strains possess the required enzymes for the utilization of all metabolic pathways. For example, Martín et al.,(2006) reported that type IIA contains enzymes for the EMP pathway but not for ED, while other strains are capable of utilizing both pathways (Oehmen et al., 2007). The

existence of different strains with different characteristics may explain the discrepancies in the literature regarding the metabolic pathways and the use or not of the Krebs cycle.

There are 5 known strains for PAO I (IA-IE) and 9 known strains for PAO II (IIA-III) although there is evidence that suggests a greater abundance (Song et al., 2019). Each type and their individual strains differ in their ability to utilize nitrate and nitrite as electron donors, as well as their tolerance to different conditions, such as limited phosphorus concentrations, high temperatures, the presence of inhibitors etc. In conditions of limited oxygen, the predominant strains were PAO IID and PAO IC (Camejo et al., 2016), while in conditions of high temperatures the strain PAO IIF displayed the highest resistance (Ong et al., 2014). Slater et al. (2010) observed that the PAO IA strain was capable of proliferating over competitor GAOs while the PAO IIC strain was incapable of competing. The PAO IIC strain, while sensitive to nitrite, predominates in anoxic phosphorus uptake when nitrite concentrations are low (<8 mg/L), whereas the PAO IID strain appears to be the most tolerant to high nitrite concentrations, while also being capable of surviving at conditions of limited carbon supply and oxygen concentration (Zeng et al., 2016a ; Zeng et al., 2017).

2.4.2 GAOs

Glycogen Accumulating Organisms (GAOs) are a microbial group that is often present in EBPR systems and are the main competitor of PAOs. Like PAOs, this bacterial group possesses the ability to take up carbon under anaerobic conditions and store it intracellularly as PHAs, but does not contribute to the removal of phosphorus (Oehmen et al., 2007). This is because, unlike PAOs, GAOs do not form intracellular polyphosphate chains which may be hydrolyzed for energy. Instead, the required energy for the anaerobic uptake of VFAs is provided entirely via glycolysis (Mino et al., 1998; Dai et al., 2007). The proliferation of GAOs over PAOs in EBPR systems is considered as the bottleneck of operation.

GAOs have the capacity to store increased amounts of glycogen which may be hydrolyzed under anaerobic conditions for energy. The redox potential for the uptake of VFAs is provided by glycolysis and to a lesser extent via the Krebs cycle (TCA) (Mino et al., 1998; Oehmen et al., 2007). The mechanisms that have been proposed for the hydrolysis of glycogen by GAOs are similar to those of PAOs; specifically, the Entner-Doudoroff (ED) pathway and the Embden, Meyerhof and Parnas (EMP) pathway (Oehmen et al., 2007), although some have suggested that GAOs may not utilize the ED pathway (Filipe et al., 2001b). The mechanism for VFA conversion to PHAs via glycolysis is as follows: Glycolysis provides the required amount of energy for the intake of VFAs and their transport inside the cell. There, the VFAs are converted to acetyl-CoA and Propionyl-CoA coenzymes, which are the precursors of PHAs. These conversions are carried out through glycolysis and the electro-propionate method, respectively. Glycolysis produces the redox potential for the electro-propionate method (Mino et al., 1998). A fraction of the redox potential is provided by the TCA cycle (Oehmen et al., 2007; Acevedo et al., 2015).

Under aerobic conditions GAOs oxidize their stored PHAs for glycogen replenishment, cell maintenance and growth. Glycogen replenishment is carried out through gluconeogenesis via the ED pathway (Oehmen et al., 2007) (Figure 2.16). The process is the same regardless of the electron acceptor. (Oehmen et al., 2010).

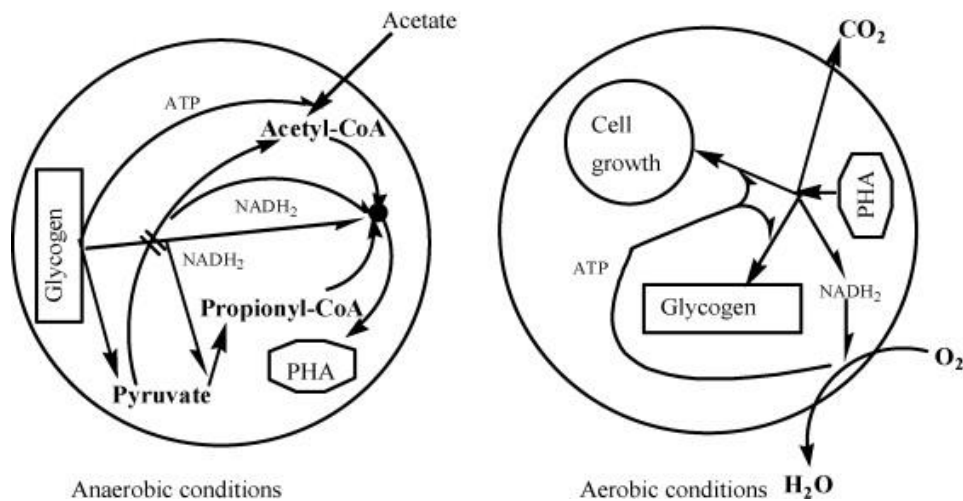


Figure 2.16. Schematic diagram of the metabolism of GAOs under anaerobic and aerobic conditions (Figure adapted from Dai et al., 2008).

To date, several microorganisms have been identified as GAOs. The most important of these are *Candidatus Competibacter* (hereafter referenced as *Competibacter*) of the Gammaproteobacteria microbial community, and *Defluviicoccus vanus* and *Sphingomonas* of the Alphaproteobacterial community (Oehmen et al., 2007; Oehmen et al., 2010; Shen and Zhou, 2016). Both *Competibacter* and *Defluviicoccus vanus* have often been observed in laboratory-scale systems but also in full-scale applications, to a lesser extent (Saunders et al., 2003; Meyer et al., 2006; Burow et al., 2007). *Competibacter* is favoured when acetate is the carbon source, for which it has a strong affinity, while *Defluviicoccus vanus* is favoured when the carbon source is propionate (Oehmen et al., 2005b; Oehmen et al., 2005c).

Competibacter are composed of at least 7 different sub-groups (GB 1-7) (Kong et al., 2002) while *Defluviicoccus vanus* are composed of at least 4 different clusters (McIlroy and Seviour, 2009). These sub-groups of each organism have varying denitrification capabilities (Kong et al., 2006; Burow et al., 2007; Wang et al., 2008). For instance, subgroups 1,4 and 5 of *Competibacter* are capable of reducing nitrate but not nitrite, while subgroups 3 and 7 are incapable of using either electron acceptor. As for *Defluviicoccus vanus*, groups DFI and DFII have been studied to some extent. Reportedly, neither group is capable of utilizing nitrite, while only DFI can reduce nitrate (Wang et al., 2008 ; Oehmen et al., 2010).

2.5 Achievement of EBPR in nitrogen removal systems

2.5.1 Peculiarities of EBPR coupled with nitrification/denitrification for low C/N wastewater treatment systems

2.5.1.1 Physicochemical characteristics of sludge liquors

The disposal of the excess sludge that is produced in WWTPs requires the decrease of its water content. This is achieved by a series of sludge treatment technologies that include thickening, dewatering and drying. These processes result in the production of several reject water streams with different quality characteristics which are typically recycled to the main wastewater treatment line. The variability of the reject water's properties is highly dependent on both the characteristics of the influent, and the sludge treatment configuration (e.g., the existence or absence of a primary treatment unit, a digestion unit, etc.).

Reject water from the anaerobic digestion process in particular contains significantly high ammonium concentrations that may reach 1500 mg N/L (Aslan and Dahab, 2008). During anaerobic digestion, organic nitrogen (mainly in the form of amines/proteins) is broken down and hydrolysed, producing ammonium, while the organic content of the sludge is consumed by heterotrophic methanogens. This results in the production of a sludge liquor with a low COD : N ratio (Ahn, 2006; Gustavsson, 2010). In addition, reject water from this process also contains a significant amount of phosphorus, which has been reported to reach concentrations of up to 250-300 mg P_{tot}/L, with approximately 84% of it being in the form of soluble phosphates (Battistoni et al., 2006). As such, the recirculation of this stream to the WWTP's inlet may significantly increase nutrient loading and reduce the influent's COD : N and COD : P ratio, thereby reducing the efficiency of the biological nutrient removal processes which require a biodegradable carbon source.

Although there are some reports on the quality characteristics of reject water, there is a general lack of systematic study regarding the characterization of all reject water sources. In their recent study, Noutsopoulos et al. (2018) presented a detailed and systematic characterization of the quality characteristics of several reject water sources of the WWTP of Psytalia (which is the largest WWTP of Greece). A layout of the sampled WWTP can be seen in Figure 2.17. The wastewater treatment line consists of a pre-treatment unit, primary sedimentation tanks and an activated sludge unit for the biological removal of organic carbon and nitrogen. Sludge treatment facilities consist of gravity thickeners for primary sludge (PS), mechanical thickeners for waste activated sludge (WAS), a thermal hydrolysis unit (in which almost 50% of the thickened WAS is processed), anaerobic digesters that process a mixture of 50% of the thickened primary sludge (PST) and the thickened WAS (WST), anaerobic digesters that process the mixture of the remaining half of the PST and the thermally hydrolyzed WAS, a dewatering unit and a thermal drying unit. The reject water streams that are generated during each stage of the sludge treatment process are depicted in Figure 2.17.

The authors reported that the reject water from the primary sludge thickening units (PST-RW) presents a neutral pH, high total COD and TSS concentrations (with average values of 4,244 mg/L and 1,863 mg/L respectively), a high VSS/TSS ratio (87%) and a low soluble COD content (at 22% of the total COD). The ammonium nitrogen content of the reject water (average concentration of 66 mg/L) accounts for 67% of the total nitrogen content, while 42% of total phosphorus is in the form of soluble phosphates (with an average concentration of 10.5 mg PO₄-P/L).

Reject water originating from the WAS mechanical thickening unit (WST-RW) exhibits a significantly lower COD, TSS, and nutrient content (with average concentrations of 184 mg COD_{tot}/L, 159 mg TSS/L, 21.5 mg TN/L and 5 mg TP/L), with a VSS/TSS ratio of 73%, and a soluble fraction of total COD equal to 20%. Ammonium nitrogen accounts for merely 15% of the total nitrogen content (as a result of nitrification in the activated sludge unit), while 60% of TP is found as phosphates.

The quality characteristics of reject water from the dewatering unit are significantly different from the respective ones of all other reject water types. Both SD-CON-RW and SD-HYD-RW are characterized by high pH values (in the order of 8.4-8.5), very high conductivity and alkalinity, moderate COD and TSS concentrations (with average concentrations between 1,956-

2,800 mg COD_{tot}/L and 919-943 mg TSS/L) and a very high ammonium nitrogen content (with average values between 1,128-1,491 mg NH₄-N/L).

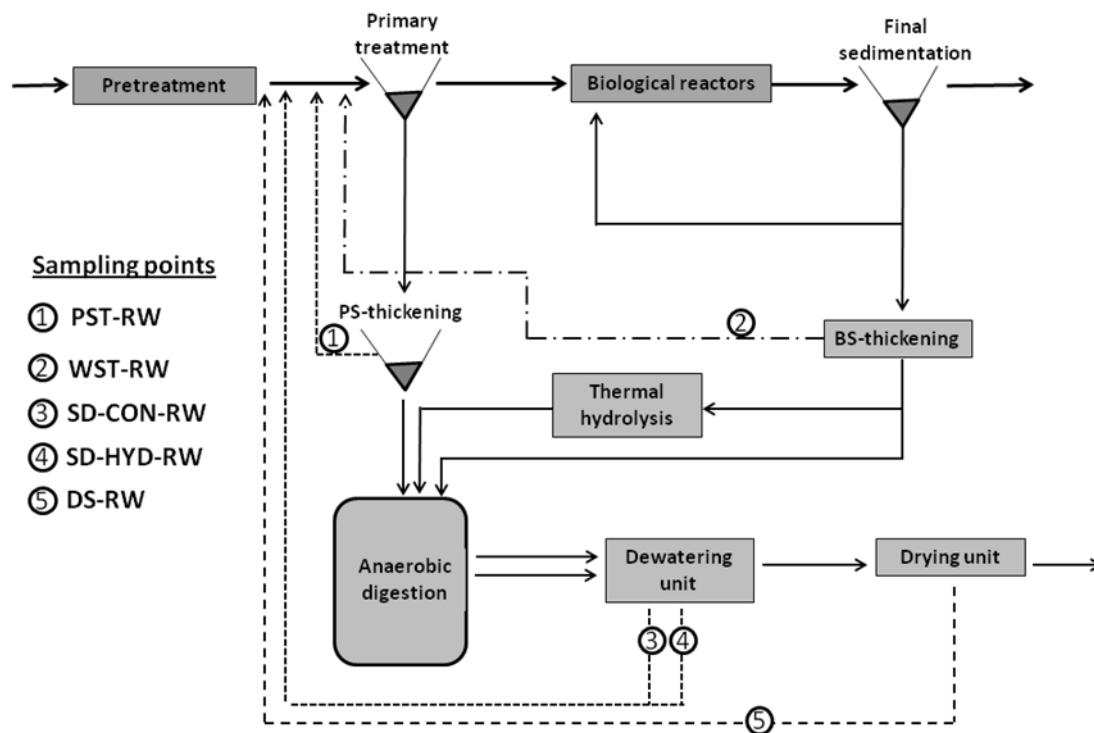


Figure 2.17. Layout of the sampled reject water (RW) according to source include: primary sludge thickening unit (PST-RW), wastage sludge mechanical thickening unit (WST-RW), dewatering unit following conventional anaerobic digestion (SD-CON-RW), dewatering unit following thermal hydrolysis – anaerobic digestion process (SD-HYD-RW) and drying sludge unit (DS-RW) (Figure adapted from Noutsopoulos et al., 2018).

Reject water from the drying process (DS-RW) is characterized by moderate conductivity and alkalinity values, as well as moderate organic carbon, suspended solids and nutrient concentrations (with average values of 688 mg COD_{tot}/L, 533 mg TSS/L, 117.4 mg TN/L and 18.7 mg TP/L). The VSS/TSS ratio is relatively low (62%), while soluble COD accounts for only 16% of the total COD. Ammonium nitrogen accounts for 59% of the total nitrogen content, while merely 27% of TP is in the form of phosphates.

According to the results, the PST-RW contains the highest easily biodegradable fraction (almost 23% of total COD), while WST-RW exhibits the lowest (practically zero, as a result of the wastewater treatment in the activated sludge unit). The two reject water types (SD-CON-RW and SD-HYD-RW) produced in the dewatering process, are characterized by a low easily biodegradable organic content (in the order of 5-10% of total COD) and an appreciable slowly biodegradable COD fraction (amounting to 37-47% of total COD). Both reject water types originating from the WAS mechanical thickening process (WST-RW) and the drying process (DS-RW) contain low total biodegradable fractions (SS and XS) and very high inert particulate organic carbon fraction (in the order of 65% and 72% respectively).

Table 2.1. Results from the qualitative characterization of several reject water sources – physicochemical characteristics, organic carbon and solids (average values \pm standard deviation) (adapted from Noutsopoulos et al., 2018).

Reject water source	pH	Conductivity ($\mu\text{S cm}^{-1}$)	Alkalinity (mg L^{-1})	COD _t (mg L^{-1})	COD _s (mg L^{-1})	TSS (mg L^{-1})	VSS (mg L^{-1})
PST-RW ¹	7 \pm 0.4	2324 \pm 336	699 \pm 170	4244 \pm 2100	916 \pm 570	1863 \pm 1100	1621 \pm 1008
WST-RW ²	7.5 \pm 0.1	1533 \pm 242	201 \pm 19	184 \pm 140	36 \pm 14	159 \pm 90	117 \pm 83
SD-CON-RW ³	8.4 \pm 0.1	9572 \pm 410	4592 \pm 367	1956 \pm 597	732 \pm 165	943 \pm 452	669 \pm 318
SD-HYD-RW ⁴	8.5 \pm 0.1	11325 \pm 573	5806 \pm 444	2800 \pm 316	1375 \pm 150	919 \pm 384	728 \pm 300
DS-RW ⁵	8.1 \pm 0.2	1876 \pm 198	478 \pm 40	688 \pm 244	113 \pm 19	533 \pm 198	330 \pm 127

¹PST-RW: reject water from primary sludge thickening unit, ²WST-RW: reject water from wastage sludge thickening unit, ³SD-CON-RW: reject water from digested sludge following conventional anaerobic digestion process, ⁴SD-HYD-RW: reject water from digested sludge following thermal hydrolysis – anaerobic digestion process, ⁵DS-RW: reject water from drying sludge unit

Table 2.2. Results from the qualitative characterization of several reject water sources –nitrogen and phosphorus (average values \pm standard deviation) (adapted from Noutsopoulos et al., 2018).

Reject water source	NH ₄ -N (mg L^{-1})	NO ₃ -N (mg L^{-1})	TKN (mg L^{-1})	TN (mg L^{-1})	PO ₄ -P (mg L^{-1})	TP (mg L^{-1})
PST-RW ¹	66.6 \pm 17	0.77 \pm 0.3	98.3 \pm 42	99 \pm 42	10.5 \pm 5	25 \pm 15
WST-RW ²	3.27 \pm 2	2.35 \pm 1	19 \pm 17	21.5 \pm 17	3 \pm 1	5 \pm 2.7
SD-CON-RW ³	1128 \pm 141	2.09 \pm 0.2	1312 \pm 161	1314 \pm 161	32.2 \pm 16	72.2 \pm 19
SD-HYD-RW ⁴	1491 \pm 141	6.55 \pm 1.1	1601 \pm 136	1608 \pm 137	16.1 \pm 10	54 \pm 13
DS-RW ⁵	69.1 \pm 9	4.84 \pm 1.6	112.6 \pm 36	117.4 \pm 36	5.13 \pm 1	18.7 \pm 5

¹PST-RW: reject water from primary sludge thickening unit, ²WST-RW: reject water from wastage sludge thickening unit, ³SD-CON-RW: reject water from digested sludge following conventional anaerobic digestion process, ⁴SD-HYD-RW: reject water from digested sludge following thermal hydrolysis – anaerobic digestion process, ⁵DS-RW: reject water from drying sludge unit

2.5.2 Factors affecting EBPR in high nitrogen loading systems

2.5.2.1 Type of substrate

The application of EBPR requires the inclusion of an anaerobic phase in which Short Chain Fatty Acids (SCFAs) are made available to be taken up by PAOs. The type of substrate affects not only the anaerobic uptake rate of SCFAs, but also the type of PHAs into which are converted and consequently the performance of PAOs in the subsequent aerobic/anoxic phase. More importantly, the type of substrate may influence the antagonism between PAOs and GAOs, as the microbial populations that make up these two groups may possess a different affinity for a specific substrate. Some of the carbon sources that have been examined in the literature are acetic acid, propionic acid, glucose, alcohols, as well as more complex organic compounds, such as glycerol and other organic wastes (Shen and Zhou, 2016). The most

commonly used substrates are acetic and propionic acid, while glucose was found to favour GAOs (Wang et al., 2010).

The type of intracellular polymer in which the taken-up carbon is converted to has an effect on the phosphorus uptake rate of PAOs (Randall and Liu, 2002). In general, PAOs convert acetate to form poly-hydroxybutyrate (PHB) (Randall and Liu, 2002), while propionate is converted to form poly-hydroxyvalerate (PHV) and poly-beta-hydroxy-2-methylvalerate (PH2MV) (Oehmen et al., 2005a). Similarly, acetotrophic GAOs have been found to convert acetate to PHB, but also to PHV at a lesser extent (Randall and Liu, 2002). Pijuan et al. (2009) developed two different microbial populations in separate reactors, with propionate being the carbon source for one reactor and acetate being the carbon source for the other reactor. The propionate-fed reactor displayed high phosphorus removal compared to the acetate-fed reactor, indicating a higher abundance of PAOs. Analysis of the biomass from the propionate reactor revealed great quantities of intracellular stored PHV and PH2MV. When the feed for this reactor was changed to acetate, analysis showed great quantities of PHB. The acetate-fed biomass, which possibly included a significant GAO population, displayed a large percentage of PHAs in the form of PHB and a low percentage in the form of PHV. According to Randall and Liu (2002), aerobic phosphorus uptake (per mol C) is greater for PHB compared to PHV when the PHA form is exclusive, but the storage of multiple forms of PHAs complicates the matter.

The choice of substrate also affects the microbial composition of the biomass due to the diverse affinity of PAO and GAO subgroups (or even individual strains) for a specific carbon type. Particularly in the case of GAOs, the two main subgroups are the Gammaproteobacterial GAOs (namely the *Competibacter spp.*) and the Alphaproteobacterial GAOs (with *Defluviicoccus vanus* being the most representative species). According to Oehmen et al. (2010), *Competibacter* are incapable of metabolizing propionate, while Alphaproteobacterial GAOs cannot utilize acetate. Oehmen et al. (2006) observed that *Competibacter* would proliferate over PAOs in an acetate-fed reactor even when high phosphorus concentrations were made available. However, in a propionate fed reactor, PAOs prevailed over GAOs when high phosphorus concentrations were made available, while *Defluviicoccus vanus* prevailed when phosphorus concentrations were low. In addition, Vargas et al. (2011) observed a wash-out of *Defluviicoccus vanus* in an anaerobic/anoxic reactor when the feed was changed from propionate to acetate. However, Dai et al. (2007) suggested that *Defluviicoccus vanus* may take up both acetate and propionate but have a higher affinity for propionate, while Wang et al. (2008) were successful in developing *Defluviicoccus vanus* with acetate as the carbon source. In the case of PAOs, Oehmen et al. (2010) reported that they displayed no particular preference between acetate and propionate whereas Carvalho et al. (2007) suggested that the choice of substrate could select specific PAO strains.

It is evident that the choice of substrate (mainly acetate vs propionate) plays a key role in the selective growth of PAOs, for the application of effective EBPR. However the matter is complex not only due to contrasts in the literature, but also due to the effect of others parameters such as pH and the presence of inhibitors on the selected microbial communities. In general, it would appear that propionate is the preferable VFA for stable EBPR performance. This is mainly due to the fact that PAOs are more capable of competing with *Defluviicoccus vanus* for propionate compared to competing with *Competibacter* for acetate (Oehmen et al., 2006). The stability of EBPR with propionate as the carbon source was also demonstrated by Pijuan et al. (2004) while

Wang et al. (2010) observed a higher phosphorus removal efficiency when propionate was used compared to when glucose, acetate and a mixture of acetate and propionate was used on a PAO-enriched biomass developed with acetate.

It should be noted however that Oehmen et al. (2005b) were successful in obtaining a stable EBPR performance in an acetate-fed reactor despite the presence of *Competibacter*. Carvalheira et al. (2014) reported that a mixture of feed (75% acetate, 25% propionate) provided PAOs with an advantage over GAOs. In agreement, Oehmen et al. (2014) suggested that propionate can provide PAOs with a competitive advantage even when the propionate fraction of the influent is relatively low and reported the achievement of good EBPR with the use of a combined feed (75% acetate, 25% propionate).

The choice of substrate may also select the growth of specific organisms differently depending on the reactor's configuration, specifically the alteration of anaerobic/aerobic or anaerobic/anoxic conditions. This is due to the different capacity of each species to utilize electron acceptors for the oxidation of the stored PHA form. In the case of anoxic phosphorus removal, the use of acetate appears problematic. Carvalho et al. (2007) observed that when the anaerobic/aerobic configuration of an acetate-fed reactor was altered to anaerobic/anoxic, it resulted in failure of EBPR. However, the propionate-fed reactor was capable of adapting to such a change after a brief period of acclimation. On the other hand, Vargas et al. (2011) observed a steady EBPR performance in a reactor, altering anaerobic and anoxic conditions and following a switch to acetate, the reactor continued to perform although with a lower removal efficiency.

The capacity of the various PAO and GAO types to utilize nitrite and nitrate differs. According to Oehmen et al. (2010), PAO I may reduce both nitrate and nitrite, whereas PAO II may only reduce nitrite. While most *Competibacter* may reduce both nitrate and nitrite, all known strains of *Defluviicoccus vanus* may only reduce nitrate. The inability of *Defluviicoccus vanus* to reduce nitrite was also demonstrated by Wang et al. (2008). As such the application of EBPR via denitrification with propionate as the sole carbon source could possibly exclude all GAO groups from the process since *Competibacter* may not utilize propionate while *Defluviicoccus vanus* may not reduce nitrite. The effectiveness of such a configuration was demonstrated by Tayà et al. (2013) who subjected a highly *Defluviicoccus vanus*-enriched biomass (70%) to these conditions and observed a shift in the biomass, in the favour of PAOs that ended making up approximately 85% of the total microbial population.

It should be noted that the capacity of PAOs (specifically the PAO I type) to reduce nitrate has been disputed in the literature with some reports suggesting that nitrate is reduced to nitrite by GAOs and that PAOs reduce the produced nitrite in a synergistic fashion. This is supported by the findings of Rubio-Rincón et al. (2017) who developed a PAO I culture and a mixed PAO I and GAO culture. Following acclimation of the biomasses to an anaerobic/anoxic/aerobic configuration, it was observed that the PAO I culture could only reduce nitrite while the mixed culture could also reduce nitrate. This synergistic cooperation was also observed by Wang et al. (2014), who reported that the prevalent PAO type in a reactor where nitrate was the electron acceptor was PAO II, which does not possess the required enzyme for nitrate reduction (Martín et al., 2006).

As PAOs reportedly have no particular preference for acetate or propionate while GAOs are divided into two groups, one of which can only take up acetate while the other has an affinity for propionate, it is likely that a regular rotation of acetate and propionate could prevent the development of GAOs. However, while propionate-fed PAOs can readily adapt to acetate, this does not appear to be the case for acetate-fed PAOs when the feed is changed to propionate. Based on the observations of Oehmen et al. (2005b) on a PAO-enriched biomass that was developed with acetate, PAOs were capable of anaerobically taking up propionate at a similar rate as acetate. However, phosphorus removal in the subsequent aerobic phase was less, most likely due to PHV and PH2MV being the new stored PHA types, for which some acclimation may be required (Oehmen et al., 2004; Oehmen et al., 2005b). As while the regular rotation between acetate and propionate may be beneficiary for PAOs, their performance may not be stable when the shift is made from acetate to propionate.

The availability and abundance of substrate during the anaerobic phase is also an important factor. Carvalho et al. (2014b) developed separate PAO and GAO cultures and observed their behaviour under limited feeding conditions. The authors reported that the decay rate of GAOs was almost 4 times that of PAOs which appeared more economical with their stored PHAs. However, Vargas et al. (2013) reported that the complete absence of substrate affected PAOs to a greater extent than GAOs, as the intracellular polyphosphate chains of PAOs were exhausted more rapidly than the stored glycogen of GAOs. In addition, Tu and Schuler (2013) examined differences between rapid and slow addition of feed during the anaerobic phase in a reactor operating at low pH (that generally favours GAOs, as will be discussed). They reported that the slow addition of feed (maintaining the substrate concentrations low) provided an advantage to PAOs, while the rapid addition of feed (providing an abundance of substrate) would result in the proliferation of GAOs and the wash-out of PAOs.

2.5.2.2 pH

The biological processes of all microorganisms are affected by the pH of the medium and each organism can only sustain within a specific range of pH. As such the pH range of the medium may control microbial populations and provide advantages to a specific group or species over others. The pH value may also control the concentration of certain inhibitors (e.g. FNA and FA) which affect microbial processes, though this will be specifically discussed in a following subsection. In regard to PAOs and GAOs, the effect of pH concerns 1) their anaerobic processes (carbon uptake – phosphorus release/glycogen consumption) and 2) their processes in the presence of an electron acceptor (oxidation of intracellular PHAs – phosphorus uptake and polyphosphate formation/glycogen formation). However, it is generally accepted that PAOs overly benefit from high pH values while GAOs prevail at lower pH.

The effect of pH on the anaerobic processes of PAOs and GAOs was studied by Filipe et al. (2001), who reported that GAOs were inhibited at higher pH whereas PAOs were practically unaffected. In particular, the rise in pH resulted in a higher energy demand for the uptake of carbon by GAOs, leading to a greater consumption of stored glycogen. Adversary, low pH values (<7.5) lowered energy demands and the consumption of glycogen, resulting in a faster uptake of carbon. The authors concluded that pH values above 7.5 during the anaerobic phase benefited PAOs.

The effect of pH on the aerobic processes of PAOs was also studied by Filipe et al. (2001) who developed separate PAO and GAO cultures at the pH range of 7.2-7.6 and 6.8-7.1 respectively. Following steady-state conditions, a series of experiments was performed on samples from each reactor, initially maintained anaerobically at the pH of 7, after which the pH was set at the values of 6.5, 7 and 7.5 for each culture. The samples were then aerated for a period in which phosphorus uptake, glycogen consumption, PHA oxidation and microbial growth were studied for each pH. The authors observed that pH had a negligible effect on the processes of GAOs, whereas PAOs performed poorly at the pH of 6.5 and best at the pH of 7.5. At the pH of 7, GAOs performed better than PAOs both in terms of PHA consumption and microbial growth. As such, pH values below 7.5 could provide an advantage to GAOs. This is also supported by the findings of Oehmen et al. (2005b) who studied the long-term effect of pH in the antagonism between PAOs and GAOs in an acetate-fed reactor and a propionate-fed reactor. Initially, both reactors performed at the pH of 7, during which phosphorus removal was particularly poor in both reactors (even more-so in the acetate-fed reactor) which displayed an abundance of GAOs. The pH of each reactor was then set to 8 which ultimately resulted in the suppression of GAOs and the proliferation of PAOs in both reactors. Notably, the proliferation of PAOs occurred faster (over 2 weeks) in the propionate-fed reactor compared to the acetate-fed reactor (over 4 weeks).

2.5.2.3 Temperature and SRT

Temperature affects all metabolic processes of microorganisms and is an important parameter in the selection of certain organisms over others. In nitrification/denitrification systems that employ EBPR, temperature may play a key role in the population dynamics of AOB and NOB, limiting full nitrification, and also the antagonism between PAOs and GAOs. The role of temperature is directly linked to the SRT of the treatment system. As temperature affects the growth and maintenance of the various species of microbial communities disproportionately, there is a critical SRT for each species, under which it cannot sustain. In the case of antagonistic groups (e.g. PAOs vs. GAOs), a range of SRT and temperature combinations may allow the presence of one group, but not the other.

Based on their capacity to grow and sustain under different temperature conditions, organisms may be divided into the following categories; psychrophiles, that are capable of growth and reproduction in temperatures as low as -10 °C, with an optimum growth rate around 15 °C, mesophiles which have an optimum growth range between 20 and 45 °C, and thermophiles which thrive under higher temperatures and are not relevant in conventional treatment systems. The effect of temperature on the specific growth rate of a microorganism is usually expressed by the Arrhenius equation:

$$\mu_{mT} = \mu_{mT^*} \times e^{k(T-T^*)}$$

where μ_{mT} is the maximum specific growth rate at T temperature, μ_{mT^*} is the maximum specific growth rate at the reference temperature of T* and k is a constant.

Figure 2.18 displays the temperature dependency of the maximum growth rates of AOB and NOB according to several studies (Chaim De Mulder, 2016). As is evident, while the effect of temperature on the growth of AOB appears consistent within the three studies presented, its effect on the growth of NOB appears to vary, likely due to differences in acclimation. In all cases

however, the growth rate of AOB is enhanced to a greater extent with the increase of temperature and at some point surpasses the growth of AOB. Therefore, high temperatures could enhance partial nitrification while a critical SRT could allow sufficient nitrification but not nitrification, owing to the wash-out of NOB. According to Philips et al. (2002), the growth rates of NOB are greater than those of AOB at temperatures below 20°C, whereas at temperatures above 25°C, the growth rates of AOB surpass them.

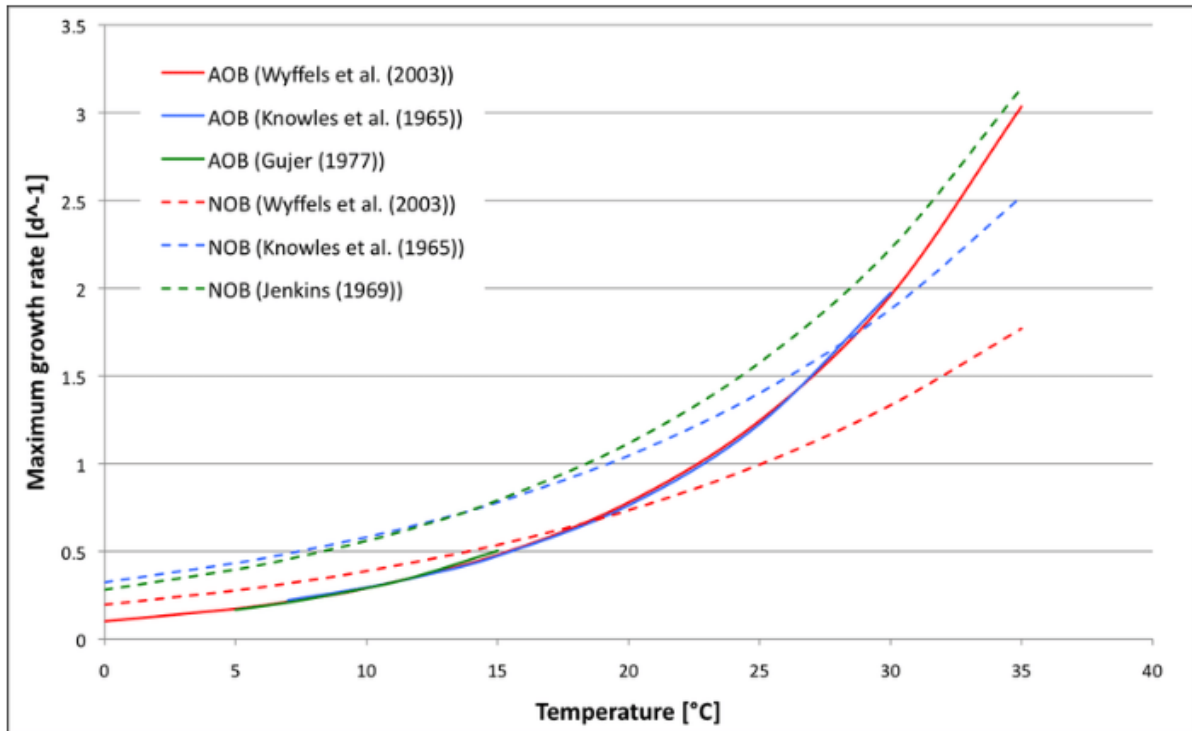


Figure 2.18. Arrhenius temperature dependency of maximum growth rate of AOB and NOB, as determined by several authors (Figure adapted from Chaim De Mulder, 2016).

It is generally accepted that PAOs are psychrophilic while GAOs are mesophilic, meaning that PAOs benefit from temperatures below 20°C, while greater temperatures provide an antagonistic advantage to GAOs. Lopez-Vazquez et al. (2009) who studied the antagonism between PAOs and GAOs in regard to temperature, pH and the carbon source reported that PAOs proliferated at the temperature of 10°C, regardless of the other factors, while the same was observed for GAOs at the temperature of 30°C. In agreement with this, Panswad et al. (2003) reported that raising the temperature above 20°C influenced the antagonism in the favour of GAOs and at 30°C no PAO activity was observed.

Temperature affects the anaerobic and aerobic/anoxic processes of PAOs and GAOs to a different extent, with the anaerobic processes being the most critical (Lopez-Vazquez et al., 2008). At temperatures below 15°C the process of glycolysis is fully inhibited, meaning that GAOs are incapable of acquiring the energy demanded for them to take up carbon, providing a full advantage to PAOs (Lopez-Vazquez et al., 2009a). In temperatures between 20 and 30°C, the anaerobic uptake rates of both PAOs and GAOs appear unaffected. However, as temperature rises, the energy requirements for cell maintenance of PAOs increases, limiting the available energy required for growth. This would provide an advantage to GAOs, which can withstand

temperatures up to 35°C where glycolysis is again inhibited (Lopez-Vazquez et al., 2008; Lopez-Vazquez et al., 2009a).

The short-term effect of temperature change on the metabolism of PAOs and GAOs has also been studied. Lopez-Vazquez et al. (2007) reported that an increase in temperature above 20°C clearly influenced the antagonism in the favour of GAOs, while at the temperatures of 10°C and 40°C the processes of both microbial groups were fully inhibited. The maximum growth rates for PAOs and GAOs were observed at the temperatures of 20°C and 30°C respectively (Lopez-Vazquez et al., 2008). It should be noted that while PAOs benefit from lower temperatures in respect to their antagonism with GAOs, a sudden drop in temperature may inhibit their activity and a period of acclimation could be required for them to resume proper function (Ren et al., 2011).

Lopez-Vazquez et al. (2009) modelled the influence of carbon source, temperature and pH on the competition between PAOs and GAOs for substrate uptake and the influence of these parameters is shown in Figure 2.19. In all cases, PAOs prevail at temperatures below 18°C. However, at greater temperatures, a higher pH is required to provide PAOs with an advantage (Carvalheira et al., 2014b).

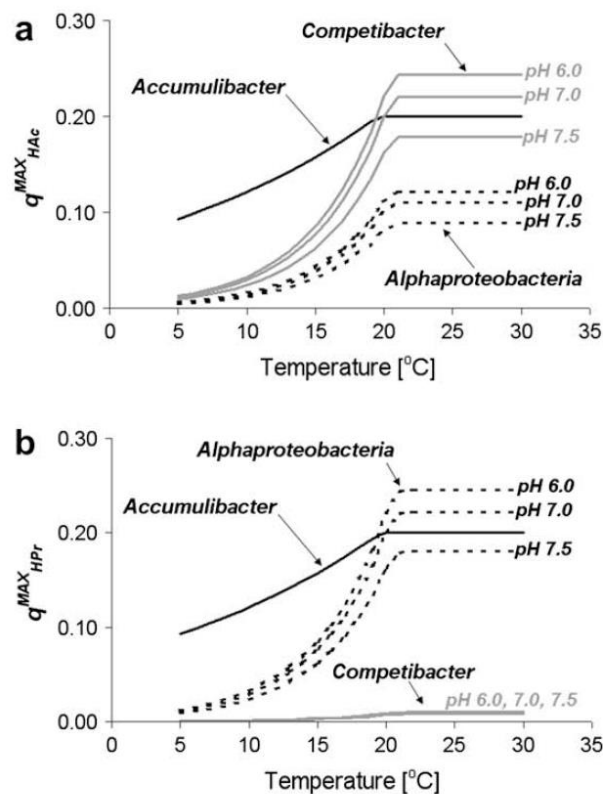


Figure 2.19. Combined temperature and pH effects on the maximum substrate uptake rates of *Accumulibacter*, *Competibacter* and Alphaproteobacteria-GAO for (a) acetate and (b) propionate. Black solid line: *Accumulibacter*; grey solid lines: *Competibacter*; and, black dotted lines: Alphaproteobacteria-GAO. Maximum substrate uptake rates of *Accumulibacter* are insensitive to pH changes. Figure adapted from Lopez-Vazquez et al., (2009)

As mentioned, the adoption of an appropriate SRT with respect to temperature may select the growth of one microbial group and limit or forbid the growth of another. Whang and Park (2006) developed a PAO-enriched biomass at the temperature of 20°C and the SRT of 10 days. After raising the temperature to 30°C, they observed a decrease in PAOs, having been overtaken by GAOs. However, after lowering the SRT to 3 days, EBPR recovered. The minimum required aerobic SRT for the cultivation of PAOs or GAOs is dependent on the PHA oxidation rate of each group (Filipe et al., 2001a). Lopez-Vazquez (2009) studied the minimum required aerobic SRT for PAO and GAO (specifically *Competibacter*) cultivation with regard to temperature, the results of which are depicted in Figure 2.20. For temperatures below 20°C, relatively high SRTs may be adopted that would prohibit the growth of GAOs while securing PAO growth. For temperatures above 20°C, a low aerobic SRT is demanded to prohibit the growth of GAOs, although PAOs themselves face the danger of wash-out.

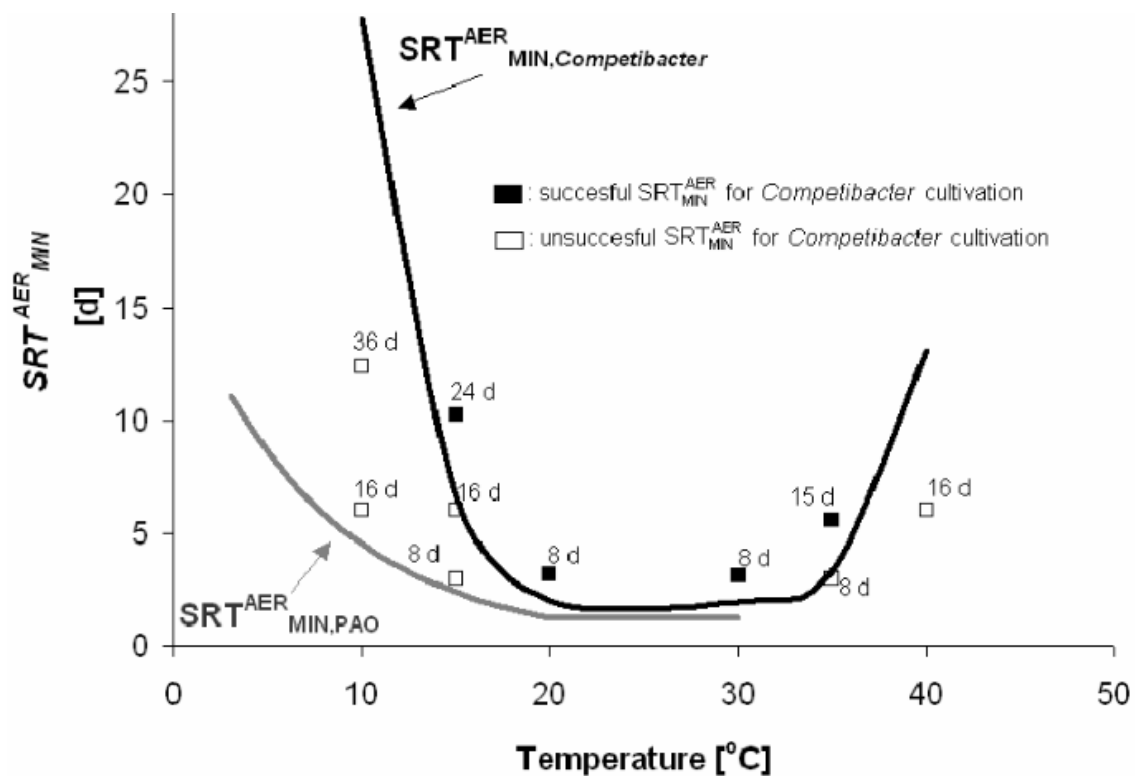


Figure 2.20. Minimum aerobic solid retention times of PAOs (Figure adapted from Lopez-Vazquez et al.,(2009))

2.5.2.4 FA and FNA

The application of the nitrification/denitrification pathway requires the shunt of NOB, which in the case of side-stream treatment of reject water is achieved by the high ammonium content of the influent. Free Ammonia (FA) is a known inhibitor of various microbial processes (including those of AOB, NOB, Anammox and others) and accounts for a percentage of the total ammonium concentration. The percentage of ammonia in this form increases at high pH values and may be calculated using the equation proposed by Levenspiel (1980):

$$[NH_3 - N] = \frac{[NH_4^+ - N + NH_3 - N] \times 10^{pH}}{10^{pH} + \exp\left(\frac{6344}{273 + T}\right)}$$

Figure 2.21 presents the FA content versus the ammonia nitrogen concentration for pH values between 6-9. Based on the equilibrium, at 20°C, an ammoniacal concentration of 500 mg N/L corresponds to 2 mg NH₃-N/L at a pH of 7 while the respective value at the pH of 8.5 is 55.8 mg NH₃-N/L. The FA content increases with temperature (2.8 mg NH₃-N/L at the pH of 7 and 76.2 mg NH₃-N/L at the pH of 8, for the same ammoniacal concentration, at 25°C).

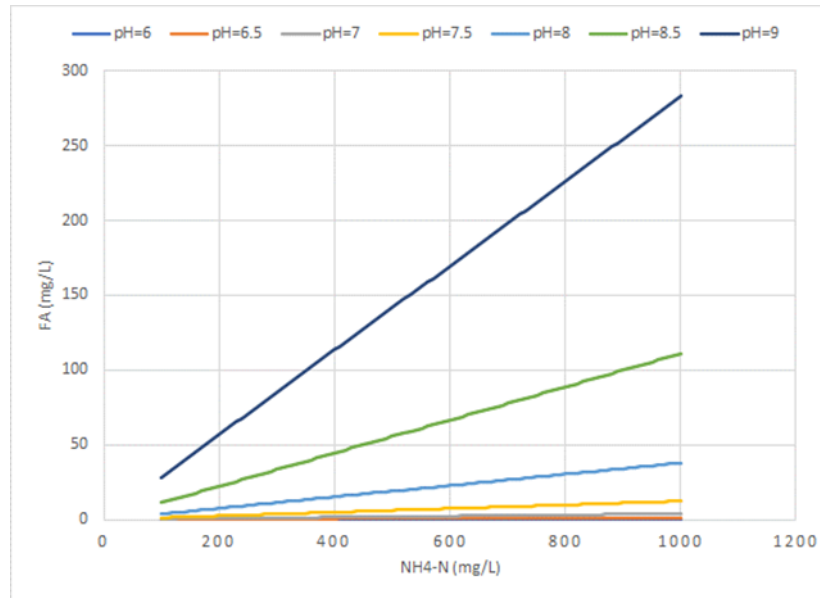


Figure 2.21. FA concentration at different NH₄-N and pH values at 20°C.

NOB shunt is achieved due to the fact that AOB are much more resilient to FA than NOB. The reported tolerances of these microbial groups to FA differ in the literature with acclimation to the inhibitor being an important factor. For instance Vadivelu et al. (2006) reported that NOB were fully inhibited at the FA concentration of 6 mg N/L while Jiang et al. (2021) reported that NOB were capable of acclimatizing to FA concentrations up to 715.3 ± 47.3 mg N/L. The authors observed that this was due to a shift of the dominant NOB genus from *Nitrospira* to *Nitroleuca*. They also noted that *Nitrosomonas* could sustain its activity at FA concentrations up to 62.1 ± 0.1 mg N/L. Park and Bae (2009) determined AOB and NOB inhibition by FA to be best described by an uncompetitive inhibition model with an inhibition constant of 4-22.4 mg N/L for AOB and 0.6 mg N/L for NOB.

In recent years, some studies have reported that PAOs can also be inhibited by FA (Zheng et al., 2013; Yang et al., 2018). These studies have focused mainly on the growth of PAOs under the prolonged influence of FA. Zheng et al. (2013) reported an FA threshold concentration of 17.76 mg N/L for PAO growth and observed that the PAO population had deteriorated significantly after exposure to said FA concentration while the population of GAOs had increased. Similarly, Yang et al. (2018) observed a severe inhibition of PAOs (by over 90%) following a 24 hour exposure to 16 mg NH₃-N/L. The results of these studies would suggest that the presence of FA may provide a competitive advantage to GAOs.

Another known inhibitor of many microorganisms is Free Nitrous Acid (FNA), which is the protonated form of nitrite. Contrary to FA, the percentage of nitrite in the form of FNA

becomes greater adversely to pH and can be calculated with the following equation (Levenspiel, 1980):

$$[HNO_2 - N] = \frac{[NO_2^- - N]}{10^{pH} \times \exp\left(-\frac{2300}{273 + T}\right)}$$

Figure 2.22 illustrates the FNA content versus the nitrite nitrogen concentration for pH values between 6-9. Based on the equilibrium, at 20°C, a 200 mg NO₂-N/L corresponds to 51.3 µg HNO₂-N/L at a pH of 7 while the respective value at the pH of 8.5 is merely 1.6 µg HNO₂-N/L.

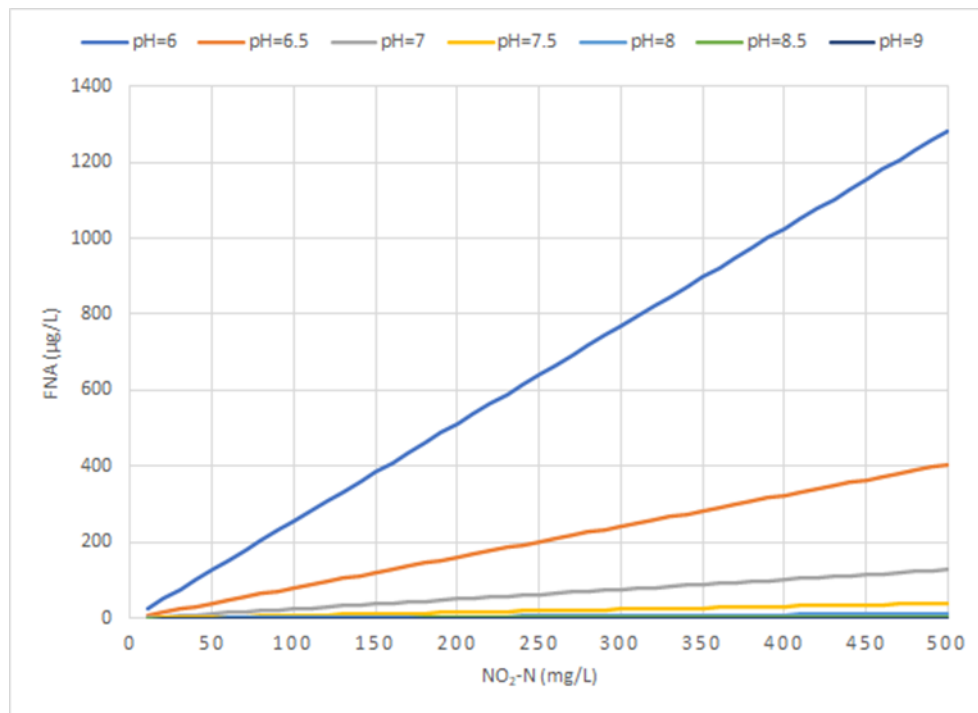


Figure 2.22. FNA concentration with respect to nitrite and pH values at 20°C

FNA is also an inhibitor of AOB and NOB and generally affects NOB to a greater extent. Park and Bae (2009) determined AOB and NOB inhibition by FNA to be best described by a non-competitive inhibition model with an inhibition constant of 168 µg N/L for AOB and 23.8-95.2 µg N/L for NOB. As such, the accumulation of FNA due to nitrite production in nitrification systems along with the biochemical drop of pH that accompanies it could further promote NOB shunt.

However, FNA has also been found to inhibit PAOs (Zhou et al., 2007). The exact mechanism of PAO inhibition by FNA is not clear as of this point. Zhou et al. (2007) suggested that the enzymes involved in the uptake of phosphorus are directly inhibited by FNA. Poly-P is synthesized by poly-P kinases (PPK), which reversibly transfer the phosphate residue from a high energy donor to the poly-P chain (Keasling et al., 2000). Increasing FNA concentrations have been found to positively correlate with reduced intracellular adenosine triphosphate (ATP) levels (Zhou et al., 2010) while also inhibiting phosphorus uptake which is likely the result of harm to PPK (Wang et al., 2011).

The effect of FNA on PAOs has been studied in regard to the uptake of phosphorus, growth and PHA oxidation with the severity of inhibition varying in the literature. Saito et al. (2004) reported that the aerobic uptake of phosphorus was fully inhibited at the FNA concentration of 1.5 $\mu\text{g N/L}$, while Pijuan et al. (2010) reported that the aerobic phosphorus uptake rate (PUR) was inhibited by 50% at 0.52 $\mu\text{g N/L}$ and by 100% at 4 $\mu\text{g N/L}$. Zhou et al. (2012) investigated the effect of FNA on an acclimated biomass and observed that aerobic phosphorus uptake was fully inhibited at the FNA concentration of 10 $\mu\text{g N/L}$, while anoxic phosphorus uptake was fully inhibited at the FNA concentration of 5 $\mu\text{g N/L}$, suggesting that the anoxic pathway is less tolerant to FNA. This would contradict the findings of Zhou et al. (2010) who reported that anoxic P-uptake ceased at the FNA concentration of 37 $\mu\text{g/L}$. Pijuan et al. (2010) also studied the effect of FNA on the growth of non-acclimated PAOs and reported 50% and 100% inhibition at the FNA concentrations of 0.36 $\mu\text{g N/L}$ and 7 $\mu\text{g N/L}$ respectively. Zhou et al. (2012) studied the effect of FNA on PAOs that were acclimated to an FNA concentration of 0.9 $\mu\text{g N/L}$ and reported that both aerobic and anoxic cell growth were fully inhibited at the FNA concentration of 10 $\mu\text{g/L}$. Regarding the effect of FNA on the catabolic processes of PAOs, Pijuan et al. (2010) observed that the PHA oxidation rate was slowed by up to 40-50% at the FNA concentration of 2 $\mu\text{g N/L}$ but did not decrease further at greater FNA concentrations. In agreement, Zhou et al. (2010) reported that the anoxic PHA oxidation rate remained constant at 60% of its original rate for FNA concentrations between 20 and 70 $\mu\text{g N/L}$.

The differences in acclimation of PAOs to FNA may be attributed to the composition of the group. In general, the PAO II type appears to display a higher tolerance to FNA than the PAO I group. The most resistant strain to FNA accumulation has been identified to be PAO IID, which is the most abundant in nitrification systems (Zeng et al., 2016a).

FNA has also been found to inhibit GAOs. Ye et al. (2010) studied the effect of FNA on the growth of *Competibacter* and reported that the growth rate was inhibited by 50% under the FNA concentration of 1.5 $\mu\text{g N/L}$ and by 100% at 7 $\mu\text{g N/L}$. After comparing the effects of FNA on glycogen production by GAOs and P-uptake by PAOs, the authors suggested that FNA inhibition may provide a competitive advantage to GAOs.

Chapter 3: Thesis objectives

As discussed in Chapter 2, the application of EBPR in short-cut nitrification systems poses certain challenges. The difficulties associated with this, mainly concern the significantly high ammonium and nitrite concentrations that characterize such systems. As seen, the inhibition of NOB for the promotion of the nitrification/denitrification pathway requires significant ammonium concentrations. As such, the removal of nitrogen will result in great accumulations of nitrite during aeration. Nitrite in the form of FNA, that is more abundant at lower pH, is a known inhibitor of PAOs. However, its reported impact on the activity of PAOs differs in the literature. This is more pronounced for the anoxic activities of PAOs, as reports regarding the tolerance of phosphorus removal via denitrification compared to aerobic P-removal appear contradictory. A reliable way of assessing the effect of FNA on PAOs is by observing its effect on the phosphorus uptake rate (PUR) of PAOs. PUR is a direct indicator of the performance of PAOs and is proportionally associated with all anabolic processes of PAOs. The highest reported tolerance of aerobic PUR inhibition by FNA is a threshold of 10 $\mu\text{g HNO}_2\text{-N/L}$ (the concentration above which PUR is fully inhibited), while the same study reports a threshold concentration of 5 $\mu\text{g HNO}_2\text{-N/L}$ for anoxic PUR. This would indicate that anoxic P-removal is less tolerant to FNA than aerobic P-removal. However, another study has reported a much higher threshold for anoxic PUR (at 37 $\mu\text{g HNO}_2\text{-N/L}$), while others report much lower threshold concentrations for aerobic PUR. These contradictions may be due to differences in acclimation to FNA of the PAO-enriched cultures that were studied. As the portion of nitrite in the form of FNA is dictated by pH, the variation of pH may play a key role in the performance of PAOs under these conditions.

In addition to the challenges posed by nitrite accumulations, there have been recent reports that ammonium, specifically FA, is also an inhibitor of PAOs. Information regarding the effect of FA on PAOs is significantly limited as of this point, as the relevant few studies are mostly focused on the prolonged exposure of PAOs to the inhibitor. As FA is required for NOB shunt, PAOs may face increasingly adverse conditions in high nitrogen loading systems. The concentration of FA is also dependent of pH, however unlike FNA, FA is more abundant at higher pH values. As such, while controlling pH at a high value may lessen the inhibitory effect of nitrite on PAOs, it would increase the inhibitory effect of ammonium. In light of this, the proper assessment of the effect of FA on PAOs could provide valuable information regarding pH manipulation for the optimum conditions for PAOs.

Based on the above, it becomes clear that nitrogen loading and pH are of great importance for the application of EBPR. As discussed in Chapter 2, reject water is generally characterized by high pH values, that transcend to high FA concentrations. As ammonium is converted to nitrite through nitrification, lower pH values result in higher overall PAO inhibition. This is problematic by itself since nitrification is accompanied by a natural biochemical drop of pH. Conditions for PAOs may improve during denitrification, as nitrite is removed along with a rise in pH. However, the residual ammonium content may prove to have a significant effect on PAOs as pH increases. In all cases, the inhibitory conditions for PAOs are governed by the combined presence of nitrite and ammonium with special regard to pH. The proper assessment of the combined effect of FA

and FNA on P-removal requires not only information regarding the effect of either FNA or FA on PAOs, but also the mode of inhibition for each inhibitor. To date, the mode of FNA inhibition on PAOs has not been established, more so for the case of FA inhibition, for which basic information is limited. In addition, experiments regarding the combined effect of FNA and FA on PAOs have not been conducted, since the adverse effect of FA has only recently come to light. Research focusing on the modes of inhibition and the combined effect of both inhibitors could help establish a combined inhibition model for PAOs, which would provide valuable information regarding nitrogen loading and pH manipulation for the effective application of EBPR.

While high nitrogen loading conditions appear threatening to EBPR in themselves, PAOs may face a higher threat from the growth and prevalence of GAOs. As the growth and performance of PAOs is negatively affected by the combined presence of FNA and FA, the tolerance of GAOs to these inhibitors is also of importance, as a higher resilience to these inhibitors may promote their differential growth over PAOs, leading to the deterioration of EBPR. While there are some reports on the effect of FNA on GAOs, information is rather limited, while no information exists on the effect of FA. Information regarding the effect of FNA and FA on GAOs and comparison with their effect on PAOs would assist in examining the feasibility of EBPR in conditions of high nitrite and ammonium accumulations. In addition, the development of strategies aiming at the suppression of GAOs are of great importance for the successful application of EBPR. Various studies have reported on such strategies with special consideration to the carbon source, pH manipulation, temperature, the SRT, as well as the capacity of each group to use nitrite as an electron acceptor. However, most strategies have been tested in systems that are closer to the characteristics of typical mainstream WWTP's, rather than systems that are characterized by high nitrogen loading. Therefore, the examination and development of such strategies in conditions of higher nitrite accumulations could help the assessment of their effectiveness for full-scale applications.

In light of the above, the overall aim of this study is to investigate the optimum conditions for the achievement of successful EBPR in high nitrogen loading systems, namely for the side-treatment of reject water that is characterized by a low C/N ratio. The study focuses on the inhibitory effect of FNA and FA on PAOs and GAOs, the development of strategies for GAO suppression and PAO proliferation, and the optimization of EBPR under these conditions. Specifically, the goals of this work may be summed up as follows:

- Determination of the effect of FNA on PAOs along with the mode of inhibition. The investigation involves a series of experiments on a PAO-enriched biomass that is developed under laboratory conditions and focuses on the effect of various nitrite concentrations at different pH values on the aerobic and anoxic PUR of PAOs. The investigation is performed in order to clearly assess the effect of FNA on PAOs, which as mentioned, shows inconsistency in the literature. The experiments aim to develop an inhibition model for the effect of FNA on PAOs, which may be used to assess the performance and growth of PAOs in conditions of high nitrite concentrations, with regard to pH.
- Determination of the effect of FA on PAOs along with the mode of inhibition. Similarly to the investigation of the effect of FNA, this assessment involves a series of

experiments on a PAO-enriched biomass, developed under laboratory conditions, and focuses on the effect of various ammonium concentrations at different pH values on the aerobic and anoxic PUR of PAOs. The experiments aim to provide valuable new information regarding the effect of FA on PAOs, which is almost non-existent, and to develop an inhibition model for the effect of FA on PAOs, which may be used to assess the performance and growth of PAOs in conditions of high ammonium concentrations, with regard to pH.

- Determination of the combined effect of FNA and FA on PAOs and optimization of pH. The investigation involves a series of experiments regarding the combined effect of ammonium and nitrite on the PUR of PAOs. The results of these experiments are used to validate a combined inhibition model, that is based on the models developed for FNA and FA, which is developed by an enzymatic approach based on the simultaneous presence of both inhibitors. The combined inhibition model is used to determine the optimum pH variation for EBPR throughout the nitrification and denitrification processes.
- Determination of the effect of FNA and FA on GAOs and their respective modes of inhibition. The investigation involves a series of experiments that focus on the effect of FNA and FA on the growth of a highly GAO-enriched biomass, developed under laboratory conditions. The investigation aims to provide new information regarding GAO inhibition by FNA and FA and to develop an inhibition model for GAOs. The results of this investigation are compared to the results regarding PAO-inhibition. The derived models provide valuable information in assessing the possible wash-out of PAOs in conditions of high FA and FNA accumulations.
- Development of strategies for the proliferation of PAOs over GAOs in conditions of high FNA accumulations. This investigation revolves around the examination of various configurations, with special regard to the carbon source and the anoxic/aerobic retention time, for the in-situ suppression of GAOs and the promotion of PAOs. The investigation aims to examine the effectiveness of various strategies for the proliferation of PAOs under inhibitive conditions.
- Optimization of EBPR under high ammonium and nitrite accumulations and proposals for full-scale operation of side-stream reject water treatment systems. This investigation utilizes the combined inhibition model and assesses the capacity for EBPR at various nitrogen loading rates (NLRs), via a series of mathematical simulations. The simulations examine the effect of ammonium and nitrite on aerobic and anoxic PUR throughout the nitrification and denitrification processes, both at an uncontrolled pH variation and at a pH variation that is optimized for EBPR. The examined configurations also take into account the developed strategies for GAO suppression. The evaluation of EBPR at various NLRs is performed with respect to the PAO population and their performance under these conditions, along with the required phosphorus removal based on the P/N ratio of the reject water, while also considering their possible wash-out by GAOs. The investigation aims to propose optimized EBPR configurations that may achieve stable and sufficient phosphorus removal at the highest possible NLR, with and without pH manipulation.

Chapter 4: Materials and methods

4.1 Experimental set-up

As stated in Chapter 3, the investigation of the inhibitory effect of FNA and FA on PAOs and GAOs along with the development of strategies for GAO suppression and PAO proliferation under conditions of nitrification/denitrification, required the development of these microbial communities under laboratory conditions. To this end, a Sequencing Batch Reactor (SBR) was set up in the Sanitary Engineering Laboratory of the Department of Water Resources and Environmental Engineering (School of Civil Engineering, National Technical University of Athens). The system's configuration has seen variation for each experimental period, depending on the goals of the investigation, but generally consisted of the following equipment (Figure 4.1).

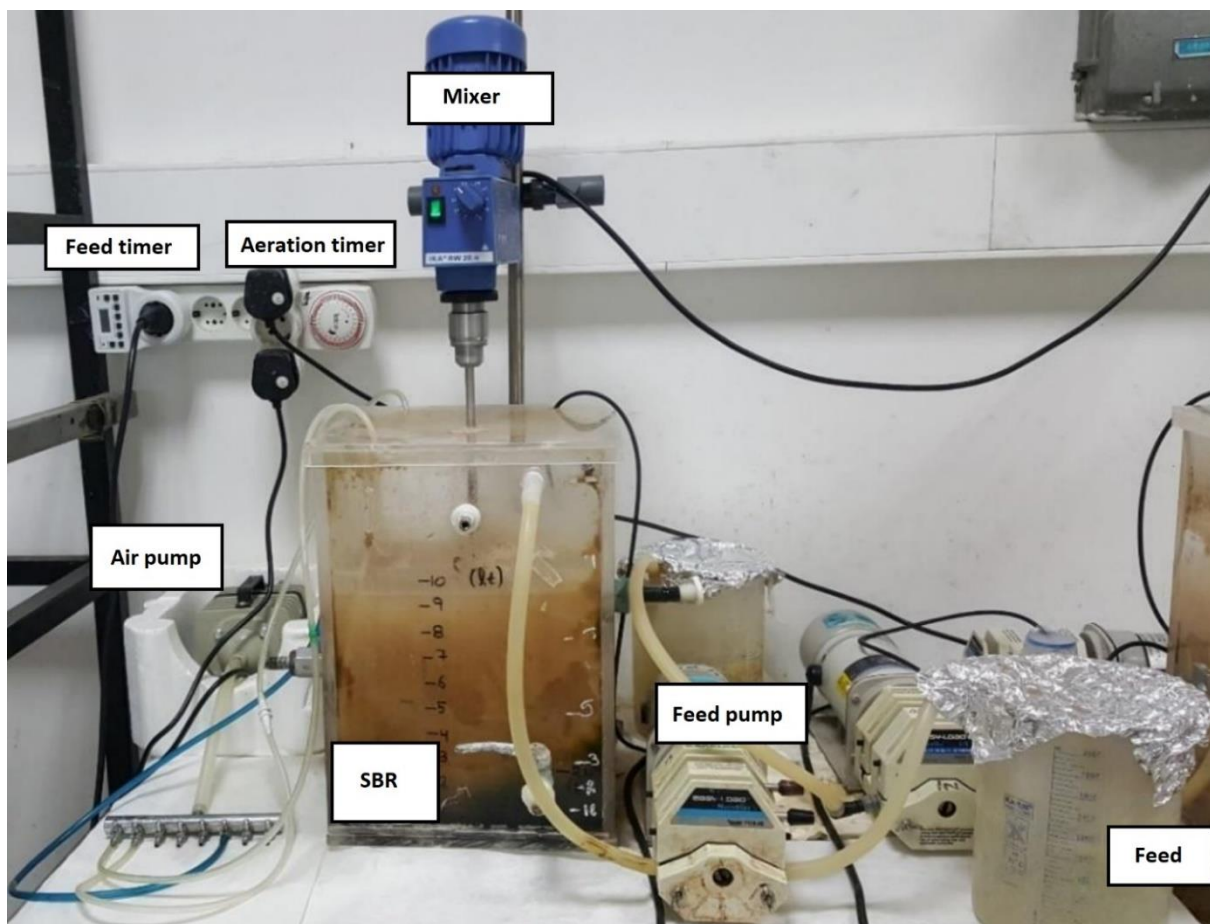


Figure 4.1. Experimental setup

The reactor was a 14 L rectangular tank, made of plexiglass. The removable cap had a suitable hole drilled down the middle, that allowed the application of a mechanical stirrer. The mixer's propeller reached a satisfactory depth (around 30 cm from the tank floor) which allowed effective mixing conditions in the reactor. Aeration was carried out through commercial air stones that were attached to the bottom of the tank and connected to an air pump via thin plastic tubes. The air pump was put in motion at the appropriate time periods, based on the

SBR's configuration, with the use of a timer. A second timer was used to activate a screw pump, at the selected time periods, that would provide feed to the SBR, via a connected plastic tube. Feed consisted of synthetic wastewater for the most part, the composition of which was specific to the objectives of each operational period.

The use of the SBR may be divided into 10 operational periods, depending on its configuration and its targeted development. At the start of each operational period, the SBR was reset and provided with a new inoculum from the WWTP of Psytalia. The configurations employed are listed below.

SBR1

SBR1 was setup in order to develop a PAO-enriched biomass that was used to fuel a series of ex-situ batch experiments regarding the effects of FNA and FA on the aerobic PUR of PAOs. During the start-up period the SBR operated on 2 daily cycles each consisting of an anaerobic phase, an aerobic phase and an anoxic phase, while settling and decanting was carried out once per day over a 2-hour period, manually. Initially the first cycle consisted of a 3-hour anaerobic phase followed by a 7-hour aerobic phase and a 2-hour anoxic phase, while the second cycle consisted of a 2-hour anaerobic phase followed by a 6 hour aerobic phase and a 2 hour anoxic phase. Following a period of approximately 15 days, both daily cycles were modified to consist of a 3-hour anaerobic phase followed by a 6-hour aerobic phase and a 1-hour anoxic phase.

Feed consisted of a concentrated mixture of acetate, ammonium and phosphorus that was introduced at the beginning of each anaerobic and each anoxic phase. The volume of each dose was 250 mL. Prior to decanting, the SBR contained 10.5 L of liquor. Following the removal of 5.5 L of effluent, 5.5 L of water was added to the SBR bringing the mixed liquor's volume to 10.5 L. Under mixing conditions, 1 L of mixed liquor was removed in order to achieve a SRT of around 10 days. Thus, with the daily addition of 1 L of the concentrated feed, the SBR's working volume averaged at 10 L simulating a HRT of around 2 days.

The addition of a carbon source at the beginning of the anaerobic phase would provide PAOs with an advantage over common heterotrophic organisms, giving them priority in the utilization of COD. During the aerobic phase, the sufficient DO concentrations (>3 mg/L) would allow PAOs to develop by oxidizing their stored PHAs, while residual acetate would be rapidly removed by other heterotrophs. Since some nitrification is expected during the aerobic phase, following the cease of aeration, feed is reintroduced to the SBR in order to allow the rapid removal of any produced nitrate or possibly nitrite via denitrification prior to the next anaerobic phase. In essence, this nominal anoxic phase is mostly anaerobic and is to ensure strictly anaerobic conditions at the beginning of the next cycle.

The daily dose of COD was gradually increased from 5 g/d to 8 g/d over a period of approximately 20 days. The dose of 8 g COD/d was regulated with respect to the aerobic SRT (≈ 6 days) in order to achieve a biomass concentration of around 2,500 mg VSS/L. The reason for the lower early dosages was primarily in order to avoid accumulations of COD that could cause bulking problems and secondarily to hasten the shift in the biomass from a mostly common heterotrophic community to a PAO-enriched sludge. More specifically, since the seed sludge contained a very low PAO population, practically all of the acetate introduced at the start of the anaerobic phase would be available at the aerobic phase. This abundance of a readily

biodegradable source of COD could in short time deteriorate the quality characteristics of biomass and lead to bulking problems, causing a strain on the system's operation. Additionally, while PAOs would always have priority over common heterotrophs in the utilization of acetate, it is possible that the presence of a large heterotrophic community could prove antagonistic in the utilization of nutrients and the availability of oxygen, slowing the growth of PAOs.

The daily dose of ammonium was gradually increased up to 600 mg N/d over a period of approximately 20 days, similarly to the dose of COD. This strategy was primarily selected in order to ensure an adequate source of nitrogen for biomass growth and also to allow some nitrification. During the start-up period, ammonium concentrations in the effluent were monitored on a daily basis and the daily dosage was modified in order to maintain effluent concentrations lower than 10 mg NH₄-N /L to prevent accumulation of ammonium in the SBR.

The daily dose of phosphorus was 200 mg PO₄-P/d, a dose much greater than the stoichiometric demand for growth of heterotrophs in order to selectively promote the growth of PAOs. This dosage would also compensate for the phosphorus that is removed via chemical precipitation, allowing the availability of an adequate phosphorus source to be taken up by PAOs throughout the aerobic phase. Access to phosphorus under aerobic conditions is important for PAOs as it is required for them to reform their intracellular polyphosphate chains. Inability to do so would result in a failure to take up acetate during the following anaerobic phase as no energy can be produced from the hydrolysis of these chains. Consequently, if the phosphorus released anaerobically by PAOs were to be removed from solution due to chemical precipitation (primarily by the formation of struvite due to an increase in pH), this would most likely result in a shift in the biomass in the favour of GAOs which do not require phosphorus and ultimately the wash-out of PAOs from the system. Since great increases in pH were observed during aeration for reasons described below, providing the SBR with a significant dosage of phosphorus was of strategic importance for the growth and maintenance of PAOs.

Having concluded the series of experiments on what was considered a non-acclimatized biomass, nitrogen loading of the SBR was gradually increased, while the SRT was lowered in an attempt to raise nitrite concentrations during the aerobic phase. Specifically, ammonium loading in the SBR was gradually increased from 0.06 kg NH₄-N/m³ d to 0.15 kg NH₄-N/m³ d over a period of 30 days, while the SRT was lowered to 8 days. The new aerobic SRT of 4.5 days would limit the presence of NOB in the biomass, resulting in less nitrite being converted to nitrate during aeration.

Following the transitional period of 30 days, the SBR was maintained under the new conditions for 15 days, after which four additional batch experiments similar to the original series were conducted. The objective of these experiments was to determine if the biomass would exhibit a stronger tolerance to FNA due to acclimation to greater FNA concentrations in the SBR.

SBR2

SBR2 was setup in order to examine the tolerance of PAOs to FNA when developed under conditions of minimum FNA presence. The SBR's configuration remained identical to that of SBR1 with the only difference being that the ammonium loading rate was lowered to 0.03 kg NH₄-N/m³ d compared to the 0.06 kg NH₄-N/m³ d loading rate of the previous configuration during steady state operation. This ammonium loading would just about satisfy the

stoichiometric demand for microbial synthesis and significantly limit nitrification, ultimately leading to the washout of AOB from the SBR.

SBR3

SBR3 was setup in order to develop a PAO-enriched biomass that was used to fuel a series of ex-situ batch experiments regarding the effects of FNA and FA on the anoxic PUR of PAOs (via denitrification). During the start-up period the SBR operated on 4 daily cycles each consisting of an anaerobic phase, an aerobic phase and an anoxic phase. Settling and decanting occurred once per day over a 2-hour period due to technical limitations. Each cycle initially consisted of a 1-hour anaerobic phase followed by a 3-hour aerobic phase and a 1.5 hour anoxic phase.

Feed consisted of reject water from the dewatering unit of the WWTP of Psytalia that was appropriately diluted and enriched with sodium propionate, potassium phosphate and in time ammonium chloride. Each day 800 mL of the mixture were pumped into the SBR in 8 doses (2 per cycle) of 100 mL. Dilution of the reject water was carried out in order to achieve the desired ammonium concentration in the feed that was dictated by the ammonium loading of each step. Prior to decanting, the SBR contained 10.4 L of liquor. Following the removal of 5.4 L of effluent, 5.4 L of water was added to the SBR bringing the mixed liquor's volume to 10.4 L. Under mixing conditions, 1 L of mixed liquor was removed in order to achieve a SRT of around 10 days. Thus, with the daily addition of 800 mL of the concentrated feed, the SBR's working volume averaged at 10 L simulating a HRT of around 2 days.

The addition of a carbon source at the beginning of the anaerobic phase would provide PAOs with an advantage over common heterotrophic organisms, giving them priority in the utilization of COD. During the aerobic phase, the sufficient DO concentrations (>3 mg/L) would allow PAOs to develop by oxidizing their stored PHAs, while the residual propionate would be rapidly removed by other heterotrophs. With the cease of aeration and the rapid depletion of the remaining DO (within 5 minutes), the SBR was left without the addition of a carbon source during the first hour of the anoxic phase. This was in aim of providing PAOs with a competitive advantage over common heterotrophs. As no propionate remained available by the start of the anoxic phase, PAOs would always have priority in the utilization of nitrite and nitrate. Feed was reintroduced 30 minutes prior to the beginning of the next cycle in order to remove any remaining nitrite and nitrate, thus ensuring proper anaerobic conditions at the start of the next phase.

Over the first 30 days of the start-up period, the daily dose of COD was gradually increased from 5 g/d to 7 g/d, while the daily dose of ammonium was gradually increased from 400 to 800 mg N/d. The daily dose of phosphorus was 500 mg $\text{PO}_4\text{-P/d}$, a dose much greater than the stoichiometric demand for growth of heterotrophs in order to selectively promote the growth of PAOs. This dosage would also compensate for the phosphorus that is removed via chemical precipitation, allowing the availability of an adequate phosphorus source to be taken up by PAOs throughout the aerobic and the subsequent anoxic phase. The COD and ammonium concentrations in the feed were regularly modified with regard to concentrations in the effluent in order to avoid their accumulation in the SBR.

The primary main objective of this initial period was to allow the growth of PAOs capable of denitrification and their acclimation to low FNA concentrations. This would require the presence

of nitrite during the anoxic phase in order to allow denitrification by PAOs but not at a concentration that would significantly inhibit their growth due to the related FNA presence during both the aerobic and anoxic phase. The relatively low aerobic SRT of 5 days would provide some suppression of NOB making nitrite available for the anoxic phase and its concentration regulated by the ammonium load. It is possible that the cultivation of PAO species with a capacity for denitrification may also be achieved via the availability of nitrate. As of this point it is not clear if PAOs have the capacity to directly reduce nitrate or if the presence of GAOs is required to first reduce nitrate to nitrite that can then be utilized by PAOs in a synergistic denitrification process. However, it is certain that this would enhance the presence of GAOs in the biomass which could endanger the growth of PAOs.

At this point the SBR's configuration was altered so that each cycle now consisted of a 1 hour anaerobic phase, a 2 hour aerobic phase and a 2.5 anoxic phase with feed being introduced at the start of the anaerobic phase and 1.5 hours into the anoxic phase. The lower aerobic SRT would allow further NOB suppression resulting in greater nitrite concentrations within the SBR. This in turn would promote the anoxic growth of PAOs via denitrification. As it has been reported that GAOs are incapable of denitrification with propionate as the sole carbon source this would provide PAOs with a significant advantage, ultimately leading to the wash-out of GAOs from the SBR.

Under the new configuration the daily dose of COD was gradually increased up to 8 g/d, while the daily dose of ammonium was gradually increased up to 1000 mg N/d over a period of 30 days and was maintained under the new conditions for a further 30 days prior to the beginning of the experiments.

SBR4

SBR4 was setup in order to investigate the combined effect of FNA and FA on PAOs. The SBR's configuration and performance was practically identical to that of SBR3. The re-setting of this configuration was in order to examine the mechanism of the combined FNA and FA inhibition both under conditions in which the biomass was not yet acclimatized, and upon acclimation to these inhibitors.

SBR5

SBR5 was setup for the development of a significantly highly GAO-enriched biomass, in order to investigate the effect of FNA and FA on GAOs.

During the start-up period the SBR operated on 4 daily cycles each consisting of a 1 h anaerobic phase, a 3 h aerobic phase and a 1.5 h endogenous phase. Settling and decanting occurred once per day over a 2-hour period due to technical limitations.

Feed consisted of a concentrated mixture of acetate and ammonium that was introduced at the beginning of each anaerobic phase. The volume of each dose was 250 mL. Before decanting, the SBR contained 10.5 L of liquor. Following the removal of 5.5 L of effluent, 5.5 L of water was added to the SBR bringing the mixed liquor's volume to 10.5 L. Under mixing conditions, 1 L of mixed liquor was removed in order to achieve a SRT of 10 days. Thus, with the daily addition of 1 L of the concentrated feed, the SBR's working volume averaged at 10 L simulating a HRT of 2 days.

In order to prevent the growth of PAOs, the concentration of phosphorus in the SBR was routinely monitored and kept below 1 mg/L with the occasional addition of a potassium phosphate solution to provide for the growth of GAOs. A thiourea solution was added daily following the refilling of the SBR as to maintain a concentration of 20 mg/L for the suppression of both AOB and NOB. The addition of a carbon source at the beginning of the anaerobic phase would provide GAOs with an advantage over common heterotrophic organisms, giving them priority in the utilization of COD. During the aerobic phase, the sufficient DO concentrations (>3 mg/L) would allow GAOs to develop by oxidizing their stored PHAs, while residual acetate would be rapidly removed by other heterotrophs. With the cease of aeration, the SBR remained without the addition of a carbon source for 1.5 h for the endogenous removal of the dissolved oxygen prior to the following anaerobic phase. Over time, by the end of the anaerobic phase less and less acetate would remain available to be oxidized by common heterotrophs, leading to the development of a practically pure GAO culture.

The daily dose of COD was 7 g/d, regulated with respect to the aerobic SRT (≈ 5 d) in order to achieve a biomass concentration of around 2,000 mg VSS/L. The daily dose of ammonium was 300 mg N/d in order to ensure an adequate source of nitrogen for biomass growth. Ammonium concentrations in the effluent were monitored on a daily basis and the daily dosage was modified in order to maintain effluent concentrations lower than 10 mg $\text{NH}_4\text{-N}$ /L to prevent accumulation of ammonium in the SBR.

SBR6, SBR7 and SBR8

SBRs 6,7 and 8 were set up in order to investigate the role of the carbon source in the PAO-GAO competition under conditions of nitrification/denitrification. The 3 operational systems shared the same configuration, with the type of carbon in the feed being the only difference. SBR6 operated with acetate as the sole carbon source, SBR7 operated with a 50-50 mixture of acetate and propionate, while SBR8 operated with the regular rotation of acetate and propionate as the sole carbon source.

In each case, the SBR operated on 3 daily cycles each consisting of a 1.5 h anaerobic phase, a 3.5 h aerobic phase and a 2.5 h anoxic phase. Settling and decanting occurred once per day over a 1.5 h period due to technical limitations. Feed consisted of a concentrated mixture of VFAs, ammonium and phosphorus that was introduced at the beginning of each anaerobic and each anoxic phase. The volume of each dose was 200 mL. Prior to decanting, the SBR contained 10.6 L of liquor. Following the removal of 5.6 L of effluent, 5.2 L of water was added to the SBR bringing the mixed liquor's volume to 10.2 L. Under mixing conditions, 0.8 L of mixed liquor was removed in order to achieve a SRT of 8 d. Thus, with the daily addition of 1.2 L of the concentrated feed, the SBR's working volume averaged at 10 L simulating a HRT of 2 d.

The addition of a carbon source at the beginning of the anaerobic phase would provide PAOs with an advantage over common heterotrophic organisms, giving them priority in the utilization of COD. During the aerobic phase, the sufficient DO concentrations (>3 mg/L) would allow PAOs to develop by oxidizing their stored PHAs, while residual acetate would be rapidly removed by other heterotrophs. Following the cease of aeration, feed was reintroduced to the SBR in order to allow the rapid removal of nitrate and nitrite that was produced during the aerobic phase via denitrification prior to the next anaerobic phase.

The daily dose of COD was gradually increased from 5 g/d to 8.5 g/d over a period of approximately 20 days. The dose of 8.5 g COD/d was regulated in order to achieve a biomass concentration of around 2,500 mg VSS/L. The daily dose of ammonium was gradually increased from 0.6 to 1.8 g NH₄-N/d over a period of approximately 20 days, similarly to the dose of COD. The dose was regulated in order to allow the gradual increase of nitrite concentrations in the SBR. This would be achieved by the partial suppression of NOB due to the relatively low aerobic retention time (3.5 d). Ammonium concentrations in the effluent were monitored on a daily basis and the daily dosage was modified in order to maintain effluent concentrations lower than 30 mg NH₄-N /L to prevent accumulation of ammonium in the SBR. The daily dose of phosphorus was 200 mg PO₄-P/d, a dose much greater than the stoichiometric demand for growth of common heterotrophs in order to selectively promote the growth of PAOs. This dosage would also compensate for the phosphorus that is removed via chemical precipitation, allowing the availability of an adequate phosphorus source to be taken up by PAOs throughout the aerobic phase.

The results of the investigations conducted are presented in section 5.6.1.

SBR9

SBR 9 was set up in order to examine the extent of the effect that FNA had on the shift in the biomass towards the proliferation of GAOs, as observed in SBR6 (in which acetate was the sole carbon source). The system's configuration remained as that of SBR6-8 with acetate as the only type of carbon in the feed, but with a lower ammonium loading rate (0.6 g NH₄-N/d) throughout operation. Ammonium concentrations in the effluent were monitored on a daily basis and the daily dosage was modified in order to maintain effluent concentrations lower than 10 mg NH₄-N /L to prevent accumulation of ammonium in the SBR. With this, nitrite (and therefore FNA) concentrations in the SBR were expected to be significantly lower than the ones observed throughout the operation of SBR6. The performance of PAOs over time in SBR9 was then compared to that observed in SBR6, for the assessment of the role of FNA in the PAO-GAO competition. The results of this investigation are presented in section 5.6.2.

SBR10

SBR10 employed the same configuration as SBR3 and SBR4 which was found to be the optimum configuration for the development of PAOs under laboratory conditions. Following its stable performance at the vNLR of 0.1 kg N/m³ d, nitrogen loading was raised to 0.15 kg N/m³ d in order to evaluate and compare the biomass's capacity for EBPR under the new conditions. Following this second phase of operation, the system was set to perform at a lower pH (6.5) in order to determine the sustainability of PAOs under high FNA accumulations without the need of increasing nitrogen loading. To achieve this, the HRT was increased to 10 days (by decanting 1 L of effluent every day, which was just enough for the 1 L of feed that would enter daily) in order to limit the renewal of the medium's alkalinity. With this, the effect of carbon stripping during aeration was minimal and the pH levels gradually dropped over a period of 7 days, reaching a value of 6.5 that would remain practically constant throughout each cycle. Following this, the SBR was operated under this constant pH for a period of 10 days, after which the system's performance was evaluated. The results of these evaluations are presented throughout section 5.6.3.

4.2 Experimental series

4.2.1 Experimental investigations regarding the activities of PAOs

A series of experimental investigations were conducted on the PAO-enriched biomasses discussed in section 4.1. These investigations concern the effect of FNA and FA on the aerobic and anoxic PUR of PAOs. The PUR displayed by PAOs is the most direct indicator of their performance, as it measures their capacity to remove phosphorus and, as discussed in chapter 2, factors that affect PUR have shown to proportionately affect the growth rate of PAOs (Mamais 1991; Pijuan et al., 2010; Zhou et al. 2012). This is of importance, as obtaining a significantly (practically pure) PAO-enriched biomass has proven extremely difficult due to the ever-present GAO populations that may sometimes exist even symbiotically with PAOs. As such, valid experiments regarding the effects of the aforementioned inhibitors on the growth rate of PAOs are hard to conduct, as the biomass's performance would not be fully representative of PAOs. While common heterotrophs (OHOs) may also take up phosphorus under various conditions for microbial synthesis, their respective uptake rates are significantly lower than that of a highly PAO-enriched biomass and may be considered negligible. Therefore, PUR inhibition by FNA and/or FA is an effective measure for the potency of these inhibitors both in terms of PAO performance and their growth.

4.2.1.1 Routine experiments for evaluating PUR

In order to properly evaluate the biomass's capacity to remove P in conditions of high DO concentration without the interference of precipitation phenomena, during each investigation period, regular ex-situ experiments were conducted under constant pH on sludge retrieved from the SBR. Typically, these experiments were conducted following feed of the SBR, where 500 ML of sludge were retrieved and placed into a container of similar working volume and stirred under anaerobic conditions for a period of 1 hour. Following this phase, the reactor was aerated for a period of up to 3 hours over which samples were retrieved every 30 minutes and analyzed for phosphorus content. Throughout the experiments, pH was controlled at its initial value with the regular addition of a 0.1N sulfuric acid solution.

PUR may be calculated as:

$$PUR \left(mg \frac{P}{g} VSS h \right) = - \frac{\Delta P}{\Delta t} \times \frac{1}{VSS} \quad (4.1)$$

where:

ΔP : the removal of phosphorus within a specific time period (Δt)

VSS: the volatile suspended solids of the examined sludge

Figure 4.2 displays the results of a typical experiment for the determination of PUR. As shown, phosphorus removal by PAOs appears to be linear throughout the experiment (which is usually the case for most experiments, especially in the absence of inhibitors). Since the biomass typically presents negligible growth within the brief time period of the experiment, PUR was generally determined based on the trendline of the experimental results for phosphorus during steady removal as:

$$PUR (mg P/g VSS h) = - \frac{dP}{dt} \times \frac{1}{VSS} \quad (4.2)$$

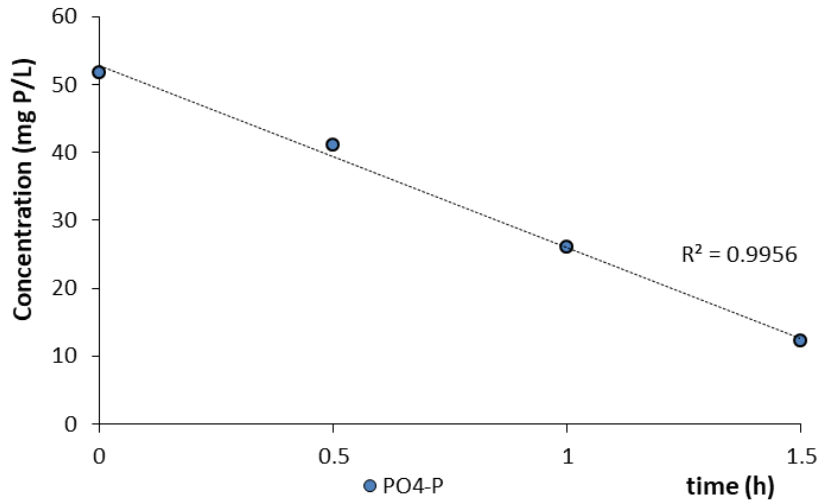


Figure 4.2. Typical ex situ batch experiment for determining aerobic PUR

In order to evaluate the biomass's capacity to remove P via denitrification, similar experiments (Figure 4.3) were routinely conducted on the sludge retrieved from the SBR. In these experiments however, following the 1 hour anaerobic period, rather than aerating the sample, an appropriate amount of a sodium nitrite solution was added in order to create an initial nitrite concentration of 10 mg N/L. This concentration was maintained at 10 ± 2 mg N/L throughout the experiment with the frequent addition of the sodium nitrite solution. The maintenance of this low concentration is due to the fact that FNA is an inhibitor of PUR, therefore greater nitrite concentrations would result in an inhibited observed PUR, especially at low pH values. As such, these routine experiments were carried out at the relatively high pH of 8. More information on the development of this experimental protocol may be found in section 5.2.2.1. When both aerobic and anoxic PURs were evaluated, both samples were maintained at the pH of 8 throughout the experiment.

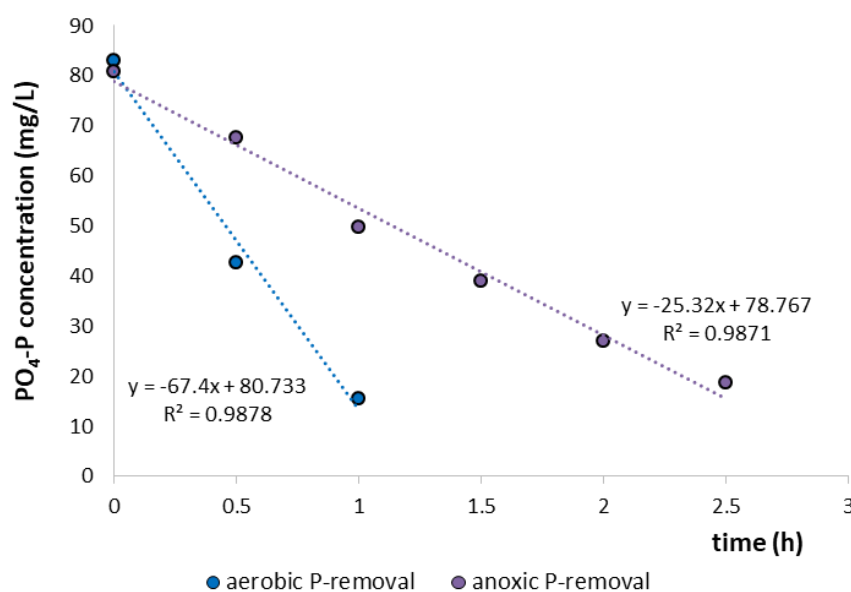


Figure 4.3. Typical ex situ batch experiment for determining aerobic and anoxic PUR

4.2.1.2 Experiments investigating PUR inhibition

The following experimental series were conducted on the developed PAO-enriched biomasses:

- Investigation of the effect of FNA on aerobic PUR (SBR1, SBR2)
- Investigation of the effect of FNA on anoxic PUR (SBR3)
- Investigation of the effect of FA on aerobic PUR (SBR1)
- Investigation of the effect of FA on anoxic PUR (SBR3)
- Investigation of the combined effect of FNA and FA on aerobic PUR (SBR4)

Each series involved multiple ex-situ batch experiments, each testing the effect of a specific inhibitor concentration on PUR. In each experiment, sludge was retrieved from the SBR and distributed into 3 containers of equal working volume (0.5 L). One container served as a control, while the others were used to test a single FNA or FA concentration as duplicate reactors. The only exception to this is the experimental series in which the combined effect of FNA and FA were investigated, wherein sludge was distributed into 4 reactors: one serving as a control, one testing a specific FNA concentration, one testing a specific FA concentration, and one containing the former concentrations of both inhibitors. Following feed and maintenance under a 1 h anaerobic period, the reactors were then either aerated or fed an appropriate amount of sodium nitrite solution in order to investigate the effects of each inhibitor concentration under either aerobic (as seen in Figure 4.4) or anoxic conditions (as seen in Figure 4.5). Throughout each experiment temperature was kept constant within a $\pm 1^\circ\text{C}$ range, via the regular appliance of ice packs to the reactors (As captured in Figure 4.5).

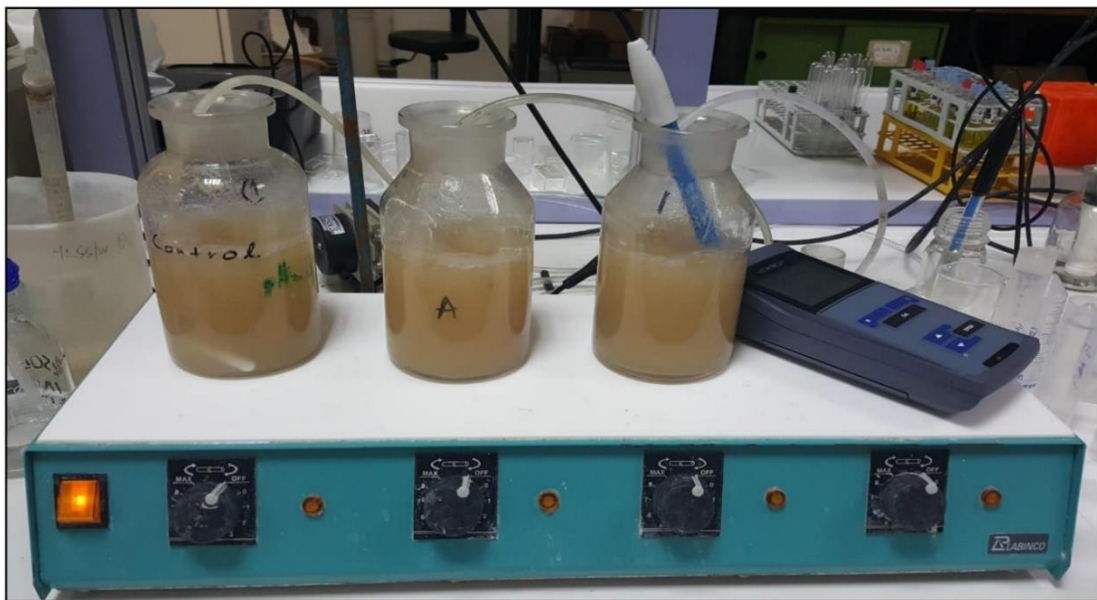


Figure 4.4. Samples during the aeration phase of a typical experiment investigating aerobic PUR.



Figure 4.5. Samples during the anoxic phase of a typical experiment investigating anoxic PUR. At this instance, ice packs have been applied to the reactors to keep temperature within the desired range.

The performance of each reactor was then compared to that of the control's in each case. The degree of PUR inhibition due to each specific inhibitor concentration was established as:

$$\text{Inhibition (\%)} = \frac{PUR_c - \frac{PUR_A + PUR_B}{2}}{PUR_c} \times 100\% \quad (4.3)$$

where

PUR_c : The PUR displayed by the control reactor (essentially PUR_{max})

PUR_A , PUR_B : The PURs displayed by the duplicate reactors

Figure 4.6 displays the results of a typical batch experiment investigating a specific inhibitor concentration. As shown, the control reactor performed at a better removal rate than the other reactors. While phosphorus removal in the control was stable from the beginning of aeration, the entry of the inhibitor in the other reactors would often cause a slight disturbance, resulting in a diminished PUR during the first 30-60 minutes of the experiment compared to their performance after. This may be due to a combination of a disturbance in the water chemistry and possibly a brief adaptation period of the biomass to the new conditions. Following this period, the reactors displayed a steady PUR up until the remaining phosphorus became significantly low or the capacity of the biomass to take up phosphorus had been largely saturated. In all cases, the PUR of each reactor was established for the duration where a stable performance was observed. As the VSS of each reactor were the same, the degree of inhibition could be calculated directly by the slopes of the removed phosphorus.

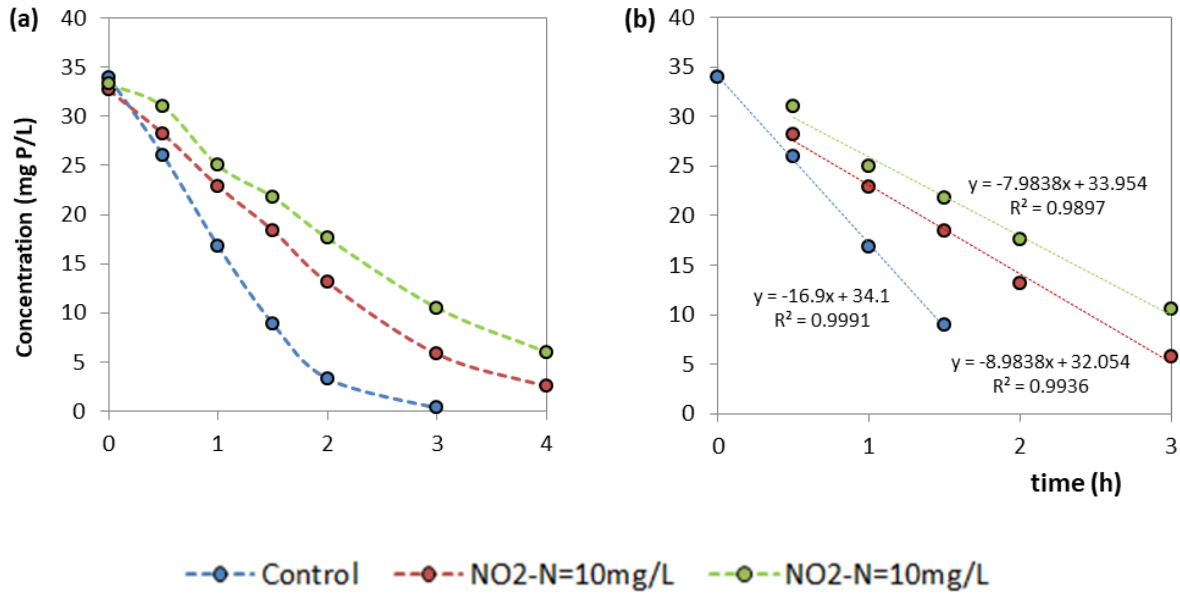


Figure 4.6. Phosphorus removal and determination of PURs of a typical batch experiment

For a better understanding of the methodology employed, an example of a typical batch experiment is provided in the results section (chapter 5) for each specific investigation. The results regarding the effect of FNA on the aerobic PUR of PAOs are presented in section 5.2.1.2.

4.2.1.3 Experiments investigating the mode of PUR inhibition

A modification of the direct linear plot method proposed by Eisenthal and Cornish-Bowden (1974) was adopted to derive the mode of inhibition from the experimental results. Based on the linear plot method, the Michaelis-Menten equation is fitted for PUR as follows:

$$PUR = PUR_{max}^{app} \frac{S}{K_m^{app} + S} \quad (4.4)$$

where

PUR: the phosphorus removal rate measured in the batch experiments

S: the initial phosphate concentration at the beginning of the experiments

PUR_{max}^{app} : the maximum apparent PUR

K_m^{app} : the half saturation apparent concentration respectively,

The linear transformation of the above equation results in the following rearrangement:

$$PUR_{max}^{app} = \frac{PUR}{S} K_m^{app} + PUR \quad (4.5)$$

For example, In the case of non-competitive inhibition the degree of inhibition depends only on the concentration of the inhibitor so an increase of the inhibitor concentration will result in a decreased PUR_{max}^{app} whereas K_m^{app} will remain the same (Figure 4.7).

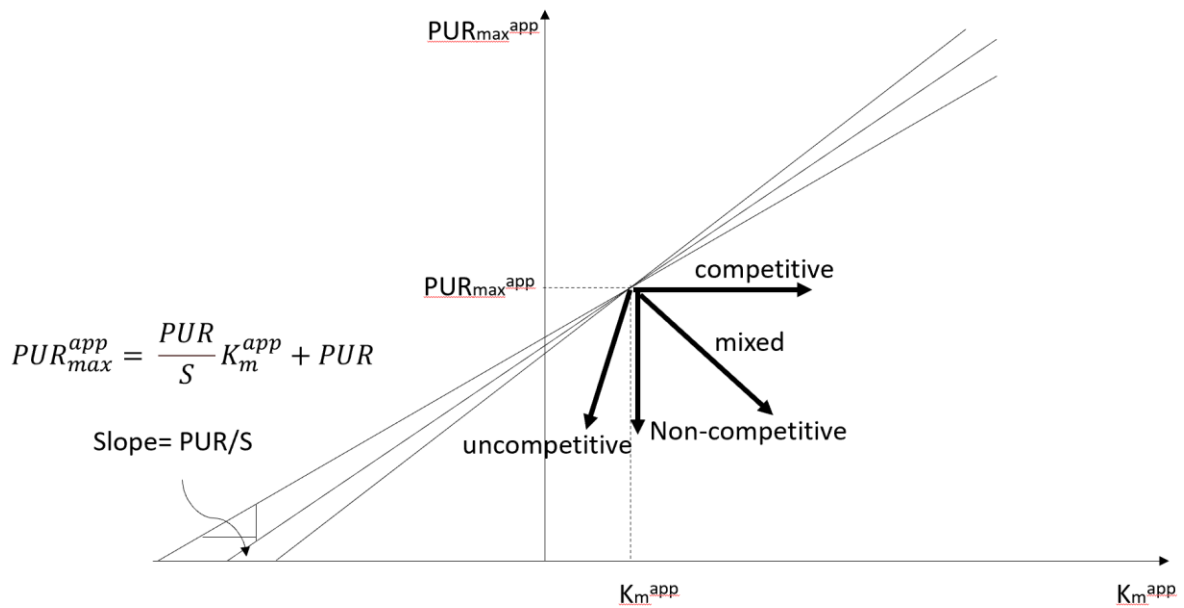


Figure 4.7. Different types of inhibition using the modified direct linear plot method

In order to examine the type of inhibition of FNA and FA on aerobic PUR, three series of batch experiments were performed for each inhibitor. In the batch experiments studying the effect of FNA, the first batch run was carried out with zero FNA presence for three different initial $\text{PO}_4\text{-P}$ concentrations and its results were compared to the other two batch runs carried out with FNA concentrations of $2.8 \mu\text{g/L}$ and $4.6 \mu\text{g/L}$ respectively (each batch run was repeated for three different initial $\text{PO}_4\text{-P}$ concentrations). The same methodology was applied for batch experiments examining the effect of FA on aerobic PUR. In the first batch run the aerobic PUR was measured for three different initial $\text{PO}_4\text{-P}$ concentrations in the absence of FA, while the other two runs were implemented for an initial FA concentration of 2 mg/L and 3.5 mg/L respectively.

Similarly, three series of batch experiments were performed for each inhibitor (FNA and FA) in order to examine the type of inhibition of FNA and FA on anoxic PUR. In the case of FA, in the first batch run the anoxic PUR was measured for three different initial $\text{PO}_4\text{-P}$ concentrations in the absence of FA, while the other two runs were implemented for an initial FA concentration of 3.2 mg N/L and 12.5 mg N/L respectively. Accordingly, in the case of FNA, the first batch run was carried out with zero FNA for three $\text{PO}_4\text{-P}$ initial concentrations and its results were compared to the other two batch runs carried out with FNA concentrations of $1 \mu\text{g N/L}$ and $3.1 \mu\text{g N/L}$ respectively.

Upon setting up axes K_{mapp} and PUR_{maxapp} as the familiar x-y axes, for each batch experiment, the measured PUR and the initial S are known and therefore creating a straight line with a slope of PUR/S and an intercept equal to PUR. By applying the same methodology for each replicate of each batch runs (each run corresponds to a certain FNA or FA concentration and different $\text{PO}_4\text{-P}$ initial concentrations) three straight lines are produced (each corresponding to different initial $\text{PO}_4\text{-P}$ concentration) which theoretically should intersect at a common point, whose coordinates gives the best fit values for PUR_{maxapp} (y-axis) and K_{mapp} (x-axis) for

each inhibitor concentration. However, almost always, there isn't any unique intersection point due to errors. In such cases it was proposed to use the median value of the apparent values of PUR_{max} and K_m instead (Eisenthal and Cornish-Bowden, 1974). In order to minimize the errors in the reading of the apparent values, the above procedure was combined with a simple statistical best fit determination of K_{mapp} value which resulted in the least sum of square errors between the calculated values of PUR_{maxapp} for each batch experiment and the average PUR_{maxapp} of the three batch tests in each run.

4.2.2 Experimental investigations regarding the activities of GAOs

The inhibition of FA and FNA on GAOs was evaluated based on their effect on their growth rate. For this, a significantly highly GAO-enriched culture was demanded (as developed by SBR5). This was in order to ensure that the effect of either FNA or FA on GAOs was accurately representative of the specific group and not influenced by the presence of other species. The high percentage of GAOs in the developed biomass that was required for a proper assessment was primarily verified by FISH analysis throughout the experimental investigation, but also by some routine experiments that were carried out throughout operation.

4.2.2.1 Routine experiments for evaluating the presence of GAOs

Similarly to the SBR configurations that focused on the development of PAOs, regular ex-situ batch experiments were performed to evaluate the biomass's capacity for phosphorus removal. This was in order to supplement verification from FISH analysis that PAOs were practically absent from the biomass. In addition, the anaerobic consumption of COD (along with the possible release of phosphorus) was regularly monitored in situ. By ensuring the absence of PAOs, the ratio of COD consumed anaerobically to the COD consumed throughout an entire cycle could provide a minimum ratio of the GAOs/Total heterotrophs of the biomass (as GAOs may also utilize COD under aerobic conditions). Nitrite and nitrate concentrations in the SBR were also regularly monitored throughout operation to ensure that NOB and AOB had been suppressed by the addition of Thiourea. All this information provided a clearer picture of the dominance of GAOs in the developed biomass, allowing the experimental data from the investigation of the effects of FNA and FA on the biomass, to be representative of their effects on GAOs.

4.2.2.2 Experiments investigating GAO growth inhibition

Having established a highly GAO enriched sludge, a series of batch experiments was conducted in order to investigate the effect of FNA on the growth rate of GAOs. In each experiment, approximately 450 ML of biomass was retrieved from the SBR and divided equally into 3 containers, each with a working volume of 1 L. The containers were then diluted up to approximately 500 ML, after which an appropriate amount of acetate, in the form of a sodium acetate solution, ammonium, in the form of a ammonium chloride solution and phosphorus, in the form of a potassium phosphate solution were added. The sludge was then further diluted up to a volume of 1 L and kept under stirring conditions. The pH of was set to the desired value and kept constant throughout the experiment. The targeted initial concentrations of each parameter were: 300 mg VSS/L, 3000 mg COD/L, 300 mg NH_4-N/L and 50 mg PO_4-P/L . The high F:M ratio of 10 along with the abundance of nutrients would provide maximum growth

conditions (Stasinakis et al., 2003). In this respect, the initial concentration of ammonium was chosen to be at 10% of the initial COD and phosphorus at just above 1.5%, which would correspond to the typical stoichiometric demands for microbial growth.

In each experiment, one of the reactors served as a control, while an appropriate amount of nitrite, in the form of a sodium nitrite solution was added to the other reactors in order to achieve the targeted FNA concentration that was to be examined, in accordance to pH. The reactors were aerated over a period of 26 hours under constant pH and temperature (25°C). The VSS of each reactor were measured on an hourly basis while samples were routinely retrieved and analyzed for nitrite to ensure a constant concentration.

Figure 4.8 presents the variation of VSS for a typical batch experiment in the absence of inhibitors. During the exponential growth phase, microbial growth may be described by the following equation (Kappeler et al., 1992):

$$\ln \left[\frac{X}{X_0} \right] = (\mu_{max} - Kd) \times t \quad (4.6)$$

where

X: the concentration of VSS at t time

X₀: the concentration of VSS at the start of the exponential phase

μ_{max}: the maximum microbial growth rate

K_d: the microbial death rate

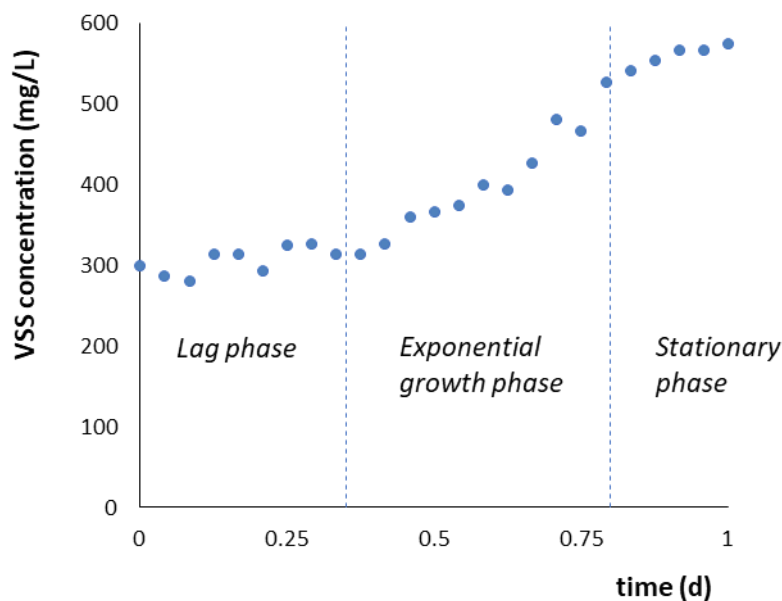


Figure 4.8. Variation of VSS in typical batch experiment.

In the presence of an inhibitor, the exponential net growth is diminished, due to a lower growth rate but also possibly due to a higher death rate:

$$\ln \left[\frac{X}{X_0} \right] = (\mu_i - K_{di}) \times t \quad (4.7)$$

where

μ_i : the (otherwise maximum) growth rate in the presence of a specific inhibitor concentration

K_{di} : the microbial death rate in the presence of the specific inhibitor concentration

As such, the degree of inhibition is determined by its effect on the net growth of the culture, and may be estimated by comparing the slopes during the exponential growth phase.

4.3 Analytical methods

4.3.1 Analysis of total and volatile suspended solids (TSS – VSS)

Determination of Total Suspended Solids (TSS) and Volatile Solids (VSS) was performed according to method 2540 D of Standard Methods for the Examination of Water and Wastewater, 22nd Edition, 2012. This method is applicable for water and treated or untreated wastewater.

The basic techniques for solids determination are separation by filtration, evaporation, combustion and weighing. Initially, during filtration, a separation is made between the suspended, non-permeable solids and the dissolved, permeable solids. Whatman GF / C layered filters with a pore size of 1.2 μm were used for this application. These filters hold the particles along their mattress, trapping them in a mesh of inorganic fibers. The filter is first placed in an oven at 550°C (Figure 4.9d) for at least 15 minutes in order to completely remove possible moisture, whereafter it is left to cool in a dryer (Figure 4.9b) and is weighed on a precision scale (Figure 4.9a) prior to filtration. The sample is stirred effectively in order to homogenize its content and is applied to the filter under vacuum. The selected volume of the sample depends on the density of the liquor.

Following filtration, the filter is placed in an oven, that is maintained at 103-105°C (Figure 4.9c), for at least 1 hour, for the complete removal of moisture (evaporation stage). After it is left briefly to cool in the dryer, the filter is then weighed once again. With this, the TSS concentration of the sample may be determined as:

$$TSS (mg/L) = \frac{M_{s1} - M_f}{V_{sample}} \quad (4.8)$$

where:

M_{s1} : the filter's weight after the evaporation process

M_f : the filter's weight prior to filtration

V_{sample} : the volume of the filtered sample

After determining the TSS of the sample, the filter may be then placed in the oven set to 550°C for a period of at least 15 minutes, for the removal of the volatile solids (combustion stage). After allowing the filter to return to room temperature in the dryer, the filter is once again weighed and the VSS concentration of the sample may be determined as:

$$VSS \text{ (mg/L)} = \frac{M_{s1} - M_{s2}}{V_{\text{sample}}} \quad (4.9)$$

where:

M_{s1} : the filter's weight after the evaporation process

M_{s2} : the filter's weight after the combustion process

V_{sample} : the volume of the filtered sample



Figure 4.9. Appliances for TSS and VSS analysis. (a): precision scale, (b): dryer, (c): evaporation oven, d): combustion oven

4.3.2 Analysis of phosphorus

The method for the determination of total phosphorus and its various fractions was performed based on the standard method 4500-P E. Ascorbic Acid of Standard Methods for the Examination of Water and Wastewater, 22nd Edition, 2012.

Phosphorus in urban wastewater is found either in inorganic form as orthophosphate radicals (PO_4^{-3} , HPO_4^{-2} , H_2PO_4) and polyphosphate chains or in organic form. The determination of organic phosphorus and polyphosphates first requires their hydrolysis to orthophosphates. For this reason, the determination of total phosphorus that includes all three forms of phosphorus (orthophosphate, polyphosphate and organic phosphorus) is performed in two stages. In the first stage, organic phosphorus and polyphosphates are digested with the aim of converting them into orthophosphate radicals and in the second stage, the total phosphorus is determined as orthophosphates ($\text{PO}_4\text{-P}$).

The amount of organic phosphorus can be determined in most samples, where chemical precipitation is not expected to occur, as the difference between the total phosphorus of an unfiltered sample and the total phosphorus concentration of the same sample after filtration through membrane type filters (0.45 μm). By bypassing the digestion step and directly filtrating a sample through a 0.45 μm membrane, it is possible to determine the orthophosphate radicals in the sample by applying the ascorbic acid method. By digestion of a filtered sample and then application of the ascorbic acid method, the total of orthophosphate radicals and polyphosphate chains is determined.

During the digestion step, the sample is heated to boiling point in the presence of sulfuric acid and a catalyst (ammonium persulfate). Under these conditions the organic matter is oxidized to CO_2 and H_2O , while the phosphorus contained in the organic matter and in the polyphosphate chains is hydrolyzed to orthophosphates. The orthophosphate concentration can then be determined by various spectroscopic methods.

The concentration of orthophosphates was determined according to the ascorbic acid method. A mixture of ammonium molybdate ($(\text{NH}_4)_6\text{MoO}_{24}$) and potassium-antimony tartrate ($(\text{K}(\text{Sb})\text{C}_4\text{H}_4\text{O}_6)$) is used, which reacts with the orthophosphates under acidic conditions, producing ammonium phosphomolybdate according to the following reaction:



Then, in the presence of ascorbic acid, the molybdenum contained in the ammonium phosphomolybdate complex is reduced to free molybdenum, giving a strong blue tint to the solution. The hue of the solution is proportional to the orthophosphate concentration (for values between 0.1 and 1.0 mg P/L) which may be determined spectrophotometrically at a wavelength of 890 nm.

Following their filtration, samples were diluted appropriately in 50 mL volumetric flasks, based on the expected phosphorus concentration (within the respective limits) and transferred to conical flasks. Then, 8 mL of mixed reagents (mix) were added to each flask and allowed to react for a period of 10 minutes, in which the reaction becomes complete. The mix consists of 50 mL 5N sulfuric acid, 5 60ypothesium antimonyl ttrate, 15 mL ammonium molybdate and 30 mL

ascorbic acid. The samples would undergo spectral analysis within the following 20 minute period as to not allow discoloration.

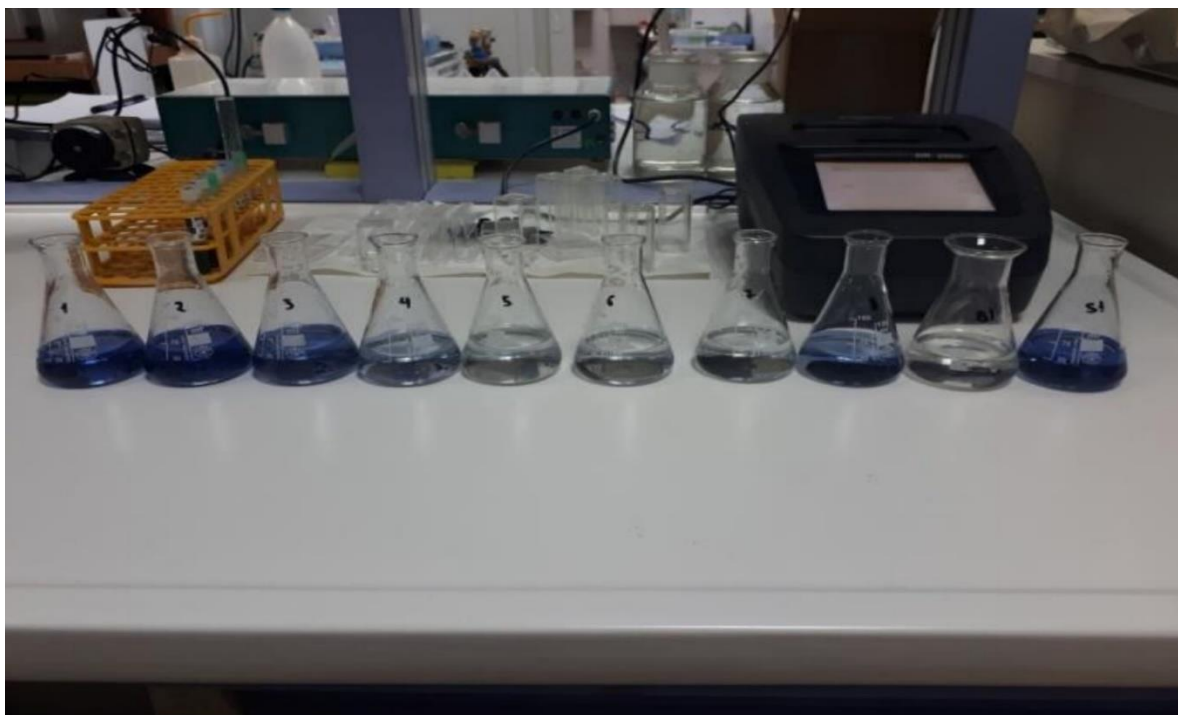
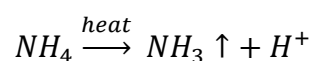


Figure 4.10. Samples prepared for spectral analysis for the determination of orthophosphates

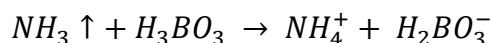
4.3.3 Analysis of ammoniacal nitrogen

The process for the determination of ammoniacal nitrogen ($\text{NH}_4\text{-N} + \text{NH}_3\text{-N}$) is based on the 4500-NH₃ C. Nesslerization Method (Direct and Following Distillation) of the Standard Methods for the Examination of Water and Wastewater, 18th Edition, 1992.

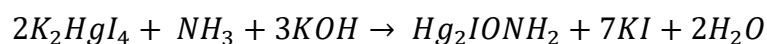
The method involves distillation in a BUCHI K-314 apparatus (Figure 4.11), where under alkaline conditions water vapor is introduced into the sample. Under these conditions the ammonia is released as follows:



A concentrated NaOH solution is first added to the sample in order to raise pH close to 9.5, while the ammonia gas is collected in an acidic boric acid solution, where it retakes the form of ammonium.



Upon completion of the distillation, the distilled solution is transferred to a 50 mL volumetric flask, after appropriate dilution, where 2 mL of the Nessler reagent are added. The Nessler reagent is a mixture of potassium iodide and mercuric iodide, which react with ammoniacal nitrogen under alkaline conditions to give a brownish-yellow colloidal solution (Figure 4.12), according to the following reaction:



The reaction of the diluted sample with the Nessler reagent requires around 10 minutes to be complete. Upon completion, the concentration of the ammoniacal nitrogen may be determined using a spectrophotometer at 425 nm, as the hue of the solution is proportional to the concentration of ammonium. Analysis was performed within 30 minutes from the completion of the reaction to avoid discolouration of the samples.



Figure 4.11. BUCHI K-314 distillation apparatus



Figure 4.12. Samples prepared for spectral analysis for the determination of ammoniacal nitrogen.

4.3.4 Analysis of nitrate nitrogen and nitrite nitrogen

Analysis for nitrate nitrogen was performed by the HACK LCK339 method, which is based on the reaction of nitrate anions with 2,6-dimethylphenol to form 4-nitro-2,6-dimethylphenol, in a solution containing sulfuric and phosphoric acid. Following filtration and appropriate dilution, 1 mL of the diluted sample was added to a vial of LANGE LCK 339 reagent along with 0.2 ml of the accompanying reagent supplied with the vial. After 15 minutes the reaction is complete, and the nitrate concentration is measured using a spectrophotometer at a wavelength of 345 nm. The range of measurement is within 0.–3 - 13.50 mg NO₃-N / L.

Analysis for nitrite nitrogen was performed with the HACK 5807 Nitrite method, which is based on the reaction of nitrite with sulfanilic acid to form a nitrogenated sulfanilic salt, which reacts with chromotropic acid to produce a pinkish color. Following filtration and appropriate dilution of the sample, a HACK Nitriver 3 reagent is added to 10 mL of the diluted sample. The sample is then stirred lightly and left over a period of 20 minutes for the completion of the reaction. Following this, the sample is analyzed spectrophotometrically at a wavelength of 507 nm. The range of measurement is within 0.002 and 0.300 mg NO₂-N / L.

4.3.5 Analysis of COD

Analysis of soluble chemically required oxygen (COD) was performed according to the 5220 D "Closed Reflux Colorimetric Method" of Standard Methods for the Examination of Water and Wastewater, 22nd Edition, 2012.

COD is defined as the chemically required oxygen for the oxidation of organic and inorganic compounds in a sample. It is essentially the amount of potassium dichromate (K₂Cr₂O₇) consumed during this oxidation. Through its measurement, the biodegradable or non-biodegradable organic load of the wastewater is determined.

A strongly acidic environment (50% H₂SO₄) is required to measure COD. A sample is digested with a strong acid solution and a quantity of potassium dichromate at a temperature of 150°C for a period of 2 hours, while Ag₂SO₄ is added as a catalyst for the more efficient oxidation of some organic compounds, such as volatile organic acids which, due to their volatility, are not oxidized as efficiently. The organic compounds under these conditions are oxidized to CO₂, H₂O, NH₄⁺, PO₄⁻³, SO₄⁻², while the Cr (VI) dichromate anion is reduced to Cr (III). These two oxidation states of chromium are characterized by orange and green colours respectively, and are absorbed at specific wavelengths(400 nm for Cr (VI) and 600 nm for Cr (III)).

For the application of the method, ready-made reagents of the company HACH were used. These reagents are contained in vials depending on the measuring range. HACH LCK314 vials are used for a measuring range of 15-150 mg / L and HACH LCK114 vials are used for a measuring range of 150-1000 mg / L. The digestion at 150°C was carried out in a compatible digester device (Figure 4.14) of the same company. The measurement of the wavelength was done in a spectrophotometer of visible light type HACH DR2800.



Figure 4.13. HACK vials for COD analysis.



Figure 4.14. COD digester.

4.3.6 Measurement of DO, pH and temperature

Measurement of DO, pH and temperature, both in the SBR as well as during the ex-situ batch experiments, was carried out with the use of a portable pH meter 3110 (Figure 4.15) and a Multi 3510 portable oxygen meter (Figure 4.16) of the company WTW (both accessories possessed a specialized probe for the measurement of temperature).



Figure 4.15. Portable pH meter 3110 manufactured by WTW.



Figure 4.16. Multi 3510 portable oxygen meter, manufactured by WTW.

4.3.7 Fluorescent In Situ Hybridization (FISH) analysis

The in-situ identification and quantification of PAOs and GAOs was carried out through FISH analysis, as detailed in Amann (1995). As mentioned, the quantification of GAOs was a prerequisite for the validity of the experiments regarding the effect of FNA and FA on their

growth, as they needed to account for a significantly high percentage (>90%) of the total microbial community of the biomass.

FISH analysis is a molecular cytogenetic technique which uses fluorescent probes that only bind to specific parts of a nucleic acid sequence, with a high degree of sequence complementarity. The method is based on the uniqueness of the oligonucleotide sequence in the ribosomal ribonucleic acid (rRNA) of each microbial species. As such, identification of specific microbial groups is achieved based on the genotype, and not from the phenotype of the microorganism. The fluorescent probe consists of a short oligonucleotide chain (known as the tracker) which is attached to a fluorescent substance. The probe penetrates the microbial cell and hybridizes with its complementary RNA sequence, where present. Probes that do not attach, due to the absence of the complementary RNA sequence, are thereafter removed during the purification step, leaving only the attached probes. The fluorescent substance on the edge of the attached tracker produces a signal under fluorescent light, enabling identification of the targeted microorganism.

The trackers can identify the strains which make up a particular microbial group and may be designed to target a specific family, genus or even species (Amann, 1995). While the sequence length of the tracker offers excellent control of its specificity, the method has several restrictions and a margin of error, as it is possible that some trackers may bind to other microorganisms with a similar oligonucleotide sequence, while some of the targeted microorganisms may not be reached by the trackers.

The samples that are prepared for FISH analysis as are also stained with 4',6-diamidino-2-phenylindole (DAPI) that attaches to the entirety of the microbial population. DAPI is a fluorescent stain that is excited with ultraviolet light and is detected through a blue/cyan filter. Images captured under the microscope with the use of a cyan filter (showing total microorganisms) may then be compared to the associate images captured with the use of the probe-specific filter (showing the targeted group). By creating composite images, with the use of an appropriate program, the common area of the overlapping images may be calculated and compared to the area of the image captured under the cyan filter. As such, the percentage of the targeted group towards the entire microbial community may be expressed as the ratio of these two areas. An increased number of images is required for a proper assessment.

Throughout the various investigations of this work, FISH analysis was regularly used to verify the existence of PAOs in the biomass. In addition, 2 major extensive quantification analyses were undertaken for 2 specific investigations. These concern SBR5, in which a significantly highly GAO-enriched biomass was demanded, and SBR10, which operated under the optimum conditions for PAOs. Each quantification was based on a total of 64 pairs of FISH images. Specifically, in each analysis, 2 separate samples were retrieved from the SBR and prepared for FISH, out of which 2 duplicate samples were examined under the microscope for each original sample. Then, 16 pairs of images were obtained for each sample under the microscope. The samples were observed under a Nikon microscope Eclipse 80 under fluorescence with the appropriate filter and the images were processed with the use of the program Image-Pro, which was used to calculate the percentage of the target group towards all microorganisms (% target group / DAPI).

In each investigation, the targeted groups and the probes that were used were the following:

PAOs were identified with the use of Cy3-labelled PAOMIX probes, in accordance with Crocetti et al. (2000). PAOMIX consists of equal quantities of PAO462, PAO651 and PAO846 trackers which target most *Accumulibacter*.

Competibacter, the main acetotrophic GAO, was identified with the use of Cy3-labelled GAOMIX probes (equal quantities of GAOQ989 and GB_G2 trackers), in accordance with Crocetti et al., 2002).

Defluviicoccus vanus, the main alphaproteobacterial GAO, was identified with the use of Cy3-labelled DF1MIX probes (equal quantities of TFO_DF218 and TFO_DF618 trackers) targeting *Defluviicoccus vanus* Cluster 1 and Cy3-labelled DF2MIX probes (DF988, DF1020 plus helper probes H966 and H1038) targeting *Defluviicoccus vanus* Cluster 2 (Wong et al., 2004).

In the experiments regarding the effect of FNA on GAOs (presented in section 5.5), additional FISH analyses were carried out in order to ensure their validity. In each experiment, samples were obtained from each reactor at the start and upon completion of the experiment and put through FISH analysis for *Competibacter*. For each sample, 16 pairs of images were captured, processed and quantified. This was to ensure that the highly GAO-enriched culture had not been contaminated by a shift in the biomass throughout the duration of the experiment, ensuring that the growth rates observed were specific to GAOs.

Chapter 5: Results and discussion

5.1 Introduction

The application of EBPR in high nitrogen loading systems that are based on nitrification/denitrification appears challenging. As discussed in chapter 2, free nitrous acid (FNA) which is the protonated form of nitrite, has been reported to be a strong inhibitor of PAOs. In addition, there have been recent reports that free ammonia (FA) is also an inhibitor of PAOs. As the percentage of nitrite in the form of FNA increases adversely to pH, while the percentage of ammonium in the form of FA increases with pH, the conditions in said systems generally appear hostile for the development of PAOs. While FNA and FA are known inhibitors of PAOs, the degree to which they inhibit EBPR is not clear as well as their mode of inhibition. The effect of FNA on PAOs has been studied to some extent, yet conclusions on its severity differ in the literature, particularly in the case of the anoxic processes of PAOs. The effect of FA on the other hand has only been observed in cases of prolonged exposure to the inhibitor. Furthermore, the combined effect of FNA and FA on PAOs has not been studied as of this point. An investigation of this could provide valuable information regarding the application of EBPR in conditions of high ammonium and nitrite accumulations, with pH control playing a key role. While the performance of PAOs is threatened under these conditions, so is their sustainability since GAOs, which are the main antagonists of PAOs, may possess a stronger tolerance to these inhibitors. As such, the effective application of EBPR should consider the inhibition of PAOs under said conditions, the inhibition of GAOs, and strategies to promote the proliferation of PAOs. In the following sections the results of the present study are explicitly presented and analyzed.

Section 5.2 presents the investigation of the effect of FNA on PAOs. The investigation focused on the effect of FNA on the phosphorus uptake rate (PUR) of PAOs under aerobic and anoxic conditions for which a series of experiments was conducted on a PAO-enriched sludge that was developed under laboratory conditions. The results were used to construct an inhibition model for the effect of FNA on PAOs. Accordingly, section 5.3 presents the investigation of the effect of FA on PAOs. The investigation focused on the effect of FA on PUR under aerobic and anoxic conditions, while also examining its effect on the anaerobic processes of PAOs. The investigation was supported by a series of experiments conducted on a PAO-enriched biomass that was developed under laboratory conditions. Based on the results an inhibition model was developed to simulate the effect of FA on PAOs. Section 5.4 presents the investigation of the combined effect of FNA and FA on PAOs. The investigation was supported by a series of experiments conducted on a PAO-enriched biomass and adopted the results of sections 5.2 and 5.3 for the development of a combined inhibition model.

Section 5.5 presents the investigation of the effects of FNA and FA on GAOs. The investigation focused on the effect of FNA and FA on the growth of GAOs under aerobic conditions, while also examining the effect of FA on the anaerobic processes of GAOs.

Section 5.6 presents the investigation of strategies to promote EBPR in conditions of nitrification/denitrification, with focus on the antagonism between PAOs and GAOs. The

investigation was undertaken by examining the effectiveness of various laboratory configurations and substrates for the sustainability of PAOs.

Finally, section 5.7 presents the assessment of optimizing conditions for EBPR in high nitrogen loading systems. The investigation is supported by a mathematical simulation model that was developed based on the findings of section 5.4 and the viability of EBPR is examined for various nitrogen loadings with the utilization of optimum strategies that were evident in section 5.6.

5.2 Inhibition of PAOs due to free nitrous acid

It has been well established that nitrite has a significant inhibitory effect on EBPR. However, the severity of this inhibition appears to vary in the literature. It is generally accepted that the protonated form of nitrite (FNA) is the actual inhibitor, meaning that pH strongly influences the effect of nitrite on PAOs. To put this into perspective, the FNA content of a specific nitrite concentration at the pH of 7 for example, is 10 times the content of the same NO_2 concentration at the pH of 8. FNA has been found to inhibit both the aerobic and anoxic activities of PAOs to varying degrees. While the exact mechanism of PAO inhibition by FNA has not been determined as of this point, it is hypothesized that it is due to the direct inhibition of the poly-P kinases (PPK) enzyme which is responsible for the synthesis of poly-P chains by transferring the phosphate residue from a high energy donor to the poly-P chain (Zhou et al., 2007). As such, FNA directly influences the uptake of phosphorus by PAOs, which in turn affects their growth. In high nitrogen loading systems, where high nitrite accumulations may be expected, the sustainability of PAOs could be threatened by the FNA content, while their performance under the effect of this inhibitor may limit the effectiveness of EBPR. Therefore, information on the degree to which FNA inhibits PAOs is important in the determination of the viability of EBPR in such systems.

In this section, the effect of FNA on PAOs is examined both under aerobic and anoxic conditions, focusing on the inhibition of the phosphorus uptake rate (PUR). In each investigation, a PAO-enriched biomass was developed under laboratory conditions, which was used in a series of batch experiments, to study the effect of various nitrite concentrations on the PUR of PAOs at different pH. Upon determining the degree of PUR inhibition by FNA, additional experiments were carried out to determine the mode of inhibition and provide kinetic parameters for the construction of an inhibition model.

5.2.1 Investigating the inhibitory effect of FNA on aerobic PUR

The effect of FNA on aerobic PUR has been well documented in the literature, although the degree of inhibition appears to vary. For instance Saito et al., (2004) reported that aerobic PUR was 100% inhibited by the FNA concentration of $1.5 \mu\text{g N/L}$, whereas Pijuan et al., (2010) reported that the process was completely inhibited at the concentration of $4 \mu\text{g N/L}$. This may be due to differences in acclimation to FNA, even though in both cases biomass was reported as non-acclimatized. Zhou et al., (2007) studied the effect of FNA on an acclimatized biomass and reported a threshold of $10 \mu\text{g HNO}_2\text{-N/L}$ (which at 20°C would correspond to $39 \text{ mg NO}_2\text{-N/L}$ at the pH of 7, or $390 \text{ mg NO}_2\text{-N/L}$ at the pH of 8).

As the reports regarding the degree of inhibition by FNA are in disagreement with each other, a comprehensive investigation regarding the effect of FNA on aerobic PUR became necessary.

Since acclimation to FNA greatly affects the tolerance of PAOs to the inhibitor, an effort was made in this investigation to determine what constitutes an acclimated biomass, in terms of prolonged exposures to FNA accumulations.

5.2.1.1 Performance of the experimental system

A lab scale SBR system was operated continuously for a period of approximately 8 months to provide a PAO-enriched biomass that was used in a series of aerobic batch experiments to study the inhibitory effect of FNA on aerobic PUR.

5.2.1.1.1 Start-up period

During the start-up period the SBR operated on 2 daily cycles each consisting of an anaerobic phase, an aerobic phase and an anoxic phase. Settling and decanting occurred once per day over a 2 hour period due to technical limitations mentioned in the materials and methods section. Initially there was a slight difference between the operational cycles. The first cycle consisted on a 3 hour anaerobic phase followed by a 7 hour aerobic phase and a 2 hour anoxic phase, while the second cycle consisted of a 2 hour anaerobic phase followed by a 6 hour aerobic phase and a 2 hour anoxic phase. Following a brief period of approximately 15 days, both daily cycles were modified to consist of a 3 hour anaerobic phase followed by a 6 hour aerobic phase and a 1 hour anoxic phase.

Feed consisted of a concentrated mixture of acetate, ammonium and phosphorus that was introduced at the beginning of each anaerobic and each anoxic phase. The volume of each dose was 250 mL. Prior to decanting, the SBR contained 10.5 L of liquor. Following the removal of 5.5 L of effluent, 5.5 L of water was added to the SBR bringing the mixed liquor's volume to 10.5 L. Under mixing conditions, 1 L of mixed liquor was removed in order to achieve an SRT of around 10 days. Thus, with the daily addition of 1 L of the concentrated feed, the SBR's working volume averaged at 10 L simulating a HRT of around 2 days.

The addition of a carbon source at the beginning of the anaerobic phase would provide PAOs with a competitive advantage, over common heterotrophic organisms in the utilization of COD. During the aerobic phase, sufficient DO concentrations (>3 mg/L) would allow PAOs to develop by oxidizing their stored PHAs, while residual acetate would be rapidly removed by other heterotrophs. Since nitrification is expected during the aerobic phase, following the cease of aeration, feed is reintroduced to the SBR in order to allow for rapid removal of any produced nitrate or possibly nitrite via denitrification prior to the next anaerobic phase. In essence, this nominal anoxic phase is mostly anaerobic and is to ensure strictly anaerobic conditions at the beginning of the next cycle.

The daily dose of COD was gradually increased from 5 g/d to 8 g/d over a period of approximately 20 days. The dose of 8 g COD/d was regulated with respect to the aerobic SRT (≈ 6 days) in order to achieve a biomass concentration of around 2,500 mg VSS/L. The reason for the lower early dosages was primarily in order to avoid accumulations of COD that could cause bulking problems and secondarily to hasten the shift in the biomass from a mostly common heterotrophic community to a PAO-enriched sludge. More specifically, since the seed sludge contained a very low PAO population, practically all of the acetate introduced at the start of the anaerobic phase would be available at the aerobic phase. This abundance of a readily

biodegradable source of COD could in short time deteriorate the quality characteristics of biomass and lead to bulking problems, causing a strain on the system's operation. Additionally, while PAOs would always have priority over common heterotrophs in the utilization of acetate, it is possible that the presence of a large heterotrophic community could prove antagonistic in the utilization of nutrients and the availability of oxygen, slowing the growth of PAOs.

The daily dose of ammonium was gradually increased up to 600 mg N/d over a period of approximately 20 days, similarly to the dose of COD. This strategy was primarily selected in order to ensure an adequate source of nitrogen for biomass growth and also to allow some nitrification. During the start-up period, ammonium concentrations in the effluent were monitored on a daily basis and the daily dosage was modified in order to maintain effluent concentrations lower than 10 NH₄-N mg/L to prevent accumulation of ammonium in the SBR.

The daily dose of phosphorus was 200 mg PO₄-P/d, a dose much greater than the stoichiometric demand for growth of heterotrophs in order to selectively promote the growth of PAOs. This dosage would also compensate for the phosphorus that is removed via chemical precipitation, allowing the availability of an adequate phosphorus source to be taken up by PAOs throughout the aerobic phase. Access to phosphorus under aerobic conditions is important for PAOs as it is required for them to reform their intracellular polyphosphate chains. Inability to do so would result in a failure to take up acetate during the following anaerobic phase as no energy can be produced from the hydrolysis of these chains. Consequently, if the phosphorus released anaerobically by PAOs were to be removed from solution due to chemical precipitation (primarily by the formation of struvite due to an increase in pH), this would most likely result in a shift in the biomass in the favour of GAOs which do not require phosphorus and ultimately the wash-out of PAOs from the system. Since great increases in pH were observed during aeration for reasons described below, providing the SBR with a significant dosage of phosphorus was of strategic importance for the growth and maintenance of PAOs.

5.2.1.1.2 Steady-state operation

The SBR was successful in developing PAOs that displayed notable activity as early as 3 weeks from the commencement of operation. Following a period of adjustments in the feed and configuration of the SBR, already described, during the first 20 days of operation, the SBR had reached steady-state operation by day 60. The strong presence of PAOs was documented by FISH analyses and was also validated by the observed anaerobic COD consumption coupled with anaerobic P-release and aerobic P-uptake that characterize the biomass.

During steady state operation, MLVSS averaged at $2,500 \pm 200$ mg/L while MLSS averaged at $2,800 \pm 200$ mg/L. The biomass concentration that was maintained in the SBR is a direct result of the chosen COD loading rate and SRT. The high MLVSS to MLSS ratio of approximately 90% is due to the use of synthetic wastewater that contained little to no solids.

The pH ranged from 7.5 to 8.5. Following decanting and re-filling of the SBR, pH would drop to 7.5 and would remain unchanged during the following anaerobic period. During aeration, pH would rise significantly due to carbon dioxide stripping and reach 8.4 during the first daily cycle and 8.5 during the second cycle. Nitrification was limited as intended and could not compensate

for this rise in pH. For the same reason, pH remained practically unaffected by denitrification during the anoxic phase.

As mentioned, feed entered the SBR at the start of each anaerobic and anoxic cycle over a 2 minute period. Each dose provided the biomass with 2 g COD, 150 mg NH₄-N and 50 mg PO₄-P that would raise the respective concentrations in the SBR by 200 mg COD/L, 15 mg NH₄-N /L and 5 mg PO₄-P/L. At the beginning of the anaerobic phase, after feed, COD concentrations in the SBR averaged at 240 ± 20 mg/L, while phosphorus concentrations averaged at 25 ± 5 mg/L.

Under anaerobic conditions, COD dropped below 100 mg/L while the concentration of phosphorus rose to 60 ± 10 mg/L as shown in Figure 5.1, indicating strong PAO activity in the SBR. Both COD uptake and P-release appear to occur faster during the first hour of the anaerobic phase with P-release rates averaging at 9.5 ± 1 mg P/g VSS h and average acetate utilization rates of 30 ± 5 mg COD/g VSS h. This would correspond to a COD_{uptake}/P_{release} ratio of 3. However, during the remaining anaerobic period, the P-release rate dropped to merely 0.15 mg P/g VSS h. This would indicate that the capacity of PAOs to release phosphorus has been largely saturated by this point. The acetate utilization rate also dropped after the first hour, performing at about half its initial rate. The much higher COD_{uptake}/P_{release} ratio that characterizes this period most likely indicates that the uptake of acetate is now achieved via glycolysis from either PAOs that have exhausted most of their intracellular polyphosphate chains, or far more likely by GAOs and specifically *Competibacter*. That have a high affinity for acetate and often accompany PAO communities. In any case it would appear that the extension of the anaerobic HRT for periods longer than 1 hour, provide little in terms of P-release and may provide an antagonistic advantage to GAOs.

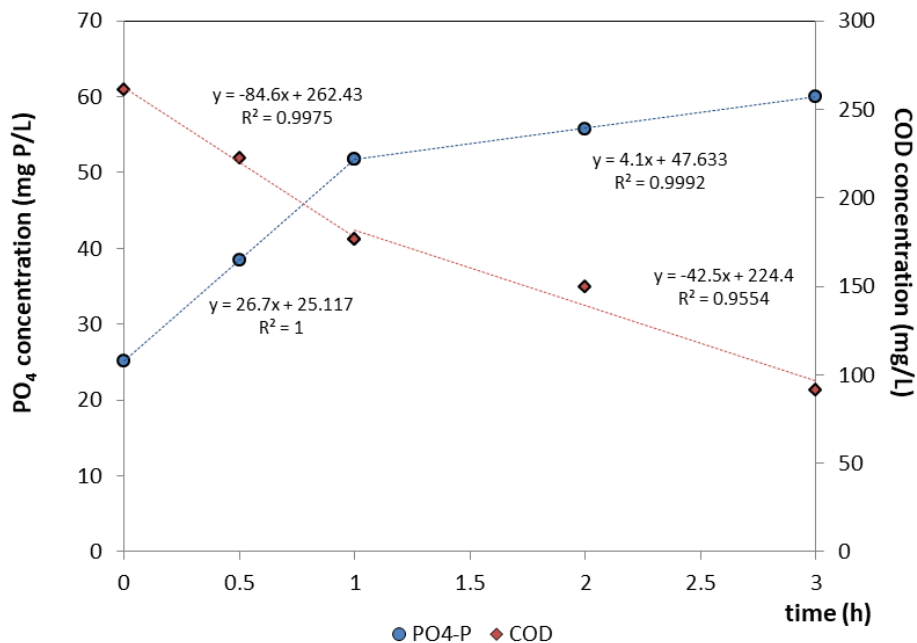


Figure 5.1. Typical variation of PO₄-P and COD concentrations in the SBR during the anaerobic phase of the first daily cycle.

During the aerobic phase, most of the phosphorus was removed within the first 2 hours of aeration, while acetate that remained after the anaerobic phase was rapidly removed within the first 30 minutes of aeration. Figure 5.2 displays the typical variation of COD and phosphorus during the first daily operational cycle. As is evident, the concentration of phosphorus is halved within the first hour of aeration and at 25% of its initial concentration by the end of the second hour of aeration. By the end of the aerobic phase, practically all phosphorus has been removed from solution. The concentration of COD remains unchanged after the first 30 minutes of aeration, averaging at 25 ± 3 mg/L. This would indicate that all biodegradable COD has been removed with almost 75% of it being taken up during the anaerobic phase and the remaining 25% being rapidly consumed by common heterotrophs very early in the aerobic phase.

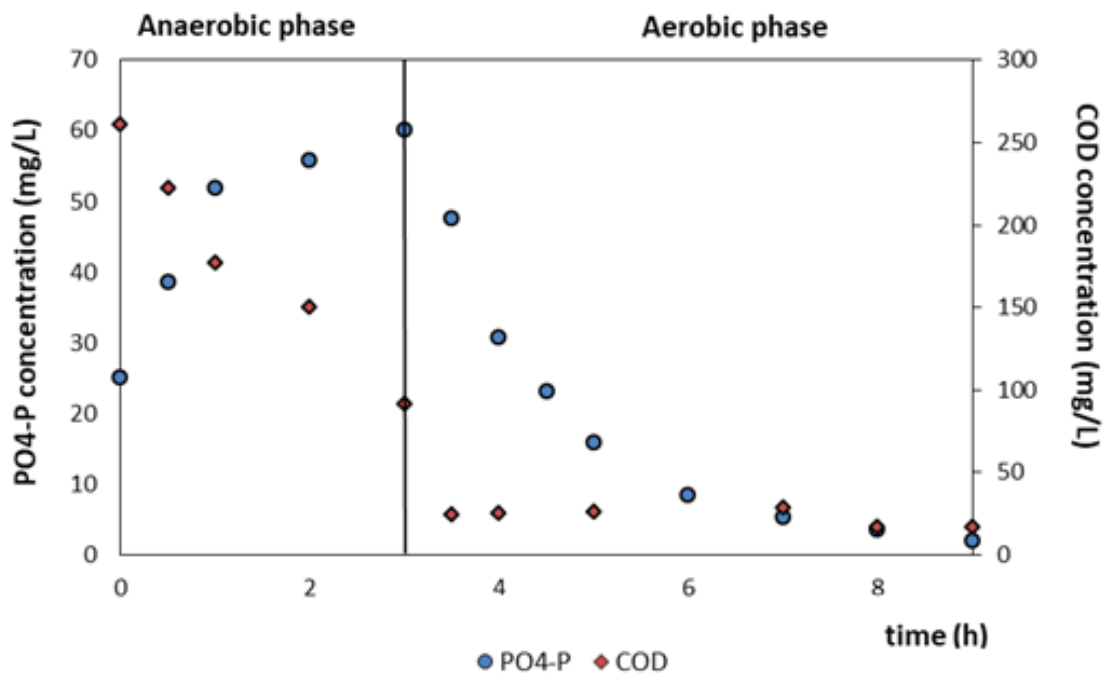


Figure 5.2. Typical variation of PO₄-P and COD in the SBR during the anaerobic and aerobic phase of the first daily cycle.

As evidenced, the biomass displayed high P-release rates coupled with COD consumption during the anaerobic phase and good P-removal during the aerobic phase with an average initial PUR of 10 ± 1 mg P/g VSS h during the first hour of aeration. However, as previously mentioned, phosphorus removal may also be influenced by precipitation reactions that occur due to changes in water chemistry, specifically the formation of struvite due to an increase in pH. Struvite is least soluble at the pH of 8 to 10, displaying the same solubility within this range, and at is most soluble at the pH of 6.5 and below. Figure 5.3 displays the removal of phosphorus during the aerobic phase with regard to pH. Within the first 30 minutes of aeration, pH is raised from 7.6 to 8 due to carbon dioxide stripping and continues to rise throughout the aerobic phase. It is likely that this initial rapid rise of pH may have contributed significantly to phosphorus removal via precipitation, especially when considering that phosphorus removal in the SBR appears to be more rapid during the first hour of aeration.

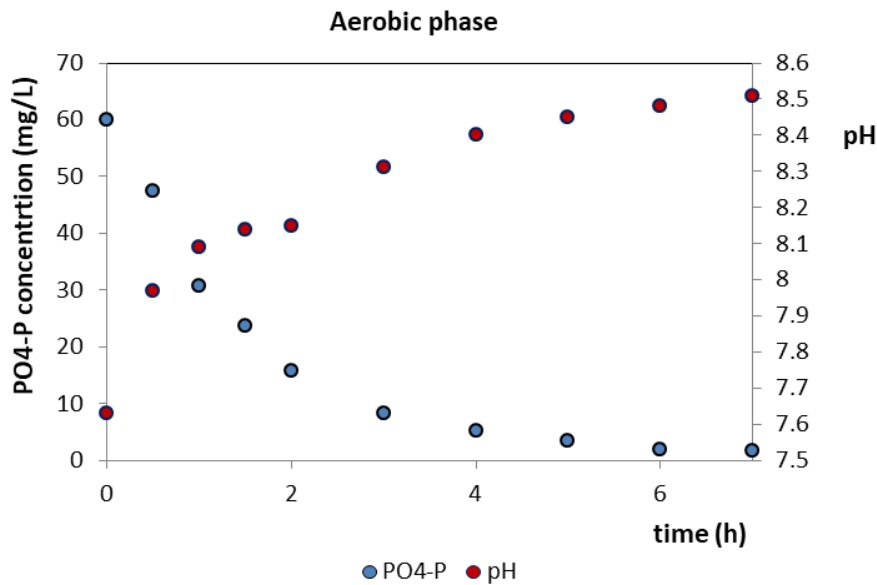


Figure 5.3. Typical variation of $\text{PO}_4\text{-P}$ and pH in the SBR during the aerobic phase of the first daily cycle

In order to properly evaluate the biomass's capacity to remove P in conditions of high DO concentration without the interference of precipitation phenomena, regular ex-situ experiments were conducted on sludge retrieved from the SBR, under controlled pH. Following feed, 500 mL of sludge were extracted and placed into a container of similar working volume and left stirring under anaerobic conditions for a period of 1 hour. Following this, the reactor was aerated for a period of up to 3 hours over which samples were retrieved every 30 minutes. Throughout the experiment pH was controlled at its initial value (7.6 ± 1).

Phosphorus removal appeared to be linear in the controlled ex-situ experiments, as shown in Figure 5.4, making the determination of PUR more reliable.

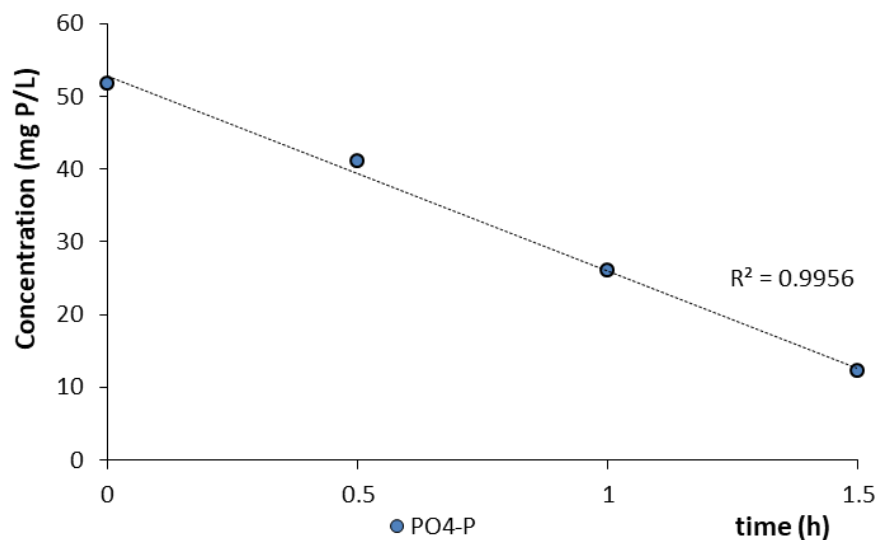


Figure 5.4. Phosphorus removal in a typical ex-situ batch experiment.

Figure 5.5 shows the profile of the oxidized forms of ammonia (nitrite and nitrate) in regard to the concentration of ammonium during the aerobic phase. Nitrification in the SBR was limited with $\text{NO}_x\text{-N}$ concentrations reaching just above 3 mg/L at the end of the 7 hour aerobic phase. Ammonium concentrations dropped steadily during aeration, primarily due to growth requirements of the biomass and secondarily due to nitrification. In total, 15 ± 2 mg/L $\text{NH}_4\text{-N}$ were removed during each aerobic phase, meaning an average daily removal of 30 mg/L. As 3 mg- $\text{NH}_4\text{-N/L}$ are ultimately converted to nitrate during each aerobic phase, the remaining 24 mg/L are utilized for the daily growth of the biomass. This would correspond to roughly 10% of the 2500 mg of biomass produced each day, which is a typical stoichiometric analogy.

Nitrite concentrations in the reactor were very low throughout operation and were noticeable only during the first hour of aeration, reaching an average peak of around 0.5 mg N/L after 30 minutes of aeration. The maximum nitrite concentration observed was just below 1 mg N/L. With regard to temperature and pH, this would mean that at no point was the biomass exposed to an FNA concentration greater than 0.08 $\mu\text{g N/L}$.

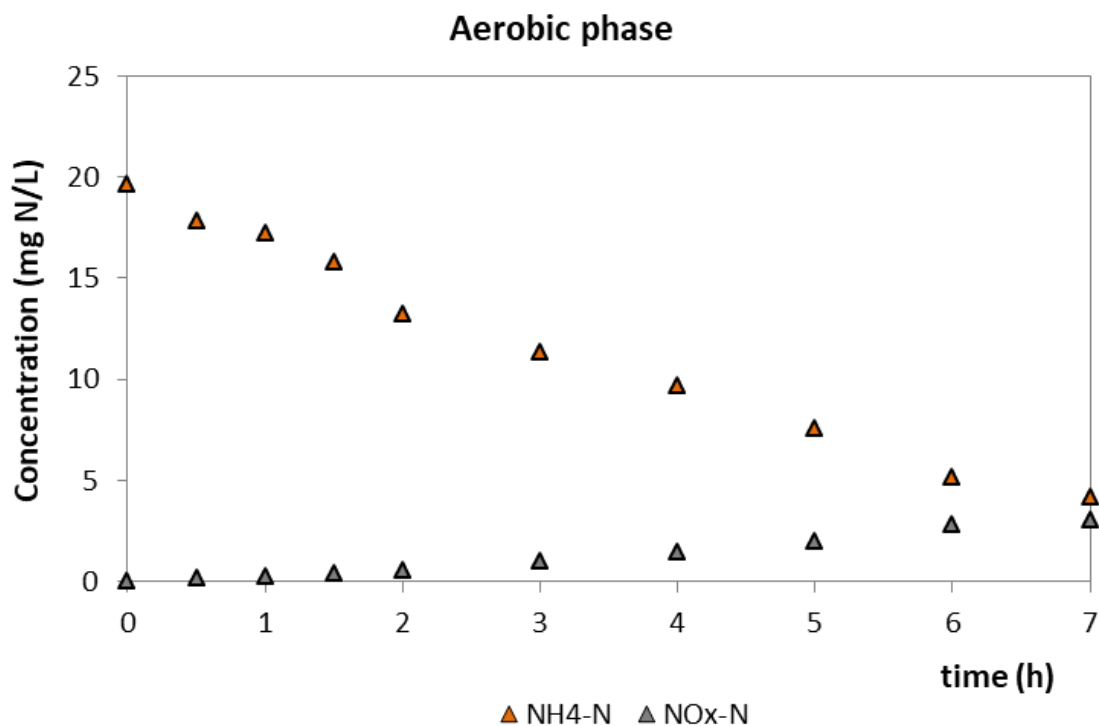


Figure 5.5. Typical variation of $\text{NH}_4\text{-N}$ and $\text{NO}_x\text{-N}$ in the SBR during the aerobic phase of the first daily cycle.

Figure 5.6 displays the concentrations of P, COD and $\text{NO}_x\text{-N}$ during the anoxic phase. As shown, the little nitrate produced during the aerobic phase is reduced very fast and the conditions throughout this phase can be mostly considered as strictly anaerobic. A large portion of the acetate entering with the feed at the start of this phase is rapidly oxidized by common heterotrophs, removing both the remaining DO and nitrate. This is why the COD concentration at the start of this phase appears to be relatively low (at about 60 mg/L) with regard to the feed. The remaining COD is taken up by the PAO-GAO community, accompanied with the release of

P. Within the first hour of this phase, all acetate has been utilized and the concentrations of P and COD remain unchanged for the remainder of this phase.

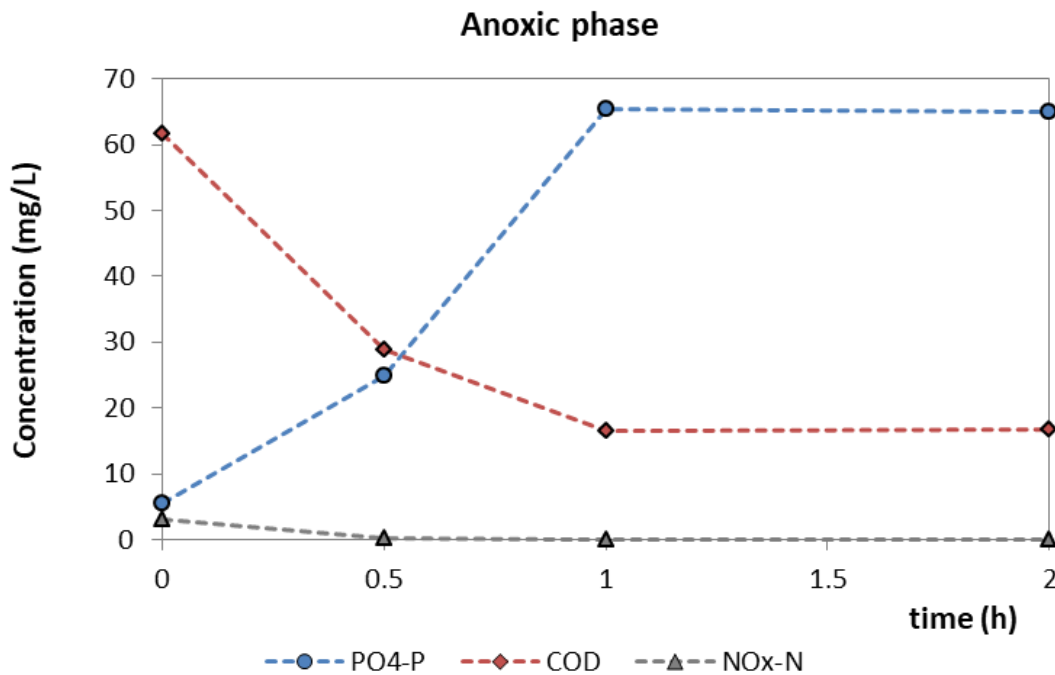


Figure 5.6. Typical variation of PO₄-P, COD and NO_x-N in the SBR during the anoxic phase of the first daily cycle.

In essence, this phase may be considered as an additional 2 hour anaerobic phase that occurs prior to the 3 hour anaerobic phase before aeration. As such, the P-release rate is much higher than the one observed during the second anaerobic period, reaching 30 mg P/g VSS.h during the first hour. This is the reason for the high phosphorus concentration observed after decanting at the start of the 3 hour anaerobic phase. The COD that is made available to PAOs following the removal of DO and NO_x is about 1/3 of the COD that it is made available during the next anaerobic phase. As such, the capacity of PAOs to take up acetate is not saturated by the end of this phase.

5.2.1.1.3 Evaluation of the PAO-enriched sludge

The SBR configuration was successful in developing a biomass with all the characteristics of a strong PAO community, displaying anaerobic P-release rates of up to 30 mg P/g VSS.h and good P-removal both in the SBR and under controlled conditions with an average aerobic PUR of 7 ± 1 mg P/g VSS.h. The strong presence of PAOs was also verified by FISH analysis (Figure 5.7).

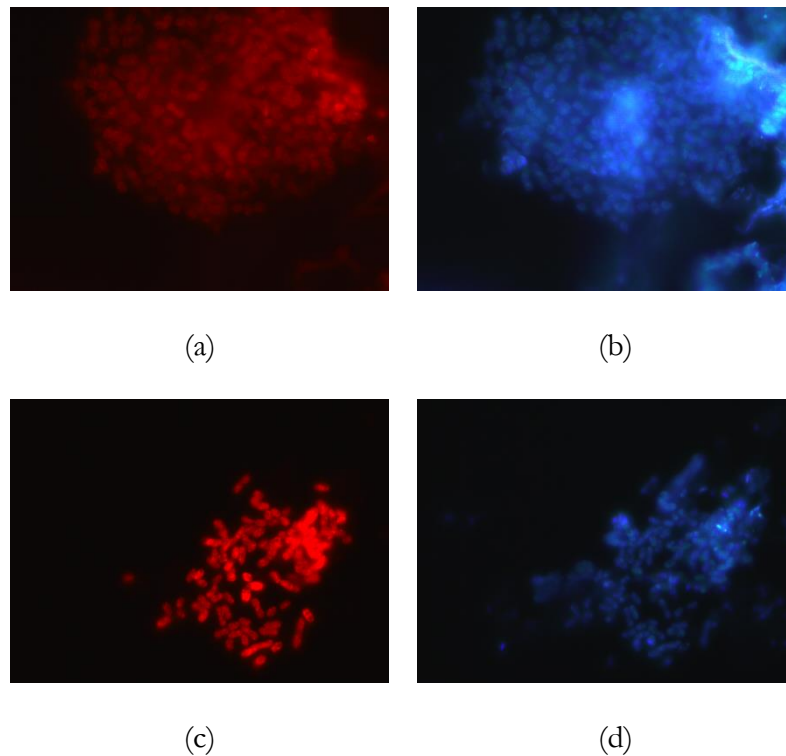


Figure 5.7. In situ identification of PAOs using Cy-3 labelled PAOMIX (PAOs depicted in red in a and c, all microorganisms stained with DAPI presented in blue in b and d).

5.2.1.2 Experimental assessment of the effect of nitrite on aerobic PUR

Having established a strong and stable PAO community, a series of ex-situ batch experiments was conducted in order to investigate the effect of FNA on the aerobic PUR of PAOs. A total of 18 batch series were performed for various nitrite concentrations at the pH values of 7, 7.5 and 8. According to the experimental protocol, a minimum of four batch series were performed at each pH. The nitrite concentrations for each series were chosen as to provide a satisfactory range of inhibition degrees at each pH with regard to the relative FNA concentration and the reported degrees of inhibition in the literature. The nitrite concentrations examined for each pH are presented in Table 5.1.

Table 5.1. Nitrite concentrations examined at each pH

pH	NO ₂ -N (mg/L)
7	5, 10, 25 50
7.5	10, 15, 20, 25, 30, 35, 45, 55, 70
8	10, 25, 50, 150, 250

At the beginning of each batch series, sludge was extracted from the SBR prior to feed and divided equally into 3 bioreactors, each with a working volume of 0.5 L. An appropriate amount of acetate, in the form of sodium acetate solution, was added to each of the reactors in order to obtain an initial COD concentration of 200 mg/L. The pH of each container was adjusted to the

targeted value just after feed addition and was kept stable for the remainder of the experiment. The reactors were then left stirring under anaerobic conditions over a 1 h period. Following the anaerobic phase, the reactors were then aerated over a period of 3–4 h. One of the bioreactors served as a control, while the other two reactors were fed with an equal amount of nitrite, in the form of a sodium nitrite solution at the start of aeration. Thus, each batch series examined the effect of a specific nitrite concentration on the duplicate reactors with respect to the control one. Nitrite was introduced to the duplicate reactors after a brief aeration period of 10 minutes at which point the initial samples were obtained. This was to ensure sufficient DO concentrations in the reactors prior to their spiking with nitrite as to not allow its removal via denitritation.

The methodology for calculating PURs and the inhibitory effect of a specific FNA concentration is detailed in the following typical batch experiment. Figure 5.8 displays the results for the nitrite concentration of 10 mg N/L at the pH of 7. As is obvious, the control reactor performed at a better removal rate than the reactors containing the nitrite concentration. While phosphorus removal of the control was at a stable rate from the beginning of aeration, the entry of nitrite in the other reactors would often cause a slight disturbance, resulting in a diminished PUR during the first 30–60 minutes of the experiment compared to their subsequent performance. This may be due to a combination of a disturbance in the water chemistry and possibly a brief adaptation period of the biomass to the new conditions. Following this period, the reactors displayed a steady PUR up until the remaining phosphorus became significantly low or the capacity of the biomass to take up phosphorus had been largely saturated.

As is made clear in Figure 5.8b, the PUR of each reactor was established for the duration where a stable performance was observed. In this particular experiment, the concentration of VSS in each reactor was 2,200 mg/L. Based on the slopes of the experimental data, the control's PUR could be calculated as 7.7 mg P/g VSS h, while the PUR of the nitrite-containing reactors averaged at 3.85 mg P/g VSS h. The nitrite concentration of 10 mg N/L at the pH of 7 was therefore found to inhibit aerobic PUR by 50%.

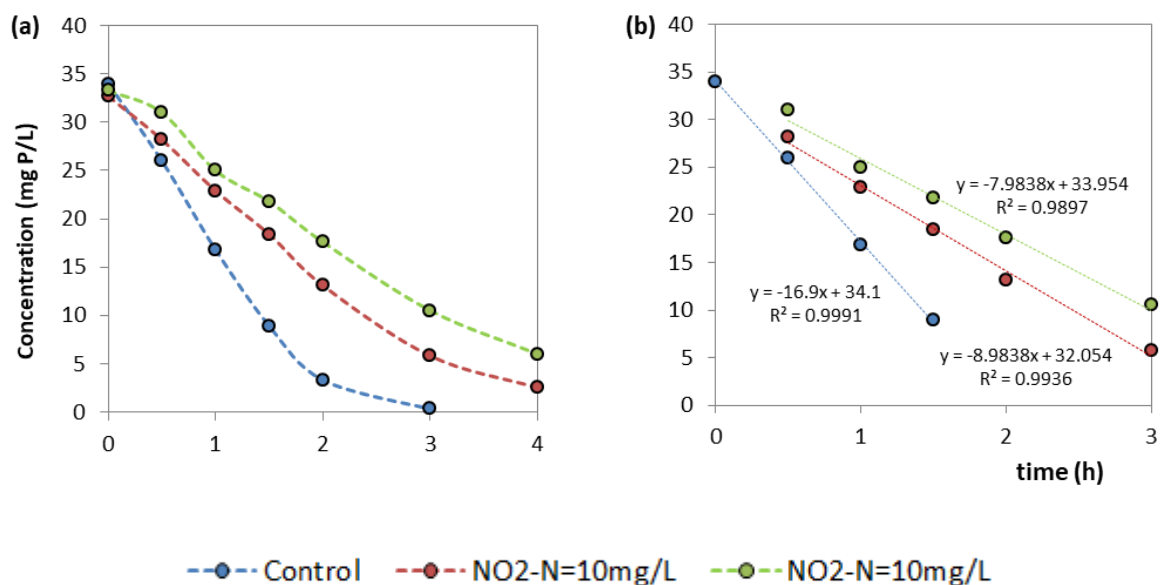


Figure 5.8. P-removal and determination of PURs for typical batch experiment (NO₂-N=10mg/L, pH=7)

The results of this series of experiments are presented in Figure 5.9 and Figure 5.10. As is shown in Figure 5.9, nitrite appears to inhibit aerobic PUR significantly more at lower pH values. This is to be expected of course as FNA has been established to be the actual inhibitor and the concentration of FNA increases inversely to pH for a specific nitrite concentration. For example, the nitrite concentration of 50 mg N/L was found to fully inhibit P-removal at the pH of 7, while at the pH of 8 it was found to inhibit the process by 50%. This is because the concentration of FNA at the pH of 7 is 10 times greater than its concentration at the pH of 8 (13 $\mu\text{g N/L}$ at pH=7 as opposed to 1.3 $\mu\text{g N/L}$ at pH=8). Aerobic PUR was found to be inhibited by 50% by a nitrite concentration of 10 mg $\text{NO}_2\text{-N/L}$ at the pH of 7, by 20 mg $\text{NO}_2\text{-N /L}$ at the pH of 7.5 and by 50 mg $\text{NO}_2\text{-N /L}$ at the pH of 8.

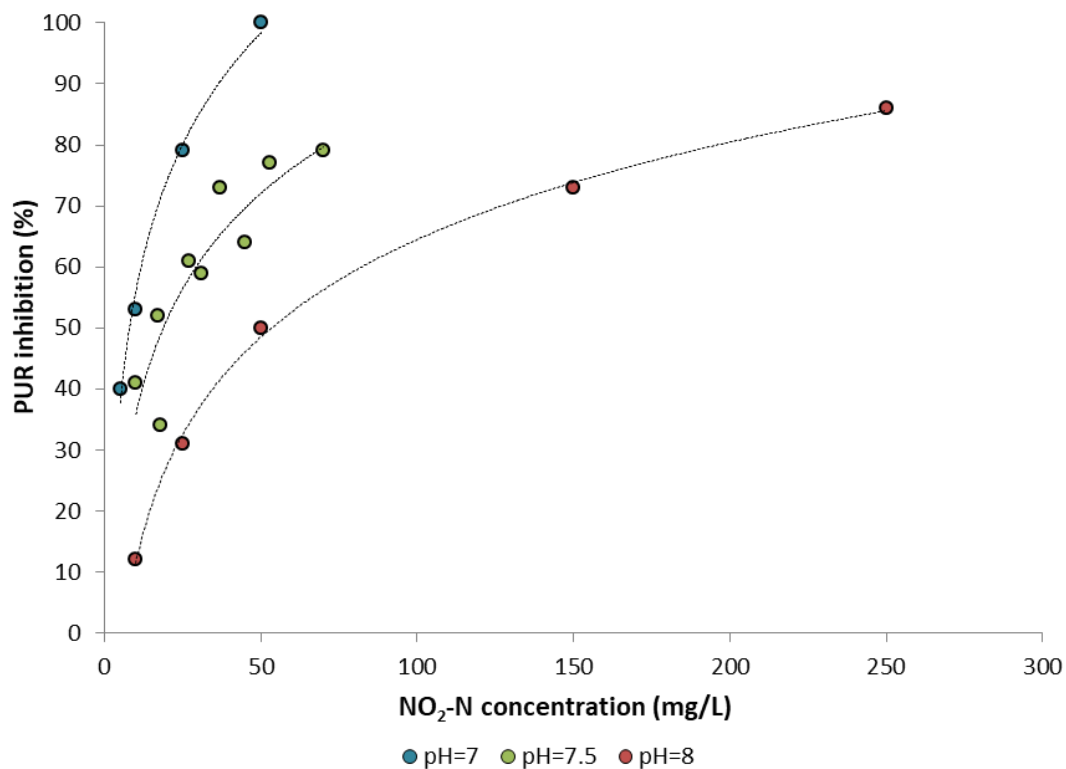


Figure 5.9. The inhibitory effect of nitrite on aerobic PUR.

The FNA concentration for each experiment was then calculated with regard to the relative nitrite concentration, pH and temperature. The inhibitory effect of FNA on aerobic PUR is presented in Figure 5.10. It is apparent that FNA practically inhibits PUR to the same degree at each pH although inhibition at the pH of 7 appears to be slightly lower than the observed inhibition at the pH of 8, while the inhibition levels at the pH of 7.5 appear to be characterized by a greater dispersion compared to the other pH values.

PUR was found to be completely inhibited by 13 $\mu\text{g HNO}_2\text{-N /L}$ and inhibited by 50% at the FNA concentration of 1.5 $\mu\text{g HNO}_2\text{-N/L}$. The degree of inhibition in relation to FNA appears to follow a logarithmic trend, similarly to the trends observed in relation to nitrite at different pH. As such, at FNA concentrations lower than 1.5 $\mu\text{g N/L}$ (the concentration that inhibits the process by 50%), the addition of FNA would inhibit the process severely more than it already is compared to the effect the same amount would have when added to a concentration greater than

that. For instance, a margin of 4–6 $\mu\text{g HNO}_2\text{-N/L}$ practically equally inhibits PUR by 80 % while just 0.25 $\mu\text{g HNO}_2\text{-N/L}$ is enough to inhibit the process by more than 10%.

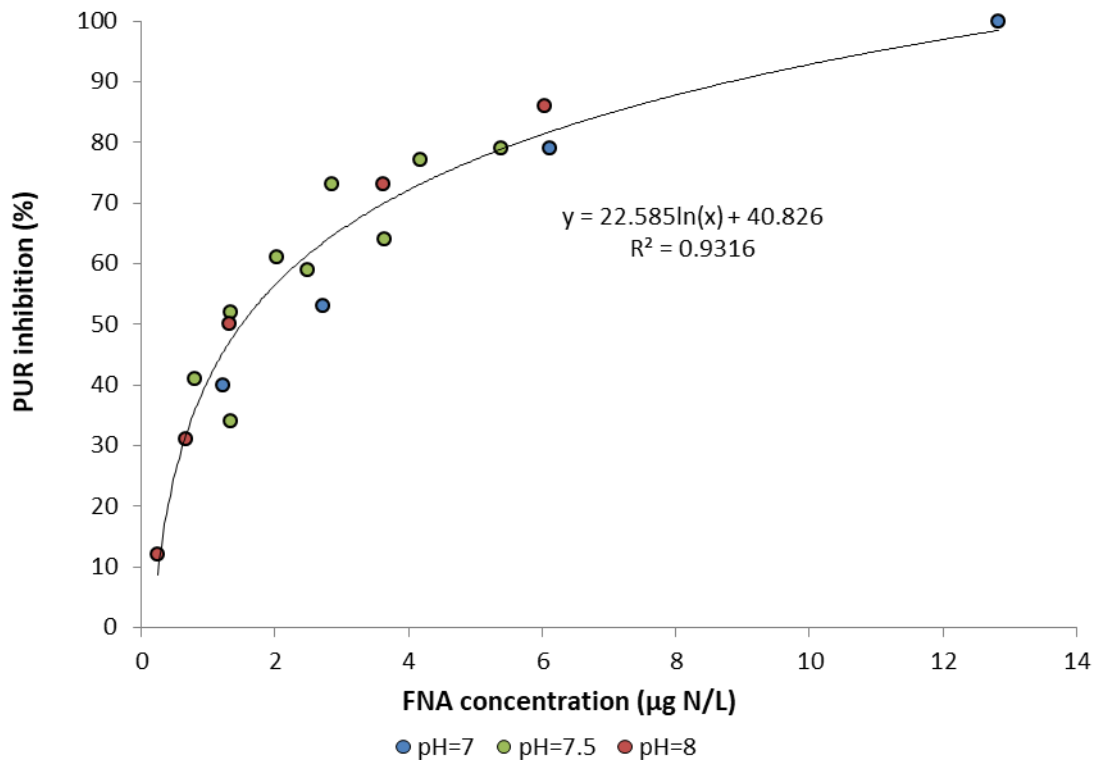


Figure 5.10. The inhibitory effect of FNA on aerobic PUR.

One point of interest is that the inhibitory effect of FNA observed seems consistent with those observed in studies where experiments were performed on a biomass that was acclimatized to the presence of nitrite. Table 5.2 presents the various degrees of aerobic PUR inhibition reported in the literature for different FNA concentrations. Saito et al. (2004) reported phosphorus removal to be fully inhibited by the FNA concentration of 1.5 $\mu\text{g N/L}$ for a non-acclimatized biomass. In the present study the same FNA concentration was found to inhibit the process by 50%. Pijuan et al. (2010) reported 50% inhibition occurring for the FNA concentration of 0.52 $\mu\text{g/L}$ and 100% inhibition for the FNA concentration of 4 $\mu\text{g/L}$. The relative FNA concentrations of this study are much higher for these degrees of inhibition for a non-acclimatized biomass as the process was found to be fully inhibited just under 13 $\mu\text{g/L}$. Interestingly, Zhou et al. (2012) reported phosphorus removal by a biomass that was acclimatized to the presence of FNA to be fully inhibited by 10 $\mu\text{g HNO}_2\text{/L}$. This would indicate that the biomass of this study displayed a slightly higher tolerance to FNA than that of the acclimatized biomass. Yoshida et al. (2006) reported that the FNA concentration of 0.7 $\mu\text{g/L}$ inhibited the aerobic PUR of a non-acclimatized biomass by 72% and the aerobic PUR of an acclimatized biomass by 20%. In this study, the specific FNA concentration was found to inhibit PUR by 30% which would suggest that the biomass's tolerance to FNA is closer associated with that of an acclimatized biomass.

Table 5.2. Comparison of studies on the effect of FNA on aerobic PUR

Study	PAOs	PUR inhibition	FNA
<i>Saito et al., 2004</i>	non-acclimatized	100%	1.5 µg/L
<i>Yoshida et al., 2006</i>	non-acclimatized	72%	0.7 µg/L
	acclimatized	20%	0.7 µg/L
<i>Pijuan et al., 2010</i>	non-acclimatized	50%	0.52 µg/L
		100%	4 µg/L
<i>Zhou et al., 2012</i>	acclimatized	100%	10 µg/L
<i>This study</i>	non-acclimatized?	50%	1.5 µg/L
		100%	13 µg/L

By all accounts it would appear that the biomass used in these experiments displayed a tolerance to FNA that is characteristic of an acclimatized biomass. As mentioned, nitrite concentrations in the SBR were particularly low and only observed during the first hour of aeration. The maximum nitrite concentration observed was just below 1 mg NO₂-N/L. With regard to the associate pH and temperature of the SBR, this would mean that the biomass was never exposed to a FNA concentration to the order of 0.08 µg N/L. According to the experimental results of this study, this FNA concentration would not inhibit PAO activity. This raises the question: Can the biomass of this study be considered acclimatized to FNA? If so, this would suggest that PAOs become acclimatized to FNA at very low concentrations.

In order to further investigate the effect of FNA on PAOs, a second series of experiments was conducted on a biomass that was acclimatized to a ten-fold greater nitrite concentration than that of the first series of experiments.

Having concluded the series of experiments on what was considered a non-acclimatized biomass, nitrogen loading of the SBR was gradually increased, while the SRT was lowered in an attempt to raise nitrite concentrations during the aerobic phase. Specifically, ammonium loading in the SBR was gradually increased from 0.06 kg NH₄-N/m³ d to 0.15 kg NH₄-N/m³ d over a period of 30 days, while the SRT was lowered to 8 days. The new aerobic SRT of 4.5 days would limit the presence of NOB in the biomass, resulting in less nitrite being converted to nitrate during aeration.

Following the transitional period of 30 days, the SBR was maintained under the new conditions for 15 days, after which four additional batch experiments similar to the original series were conducted. The objective of these experiments was to determine if the biomass would exhibit a stronger tolerance to FNA due to acclimation to greater FNA concentrations in the SBR.

Under the new configuration, nitrite concentrations in the SBR increased significantly reaching 15 mg NO₂-N/L while nitrate nitrogen represented a fraction of 1/4 - 1/3 of total NO_x-N.

Figure 5.11 displays a typical variation of $\text{NO}_2\text{-N}$ and $\text{NO}_x\text{-N}$ during aeration, while Figure 5.12 shows the variation of pH and the respective FNA concentrations. According to this, the biomass was regularly exposed to FNA concentrations up to $0.35 \mu\text{g/L}$. Based on the results of the experiments previously conducted, this FNA concentration would inhibit aerobic PUR by 15-20%. The highest FNA concentration observed was $0.7 \mu\text{g/L}$ ($10 \text{ mg NO}_2\text{-N/L}$ at $\text{pH}=7.6$), a concentration almost tenfold the maximum concentration observed in the SBR during the first series of experiments and one that was found to inhibit PUR by more than 30%.

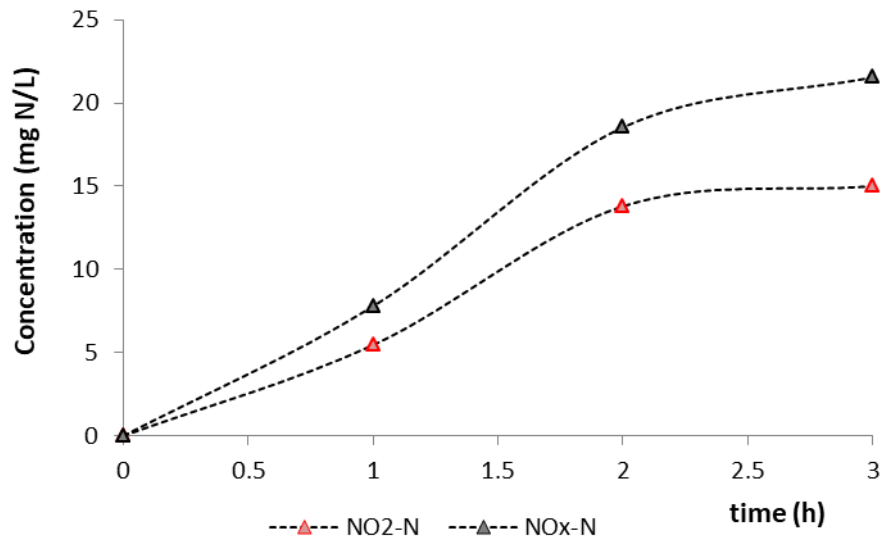


Figure 5.11. Typical variation of $\text{NO}_2\text{-N}$ and $\text{NO}_x\text{-N}$ in the SBR during the aerobic phase of the first daily cycle

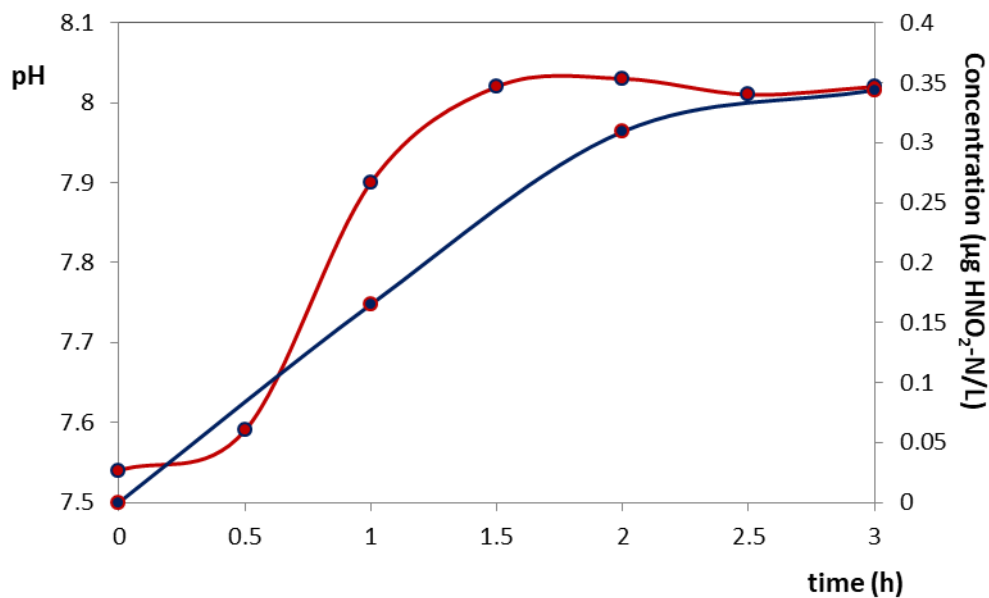


Figure 5.12. Typical variation of FNA and pH in the SBR during the aerobic phase of the first daily cycle

While the SBR achieved a relatively steady performance in regard to nitrification/denitrification, this was not the case for phosphorus removal. Following the 15 day maintenance of the SBR under the new conditions, the 4 additional batch experiments were performed within 7 days. During this time, the biomass's capacity for phosphorus removal steadily decreased from 6.5 mg P/g VSS h to 3 mg P/g VSS h. After the conclusion of the fourth batch experiment, the biomass displayed little to no phosphorus removal indicating that PAOs were likely washed out of the system.

The nitrite concentrations examined in each experiment were 40, 70, 120 and 300 mg NO₂-N/L at the pH of 8. The respective FNA concentrations for each experiment were 1.1, 1.7, 2.7 and 8.35 µg HNO₂-N/L. The results of these experiments are displayed in Figure 5.13 and are compared to the results of the previous experimental series. As shown, the biomass appeared to display the same tolerance to FNA in terms of PUR inhibition as it had under the initial conditions of the SBR, meaning that exposure to much greater FNA concentrations had not improved its resilience.

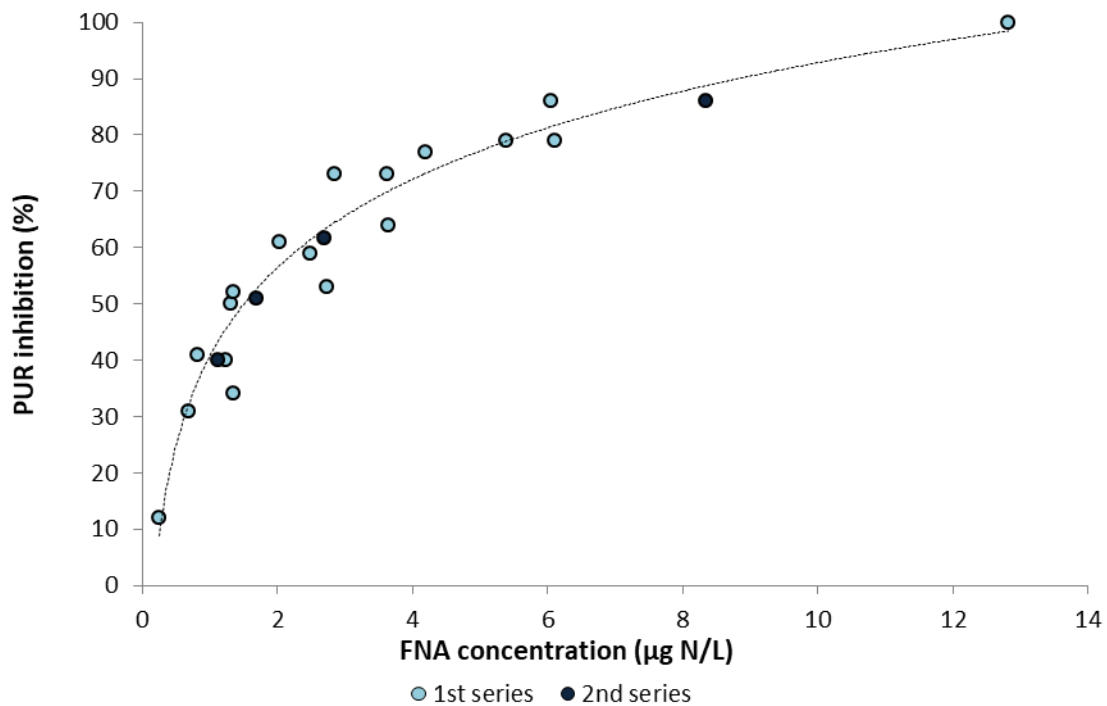


Figure 5.13. Experimental results on the effect of FNA for the first and second series of experiments.

It should be noted that the 15 day period may not be considered a sufficient length of time to achieve new steady-state conditions and consequently may not be enough time to observe changes in acclimation. However, as the sludge was exposed to a gradual increase of FNA concentrations over 40 days prior to this, by the time of the experiments some difference in FNA tolerance could be expected. While exposure to greater FNA concentrations had no effect on the degree of inhibition on PUR, the growth of PAOs in the SBR suffered as a result. Since their tolerance of FNA did not improve, the PAO population decreased over time as their inhibited growth could not compensate for their removal with the excess sludge. This inhibition

also provided an advantage to GAOs that are known to possess a higher tolerance to FNA, thus shifting the biomass populations in favour of them over time, hastening the wash-out of PAOs. By day 24 under the new conditions, all PAO activity had ceased while there was a strong presence of GAOs (*Competibacter*) that was observed by the anaerobic intake of acetate without simultaneous P-release and documented by FISH analysis.

The results of this series of experiments would suggest that PAOs had already reached their maximum tolerance to FNA during the first series of experiments and therefore may be considered acclimated to FNA. This would be in agreement with other studies on the effect of FNA as the degree of inhibition observed seems to be consistent with those observed for an acclimated biomass (Figure 5.14). Based on this, it is possible that PAOs are acclimated to FNA at relatively low concentrations.

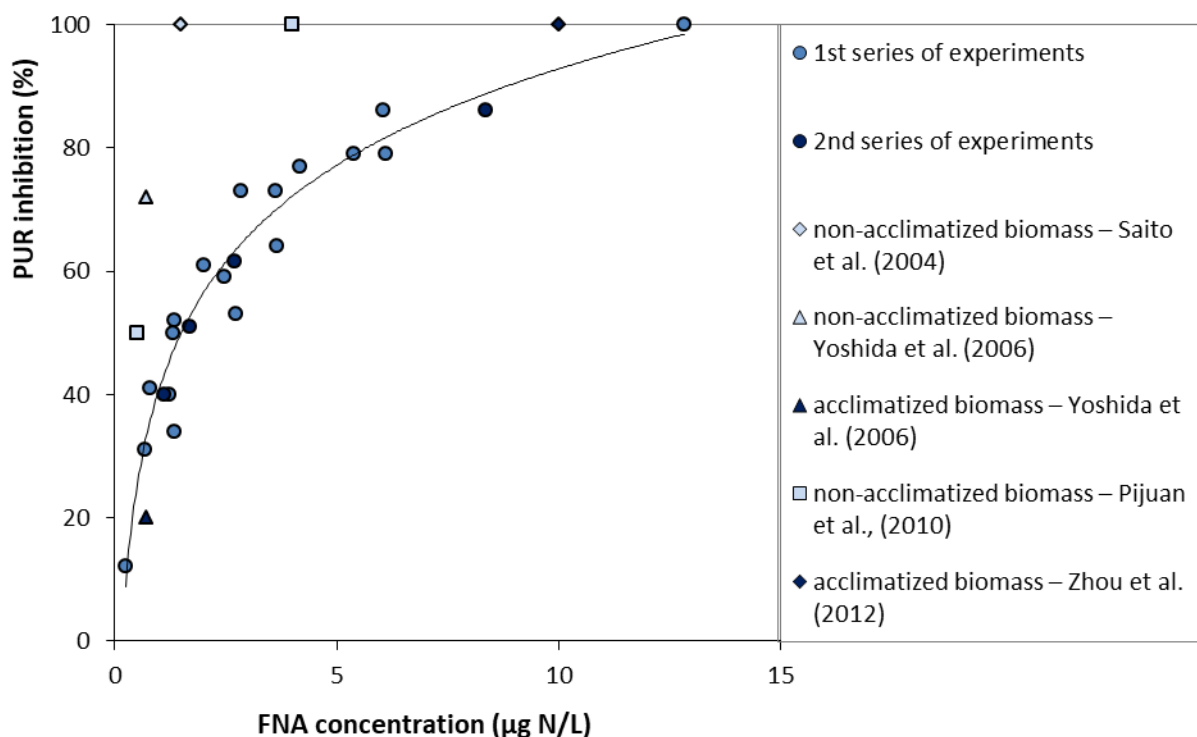


Figure 5.14. Comparison of studies on the effect of FNA on aerobic PUR.

In order to examine the tolerance of PAOs to FNA when developed under conditions of minimum FNA presence, a new series of experiments was conducted. The SBR was re-set and a new seed sludge from the WWTP of Psytalia was used to develop PAOs. The SBR configuration was as described in section 5.2.1.1 with one major difference; the ammonium loading rate was lowered to $0.03 \text{ kg NH}_4\text{-N/m}^3 \text{ d}$ compared to the $0.06 \text{ kg NH}_4\text{-N/m}^3 \text{ d}$ loading rate of the previous configuration during steady state operation. This ammonium loading would just about cover the stoichiometric demand for microbial synthesis and significantly limit nitrification, ultimately leading to the washout of AOB from the SBR.

After 37 days of operation, the SBR had already successfully developed PAOs with phosphorus removal being observed both in the SBRs performance and in ex-situ batch experiments under

controlled conditions. At this point, nitrite concentrations in the reactor were very low throughout operation (<0.1 mg $\text{NO}_2\text{-N/L}$), enabling an FNA-free environment for the growth of PAOs.

On day 37, an experiment similar to the ones described previously was conducted on sludge from the SBR, investigating the effect of 45 mg $\text{NO}_2\text{-N/L}$ at the pH of 7.5 (3.58 $\mu\text{g HNO}_2\text{-N/L}$). The control performed at a PUR of 8.41 mg P/g VSS h, while the PUR of the reactors containing the nitrite concentration averaged at 1.17 mg P/g VSS h. This meant that PUR was inhibited by this nitrite concentration by approximately 86%, whereas the previous series of experiments found this concentration to inhibit PUR by approximately 64% at the same pH. It would appear that nitrite was affecting PAOs noticeably more than previously.

On day 44, the effect of 35 mg $\text{NO}_2\text{-N/L}$ at the pH of 7.5 (2.7 $\mu\text{g HNO}_2\text{-N/L}$) was investigated in a similar manner. While the control performed with a PUR of 6.9 mg P/g VSS h, phosphorus removal in the other reactors was found to be fully inhibited. On day 52, the concentration of 16 mg $\text{NO}_2\text{-N/L}$ at the pH of 7.5 (1.22 $\mu\text{g HNO}_2\text{-N/L}$) was found to inhibit PUR by 95%. By day 63, a mere 6 mg $\text{NO}_2\text{-N/L}$ at the pH of 8 (0.14 $\mu\text{g HNO}_2\text{-N/L}$) was found to inhibit PUR by more than 90%.

It became evident that under these conditions, PAOs were losing their tolerance to FNA over time. Interestingly, by the end of this series of experiments, the biomass was displaying very good P-removal with PURs of up to 17.6 mg P/g VSS h, as shown in Figure 5.15.

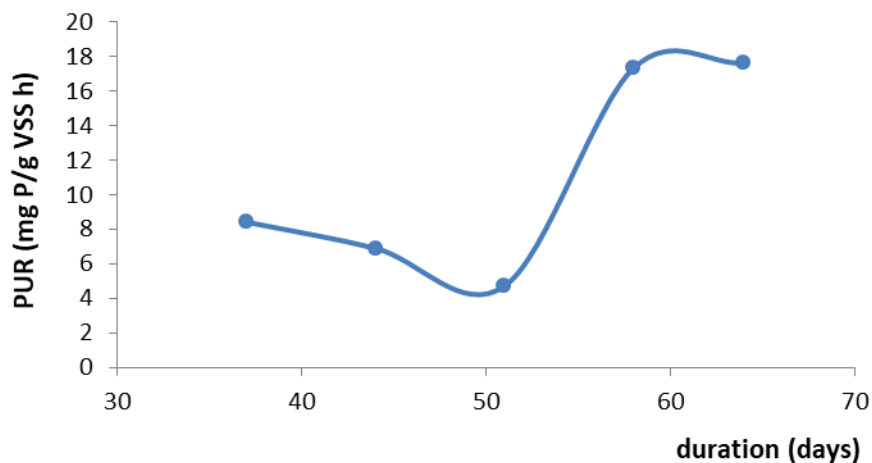


Figure 5.15. Variation of PUR throughout operation.

A possible explanation for this is the following. PAO populations are made up from individual strains that possess different characteristics such as the affinity for a specific carbon source, the capacity to utilize nitrite or nitrate and their tolerance to inhibitors. In that respect, each individual strain may be characterized by a specific k_{IFNA} or inhibition constant that corresponds to the FNA concentration that inhibits its aerobic metabolism by 50%. Under conditions where FNA is present, strains with a higher k_{IFNA} will persevere over strains with a low k_{IFNA} whose

growth will be inhibited to a greater extent. Under developing conditions, this shift in the biomass will be accompanied by a higher observed overall k_{iFNA} .

Under developing conditions where FNA is practically absent however, strains with a higher k_{iFNA} lose this advantage, allowing other strains that are less tolerant to FNA to grow. These strains may also possess certain advantages over others such as faster growth rates, leading to the wash-out of the more FNA-tolerant strains. A shift in the biomass in their favour would be accompanied by a lowering of the observed overall k_{iFNA} of the biomass.

In further investigation (presented in section 5.2.1.3), the effect of FNA on PAOs was determined to be best described by a non-competitive inhibition model. Therefore, the PURs under the effect of FNA and in its absence observed in these experiments may be correlated accordingly:

$$PUR = PUR_{control} \times \frac{k_{iFNA}}{k_{iFNA} + S_{FNA}} \quad (5.1)$$

where S_{FNA} is the FNA concentration of the reactor and k_{iFNA} is the half saturation inhibition constant of the overall biomass.

As the biomass loses its tolerance to nitrite over time, so does the k_{iFNA} drop. The k_{iFNA} in each experiment can be determined as:

$$k_{iFNA} = \frac{PUR \times S_{FNA}}{PUR_{control} - PUR} \quad (5.2)$$

Figure 5.16 displays the change in the overall k_{iFNA} of the biomass over time from the day of the first experiment of the series. As is apparent the biomass loses its tolerance to FNA over time as less tolerant PAO strains become prevalent and displace the more resilient strains. The high PUR rates observed by the end of the series may explain this shift in the PAO population as it is indicative of higher growth rates.

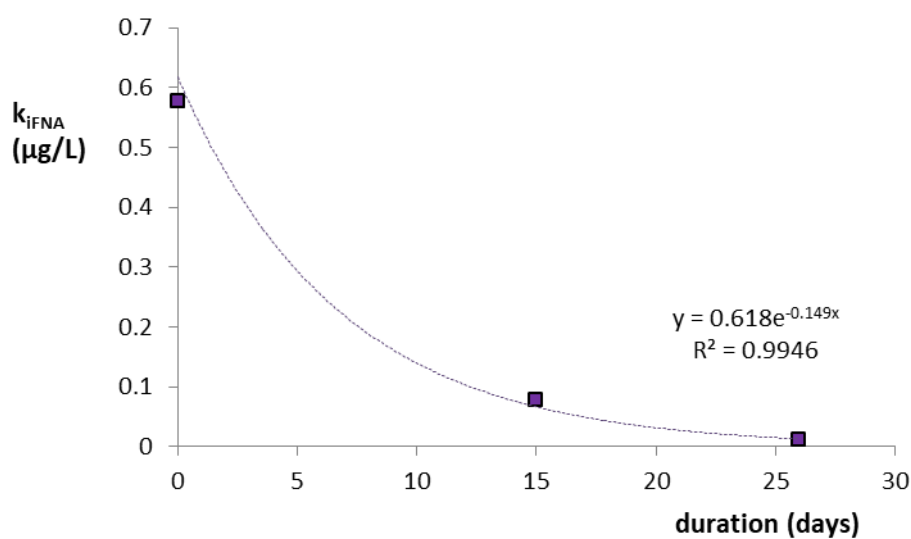


Figure 5.16. Diminishment of overall K_{iFNA} over time.

The results of the experimental series that have been presented so far indicate that PAOs could be acclimatized to FNA at concentrations as low as $0.08 \mu\text{g HNO}_2\text{-N/L}$, as PAOs that were developed in conditions of FNA accumulations up to $0.35 \mu\text{g HNO}_2\text{-N/L}$ possessed no greater tolerance to the inhibitor. Both biomasses were found to be inhibited by 50%, in regard to PUR, by an FNA concentration of $1.5 \mu\text{g HNO}_2\text{-N/L}$, and displayed practically identical degrees of inhibition over the range of the FNA concentrations that were examined. On the other hand, PAOs that were developed in the absence of FNA were found to be severely inhibited (>90%) by an FNA concentration of only $0.14 \mu\text{g HNO}_2\text{-N/L}$. Therefore, it is likely that the development of PAOs in conditions of even greater FNA accumulations, may not improve their tolerance to the inhibitor. As such, the effect of FNA on aerobic PUR that has been presented may concern an acclimated biomass. However, it is possible that more tolerant PAO strains may be in existence but could not be developed under the conditions of the experimental system.

Having established the inhibitory effect of FNA on aerobic PUR, it was questioned if PAOs had the capacity to recover from an acute exposure to FNA. In order to examine the recovery potential of PAOs, an additional experiment was carried out. This experiment was conducted upon completion of the first experimental series, with a similar protocol that differed as follows: The effect of a nitrite concentration of 35 mg N/L on aerobic PUR was examined, and compared to a control, over an aerobic period of 2 h at the pH of 7.8 ± 0.1 . After aeration, the original amount of acetate (which would provide 200 mg COD/L) was once again added in order to remove the nitrite concentration via denitritation and the reactors were maintained under stirring conditions for an anoxic/anaerobic period of 2 h. Following this, the reactors were once again aerated for a period of 2 h. The performance of the reactors during the second aerobic phase was then compared to that of the control to determine the recovery potential of PAOs.

The results of the experiment are presented in Figure 5.17. During the first phase of aeration, the reactor containing the nitrite concentration of $35 \text{ mg NO}_2\text{-N/L}$ performed poorly in comparison to the control reactor, as expected. However, following the anoxic removal of nitrite and the anaerobic release of phosphorous, the reactor appeared to remove phosphorus at an almost identical rate (5% difference) to that of the control reactor, during the second aerobic period. This would indicate that the capacity of PAOs to take up phosphorus had fully recovered from the presence of FNA. As such, it may be concluded that FNA has no acute toxic effect on PAOs and EBPR may recover quickly from nitrite shock loads, that have a short duration.

5.2.1.3 Modelling aerobic PUR inhibition due to FNA

The exact inhibitive mechanism of FNA on PAOs has not been well evidenced yet. There are reports referring to the decrease of energy generation rate (i.e. ATP production) (Zhou et al., 2010 ; Zhou et al., 2011), while others report on its negative impact on the action of some crucial enzymes and more specifically on the -PPK (Saito et al., 2004; Zhou et al., 2007; Wang et al., 2011).

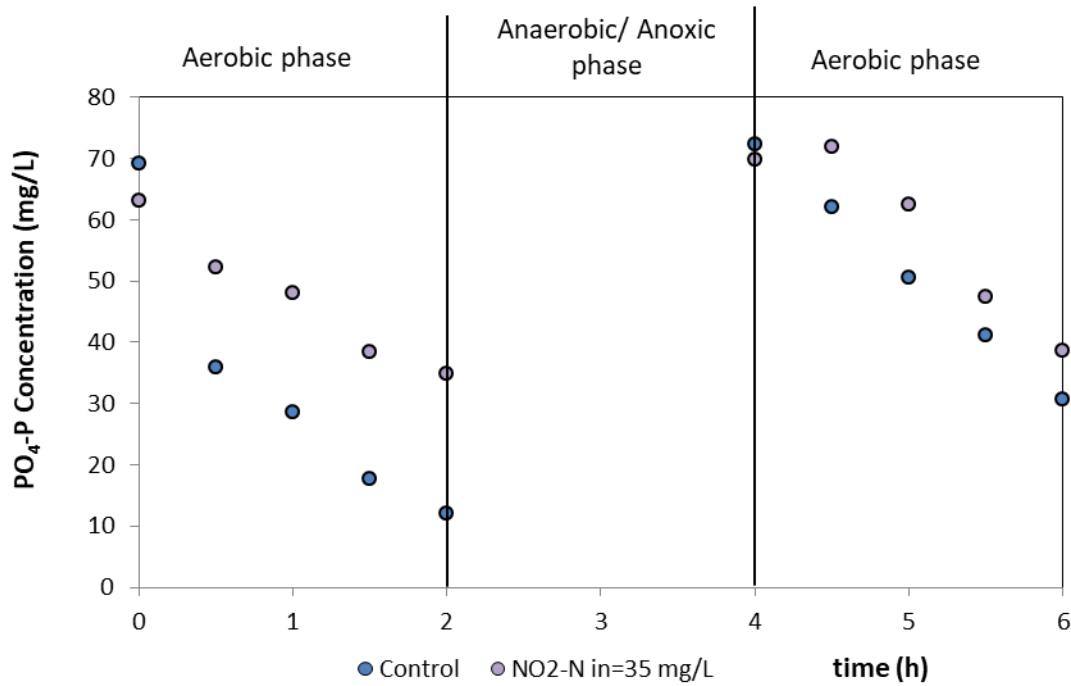


Figure 5.17. Phosphorus removal under the effect of 35 mg NO₂-N/L and after its removal.

By applying the modified direct linear plot method described in Materials and Methods (chapter 4), the values of PUR_{max}^{app} and K_m^{app} were calculated for all experimental runs. According to the results PUR_{max}^{app} decreased from 21.9 mg PO₄-P/g VSS h at the zero FNA experiment to 7.3 mg PO₄-P/g VSS h and 6.2 mg PO₄-P/g VSS h for the experiments performed with an FNA content of 2.8 µg/L and 4.6 µg/L respectively. Furthermore, K_m^{app} value for all experiments was almost constant presenting an average value equal to 4.5 mg/L and a relative low coefficient of variation (6%). The decrease of the PUR_{max}^{app} with the increase of FNA concentration and the steadiness of K_m^{app} value clearly indicates a non-competitive mode of inhibition.

A possible inhibition mechanism of FNA on PAOs activity may be described by the ability of FNA to bind equally well to both the PPK enzyme and the enzyme-substrate complex. In non-competitive inhibition it is assumed that both bindings occur at a site distinct from the active binding site that is being occupied by the substrate (allosteric site). The binding of FNA to the allosteric site results in a conformational change to the active site of the enzyme thus resulting in the decrease of product formation and therefore the decrease of PUR_{max}^{app} , while the affinity of the enzyme for phosphates (substrate) is practically unaffected as FNA does not compete with phosphates for the active site. Similarly, the effect of FNA on AOB and anammox activities has been regarded to follow the non-competitive inhibition model (Jiménez et al., 2012; Puyol et al., 2014).

In order to model FNA effect to aerobic PUR the non-competitive inhibition kinetics were adopted:

$$PUR = PUR_{max} \frac{K_{iFNA}}{S_{FNA} + K_{iFNA}} \quad (5.1)$$

where K_{iFNA} is the inhibition constant corresponding to the FNA concentration that inhibits the process by 50%, S_{FNA} is the FNA concentration in the tank and PUR_{max} refers to the maximum aerated PUR at conditions with zero inhibition (practically refers to the PUR measured at the control system of each experimental batch series).

The ability of the aforementioned non-competitive inhibition model was also compared with the model proposed by Levenspiel (1980) (equation 5.3), the Andrew's inhibition model (Andrews, 1968, equation 5.4) and the model proposed by Zhou et al. (2007) to describe FNA effect on anoxic PUR (equation 5.5). It is emphasized that both Andrews's and Levenspiel's models are substrate inhibition models which are widely used due to their simplicity. In the present study both models are used only for comparison with the simple non-competitive model.

$$PUR = PUR_{max} \left(1 - \frac{S_{FNA}}{S_{FNA}^*}\right)^n \quad (5.3)$$

where S_{FNA}^* is the critical FNA concentration in the tank at which PUR is completely inhibited and n is a constant.

$$PUR = PUR_{max} \frac{S_{FNA}}{K_S + S_{FNA} + \frac{S_{FNA}^2}{K_{iFNA}}} \quad (5.4)$$

$$PUR = PUR_{max} \frac{S_{FNA}}{K_S + S_{FNA}} e^{-\alpha S_{FNA}} \quad (5.5)$$

where S_{FNA}^* is the critical FNA concentration in the tank at which PUR is completely inhibited, K_S is the affinity coefficient constant and n, α constants.

The Nash-Sutcliffe efficiency coefficient (NSE) and the percent bias (PBIAS) were used as statistic indices to evaluate models' performances as proposed by Moriasi et al. (2007). Performance criteria used to accept each model's predictivity were $NSE > 0.8$ and PBIAS within $\pm 20\%$.

Models parametric values were calculated by performing best fit analysis to the experimental data in order to obtain the least sum of square errors (SSE). Based on this methodology an FNA inhibition constant of $1.5 \mu\text{g/L}$ was calculated for the simple non-competitive model (eq. 5.1). Accordingly, by using a S_{FNA}^* value of $13 \mu\text{g/L}$ (based on the experimental results), an n value equal to 4.4 gave the best fit of this model. Both Andrews's and Zhou's models were applied by adopting a K_S value of $0.031 \mu\text{g/L}$ as proposed by Zhou et al. (2007), while in Andrews's model, K_{iFNA} best fit value was equal to the value calculated for the simple non-competitive inhibition model ($1.5 \mu\text{g/L}$). Under best fit conditions the four models SSE were equal to 696, 1,627, 807 and 1,038 for the simple non-competitive, Levenspiel's, Andrews's and the model proposed by Zhou et al. (2007) respectively, thus highlighting that the former kinetic model is the more accurate one (eq. 5.1). The same conclusion can be drawn upon considering the other statistical indices as well (Table 5.3).

Table 5.3. Statistic indices for the FNA inhibition models examined for aerobic PUR

Statistical Index	Non-competitive	Levenspiel (1980)	Andrews (1968)	Zhou et al., (2007)
SSE-FNA	696	1627	807	1038
NSE-FNA	0.92	0.81	0.90	0.88
PBIAS-FNA	0.42%	0.44%	-0.59%	-1.07%

Figure 5.18 illustrates the graphical comparison between the experimental results and the non-competitive model's output.

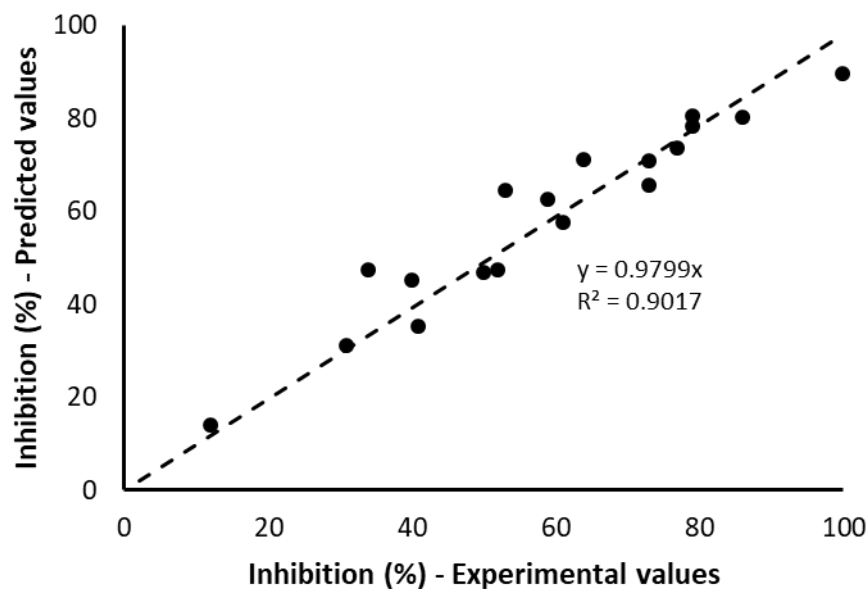


Figure 5.18. Comparison of experimental and predicted results regarding the inhibitive effect of FNA on aerobic PUR.

5.2.2 Investigating the inhibitory effect of FNA on anoxic PUR

The effect of FNA on anoxic PUR has been studied to a lesser extent compared to its effect on aerobic PUR and the reports in the literature appear to be in disagreement. For instance, Zhou et al. (2010) reported that anoxic PUR was inhibited by 100% at the FNA concentration of 37 $\mu\text{g N/L}$ (a concentration significantly higher than the threshold reported for aerobic PUR), whereas Zhou et al. (2012) reported that full inhibition was observed at the concentration of 5 $\mu\text{g N/L}$ (half the threshold for aerobic PUR). In the absence of definitive information regarding the degree of anoxic PUR inhibition and the tolerance of the anoxic pathway in comparison to the

aerobic pathway, an SBR was set-up to develop PAOs that were capable of denitrification, in order to fuel a series of experiments that focused on anoxic PUR inhibition by FNA.

5.2.2.1 Performance of the experimental system

5.2.2.1.1 Start-up period

During the start-up period the SBR operated on 4 daily cycles each consisting of an anaerobic phase, an aerobic phase and an anoxic phase. Settling and decanting occurred once per day over a 2 hour period due to technical limitations mentioned in the materials and methods section. Each cycle initially consisted of a 1 hour anaerobic phase followed by a 3 hour aerobic phase and a 1.5 hour anoxic phase.

Feed consisted of reject water from the dewatering unit of the WWTP of Psytalia that was appropriately diluted and enriched with sodium propionate, potassium phosphate and in time ammonium chloride. Each day 800 mL of the mixture were pumped into the SBR in 8 doses (2 per cycle) of 100 mL. Dilution of the reject water was carried out in order to achieve the desired ammonium concentration in the feed that was dictated by the ammonium loading of each step. Prior to decanting, the SBR contained 10.4 L of liquor. Following the removal of 5.4 L of effluent, 5.4 L of water was added to the SBR bringing the mixed liquor's volume to 10.4 L. Under mixing conditions, 1 L of mixed liquor was removed in order to achieve a SRT of around 10 days. Thus, with the daily addition of 800 mL of the concentrated feed, the SBR's working volume averaged at 10 L simulating a HRT of around 2 days.

The addition of a carbon source at the beginning of the anaerobic phase would provide PAOs with an advantage over common heterotrophic organisms, giving them priority in the utilization of COD. During the aerobic phase, the sufficient DO concentrations (>3 mg/L) would allow PAOs to develop by oxidizing their stored PHAs, while the residual propionate would be rapidly removed by other heterotrophs. With the cease of aeration and the rapid depletion of the remaining DO (within 5 minutes), the SBR was left without the addition of a carbon source during the first hour of the anoxic phase. This was to provide PAOs with a competitive advantage over common heterotrophs. As no propionate remained available by the start of the anoxic phase, PAOs would always have priority in the utilization of nitrite and nitrate. Feed was reintroduced 30 minutes prior to the beginning of the next cycle in order to remove any remaining nitrite and nitrate, thus ensuring proper anaerobic conditions at the start of the next phase.

Over the first 30 days of the start-up period, the daily dose of COD was gradually increased from 5 g/d to 7 g/d, while the daily dose of ammonium was gradually increased from 400 to 800 mg N/d. The daily dose of phosphorus was 500 mg $\text{PO}_4\text{-P/d}$, a dose much greater than the stoichiometric demand for growth of heterotrophs in order to selectively promote the growth of PAOs. This dosage would also compensate for the phosphorus that is removed via chemical precipitation, allowing the availability of an adequate phosphorus source to be taken up by PAOs throughout the aerobic and the subsequent anoxic phase. The COD and ammonium concentrations in the feed were regularly modified with regard to concentrations in the effluent in order to avoid their accumulation in the SBR.

The main objective of this initial period was to allow for the growth of PAOs that were capable of denitrification and their acclimation to low FNA concentrations. This would require the presence of nitrite during the anoxic phase in order to allow denitrification by PAOs but not at a concentration that would significantly inhibit their growth due to the related FNA presence during both the aerobic and anoxic phase. The relatively low aerobic SRT of 5 days would provide some suppression of NOB making nitrite available for the anoxic phase and its concentration regulated by the ammonium load. It is possible that the cultivation of PAO species with a capacity for denitrification may also be achieved via the availability of nitrate. As of this point it is not clear if PAOs have the capacity to directly reduce nitrate or if the presence of GAOs is required to first reduce nitrate to nitrite that can then be utilized by PAOs in a synergistic denitrification process. However, it is certain that this would enhance the presence of GAOs in the biomass which could endanger the growth of PAOs.

After 30 days of operation the biomass started displaying noticeable PAO activity with aerobic PUR rates of up to 7.5 mg P/gVSS h observed. In addition, some phosphorus removal via denitrification was observed as phosphorus removal continued during the anoxic phase along with the removal of nitrite and nitrate.

While it became clear that the cultivated PAOs were capable of removing phosphorus via denitrification, examination of their capacity to do so was limited in the SBR conditions due to the following factors:

1. Phosphorus concentrations at the end of the aerobic phase were relatively low in order to accurately examine anoxic P-removal.
2. The presence of nitrate may cloud an accurate assessment of P-removal via denitrification as it may or may not be reduced, fully or partially, by other organisms.
3. While the range of pH during the anoxic phase is likely to have little effect on precipitation reactions, or the percentage of nitrite in the form of FNA, a proper assessment requires the study of anoxic P-removal under a constant pH.

Thus, the examination of P-removal via denitrification demanded regular ex-situ experiments under controlled conditions in which phosphorous and nitrite were made available. In order to form an experimental protocol, the following batch test was conducted at this point.

Following feed, 500 mL of sludge was extracted from the SBR and placed into a container of similar working volume and left stirring under anaerobic conditions for a period of 1 hour. Following this, an appropriate amount of nitrite, in the form of sodium nitrite was added in order to obtain an initial NO_2 concentration of 40 mg N/L. From then after, samples were taken every 30 minutes for a period of 3 hours and were analysed for phosphorus and nitrite. Temperature and pH were kept constant throughout the experiment at 22 ± 1 °C and 7.65 respectively. The concentration of VSS was 2.2 g/L.

The results of this pilot experiment are displayed in Figure 5.19. As shown, phosphorus is removed steadily throughout the experiment, while nitrite is reduced at a much higher rate during the first hour of the experiment. This is because at this stage, not all of the propionate is taken up by PAOs anaerobically, leaving a residual concentration that may be utilized by common heterotrophs in the presence of nitrite. With the residual carbon source having been used, denitrification thereafter occurs at a slower rate and can be attributed mainly to PAOs, which

continue to take up phosphorus at a steady pace. The denitrification rate for heterotrophs alongside PAOs is 7.9 mg N/g VSS h, while the denitrification rate for PAOs alone is 2 mg N/g VSS h, accompanying a PUR of 2 mg P/g VSS h.

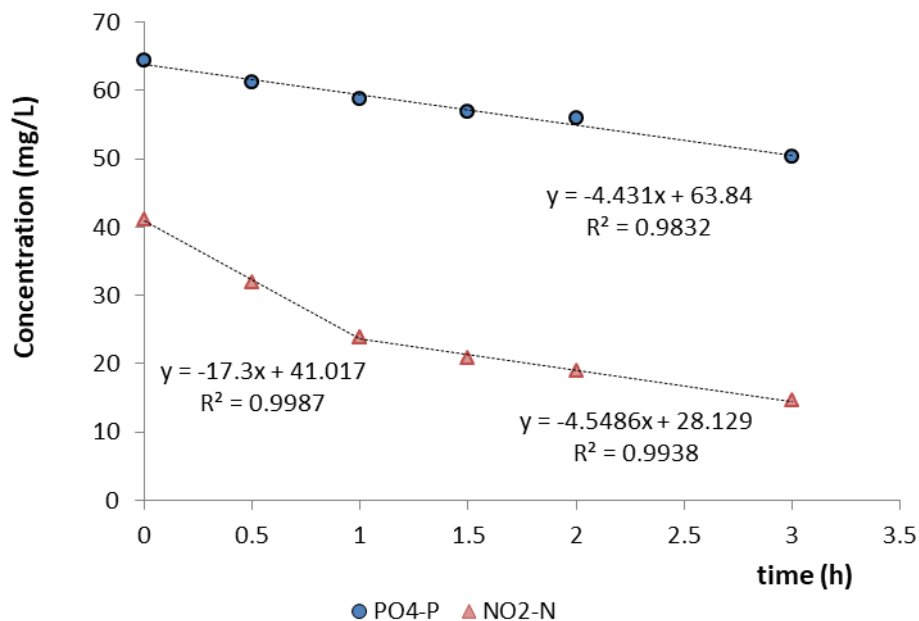


Figure 5.19. Variation of PO₄-P and NO₂-N during the ex-situ batch experiment

While the removal of phosphorus here may appear limited, it should be noted that the initial nitrite concentration with regard to temperature and pH of the reactor would result in an FNA concentration of 2.3 µg N/L. According to the experiments regarding the effect of FNA on aerobic PUR (section 5.2.1), this concentration would inhibit PAOs by more than 50%. Therefore, in order to accurately assess the capacity of PAOs for denitrification, FNA concentrations in the ex-situ batch tests are required to be at a minimum. This would require a high pH and a relatively low yet abundant nitrite concentration.

The examination of P-removal via denitrification was hereafter examined in similar ex-situ batch tests in which the nitrite concentration was kept constant at 8 ± 2 mg N/L with the frequent addition of a sodium nitrite solution. The pH of each experiment was kept constant at the value of 8, a relatively high pH that would limit the concentration of FNA. According to the experiments regarding the effect of FNA on aerobic PUR, this concentration would inhibit PAOs by less than 10%.

At this point the SBR's configuration was altered so that each cycle now consisted of a 1 hour anaerobic phase, a 2 hour aerobic phase and a 2.5 anoxic phase with feed being introduced at the start of the anaerobic phase and 1.5 hours into the anoxic phase. The lower aerobic SRT would allow further NOB suppression resulting in greater nitrite concentrations within the SBR. This in turn would promote the anoxic growth of PAOs via denitrification. As it has been reported that GAOs are incapable of denitrification with propionate as the sole carbon source this would provide PAOs with a significant advantage, ultimately leading to the wash-out of GAOs from the SBR.

Under the new configuration the daily dose of COD was gradually increased up to 8 g/d, while the daily dose of ammonium was gradually increased up to 1000 mg N/d over a period of 30 days and was maintained under the new conditions for a further 30 days prior to the beginning of the experiments.

5.2.2.1.2 Steady-state operation

Following a period of adjustments in the feed and configuration of the SBR already described during the first 60 days of operation, the SBR had reached steady-state operation by day 90. The SBR was successful in developing a strong PAO population as was documented by FISH analyses and validated by the observed anaerobic COD consumption coupled with significant anaerobic P-release and aerobic P-uptake that characterize the biomass. In addition, the biomass maintained a capacity for anoxic P-removal that was noticeable as early as 30 days from the commencement of operation. Over time, the anoxic/aerobic PUR ratio displayed by the biomass increased and remained constant from day 80 onwards.

During steady state operation, MLVSS averaged at $2,500 \pm 300$ mg/L, while MLSS averaged at $2,800 \pm 400$ mg/L. The biomass concentration that was maintained in the SBR is a direct result of the chosen COD loading rate and SRT. The pH ranged from 7.5 to 8.3. Following decanting and re-filling of the SBR, pH would drop to 7.5 and would remain unchanged during the following anaerobic period. During aeration, pH would rise due to carbon stripping and reach 8.2 ± 0.05 by the end of the aerobic phase. During the anoxic phase, pH rose up to 8.3 due to denitrification.

As mentioned, feed entered the SBR at the start of each anaerobic cycle and 1.5 hours into the anoxic cycle over a 2 minute period. Each dose provided the biomass with 1 g COD, 125 mg $\text{NH}_4\text{-N}$ and 62.5 mg $\text{PO}_4\text{-P}$ that would raise the respective concentrations in the SBR by 100 mg COD/L, 12.5 mg $\text{NH}_4\text{-N}$ /L and 6.25 mg $\text{PO}_4\text{-P}$ /L. At the beginning of the anaerobic phase, after feed, COD concentrations in the SBR averaged at 170 ± 20 mg/L, while phosphorus concentrations averaged at 22 ± 4 mg/L.

Under anaerobic conditions, COD concentration dropped to values less than 100 mg/L, while the concentration of phosphorus rose to 70 ± 10 mg/L as shown in Figure 5.20, indicating strong PAO activity in the SBR. The average P-release rate was 22 ± 2 mg P/g VSS h, while the average propionate uptake rate was 44 ± 5 mg COD/g VSS h. This would correspond to a $\text{COD}_{\text{uptake}}/\text{P}_{\text{release}}$ ratio of 2.

During the aerobic phase, the residual biodegradable COD was rapidly removed over the first 30 minutes of aeration, while phosphorus concentrations dropped dramatically during the first hour of aeration, displaying a PUR of 22 ± 3 mg P/g VSS h. It is possible that the removal of phosphorus may have been assisted to some extent by the formation of struvite due to the rise of pH, especially during the first 30 minutes of aeration (Figure 5.21). By the end of the aerobic phase, the remaining phosphorus concentration was 5 ± 2 mg P/L. After the cease of aeration, the remaining phosphorus was taken up by PAOs by reducing the nitrite produced during the aerobic phase. In this case it is unlikely that chemical precipitation contributed to phosphorus removal as the solubility of struvite remains unchanged at pH above 8. Furthermore, the re-entry of feed 4.5 hours since the beginning of the cycle did not result in P-release

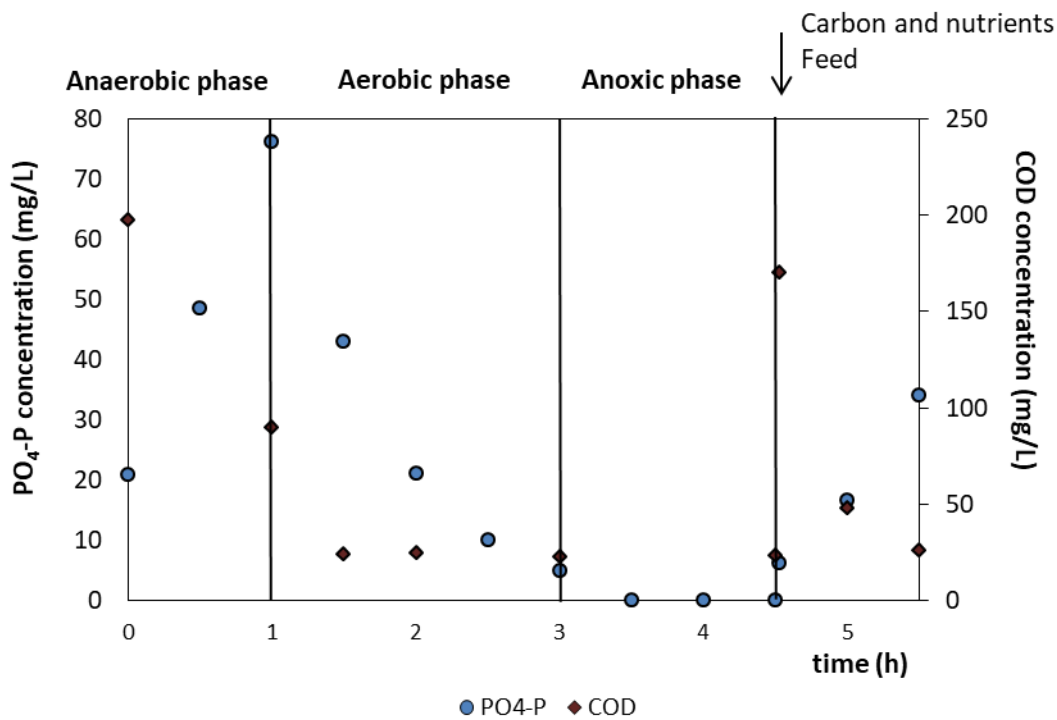


Figure 5.20. Typical variation of PO₄-P and COD in the SBR during the first daily cycle.

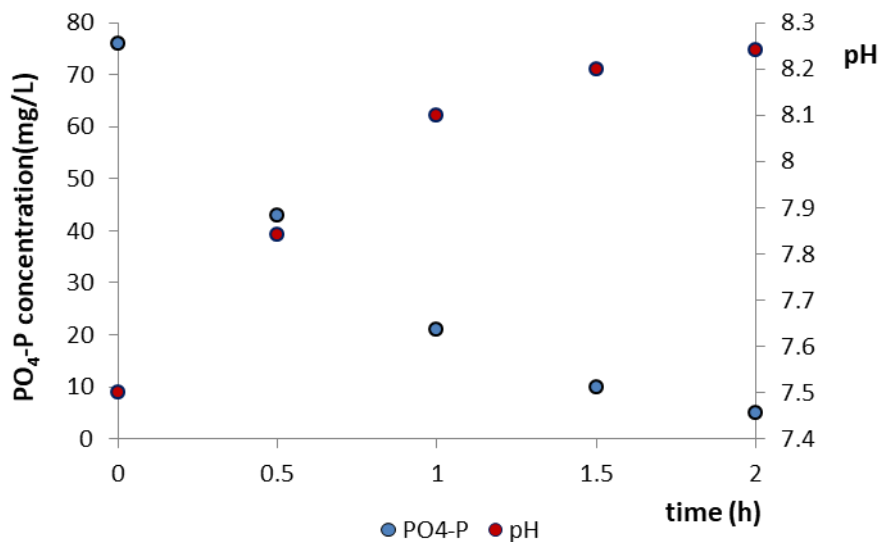


Figure 5.21. Typical variation of PO₄-P and pH in the SBR during the aerobic phase of the first daily cycle.

Figure 5.22 shows the profiles of nitrite, nitrate and ammonium nitrogen during the aerobic phase. At the end of the aerobic phase the concentration of total NO_x-N was 15 ± 3 mg/L with nitrite representing 2/3 of this amount. This was due to the intended NOB shunt that was partially achieved by the low aerobic retention time. During the 1.5 hour period after the cease of aeration approximately 80% of both nitrite and nitrate was removed by PAOs (and possibly by

other heterotrophs via endogenous respiration), taking up P in the process. The remaining NO_x were rapidly removed with the re-entry of feed. Ammonium concentrations dropped steadily during aeration due to oxidation and secondary due to the growth requirements of the biomass. In total, 21 ± 4 mg/L NH₄-N were removed during each cycle, meaning that an average of 6 mg N/L per cycle or 24 mg N/L per day were utilized for the daily growth of the biomass. This would correspond to roughly 10% of the 2,500 mg of biomass produced each day, which is a typical stoichiometric analogy.

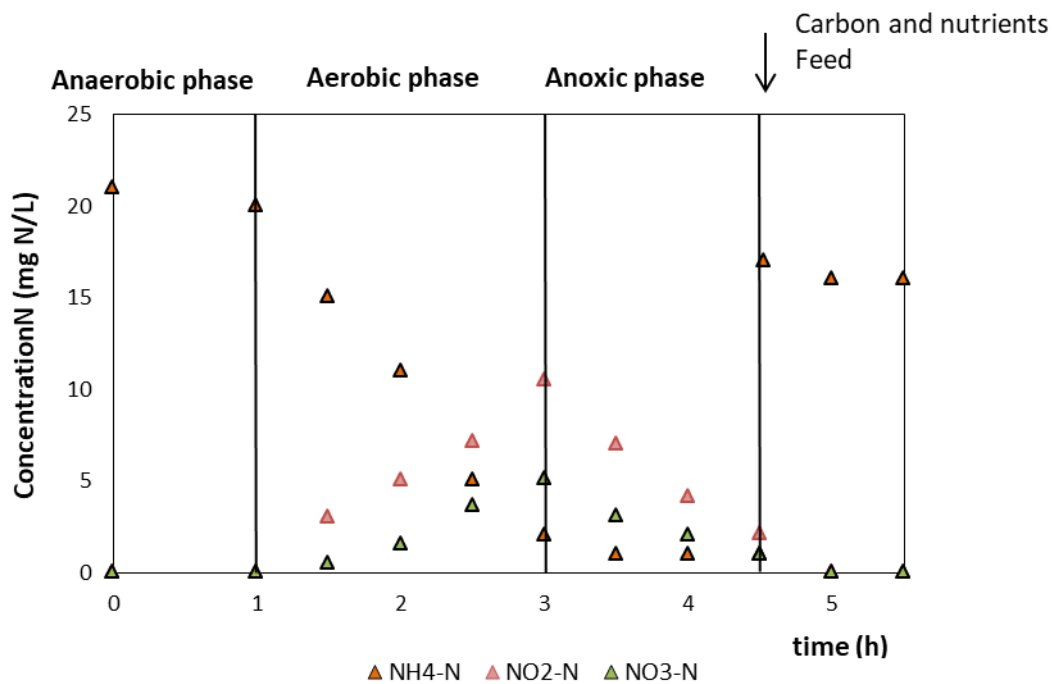


Figure 5.22. Typical variation of ammonium, nitrite and nitrate in the SBR during the first daily cycle.

Figure 5.23 displays the typical variation of FNA in the SBR during the aerobic phase of the first daily cycle with regard to pH. As shown, for most of the duration, PAOs were exposed to an FNA concentration greater than $0.1 \mu\text{g N/L}$ which would peak with the completion of nitrification at a concentration of just below $0.16 \mu\text{g N/L}$. According to the results of the experimental series regarding the effect of FNA on aerobic PUR (section 5.2.1), concentrations of this magnitude would have little effect on PAOs but may be considered adequate for their acclimation to FNA.

As mentioned, in order to properly evaluate the biomass's capacity for phosphorus removal under both aerobic and under anoxic conditions, regular batch experiments were conducted on sludge samples retrieved from the SBR. In each experiment, 1 L of sludge from the SBR was divided equally into 2 containers each with a working volume of 500 mL. The pH of each reactor was set to 8 and kept constant throughout the duration of the experiment. Aerobic PUR was examined as previously described in section 5.2.1.1., while anoxic PUR was evaluated according to the experimental protocol developed during the start-up period.

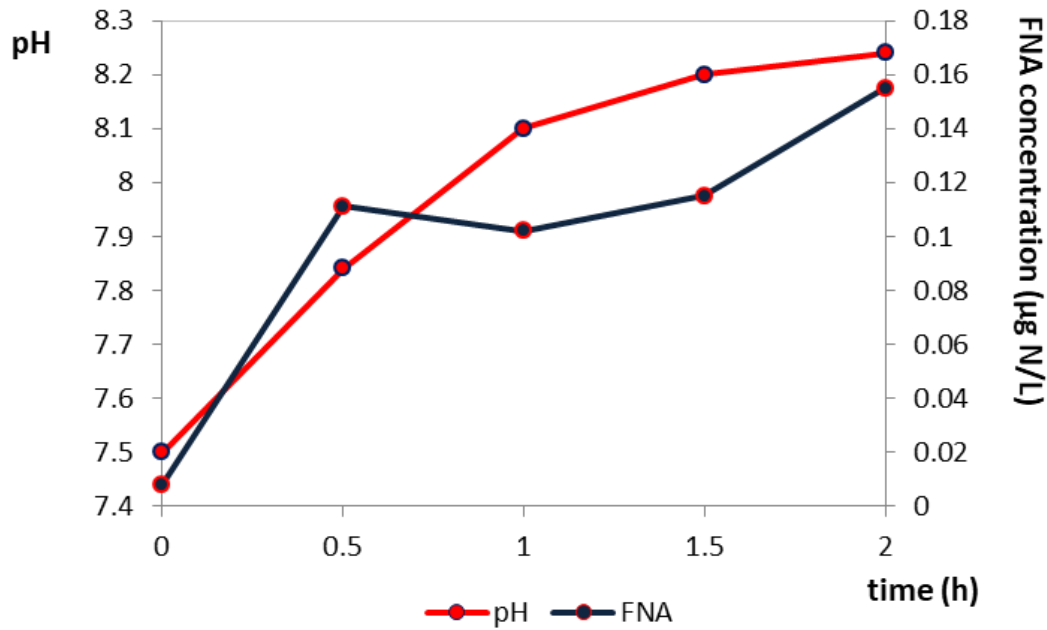


Figure 5.23. Typical variation of FNA and pH in the SBR during the aerobic phase of the first daily cycle.

The biomass displayed phenomenally high aerobic PURs of up to 29 mg P/g VSS h and anoxic PURs up to 13 mg P/g VSS h throughout operation. Figure 5.24 displays the results of a routine batch experiment. The concentration of VSS was 2,460 mg/L and based on the slopes of the experimental data, the aerobic PUR could be calculated as 27.4 mg P/g VSS h and the anoxic PUR (via nitrite) as 10.3 mg P/g VSS h (approximately 38% of the aerobic PUR).

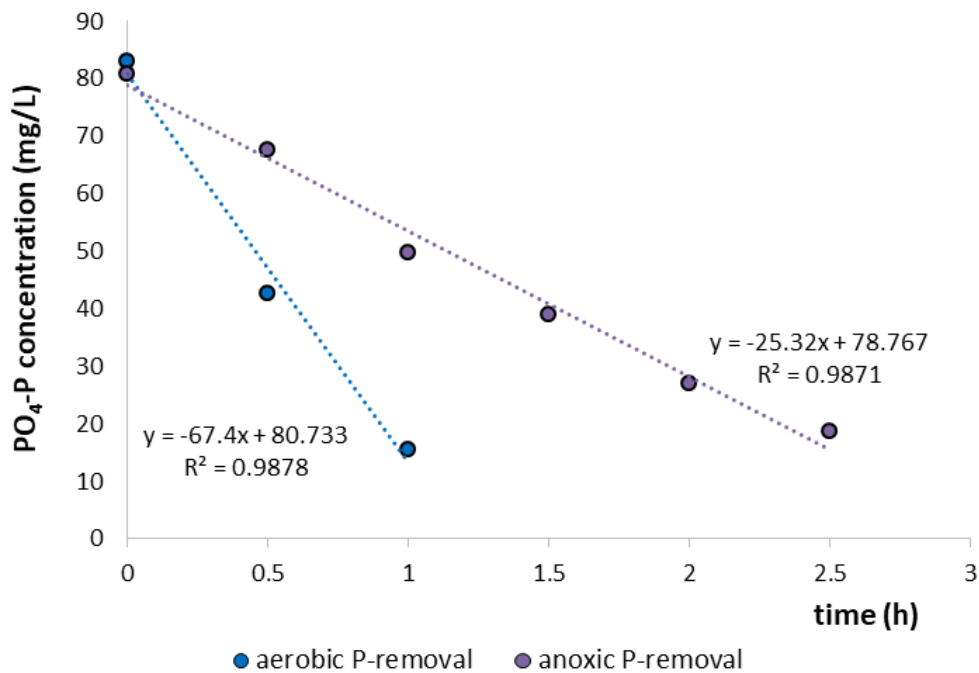


Figure 5.24. Phosphorus removal under anoxic and aerobic conditions of the typical ex-situ batch experiment.

Figure 5.25 displays a comparison of the aerobic and anoxic PURs observed in the routine batch experiments throughout operation. The aerobic PUR averaged at 25 ± 4 mg P/g VSS h, while the anoxic PUR averaged at 10 ± 3 mg P/g VSS h. The anoxic/aerobic PUR ratio appeared relatively steady throughout operation with anoxic PUR being observed to occur at approximately 40% of the aerobic PUR. It is possible that not all PAOs were capable of denitrification although, given the SBR's configuration and its stable performance it is more likely that all PAOs had this capacity and that anoxic P-removal is thermodynamically considerably slower than aerobic P-removal. Based on this finding it is anticipated that upon modelling biological phosphorus removal processes, a n_{NO_x} coefficient of around 0.4 can be used to simulate anoxic phosphorus removal with respect to the respective aerobic process. This value is lower than the one proposed in ASM2d (0.6) to simulate biological phosphorus removal in conventional activated sludge systems (IWA, 2000).

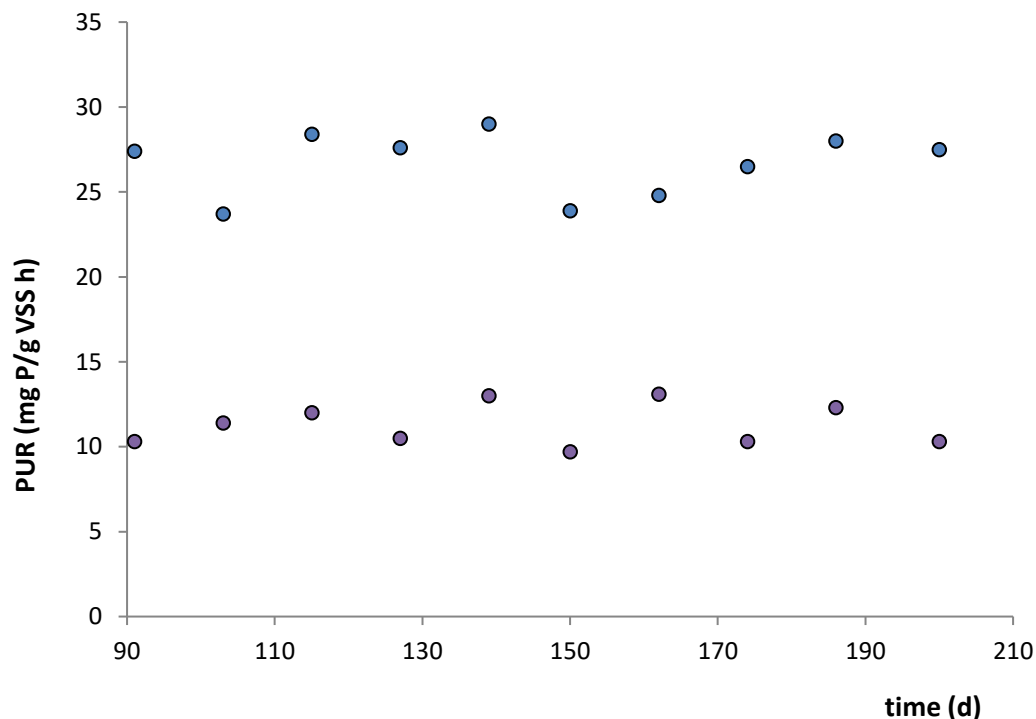


Figure 5.25. Variation of anoxic and aerobic PUR throughout operation.

5.2.2.1.3 Evaluation of the PAO-enriched sludge

The SBR configuration was successful in developing a biomass with all the characteristics of a strong PAO community, displaying very good phosphorus removal both under aerobic and anoxic conditions with an average aerobic PUR of 25 ± 4 mg P/g VSS h and an average anoxic PUR of 10 ± 3 mg P/g VSS h. The strong presence of PAOs was also verified by FISH analysis (Figure 5.26). Quantification of 4 samples revealed that *Accumulibacter* (the main PAO group), accounted for approximately 48% of the total microbial population.

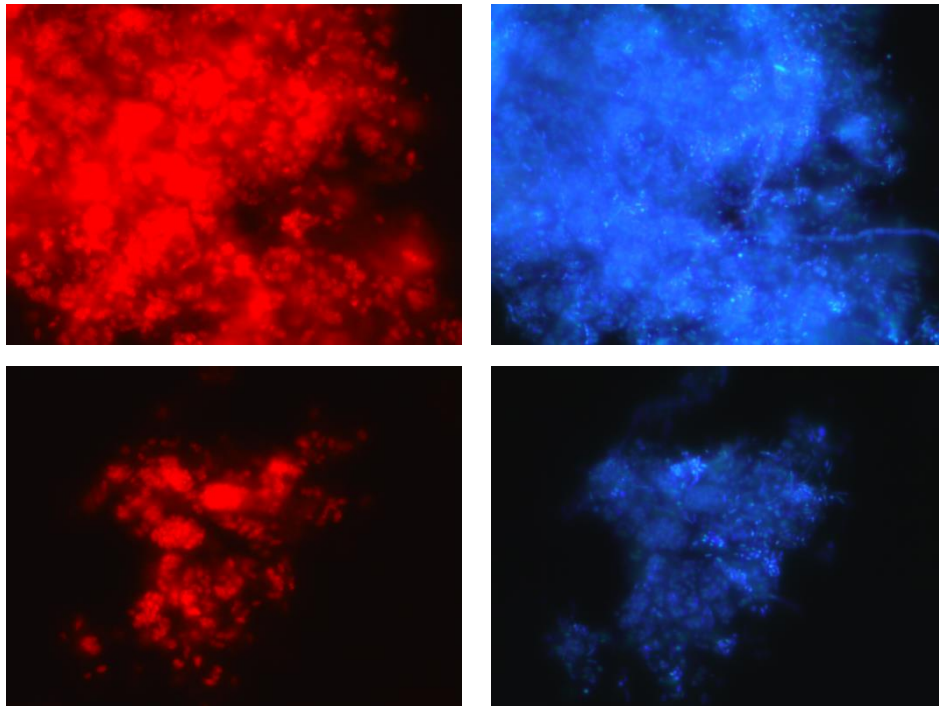


Figure 5.26. In situ identification of PAOs using Cy-3 labelled PAOMIX (PAOs depicted in red, all microorganisms stained with DAPI presented in blue).

5.2.2.2 Experimental assessment of the effect of nitrite on anoxic PUR

Having established a strong and stable PAO community, a series of ex-situ batch experiments was conducted in order to investigate the effect of FNA on the anoxic PUR of PAOs. A total of 6 batch series were performed for various nitrite concentrations at the pH of 8. The nitrite concentrations investigated were 25, 35, 75, 170, 270 and 350 mg NO₂-N/L. The respective FNA concentrations are 0.58, 0.82, 1.82, 4.73, 7.12 and 8.51 µg HNO₂-N/L. At the beginning of each experiment, sludge was extracted from the SBR prior to feed and divided equally into 3 bioreactors, each with a working volume of 0.5 L. The pH of each reactor was set to 8 ± 0.05 and kept constant over the duration of each experiment. Each reactor was fed with readily biodegradable organic carbon, in the form of a sodium acetate solution, in order to obtain an initial COD concentration of 100 mg/L and was stirred for 1 h under anaerobic conditions. Following the anaerobic phase, nitrite in the form of a sodium nitrite solution was added to the bioreactors in order to study phosphorus removal via denitrification. In each experiment, one of the bioreactors served as a control and received an initial nitrite concentration of 10 mg NO₂-N/L. Throughout the experiment, the control's nitrite concentration was kept constant at 8 ± 2 mg N/L by regular addition of the sodium nitrite solution. In each experiment, the effect of a specific NO₂-N concentration on anoxic PUR was evaluated in duplicates over a 3 h period.

After the completion of the series of experiments described above, the following supplementary batch tests were conducted:

- In order to examine any possible differences in the inhibitory effect of FNA on anoxic PUR with regard to the type of carbon source, a similar experiment was conducted with sodium propionate instead of sodium acetate being added to provide the initial 100

mg/L COD concentration. The nitrite concentration in the duplicate reactors for this experiment was 50 mg NO₂-N/L and the pH throughout the experiment was kept stable at 8 ± 0.05 .

- In order to confirm the effect of FNA on anoxic PUR at lower pH, a similar experiment was carried out in which the performance of a control reactor, as described above, was compared to that of two bioreactors under the same NO₂-N concentration of 30 mg/L at the different pH values of 7 and 8. The experiment was replicated twice to ensure repeatability.
- In order to accurately compare the effect of FNA on anoxic PUR with its effect on aerobic PUR, an additional experiment was conducted on the same biomass. In this experiment, following a similar 1 h anaerobic phase, the reactors were aerated for a period of 3 hours. One reactor containing no nitrite served as a control, while the other 2 bioreactors obtained a nitrite concentration of 50 mg NO₂-N/L. This experiment was conducted to ensure that the biomass used in this series of experiments had the same acclimation to FNA with the biomass on which the experiments focusing on aerobic PUR had been conducted (section 5.2.1.2).

The methodology for calculating PURs and the inhibitory effect of a specific FNA concentration is detailed in the following typical batch experiment. Figure 5.27 displays the results for the nitrite concentration of 170 mg N/L at the pH of 8. As shown, while phosphorus removal generally occurred at a steady rate, the entry of sodium nitrite in the reactors would often cause a slight disturbance, resulting in a diminished PUR during the first 30 minutes of the experiment compared to their subsequent performance. This may be due to a combination of a disturbance in the water chemistry and possibly a brief adaptation period of the biomass to the new conditions. Following this period, the reactors displayed a steady PUR up until the remaining phosphorus became significantly low or the capacity of the biomass to take up phosphorus had been largely exhausted.

As it is made clear in Figure 5.27, the PUR of each reactor was established for the duration where a stable performance was observed. In this particular experiment, the concentration of VSS in each reactor was 2,140 mg/L. Based on the slopes of the experimental data, the control's PUR could be calculated as 6.1 mg P/g VSS h, while the PUR of the other reactors averaged at 2.15 mg P/g VSS h. The nitrite concentration of 170 mg N/L at the pH of 8 was therefore found to inhibit anoxic PUR by 65%.

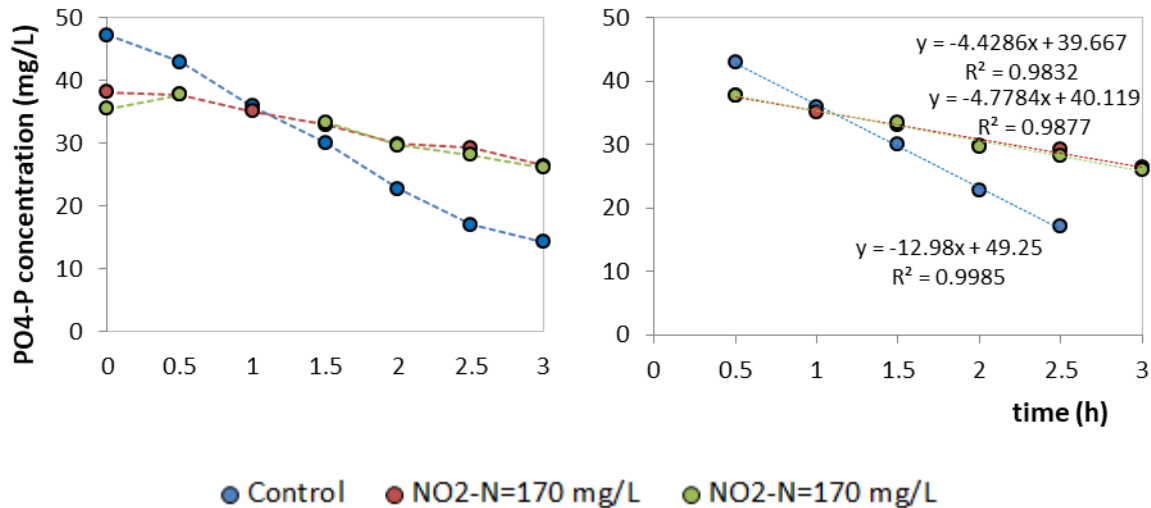


Figure 5.27. PURs for a typical batch experiment ($\text{NO}_2\text{-N}=170$ mg/L, pH=8)

While the nitrite concentration in the control reactor was kept constant at 8 ± 2 mg N/L, there was no replenishment of nitrite in the duplicate reactors in order to study the denitritation rates under these conditions. Figure 5.28 displays the variation of nitrite in the duplicate reactors for the typical batch experiment mentioned above. As shown, the reactors performed at a practically identical denitritation rate (6.2 mg $\text{NO}_2\text{-N}/\text{g VSS h}$) with nitrite being reduced from an initial concentration of $175\text{-}180$ mg $\text{NO}_2\text{-N}/\text{L}$ to $145\text{-}150$ mg $\text{NO}_2\text{-N}/\text{L}$ by the end of the experiment. In this range of concentrations, nitrite would have practically the same effect on PAOs. Generally, it was accepted that the initial nitrite (or rather the associated FNA) concentration affected the process throughout the experiment as it was considered unlikely that PAOs were capable of recovering directly along with the removal of nitrite in this short period of time. This would be backed up by the fact that both phosphorus and nitrite removal in each experiment did not appear to improve over time with the removal of nitrite and displayed steady rates.

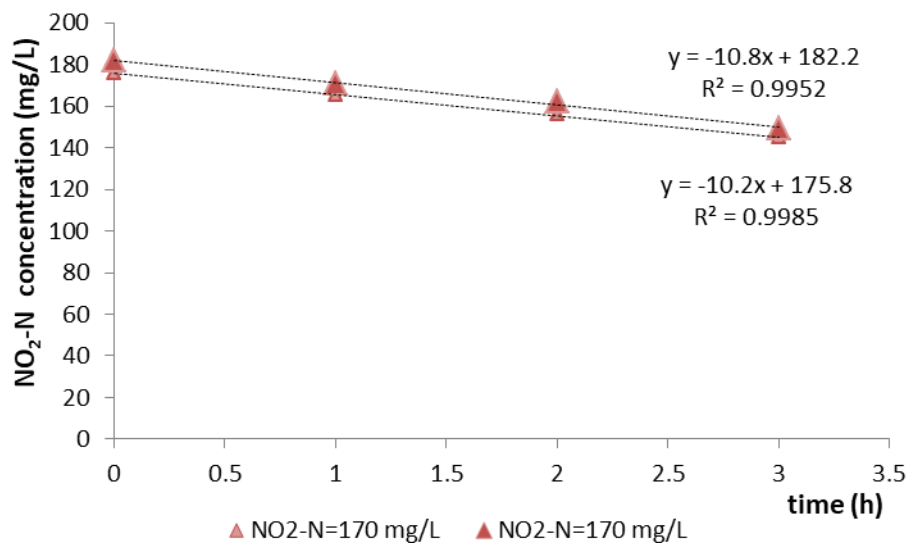


Figure 5.28. Denitritation in the typical batch experiment ($\text{NO}_2\text{-N}=170$ mg/L, pH=8).

Figure 5.29 and Figure 5.30 present the results of the experiment investigating the effect of nitrite on anoxic PUR at 2 different pH values (30 mg NO₂-N/L at the pH of 7 & 8). As expected, nitrite inhibited anoxic PUR significantly more at the low pH of 7 due to the higher FNA content (tenfold the concentration compared to the pH of 8). This can be observed not only by the diminished PUR but also by the slower denitritation rate at the pH of 7.

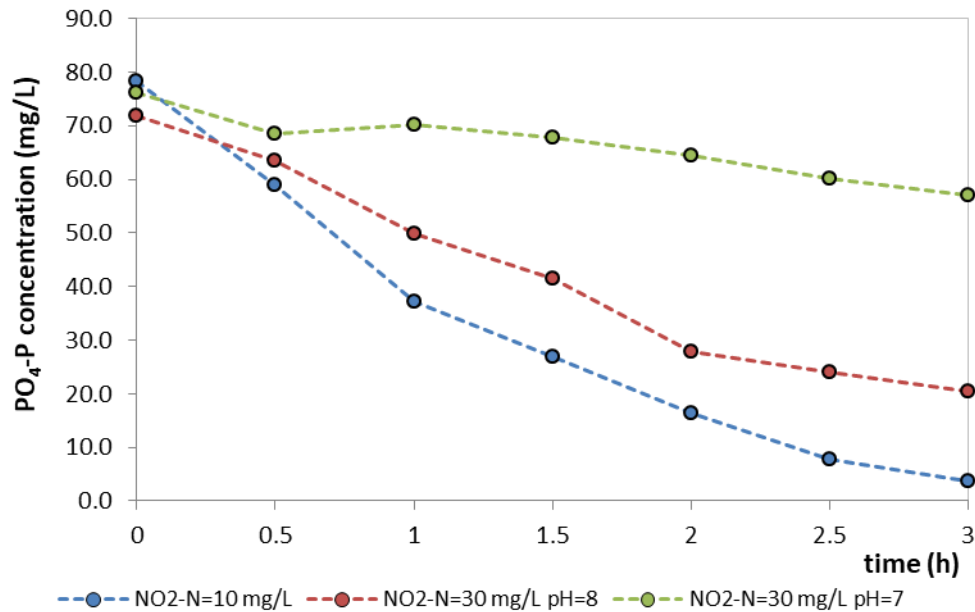


Figure 5.29. Variation of phosphorus during the typical experiment.

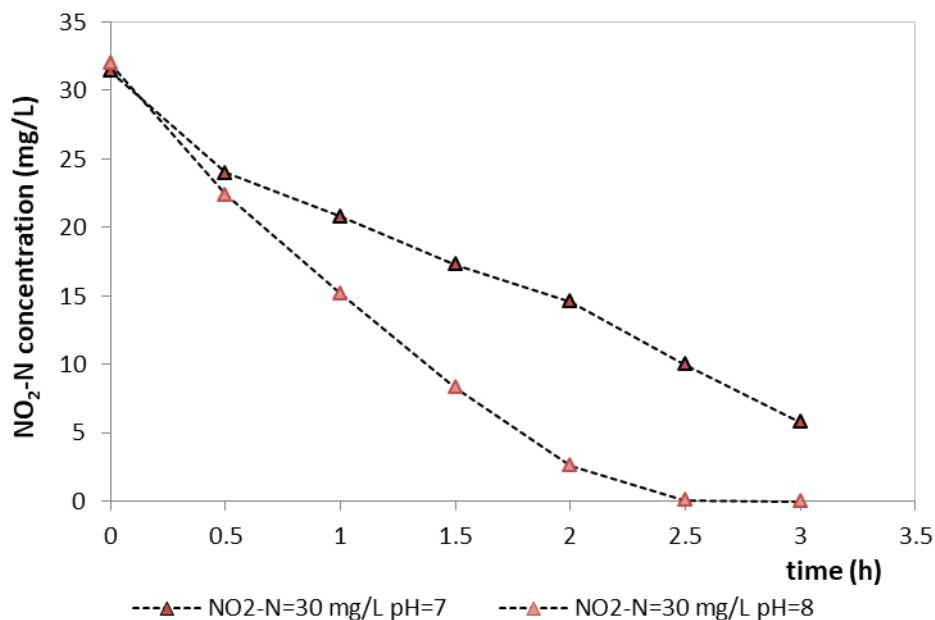


Figure 5.30. Variation of nitrite during the typical experiment.

In order to properly assess the experimental data, several considerations must be taken into account. In particular:

- Nitrite concentrations appear to drop at a higher rate during the first 30 minutes of the experiment. This is most likely due to the presence of some residual carbon that was not taken up anaerobically and was made available for common heterotrophs with the introduction of nitrite. Nitrite removal during this step also appears to be much less affected by pH which seems to validate the above hypothesis. Therefore, this period of time should not be taken into consideration when evaluating the denitrification rates of PAOs. This, however, does not affect the PURs of PAOs.
- Nitrite in the reactor with pH=8 drops to very low concentrations after 1.5 hours. This not only affects the denitrification rate of PAOs but also their PUR. Therefore, no data after this point should be used to determine removal rates for this reactor.
- Phosphorus concentrations in the control reactor become lower than 10 mg/L after 2 hours which could affect PUR as phosphorus is not in abundance. Therefore, the control's PUR should derive from its performance during the first 2 hours of the experiment.
- Both phosphorus and nitrite, in the reactors containing the initial 30 mg NO₂-N/L, appear to be removed at a steady rate, despite the removal of nitrite (with 15 mg NO₂-N/L remaining after 1 h at the reactor of pH=8 and after 2 h at the reactor of pH=7). This would validate the assumption that PAOs do not recover immediately along with the removal of nitrite and that for short-time experiments such as the present ones, the degree of PUR inhibition may be attributed to the initial nitrite concentration of 30 mg N/L.

In view of the above, the denitrification and phosphorus uptake rates were established according to the data presented in Figure 5.31 and Figure 5.32. With regard to the VSS concentration (2,550 mg/L), the PUR of the control reactor was calculated at 12.2 mg P/g VSS h, while the PUR of the reactor containing 30 mg NO₂-N/L at the pH of 8 was found to be 8.16 mg P/g VSS h. The PUR of the reactor at the pH of 7 was calculated at 2.23 mg P/g VSS h when taking into account the first hour of the experiment and at 2.66 mg P/g VSS h when disregarding it. These values would correlate to inhibition degrees of 78-82% compared to the control's performance. The average value of 2.45 mg P/g VSS h was determined to best represent the reactors performance, meaning that the concentration of 30 mg HNO₂-N/L at the pH of 7 was found to inhibit anoxic PUR by 80%. At the pH of 8, the same concentration was found to inhibit anoxic PUR by 33%.

The denitrification rate was 5.51 mg N/g VSS h at the pH of 8 and 2.77 at the pH of 7. While the performances in denitrification do not directly correlate to the respective performances in phosphorus removal, this is to be expected as it is likely that a portion of nitrite is denitrified by other heterotrophic organisms present via endogenous respiration.

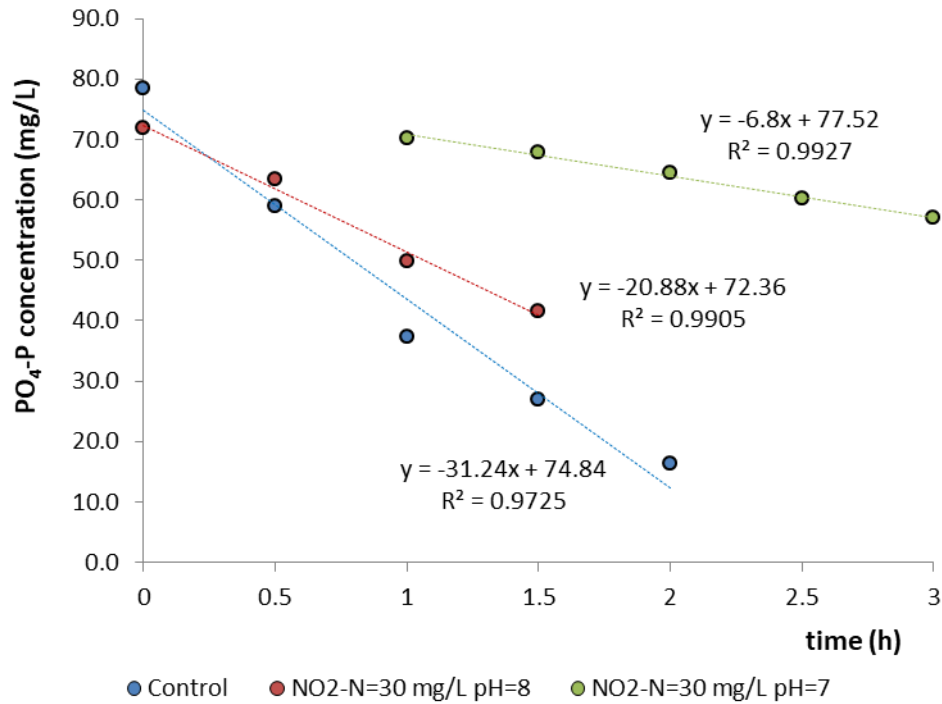


Figure 5.31. Determination of PURs for the ex-situ experiment.

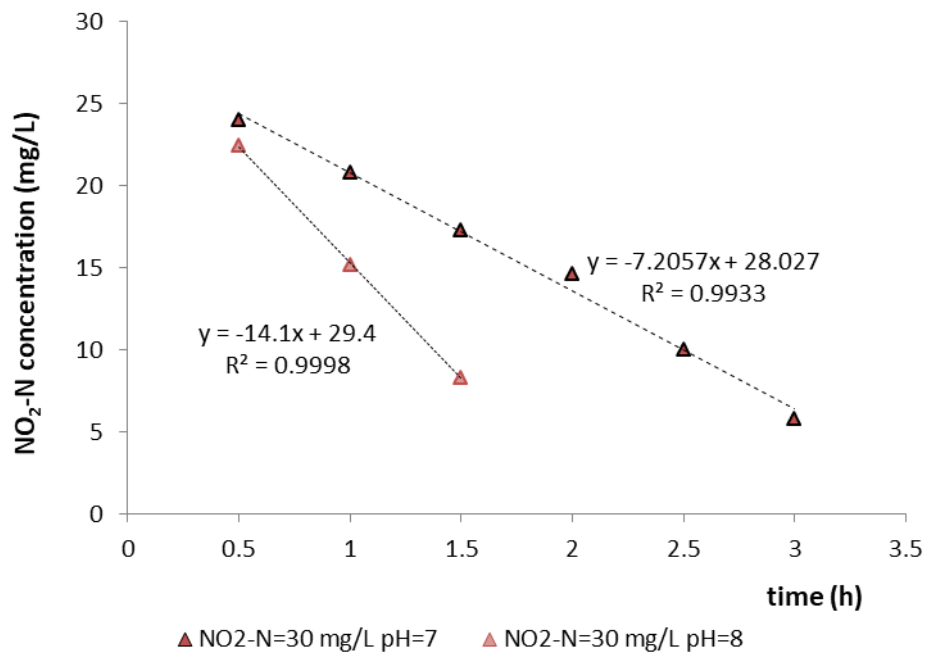


Figure 5.32. Determination of the denitrification rates for the ex-situ experiment.

The results of this series of experiments are presented in Figure 5.33 and Figure 5.34. The FNA concentrations in each experiment were calculated with regard to the relative nitrite concentration, pH and temperature. As expected, FNA appears to be a strong inhibitor of the anoxic metabolism of PAOs with 50% inhibition of the anoxic PUR being observed at the FNA concentration of 1.8 $\mu\text{g HNO}_2\text{-N/L}$ (75 mg NO₂-N/L at pH=8).

The degree of inhibition due to FNA in the experiment at the pH of 7 seems to correlate well with those observed at the pH of 8, as could be expected, since temperature and pH control the percentage of nitrite in its protonated form. Therefore, the inhibitory effect of nitrite at low pH may be accurately predicted accordingly.

When propionate was used instead of acetate as the carbon source, the control reactor performed at a very similar PUR to the ones observed when acetate was used and the degree of PUR inhibition observed for the nitrite concentration examined appears to be in agreement with the results of the previous experiments. As such, it would appear that the effect of FNA on the anoxic metabolism of PAOS is the same in the case of propionate and acetate.

In the experiment examining the inhibition of aerobic PUR, the concentration of 50 mg NO₂-N/L at the pH of 8 was found to inhibit the process by 49%. In the series of experiments investigating the effect of FNA on aerobic PUR (section 5.2.1.2), the same concentration was found to inhibit PUR by 50%. As such, the biomass in this series of experiments possesses the same tolerance to FNA as the biomass used in the aerobic experiments. Therefore, the effect of FNA on the anoxic metabolism of PAOs as observed in this series of experiments may be compared with that on the aerobic metabolism observed in the previous series of experiments.

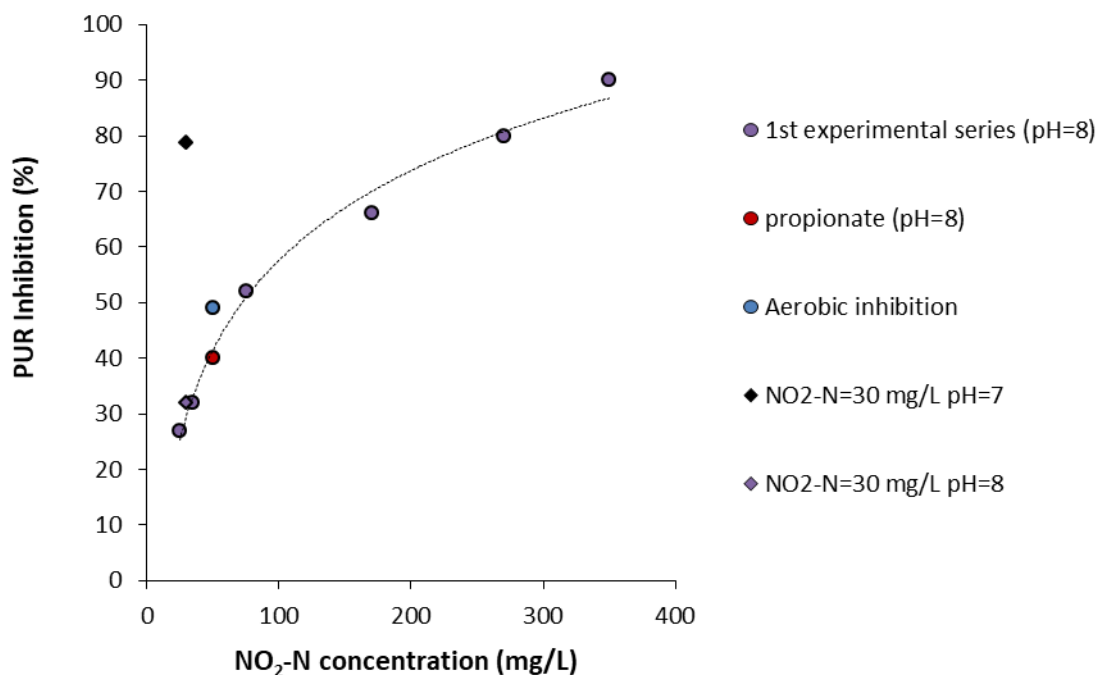


Figure 5.33. Effect of nitrite on anoxic PUR.

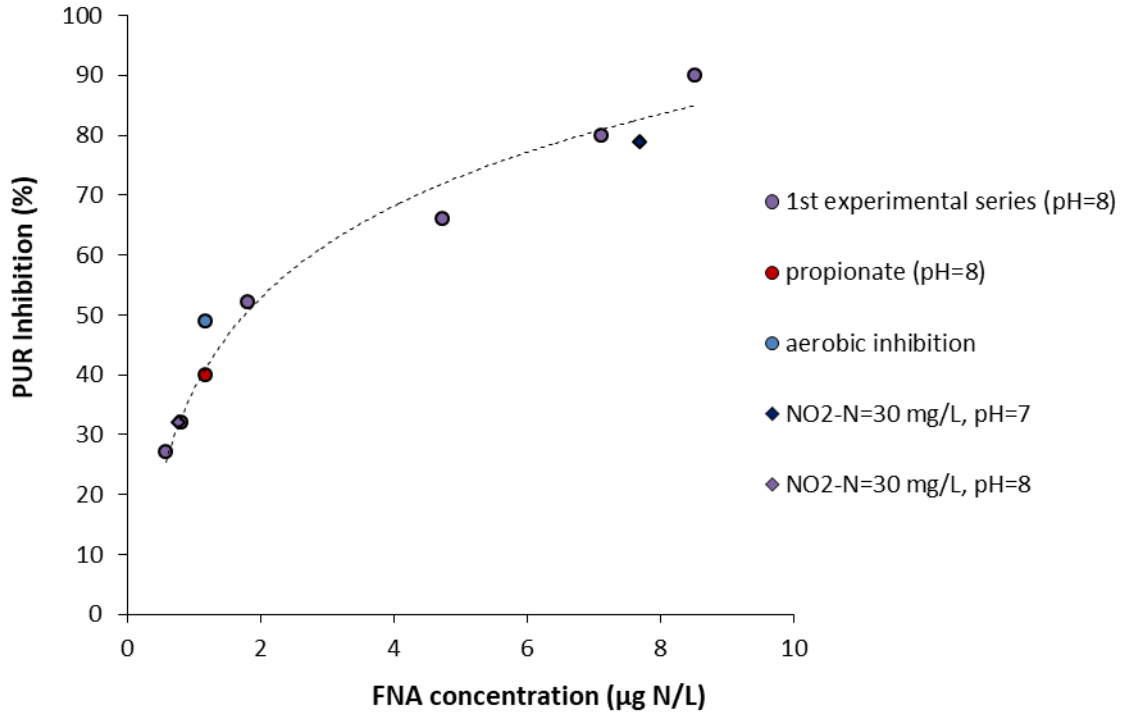


Figure 5.34. Effect of FNA on anoxic PUR.

Figure 5.35 displays the inhibitory effect of FNA on anoxic PUR compared to its effect on aerobic PUR. Interestingly, the inhibitory effect of FNA on anoxic PUR was found to be very similar to that observed on aerobic PUR. At first glance it would appear that anoxic phosphorus removal has a slightly greater tolerance to FNA than aerobic P removal. However, it should be pointed out that the control reactors in the experiments examining anoxic inhibition maintained a nitrite concentration of 8 ± 2 mg $\text{NO}_2\text{-N/L}$ in order to allow sufficient denitritation. At pH=8 at room temperature, this nitrite concentration has been found to inhibit aerobic PUR by approximately 10%. Assuming that the anoxic pathway has the same tolerance to FNA as the aerobic pathway, the inhibitions observed in the anoxic experiments may be corrected as so:

If the control reactor is inhibited by Control_{inh} , then the PUR observed is:

$$PUR_c = (1 - \text{Control}_{inh}) \times PUR_{max} \quad (5.6)$$

where PUR_{max} is the theoretical anoxic PUR in the complete absence of FNA.

The inhibitions for the various FNA concentrations in this series of experiments were determined based on the performance of the control reactor as so:

$$\text{Inhibition}_{observed} = \frac{PUR_c - PUR_{inh}}{PUR_c} \quad (5.7)$$

where PUR_{inh} is the PUR of the duplicate reactors containing the examined nitrite concentrations. The real inhibitory effect of each FNA concentration is:

$$\text{Inhibition} = \frac{PUR_{max} - PUR_{inh}}{PUR_{max}} \quad (5.8)$$

Therefore:

$$(5.7) \stackrel{(5.6)}{\Rightarrow} Inhibition_{observed} = \frac{(1 - Control_{inh}) \times PUR_{max} - PUR_{inh}}{(1 - Control_{inh}) \times PUR_{max}} \Rightarrow$$

$$\Rightarrow PUR_{inh} = (1 - Control_{inh}) \times PUR_{max} \times (1 - Inhibition_{observed}) \quad (5.9)$$

$$(5.8) \Rightarrow Inhibition = 1 - \frac{PUR_{inh}}{PUR_{max}} \stackrel{(5.9)}{\Rightarrow}$$

$$Inhibition = 1 - (1 - Control_{inh}) \times (1 - Inhibition_{observed}) \Rightarrow$$

$$\Rightarrow Inhibition = Control_{inh} + (1 - Control_{inh}) \times Inhibition_{observed}$$

or

$$Inhibition(\%) = 10(\%) + 0.9 \times Inhibition_{observed}(\%) \quad (5.10)$$

Figure 5.36 displays the modified anoxic inhibition values in comparison with the aerobic ones. The results strongly suggest that FNA inhibits aerobic and anoxic PUR to the same degree.

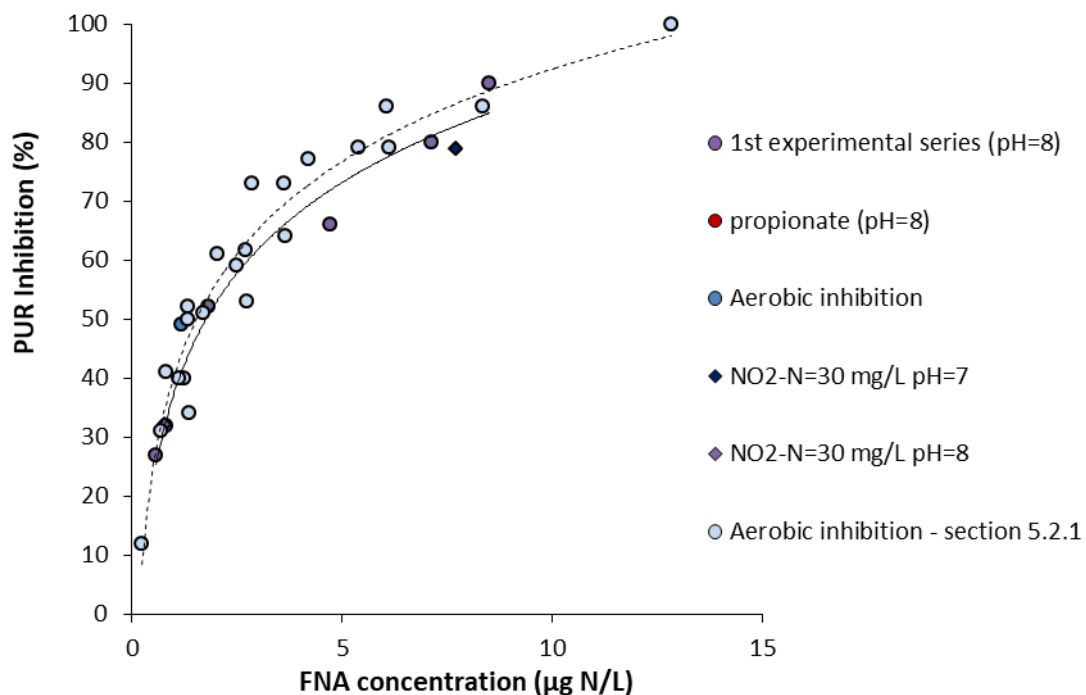


Figure 5.35. Comparison of anoxic PUR inhibition with aerobic PUR inhibition.

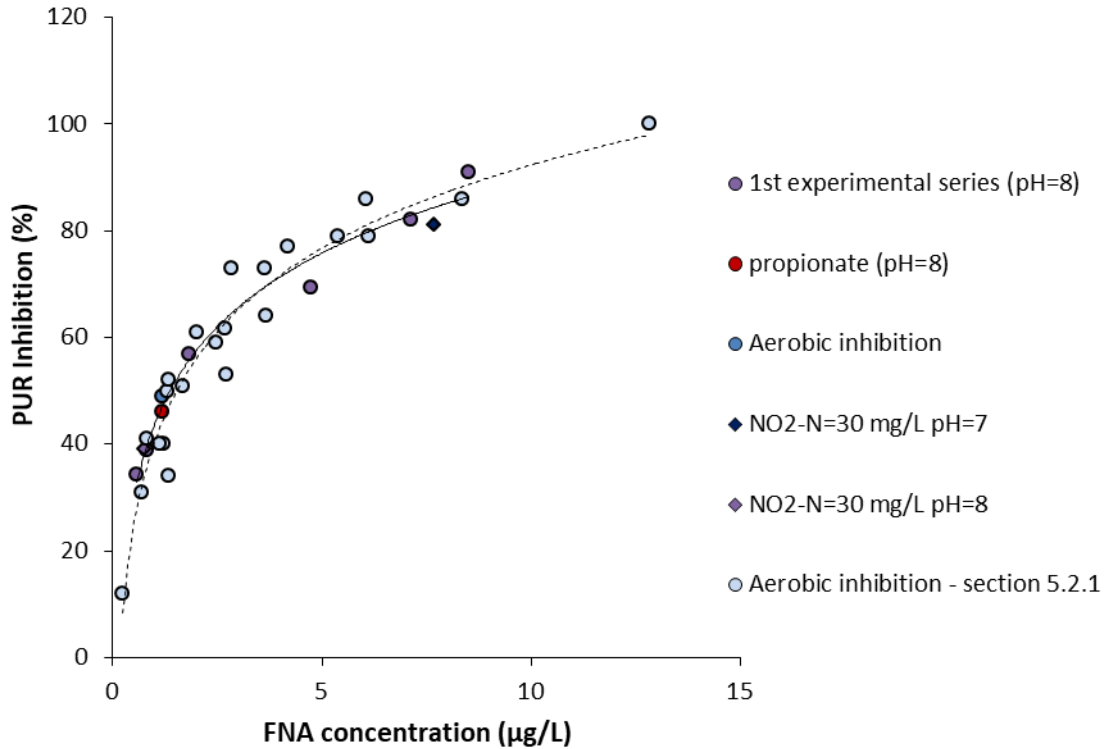


Figure 5.36. Comparison of modified anoxic PUR inhibition with aerobic PUR inhibition.

5.2.2.3 Modelling anoxic PUR inhibition due to FNA

According to the method described in Chapter 2, the values of PUR_{max}^{app} and K_m^{app} were calculated for all experimental runs. Based on the results, PUR_{max}^{app} decreased from 11.9 mg $PO_4\text{-P/g VSS h}$ at the $FNA=0$ experiment to 9.8 mg $PO_4\text{-P/g VSS h}$ and 2.9 mg $PO_4\text{-P/g VSS h}$ for the experiments performed with an FNA content of 1 $\mu\text{g/L}$ and 3.1 $\mu\text{g/L}$ respectively. The K_m^{app} value for all experiments was almost constant presenting an average value equal to 6.4 $\mu\text{g/L}$ and a low coefficient of variation (2%). These results (decrease of the PUR_{max}^{app} and constant K_m^{app}) clearly point to a non-competitive inhibition model. Similar findings are recorded regarding the effect of FNA on AOB and anammox activities as well (Jiménez et al., 2012; Puyol et al., 2014).

The non-competitive inhibition kinetics can be mathematically described as follows:

$$PUR = PUR_{max} \frac{K_{iFNA}}{S_{FNA} + K_{iFNA}} \quad (5.1)$$

where K_{iFNA} is the inhibition constant corresponding to the FNA concentration that inhibits the process by 50%, S_{FNA} is the FNA concentration in the mixed liquor and PUR_{max} refers to the maximum anoxic PUR at conditions with zero inhibition (practically refers to the PUR measured at the control system of each experimental batch series). In order to conclude on the mathematical expression that optimally describes the inhibition phenomenon, the simple non-competitive model described in equation (5.1) was compared with the model proposed by Levenspiel (1980) (equation 5.3), the Andrews inhibition model (Andrews, 1968, equation 5.4),

the Hill-type model (Prinz, 2010, equation 5.11) and the model proposed by Zhou et al. (2007) to describe FNA effect on anoxic PUR (equation 5.5):

$$PUR = PUR_{max} \left(1 - \frac{S_{FNA}}{S_{FNA}^*}\right)^m \quad (5.3)$$

$$PUR = PUR_{max} \frac{S_{FNA}}{K_S + S_{FNA} + \frac{S_{FNA}^2}{K_{iFNA}}} \quad (5.4)$$

$$PUR = PUR_{max} \frac{K_{iFNA}^n}{S_{FNA}^n + K_{iFNA}^n} \quad (5.11)$$

$$PUR = PUR_{max} \frac{S_{FNA}}{K_S + S_{FNA}} e^{\alpha S_{FNA}} \quad (5.5)$$

where S_{FNA}^* is the critical FNA concentration in the mixed liquor at which PUR is completely inhibited, K_s is the affinity coefficient constant, m , α are constants and n is the Hill coefficient representing the number of bound ligands.

The Nash-Sutcliffe efficiency coefficient (NSE) and the percent bias (PBIAS) were used as statistic indices to evaluate performance of each model, as proposed by Moriasi et al. (2007). Performance criteria used to accept each model's predictivity were $NSE > 0.8$ and PBIAS within $\pm 20\%$.

The values of models' parameters were calculated by performing a best fit analysis against to the experimental data in order to obtain the least sum of square errors (SSE) for each inhibition model. Based on this methodology, an FNA inhibition constant of $1.6 \mu\text{g N/L}$ was calculated for the simple non-competitive inhibition model (eq. 5.1), a value which is practically identical to the one found for the case of FNA inhibition on aerobic PUR ($1.5 \mu\text{g N/L}$). Accordingly, by using a S_{FNA}^* value of $12.8 \mu\text{g/L}$ (based on the experimental results), an m value equal to 4.5 gave the best fit for Levenspiel's model. Both Andrews's and Zhou's models (equations 5.4, 5.5) were applied by using a K_s value of $0.031 \mu\text{g/L}$ as proposed by Zhou et al. (2007), while in Andrews's model, best fit analysis resulted in a K_{iFNA} value of $1.6 \mu\text{g/L}$, equal to the value calculated for the simple non-competitive inhibition model. The optimum fitting of the dose-response Hill-type model (equation 5.11) was achieved for a Hill coefficient value of 1.15 which approximates the simple non-competitive inhibition model ($n=1$) and indicates noncooperative (independent binding). The statistics of the five inhibition models are presented in Table 5.4.

Table 5.4. Statistic indices for the FNA inhibition models examined for anoxic PUR

Statistical Index	Simple non-competitive	Levenspiel (1980)	Andrews (1968)	Hill-type (Printz, 2010)	Zhou et al. (2007)
SSE	162	1154	168	160	634
NSE	0.95	0.65	0.95	0.95	0.81
PBIAS	-0.12%	-4.45%	-1.56%	0.43%	-1.90%

Under best fit conditions, the simple non-competitive model and the dose response Hill-type model can equally describe the FNA inhibition on anoxic PUR very satisfactorily as evidenced from the statistical indices (Table 5.4).

Figure 5.37 provides a graphical comparison between the experimental data and the simulation values based on the simple non-competitive model.

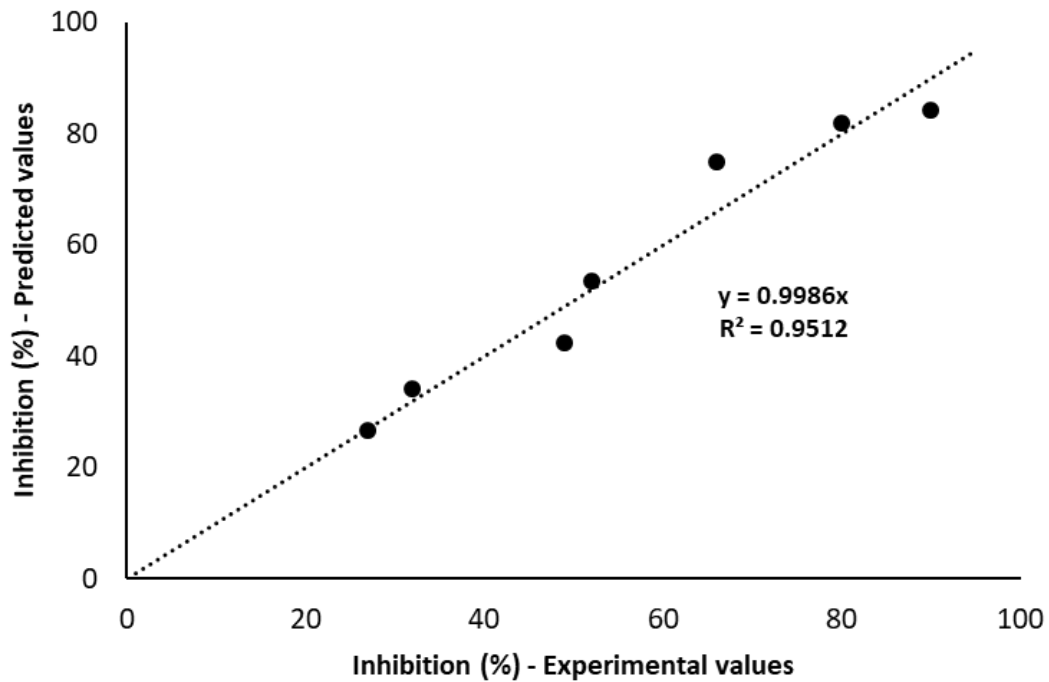


Figure 5.37. Comparison of experimental and predicted results regarding the inhibitive effect of FNA on anoxic PUR

5.3 Inhibition of PAO activities due to free ammonia

Recently there have been reports that PAOs can also be inhibited by free ammonia (FA) (Zheng et al., 2013; Yang et al., 2018). The studies conducted up to this point mainly focused on the prolonged effect of FA on the growth of PAOs. Zheng et al. (2013) reported that the FA threshold concentration for PAOs was 17.76 mg NH₃-N/L and that analyses before and after treatment with such FA content showed that the PAO population had deteriorated significantly, while the GAO population had increased. In agreement to this, Yang et al. (2018) reported that PAOs were significantly inhibited (by over 90 %) after a 1-day exposure to 16 mg NH₃-N/L. However, detailed information on the inhibition of PAOs by FA is limited, especially in regard to its effect on PUR. In addition, EBPR under high nitrogen loading conditions would likely be inhibited by the simultaneous presence of FA and FNA. Therefore, assessing the applicability of EBPR for such systems would require knowledge of the mode of inhibition by FA, in order to determine the severity of the combined inhibition of PUR.

In view of the above, a series of experiments was conducted to investigate the effect of FA on aerobic and anoxic PUR along with the effect of FA on the anaerobic processes of PAOs.

5.3.1 Investigating the inhibitory effect of FA on aerobic PUR

5.3.1.1 Experimental assessment of the effect of free ammonia on aerobic PUR

Parallel to the series of experiments investigating the effect of nitrite on aerobic PUR, a second series of ex-situ batch tests was conducted to investigate the effect of ammonium on the aerobic PUR of PAOs. All batch experiments were performed with the PAO – enriched biomass developed in the experimental system which has already been described in section 5.2.1.1. A total of 19 batch experiments were performed for various ammonium concentrations at the pH values of 7, 7.5, 8 and 8.5. According to the experimental protocol, a minimum of four batch tests were performed at each pH and the ammonium concentrations for each series were chosen as to provide a satisfactory range of inhibition degrees at each pH. The ammonium concentrations examined for each pH are presented in Table 5.5.

Table 5.5. Ammonium concentrations examined at each pH

pH	NH ₄ -N (mg/L)
7	80, 180, 300, 450, 740
7.5	190, 350, 680, 980
8	80, 170, 350, 450, 420
8.5	45, 85, 110, 165

At the start of each experiment, sludge was retrieved from the SBR and divided equally into 3 containers, each with a working volume of 0.5 L. Each container was then fed an amount of acetate in order to obtain an initial COD concentration of 200 mg/L and was left stirring under anaerobic conditions over a 1 h period. One of the bioreactors served as a control while the other two reactors were fed with an equal amount of ammonium, in the form of an ammonium chloride solution to obtain the desired ammonium concentration that was to be investigated. The pH of each container was adjusted to the targeted value just after feed and was kept stable for the remainder of the experiment. The reactors were then aerated over a period of 3-4 h. Each batch test examined the effect of a specific ammonium concentration on the duplicate reactors with respect to the control.

Figure 5.38 displays the variation of phosphorus throughout a typical experiment in which PUR inhibition is examined for the ammonium concentration of 85 mg N/L at the pH of 8.5. In addition to the aerobic uptake of phosphorus, the anaerobic release under the effect of phosphorus is also examined. One point of interest is that the initial PO₄-P concentration in the control reactor at the start of the anaerobic phase appears to be lesser than its concentration in the duplicate samples that were fed ammonium at this point. In addition, phosphorus release during the anaerobic phase appears to be greater in the presence of ammonium. This may be due to a combination of the following reasons:

- ⇒ The introduction of the ammonium chloride influences precipitation/dissolution reactions involving phosphorus.

- ⇒ The high FA concentration (approximately 14.3 mg N/L) that was introduced to the duplicate reactors had an acute toxic effect on a variety of microorganisms, resulting in their demise and the subsequent release of phosphorus in the medium.
- ⇒ The capacity of PAOs to take up VFAs is inhibited by FA meaning a possible greater energy demand for the process. As this energy is provided via the hydrolysis of their intracellular polyphosphate chains, there is an increased release of phosphorus.

The effect of ammonium on the anaerobic activity of PAOs is discussed in section 5.3.3. While there are some implications regarding the growth of PAOs in conditions where FA is present during anaerobic VFA uptake, aerobic PUR appears to be influenced by FA regardless if it was present prior to aeration.

The control reactor performed at a higher PUR as expected (Figure 5.39). Upon the second hour of aeration, the control's capacity to remove phosphorus appeared to be largely exhausted. The duplicate reactors on the other hand performed steadily at a diminished PUR throughout the duration of the experiment. The PUR for each reactor was established for the duration where a stable performance was observed. Based on the slopes of the experimental data, the control's PUR could be calculated at 7.5 mg P/g VSS h, while the PUR of the ammonium-containing reactors averaged at 2.8 mg P/g VSS h. The ammonium concentration of 85 mg N/L at the pH of 8.5 was therefore found to inhibit aerobic PUR by 63%.

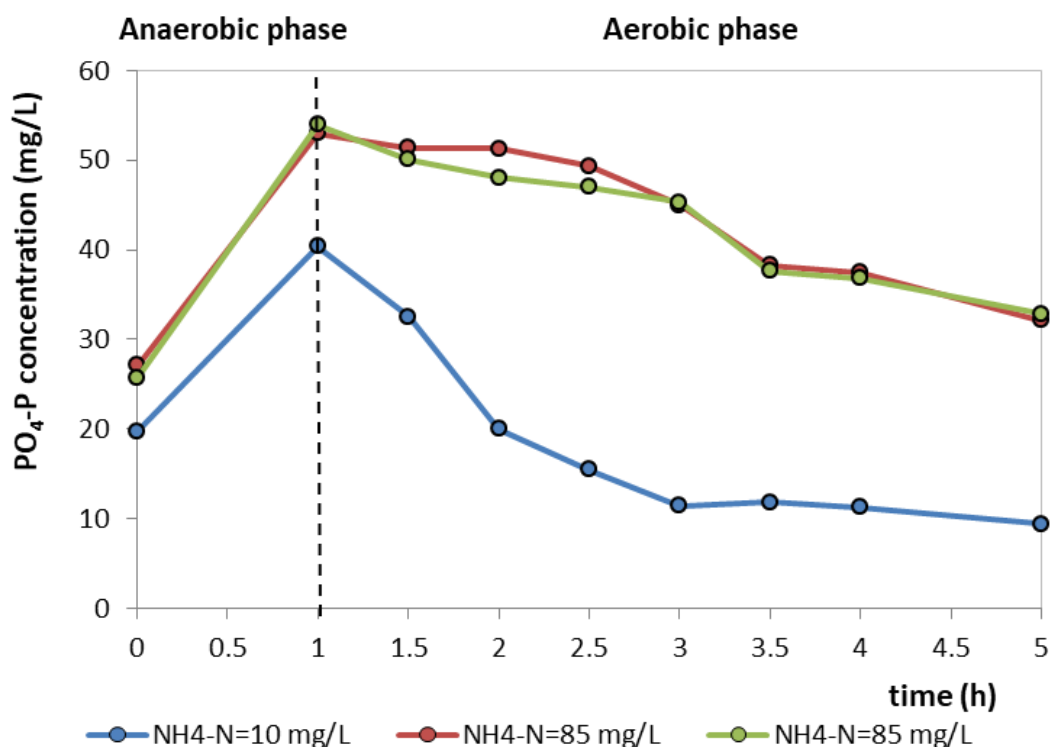


Figure 5.38. Phosphorus variation for typical batch experiment (NH₄-N=85 mg/L, pH=8.5)

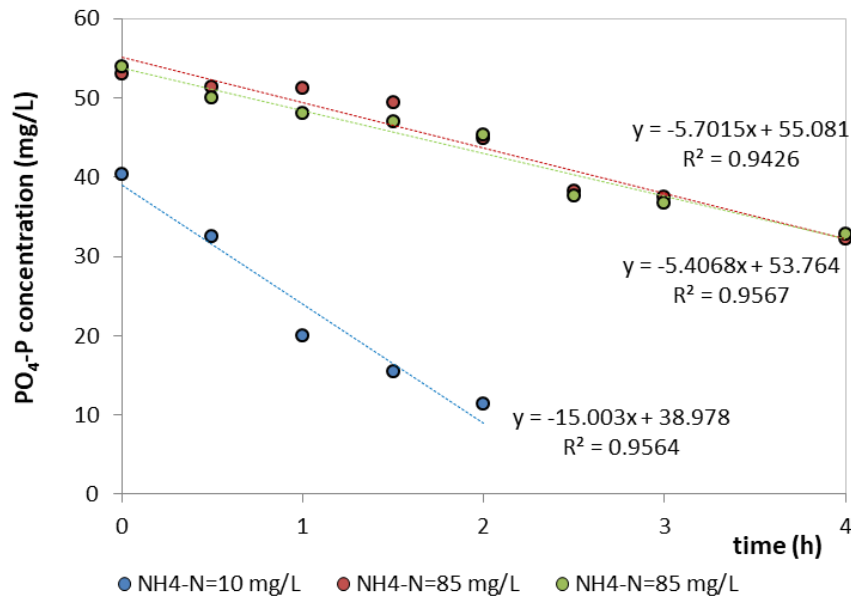


Figure 5.39. Aerobic PURs for typical batch experiment (NH₄-N=85 mg/L, pH=8.5)

The results of the batch experiments regarding the inhibitory effect of ammonium on aerobic PUR are shown in Figure 5.40. Based on the results it appears that elevated ammonium concentrations inhibit PUR significantly more at higher pH values. At the pH of 7, PUR was inhibited by 10% for the NH₄-N concentration of 300 mg/L, while at the pH of 8.5, PUR was inhibited by 50% for the relatively low NH₄-N concentration of 45 mg/L. At the pH of 7, this concentration would likely have no effect on the process as the ammonium concentration of 80 mg/L was observed to have minimum impact on PUR at this pH. The role of pH in the severity of the inhibitory effect of ammonium on aerobic PUR is clearly of great significance as approximately 85% inhibition occurs for 165 mg NH₄-N/L at the pH of 8.5, 620 mg NH₄-N/L at the pH of 8 and around 1000 mg NH₄-N/L at the pH of 7.5.

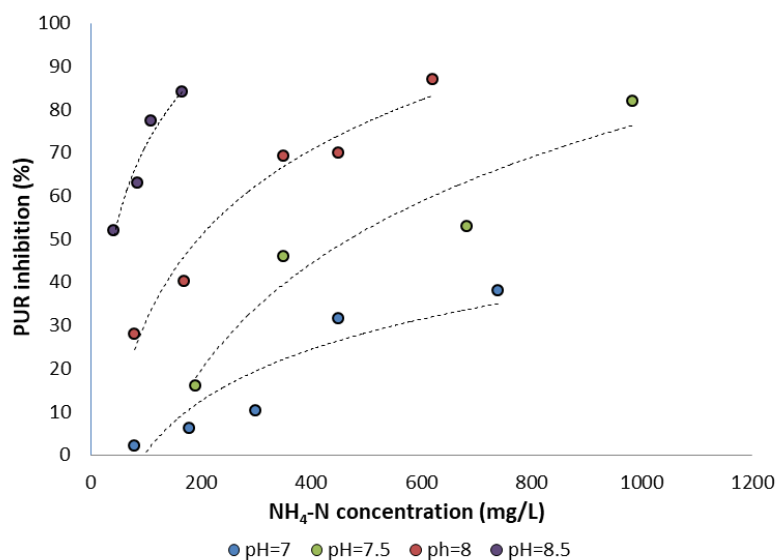


Figure 5.40. The effect of ammonium nitrogen on aerobic PUR inhibition for the pH of 7, 7.5, 8 and pH=8.5.

The correlation of the degree of inhibition to pH would suggest that FA rather than ammonium is the actual inhibitor of the process, as FA is more abundant at higher pH values. The FA concentrations for each experiment were calculated with regard to the ammonium concentration, pH and temperature and the associated PUR inhibitions observed are displayed in Figure 5.41. As shown, the inhibitions observed at all examined pH seem to correlate very satisfactorily with the associated FA concentrations, indicating that FA rather than ammonium is the actual inhibitor of PAOs. This could be anticipated as FA is a known inhibitor of various microbial processes and is the main suppressor of NOB in high nitrogen loading systems.

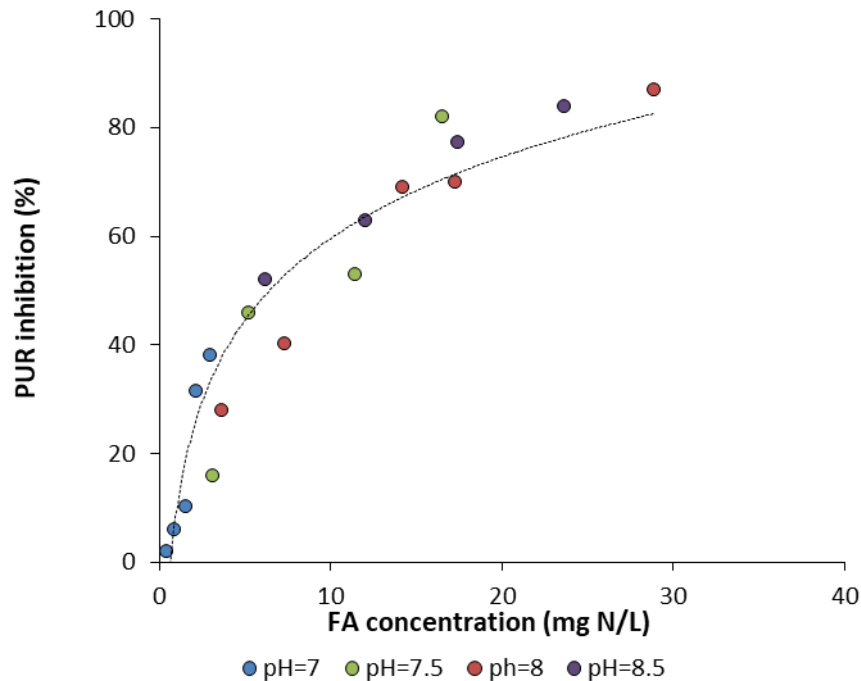


Figure 5.41. The effect of FA on aerobic PUR inhibition for the pH of 7, 7.5, 8 and 8.5.

According to the results it is concluded that the aerobic PUR of PAOs is inhibited by 50% under a FA concentration of 8 mg NH₃-N/L, while FA concentrations above 30 mg/L appear to severely inhibit the process by more than 90%. This would be in agreement with the findings of Zheng et al. (2013) and Yang et al. (2018) who observed that EBPR would completely deteriorate after a prolonged exposure to FA concentrations greater than 18 mg NH₃-N/L. Based on the results of this series of experiments, concentrations of this magnitude would inhibit aerobic PUR by 70-80%. The diminished PUR observed under these FA concentrations would most likely support these observations when taking the exposure time into account, alongside a possible greater resilience to FA by other antagonistic microbial groups.

While it is clear that FA inhibits aerobic PAO activity, it is a much less strong inhibitor than FNA in terms of nitrogen (with 6400 µg N/L FA having the same effect as 1.5 µg N/L FNA). However, this in no way constitutes the effect of FA as of unimportant significance since in the typical pH range of the treated media, the percentage of ammonium nitrogen in the form of FA is much higher than the percentage of nitrite nitrogen in the form of FNA. For example, at the pH of 8 at 20°C, approximately 4.7% of ammonium nitrogen is in the form of FA while a mere

0.0026% of nitrite nitrogen is in the form of FNA. As the percentage of ammonium nitrogen in the form of FA rises exponentially with rising pH while the percentage of nitrite nitrogen in the form of FNA rises exponentially adversely to pH, there are certain implications for high nitrogen loading systems that rely on nitrification/denitrification. These implications are discussed extensively in section 5.4 where the combined effect of FNA and FA on EBPR is also examined.

5.3.1.2 Modelling aerobic PUR inhibition due to FA

The exact mechanism of FA inhibitive effect on PAOs activity is practically unknown. There are studies reporting on the effect of FA in intracellular pH (Liu et al., 2019) and therefore in either the potassium availability for enzyme production or in the increase of maintenance energy requirements, thus slowing down process kinetics (Dai et al., 2017; Rajagopal et al., 2013). Other studies reporting low enzyme activity in many processes taking place during anaerobic metabolism (e.g. hydrolysis, acetate production, methanogenesis) due to the effect of FA (Wang et al., 2018; Zhao et al., 2018). Park and Bae (2009) studied the kinetics of FA inhibition on AOB and NOB activity. According to the authors, FA inhibition in both bacterial groups can be predicted by the uncompetitive model. However, all of these studies were focused on the inhibitive effect of FA on anaerobic microorganisms (mostly methanogens) or nitrifiers rather than on PAOs activity. Therefore, the type of FA inhibition on PAO has not been documented yet.

By applying the modified direct linear plot method described in Chapter 4, the values of PUR_{max}^{app} and K_m^{app} were calculated for all experimental runs. According to the results PUR_{max}^{app} decreased from 21.9 mg PO₄-P/g VSS h at the zero FA experiment to 18.8 mg PO₄-P/gVSS h and 18 mg PO₄-P/g VSS h for the experiments performed with an FA content of 2 mg N/L and 3.5 mg N/L respectively. Furthermore, the increase of FA resulted in a gradual decrease of the K_m^{app} value, from 4.5 mg N/L in the control experiment to 4.2 mg N/L and 3 mg N/L for the experiments performed with an FA content of 2 mg N/L and 3.5 mg N/L respectively. The decrease of both apparent values of PUR_{max} and K_m is a clear indication of an uncompetitive mode of inhibition. According to the general principles of uncompetitive inhibition, a possible rationale regarding the effect of FA to aerobic PUR is the following: FA binds only to the enzyme-substrate complex (ES) rather than directly to free enzyme. As a result, the advanced enzyme-substrate-inhibitor complex (ESI) cannot end up to products thus decreasing the PUR_{max}^{app} . At the same time, following Le Chatelier's principle, as the ESI is constantly produced and ES is rather depleted, in order to maintain equilibrium between ESI and ES the reaction moves towards ES formation thus improving ES affinity and ultimately decreasing the K_m^{app} . The uncompetitive inhibition model has also been proposed as the most appropriate to simulate the inhibitory effect of FA to nitrifiers (AOB and NOB) by Park and Bae (2009).

In order to model FNA effect to aerobic PUR the uncompetitive inhibition kinetics were adopted:

$$PUR = PUR_{max} \frac{S}{S \cdot \left(1 + \frac{S_{FA}}{K_{iFA}}\right) + K_S} \quad (5.12)$$

where K_{iFA} is the inhibition constant, S_{FA} is the concentration of FA in the tank, S is the concentration of PO₄-P in the tank, K_S is the half saturation coefficient for PO₄-P and PUR_{max}

refers to the maximum aerated PUR at conditions with zero inhibition (practically refers to the PUR measured at the control system of each experimental batch series). The predictive capacity of the aforementioned inhibition model was tested against to the model proposed by Levenspiel (1980) and described by the following equation:

$$PUR = PUR_{max} \left(1 - \frac{S_{FA}}{S_{FA}^*}\right)^n \quad (5.13)$$

where S_{FA}^* is the critical FA concentration in the tank at which PUR is completely inhibited and n is a constant.

As already explained each model's parametric values were calculated by performing best fit analysis to the experimental data in order to obtain the least SSE. Based on this methodology an FA inhibition constant (K_{iFA}) of 10 mg N/L was calculated for the simple model (eq. 5.12). Accordingly, by using a S_{FA}^* value of 40 mg/L (based on the experimental results), an n value equal to 2.3 gave the best fit of this model. By comparing the statistical indices of the two models it is concluded that the conventional un-competitive model described by equation 5.11 exhibits better fit to experimental data than Levenspiel's model. Both performance indices examined (NSE and PBIAS) showed very satisfactory values; NSE was equal to 0.90 while PBIAS was equal to -0.71% (Table 5.6).

Table 5.6. Statistic indices for the FA inhibition models examined

Statistical Index	Uncompetitive	Levenspiel (1980)
SSE-FA	1465	1624
NSE-FA	0.90	0.88
PBIAS-FA	-0.71%	1.53%

Figure 5.42 illustrates the satisfactory comparison between the experimental results and the model's output. Therefore, it is anticipated that equation 5.12 can provide for an accurate simulation of the inhibition of FA on the aerated PUR of PAOs.

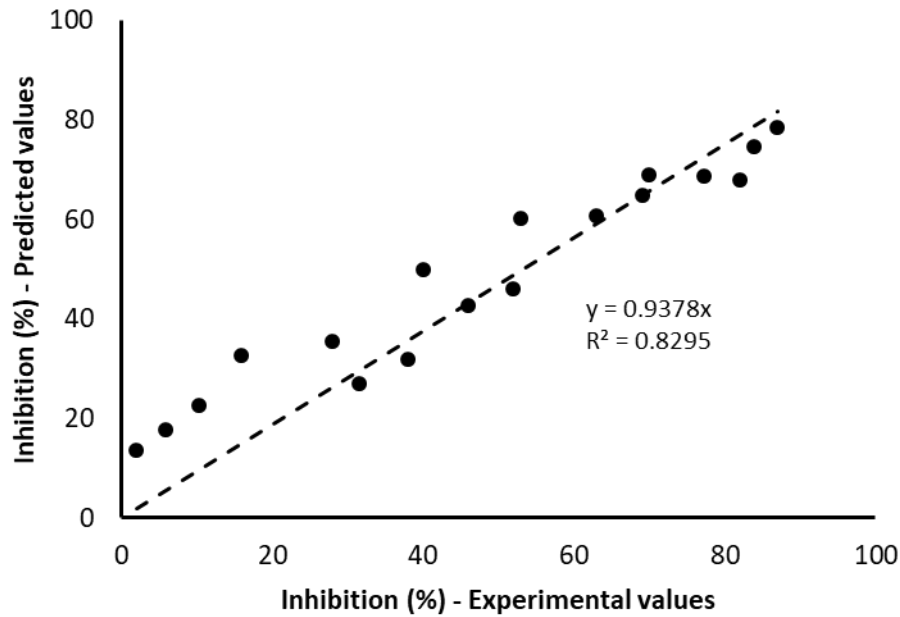


Figure 5.42. Comparison of experimental and predicted results regarding the inhibitive effect of FA on aerobic PUR.

5.3.2 Investigating the inhibitory effect of FA on anoxic PUR

5.3.2.1 Experimental assessment of the effect of free ammonia on anoxic PUR

Parallel to the series of experiments investigating the effect of nitrite on anoxic PUR, a second series of ex-situ batch tests was conducted to investigate the effect of ammonium on the anoxic PUR of PAOs. All batch experiments were performed with the PAO-enriched biomass developed in the experimental system which has already been described in section 5.2.2.1. A total of 8 batch series were performed for various ammonium concentrations at the pH values of 8 and 8.5. The ammonium concentrations for each series were chosen as to provide a satisfactory range of inhibition degrees at each pH. The ammonium concentrations examined for each pH are presented in Table 5.7.

Table 5.7. Ammonium concentrations examined at each pH

pH	NH ₄ -N (mg/L)
8	140, 360, 530
8.5	70, 100, 130, 180, 240

At the start of each experiment, sludge was retrieved from the SBR and divided equally into 3 containers, each with a working volume of 0.5 L. One of the bioreactors served as a control, while the other two reactors were fed with an equal amount of ammonium, in the form of an ammonium chloride solution in order to obtain the targeted ammonium concentration that was to be examined. The pH of each reactor was then set to the targeted value and remained constant over the duration of the experiments. The reactors were then kept under stirring

conditions for 1 h prior to the addition of feed. This was in order to limit the influence of the added ammonium chloride that was observed in the experiments regarding aerobic PUR (section 5.3.1.1). Each container was then fed an amount of acetate in order to obtain an initial COD concentration of 100 mg/L and was stirred for 1 h under anaerobic conditions. Following this 1 h anaerobic period, nitrite in the form of a sodium nitrite solution was introduced to the bioreactors in order to achieve an initial nitrite concentration of 10 mg NO₂-N/L that was kept constant at 8 ± 2 mg N/L over the duration of the experiment with the frequent addition of sodium nitrite every 15 minutes. The anoxic removal of phosphorus was studied over a period of 2.5 hours.

Figure 5.43 displays the variation of phosphorus throughout a typical experiment in which the effect of ammonium on anoxic PUR is examined for the ammonium concentration 100 mg N/L at the pH of 8.5. The control reactor displayed a slightly higher release of phosphorus during the anaerobic phase compared to the duplicate reactors and a clearly higher PUR during the anoxic phase.

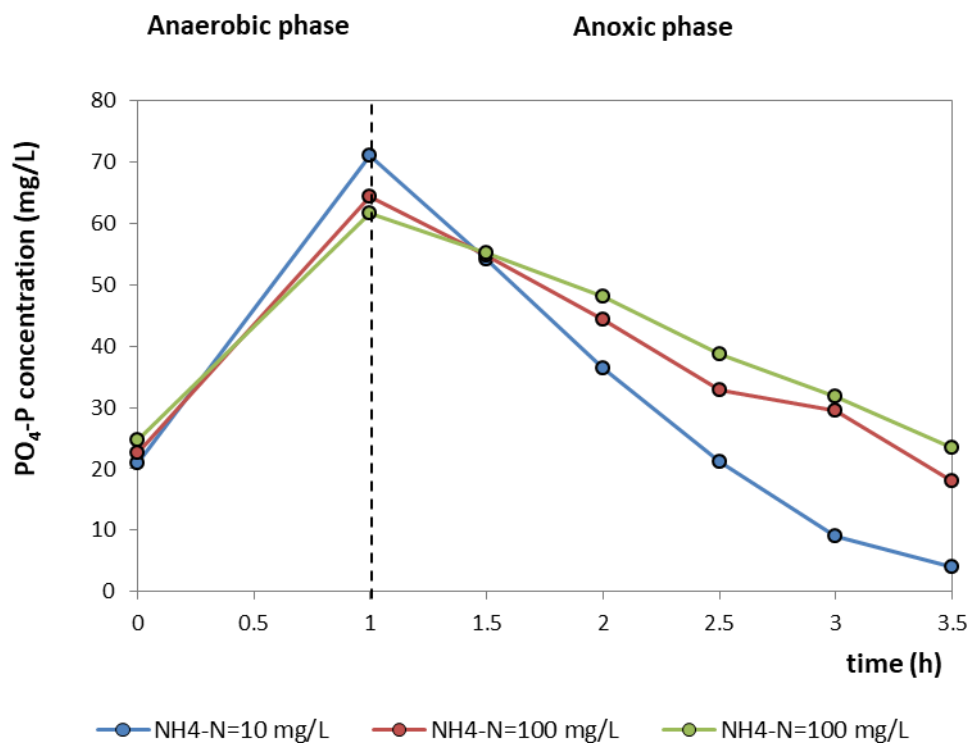


Figure 5.43. Phosphorus variations for typical batch experiment (NH₄-N=100 mg/L, pH=8.5)

The PUR for each reactor was established for the duration where a stable performance was observed. Based on the slopes of the experimental data, the control's PUR could be calculated as 12.7 mg P/g VSS h, while the PUR of the ammonium-containing reactors averaged at 6.1 mg P/g VSS h. The ammonium concentration of 100 mg N/L at the pH of 8.5 was therefore found to inhibit anoxic PUR by 52%.

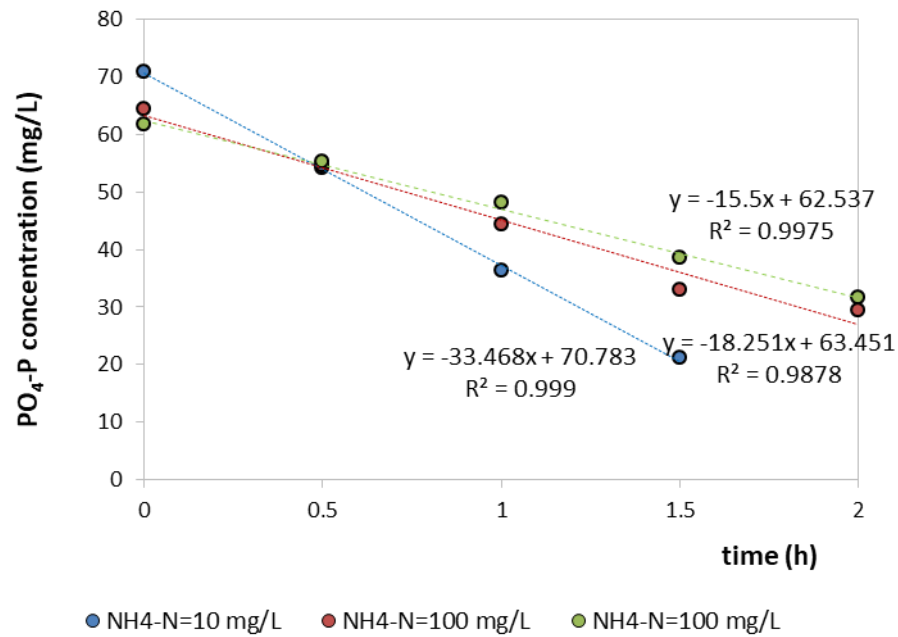


Figure 5.44. PURs for typical batch experiment (NH₄-N=100 mg/L, pH=8.5)

The results of the batch experiments regarding the inhibitory effect of ammonium on anoxic PUR are shown in Figure 5.45. In agreement with the observations regarding the effect of ammonium on aerobic PUR, anoxic PUR is inhibited by elevated ammonium concentrations significantly more at higher pH values, suggesting that FA is the actual inhibitor of PAOs. Anoxic PUR is inhibited by approximately 50% by a NH₄-N concentration of 360 mg/L at the pH of 8, while at the pH of 8.5 the process is equally inhibited by a mere 100 mg NH₄-N/L.

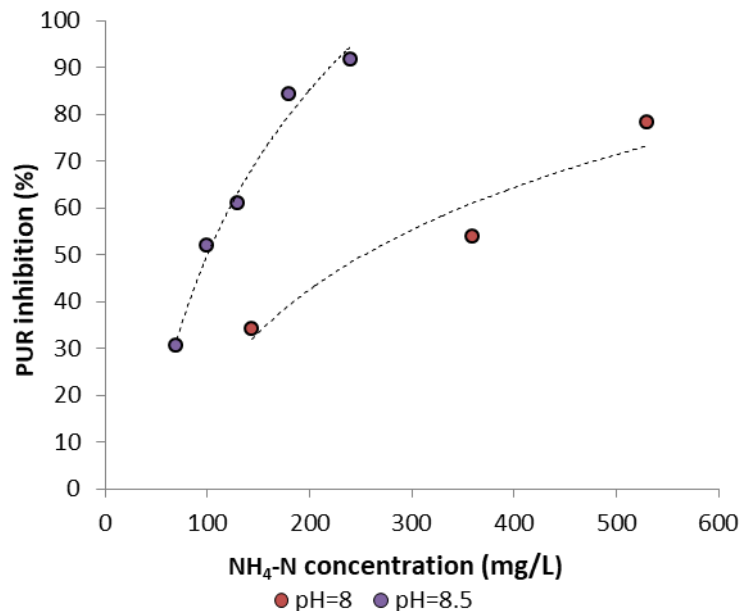


Figure 5.45. The effect of ammonium on anoxic PUR for pH=8 and pH=8.5.

The FA concentrations for each experiment were calculated with regard to the ammonium concentration, pH and temperature and the associated PUR inhibitions observed are displayed in

Figure 5.46. As shown, the inhibitions observed seem to correlate very satisfactorily with the associated FA concentrations, indicating once again that FA rather than ammonium is the actual inhibitor of PAOs. Anoxic PUR was observed to be inhibited by 50% under the FA concentration of 10 mg N/L, while the process was found to be inhibited by over 90% under the FA concentration of 26 mg N/L.

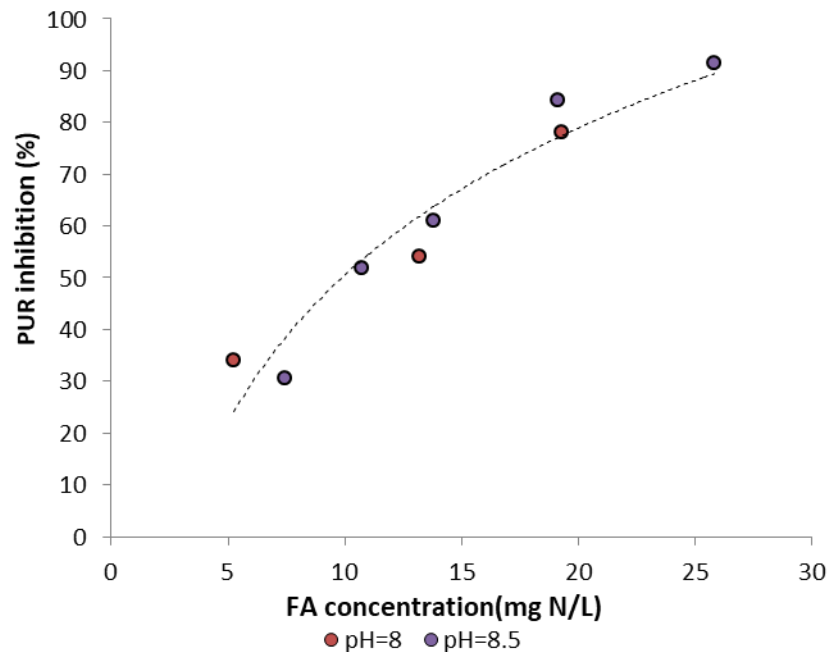


Figure 5.46. The effect of FA on anoxic PUR for pH=8 and 8.5.

Figure 5.47 displays a comparison of the effect of FA on anoxic PUR with its effect on aerobic PUR. It appears that P-removal via denitrification shows no greater tolerance to FA than that displayed in the case of aerobic P-removal. It should be pointed out that in nitrification-denitrification systems, most of the ammonium is converted to nitrite during aeration and therefore the inhibitory effect of ammonium on EBPR mainly concerns the aerobic pathway. However, the residual ammonium at the beginning of the denitrification phase may prove to have a considerable adverse effect on anoxic P-removal as well, especially if the medium's pH is high. Therefore, while a high pH may be beneficial in lowering the FNA concentration due to the significant nitrite content at the start of the anoxic phase, the residual ammonium concentration should also be taken into consideration.

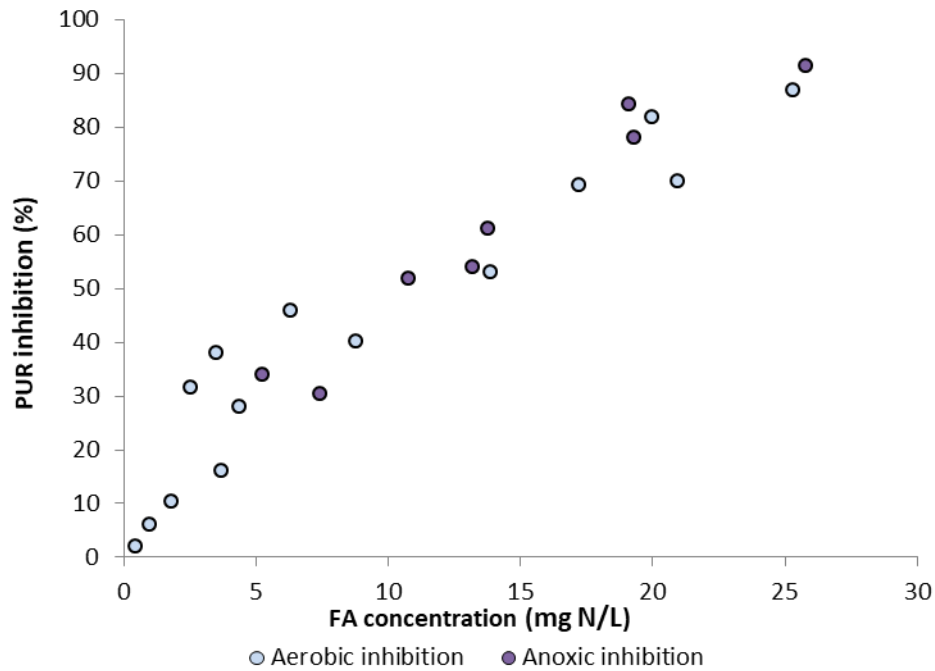


Figure 5.47. Comparison of anoxic PUR inhibition with aerobic PUR inhibition by FA.

5.3.2.2 Modelling anoxic PUR inhibition due to FA

By applying the method described in Chapter 4, the values of PUR_{max}^{app} and K_m^{app} were calculated for all experimental runs. Based on the results the increase of FA concentration from 0 to 2.5 mg N/L and 12.5 mg N/L resulted in a decrease of PUR_{max}^{app} from 11 mg PO_4 -P/g VSS h to 6.1 mg PO_4 -P/g VSS h and 4.5 mg PO_4 -P/g VSS h respectively and a gradual decrease of the K_m^{app} value, from 5.6 mg/L to 5.0 mg/L and 3.2 mg/L respectively. The decrease of both apparent values of PUR_{max} and K_m with the increase of the inhibitor (FA) is a clear indication of an un-competitive mode of inhibition. Therefore, in order to model FA effect to anoxic PUR the simple un-competitive inhibition model was adopted (equation 5.12):

$$PUR = PUR_{max} \frac{S}{S \cdot \left(1 + \frac{S_{FA}}{K_{iFA}}\right) + K_S} \quad (5.12)$$

where K_{iFA} is the inhibition constant, S_{FA} is the concentration of FA in the tank, S is the concentration of PO_4 -P in the tank, K_S is the half saturation coefficient for PO_4 -P and PUR_{max} refers to the maximum anoxic PUR at conditions with zero inhibition (practically refers to the PUR measured at the control system of each experimental batch series). The predictive capacity of the aforementioned inhibition model was tested against to the model proposed by Levenspiel (1980) and described by equation (5.13) and the dose-response Hill-type model described by equation (5.11) by substituting S_{FNA} , S_{FNA}^* and K_{iFNA} with S_{FA} , S_{FA}^* and K_{iFA} .

Based on the methodology followed in the case of FNA the calculation of models' parameters was performed by employing best fit analysis to the experimental data in order to obtain the least SSE. According to the results, an FA inhibition constant (K_{iFA}) of 8 mg N/L was calculated for the simple model (eq. 5.12), a value very similar to the one that was calculated for the case of FA inhibition on aerobic PUR. In the case of Levenspiel's model, an S_{FA}^* value of 37 mg/L and an

n value equal to 2.5 gave the best fit of this model. For the Hill-type model an n coefficient of 1.5 resulted to best fitting thus suggesting positively cooperative binding. The SSE values of the three models were equal to 1053, 678 and 734 respectively, while the NSA and PBIAS values were equal to 0.70, 0.80 and 0.79 and 2.2%, 0.42% and -0.37% respectively, suggesting that the predictive capacity of Levenspiel's model is better than the one of the simple un-competitive model and the dose-response model.

Figure 5.48 presents the satisfactory comparison between the experimental results and the predicted values based on Levenspiel's model.

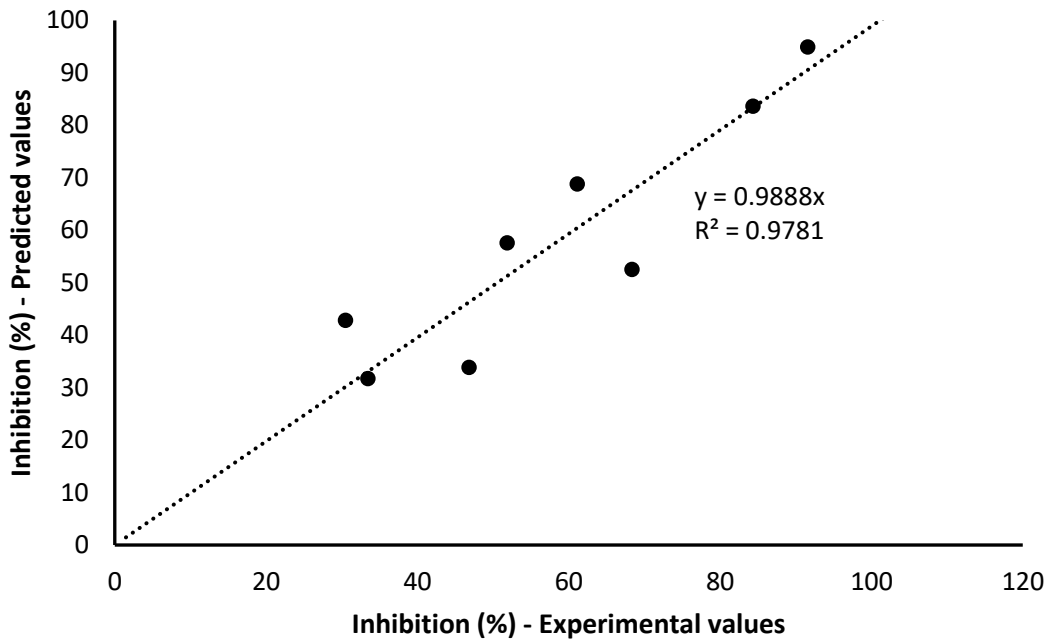


Figure 5.48. Comparison of experimental and predicted results regarding the inhibitive effect of FA on anoxic PUR

5.3.3 Investigating the effect of FA on anaerobic PAO activity

Parallel to the series of experiments investigating the effect of ammonium on aerobic PUR, a number of experiments were conducted focusing on the effect of FA on the anaerobic processes of PAOs, specifically the anaerobic phosphorus release rate and COD uptake rate. The biomass used in these experiments was developed as described in section 5.2.1.1.

Initially two series of batch experiments were conducted. The first investigated the effect of 85 mg NH₄-N/L at the pH of 8.5 (14.3 mg NH₃-N/L), while the second assessed the effect of ammonium concentration of 165 mg N/L (28.1 mg NH₃-N/L) in anaerobic rates. In each series, sludge was retrieved from the SBR and divided equally into 3 containers, each with a working volume of 0.5 L. The pH of each reactor was set to 8.5 ± 0.05 and kept constant for the duration of the experiment. Each reactor was fed with readily biodegradable organic carbon, in the form of a sodium acetate solution, in order to obtain an initial COD concentration of 200 mg/L. One of the bioreactors served as a control while the other two reactors were fed with an equal amount of ammonium, in the form of an ammonium chloride solution to obtain the desired

ammonium concentration that was to be investigated. The reactors were maintained under anaerobic conditions for a period of 1 hour in which the release of phosphorus and the uptake of COD were studied.

The FA concentration of 14.3 mg N/L was found to inhibit the anaerobic uptake of COD by 24%. The control performed at a rate of 112 mg COD/g VSS h, while the reactors under the presence of FA performed at 85 and 86 mg COD/g VSS. Interestingly, phosphorus release appeared slightly greater in the duplicate reactors (13.1 and 13.4 mg P/g VSS h) compared to the control reactor (11.5 mg P/g VSS h).

The FA concentration of 28.1 mg N/L was found to inhibit the anaerobic uptake of COD by 56%. The control performed at a rate of 99.2 mg COD/g VSS h, while the reactors under the presence of FA performed at 40.6 and 40.7 mg COD/g VSS. This time, the phosphorus release rate of the duplicate reactors (4.5 mg P/g VSS h) was considerably lower than that of the control (10.1 mg P/g VSS h).

According to the experimental results it would appear that FA inhibits the anaerobic uptake of carbon, though its influence on phosphorus release is not clear. This may be due to the fact that not enough time was given after the addition of ammonium chloride and the setting of the new pH prior to the addition of COD which may have influenced precipitation/dissolution reactions involving phosphorus. Additionally, it is unclear if the diminished COD uptake rate regards only PAOs or if it involves GAOs as well. However, further experiments highlighted that ammonium concentrations lower than 140 mg NH₄-N/L at the pH of 8.5 had minimal effect on the COD uptake rate of GAOs (section 5.5.2), suggesting that the inhibitions observed here mostly concern PAOs.

An additional experiment was conducted, investigating the effect of the ammonium concentration of 280 mg N/L at pH=8.5 (44 mg NH₃-N/L) on the anaerobic phosphorus release rate and COD uptake rate. In this experiment however, following the setting of pH and the addition of ammonium chloride, the reactors were kept stirring under anaerobic conditions for a time period of 1 h prior to the addition of sodium acetate. The reactors were then maintained under anaerobic conditions for a period of 1.5 hour in which the release of phosphorus and the uptake of COD were studied. The COD uptake rates, and phosphorus release rates were established for the first hour following the addition of acetate. The extension of the anaerobic period by 0.5 h was in order to ensure that the capacity of PAOs to take up carbon and release phosphorus had not been exhausted.

The results of this experiment are presented in Figure 5.49 and Figure 5.50. It would appear that under these conditions, ammonium has a negligible effect on both the uptake of COD and phosphorus release. The experiment was later replicated on the biomass developed according to section 5.5.2.1 to similar results, with the control reactor performing at a COD uptake rate of 38 mg COD/g VSS h and a phosphorus release rate of 21 mg P/g VSS h, and the duplicate reactors performing at an average of 38 mg COD/g VSS h and 20 mg P/g VSS h.

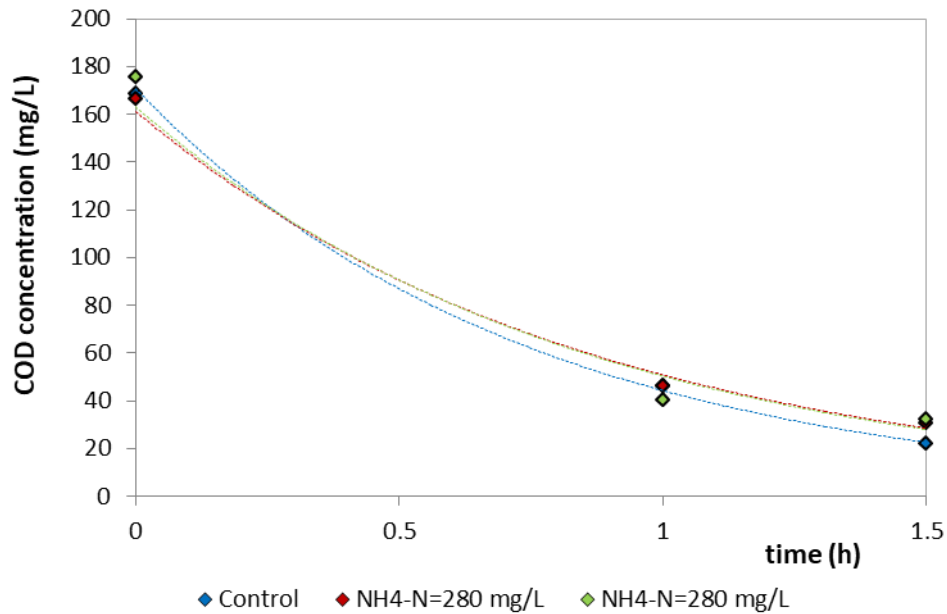


Figure 5.49. The effect of ammonium on the anaerobic COD uptake of PAOs.

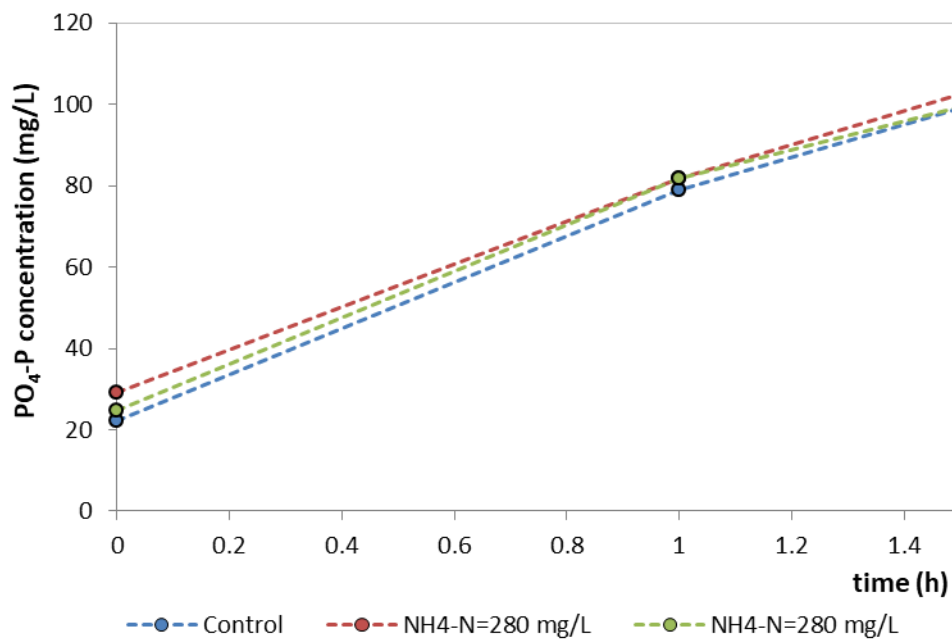


Figure 5.50. The effect of ammonium on the anaerobic P-release of PAOs.

The FA concentration in these experiments was 42.5 mg NH₃-N/L, a concentration which according to the results of section 5.3.1 would practically fully inhibit the aerobic and anoxic activity of PAOs. Therefore, it can be concluded that on a practical scale, FA has no effect on the anaerobic activity of PAOs.

However, as it was noticed in the first batch experiments, an ammonium shock load may have a brief negative effect on the anaerobic processes of PAOs which require some time to recover. As is evident from the follow-up experiments, PAOs were capable of making a full recovery within 1 hour. The implications for this observation are discussed below.

Experiments regarding the effect of the anaerobic retention time that are discussed in section 5.6.2, showed that when acetate and/or propionate was used as the carbon source, the extension of the anaerobic retention time beyond the duration of 1 h had little beneficiary effect on anaerobic P-release and the subsequent PUR during aeration. Therefore, an optimal configuration would rely on an anaerobic retention time of 1 hour. However, if a high ammonium load was to enter this phase, it could jeopardize PAOs since under these conditions their anaerobic activity would be delayed.

EBPR in high nitrogen loading systems mainly concerns the treatment of reject water produced during the sludge anaerobic stabilization processes and the subsequent dewatering process. In addition to high ammonium and phosphorus concentrations, these sludge liquors also contain an appreciable concentration of COD. Therefore it may seem like an attractive option to load the reject water at the beginning of the anaerobic phase as to allow PAOs to take up the organics present, minimizing the requirement for an external carbon source. As it has been demonstrated though, the high ammonium concentration could shortly inhibit PAOs, revealing the requirement for longer anaerobic detention times.

In light of the above, the following optimal strategies may be employed:

- The first option would be to base the growth of PAOs solely on an external readily biodegradable carbon source (acetate or propionate) that is added at the start of the anaerobic phase, and to load the reject water at the beginning of the aerobic phase. This would allow low anaerobic retention times, due to VFAs being the carbon source which can be easily taken up by PAOs, and the absence of high ammonium concentrations during this phase. In addition, this allows the employment of certain strategies centred around the type of carbon source that may give PAOs an antagonistic advantage over GAOs (e.g. the promotion of anoxic EBPR with the use of propionate that is discussed in section 5.6.7). While the biodegradable organic content of the reject water is not utilized by PAOs, it is reduced by common heterotrophs whose growth is a requirement anyway. The low COD/N ratio that characterizes reject water generally necessitates the external addition of carbon. The downside of this strategy is the elevated cost of the external carbon that is to be taken up by PAOs.
- The second option would be to introduce the reject water at the start of the anaerobic phase and employ longer anaerobic retention times. While anaerobic PAO activity may be delayed due to the ammonium shock load, the increased anaerobic retention time would secure their proper function and could also allow effective hydrolysis and fermentation of the organic content of the reject water, producing more VFAs that can be taken up by PAOs. This strategy may also employ the use of cheap by-products such as glycerol as an external carbon source added at this phase that can be fermented to produce VFAs. As VFAs are slowly produced and subsequently taken up by PAOs, their concentration in the reactor would be minimal throughout the anaerobic phase. This may provide an antagonistic advantage to PAOs as it has been reported that PAOs prevail over GAOs in conditions of scarcity (Tu and Schuler, 2013). The downside of this strategy is the requirement for longer anaerobic times, meaning greater reactor volumes for a given influent load.

- A final option may be to load the reject water at the beginning of the anaerobic phase and maintain a low anaerobic retention time by effectively lowering the pH during this phase, minimizing the FA content of the medium. While this approach provides no significant benefit compared to the aforementioned strategies, since an external readily biodegradable carbon source would likely still be required, it is a viable option especially since a relatively low pH at the start of aeration may be deemed necessary to combat the effect of ammonium on aerobic PUR.

In general, the preferred strategy will depend on the characteristics of the reject water, limitations and associated costs of the installation and maintenance of the reactors, and the supply and associated costs of the required external carbon source.

In conclusion, while ammonium may have a short-term inhibitory effect on the anaerobic processes of PAOs which should be considered, it constitutes no significant challenge for EBPR under high nitrogen loading conditions.

5.4 Assessment of the combined effect of FNA and FA and validation of the inhibition models

As demonstrated in sections 5.2 and 5.3, it appears that both nitrite and ammonium can inhibit EBPR based on their effect on PUR. Since FNA and FA seem to be the actual inhibitors, pH is of great importance as it dictates the percentage of nitrite in its protonated form along with the portion of ammonium as FA. For a given nitrite concentration, the concentration of FNA increases inversely to pH, while the FA content for a given ammonium concentration increases along with pH increase. Therefore, manipulation of pH in an effort to combat the effect of one inhibitor would result in enhancing the effect of the other.

Figure 5.51 displays the predicted inhibitions of PUR due to either nitrite or ammonium with respect to pH for the temperature of 20°C. The corresponding inhibitions on PUR by nitrite were predicted with the use of a non-competitive inhibition model that was found to best describe inhibition by FNA using a K_{iFNA} of 1.5 µg N/L (Section 5.2.2.3). Accordingly, inhibition by ammonium was predicted by a simple uncompetitive model that was found to best describe inhibition by FA using a K_{iFA} of 10 mg N/L and an abundance of phosphorus ($S \gg K_s$) (Section 5.3.1.2). According to this nomograph, operating under a high pH could tackle EBPR inhibition due to FNA, but the process would be inhibited by the high concentrations of FA. Nitrogen loading is a key factor as high FA concentrations are practically required to stimulate the NOB shunt and therefore the achievement of the nitrification-denitrification process, but at the same time may hinder EBPR due to the high FA and/or FNA content. Raising pH during the nitrification process may assist EBPR as ammonium is oxidized to nitrite. When the residual concentration of ammonium nitrogen becomes equal to the concentration of nitrite nitrogen, the optimal pH of operation is just over 8.2. The adjustment of pH would have to combat the biochemical drop of pH during nitrification. Therefore it seems that the use of an on-line monitoring strategy is urgently needed to avoid severe inhibition effect on PAOs activity in nitrification-denitrification systems. However even with the application of this optimal approach, nitrogen concentrations that are typically present in sludge liquors may prove to limit EBPR under these conditions. For instance, according to the diagram, a nitrogen concentration of 200 mg/L (a concentration much

less than the concentrations generally found in sludge liquors) would mean that when nitrite nitrogen and ammonium nitrogen are at equilibrium under optimal pH, EBPR would be inhibited by 50% by the presence of FNA alone and that the presence of FA alone would inhibit the process also by 50%. The combined effect of both inhibitors will be studied in the following section. However, it is very likely that EBPR would be severely deteriorated under these conditions.

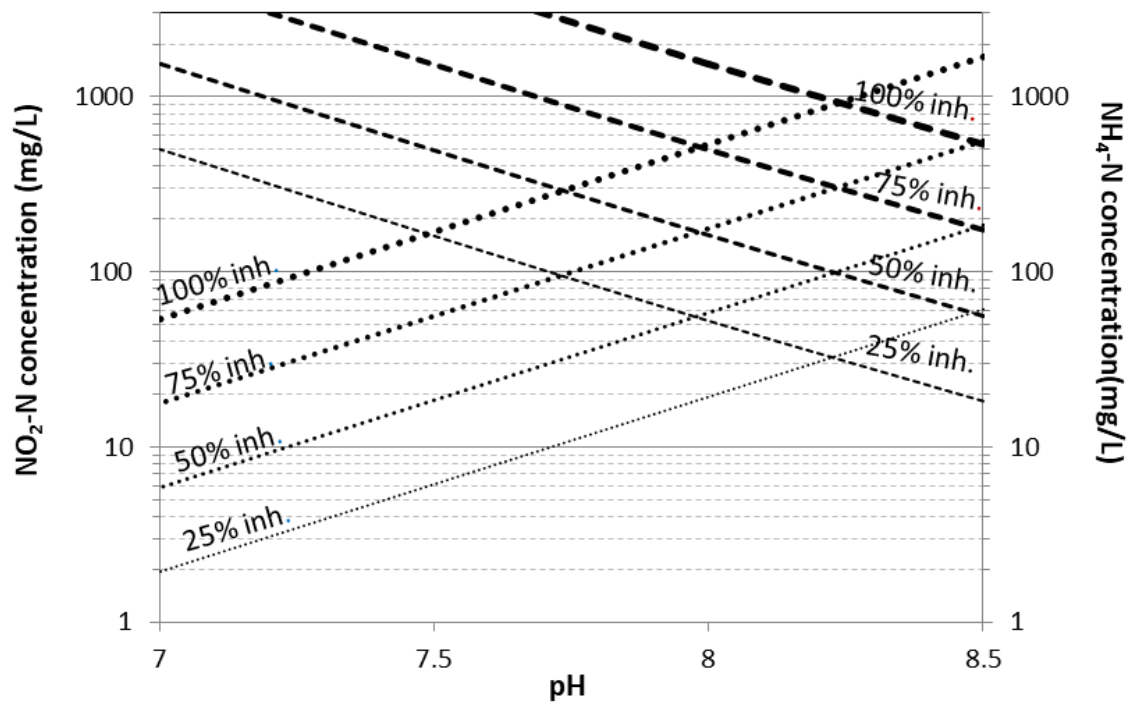


Figure 5.51. Predicted effect of nitrogen loading on aerobic PUR with respect to pH and distribution between nitrite (···) and ammonium (---) nitrogen at $T=20^{\circ}\text{C}$ (Nitrogen concentrations for both nitrite and ammonium are presented in logarithmical scale).

5.4.1 Experimental assessment of the combined effect of FNA and FA on aerobic PUR

In order to investigate the combined effect of FNA and FA on PUR, the SBR was reset and provided with a new inoculum. The SBRs configuration and performance was practically identical to that described in section 5.2.2.1. This was in order to examine the mechanism of the combined FNA and FA inhibition regardless of biomass acclimation. As such, the series of experiments focusing on the combined effect of FNA and FA on PUR started 30 days from the beginning of operation when noticeable PAO activity was displayed.

At the beginning of each experiment, 2 L of sludge was extracted from the SBR prior to feed and divided equally into 4 bioreactors, each with a working volume of 0.5 L. An appropriate amount of acetate, in the form of sodium acetate solution, was added to each of the reactors in order to obtain an initial COD concentration of 200 mg/L. The pH of each container was adjusted to the targeted value just after feed and was kept stable for the remainder of the experiment. The

reactors were then left stirring under anaerobic conditions over a 1 h period. Following the anaerobic phase, the reactors were then aerated over a period of 3 h. The first reactor served as a control ($\text{NO}_2\text{-N}=0$ mg/L, $\text{NH}_4\text{-N}=10$ mg/L). The second reactor was fed with a sodium nitrite solution at the start of aeration in order to achieve a desired initial nitrite concentration to be examined ($\text{NO}_2\text{-N}=\text{X}$ mg/L, $\text{NH}_4\text{-N}=10$ mg/L). The third reactor was fed with an ammonium chloride solution at the start of aeration in order to achieve a desired initial ammonium concentration to be examined ($\text{NO}_2\text{-N}=0$ mg/L, $\text{NH}_4\text{-N}=\text{Y}$ mg/L). Finally, the fourth reactor was fed both amounts of ammonium chloride and sodium nitrite in order to achieve the nitrite concentration of reactor 2 and the ammonium concentration of reactor 3 ($\text{NO}_2\text{-N}=\text{X}$ mg/L, $\text{NH}_4\text{-N}=\text{Y}$ mg/L). Thus, each batch series examined the effect of a specific nitrite concentration and a specific ammonium concentration on PUR both separately and in combination at various pH. A total of 9 experiments were performed. The various combinations of nitrite and ammonium concentrations examined at different pH are presented in Table 5.8.

Table 5.8. Conditions for batch experiments.

#	pH	$\text{NO}_2\text{-N}$ (mg/L)	$\text{NH}_4\text{-N}$ (mg/L)	FNA acclimation
1	7.3	25	700	YES
2	7.3	50	250	YES
3	7.5	20	250	YES
4	7.7	120	250	YES
5	7.7	30	300	NO
6	7.9	50	150	NO
7	7.9	60	150	NO
8	8.2	65	110	NO
9	8.2	90	110	NO

The methodology for estimating the combined inhibitory effect of nitrite and ammonium is detailed in the following typical batch experiment investigating the effect of 50 mg $\text{NO}_2\text{-N/L}$ and 250 mg $\text{NH}_4\text{-N/L}$ at the pH of 7.5. Figure 5.52 displays the evolution of phosphate-phosphorus concentration in all reactors throughout the duration of the experiments. As it is apparent, the addition of the external solutions in the reactors other than the control, resulted in the release of phosphorus early in the experiment. This may be attributed to either a disturbance in the water chemistry that caused the dissolution of phosphorus-containing compounds, or an initial shock experienced by the PAO population due to the rapid change of conditions. This is especially apparent in the reactor where both solutions were added. As such the PUR of each reactor was established for the period after which conditions had settled.

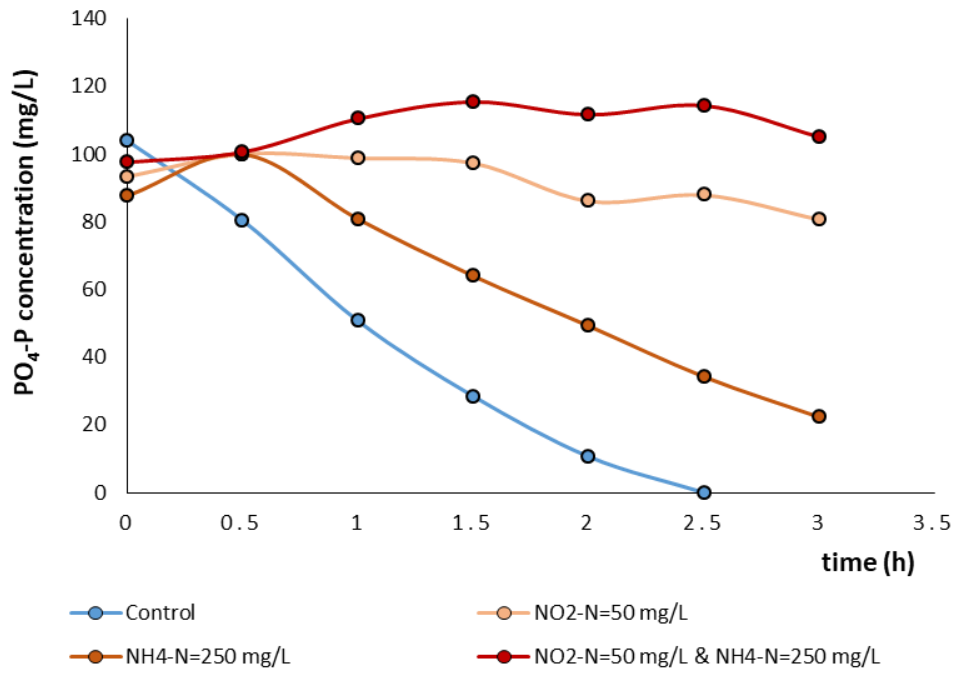


Figure 5.52. Experimental results of typical batch experiment

The PUR of each reactor was calculated according to Figure 5.53 with respect to VSS (2,480 mg/L). The control reactor performed at a PUR of 19.2 mg P/g VSS h, while the reactor containing 50 mg NO₂-N/L performed at 3.7 mg P/g VSS h, the reactor containing 250 mg NH₄-N/L performed at 12.5 mg P/g VSS h and the reactor containing both nitrite and ammonium performed at 2.4 mg P/g VSS h. As such, the specific nitrite concentration was found to inhibit PUR by approximately 81% and the specific ammonium concentration by approximately 35%. When both were present, the process was inhibited by approximately 87%.

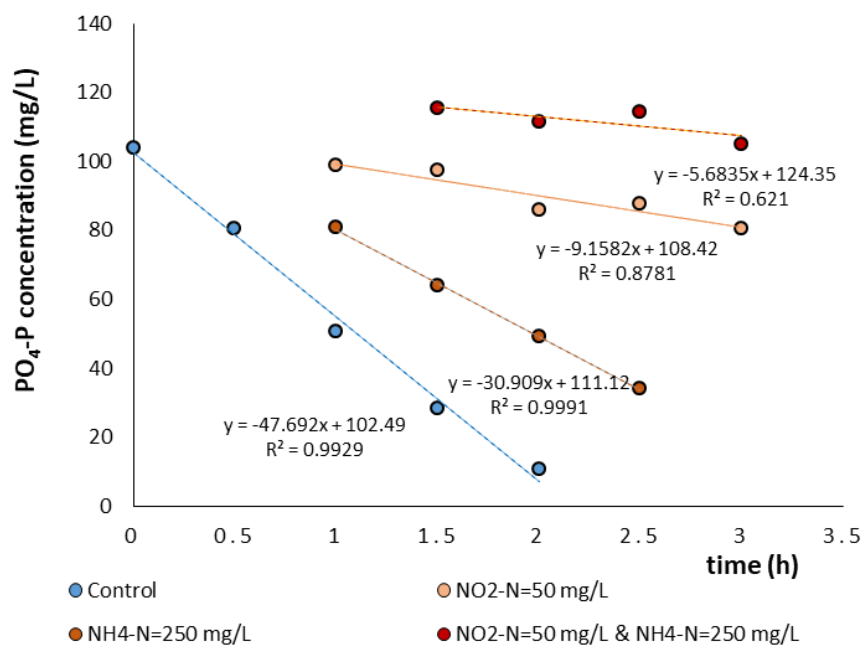


Figure 5.53. Determination of PURs for typical batch experiment

As the performance of the reactors containing either solely FNA or FA may be compared to that of the controls by:

$$PUR_{FNA} = PUR_{control}(1 - Inh_{FNA}) \quad (5.14)$$

$$PUR_{FA} = PUR_{control}(1 - Inh_{FA}) \quad (5.15)$$

where Inh_{FNA} and Inh_{FA} are the degrees of PUR inhibition for the specific FNA and FA concentrations, it is likely that the performance of the reactor containing both inhibitors may be described as:

$$PUR_{FNA\&FA} = PUR_{control} \times (1 - Inh_{FNA}) \times (1 - Inh_{FA})$$

or:

$$Inh_{FNA\&FA} = 1 - (1 - Inh_{FNA}) \times (1 - Inh_{FA}) \quad (5.16)$$

In the case of this experiment:

$$Inh_{FNA\&FA} = 1 - (1 - 0.81) \times (1 - 0.35) \Rightarrow$$

$$Inh_{FNA\&FA} = 0.877 \text{ or } 87.7\%$$

This would be in satisfactory agreement with the degree of inhibition observed in the reactor containing both inhibitors (87%).

Figure 5.54 displays a comparison of the experimental inhibition values observed for the simultaneous presence of nitrite and ammonium with the predicted values according to eq. 5.16, using the data from the respective experiments. As it is evident, the dual effect of FNA and FA may be predicted to a satisfying degree by equation 5.16.

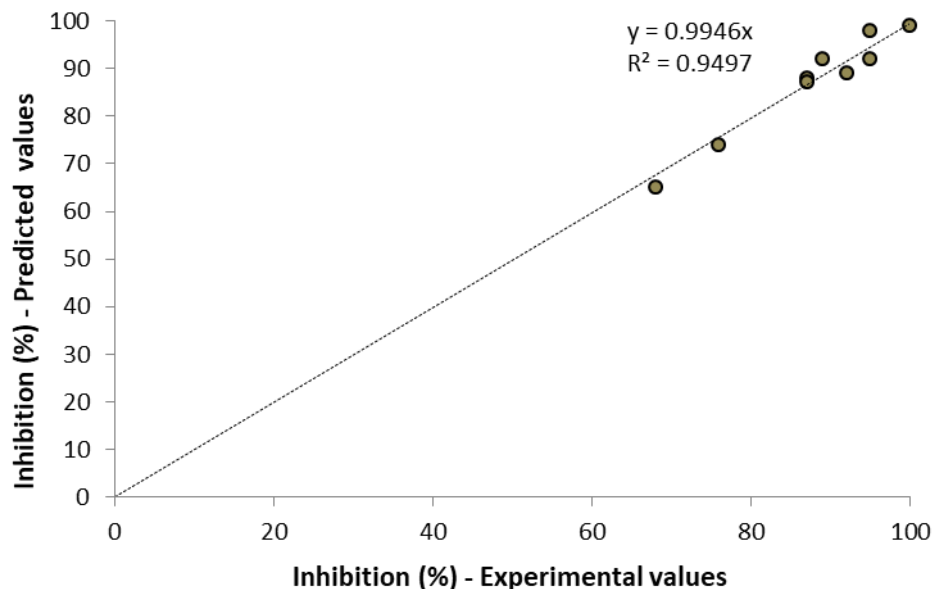


Figure 5.54. Correlation of the experimental and the predicted inhibition values for the simultaneous presence of FNA and FA.

5.4.2 Validation of the inhibition models

The experiments detailed in sections 5.2.1.3 and 5.3.1.2 regarding the nature of PUR inhibition by FNA and FA found aerobic PUR inhibition by FNA to be best described by a non-competitive inhibition model, while inhibition by FA was best described by an uncompetitive inhibition model. Therefore, in the presence of a single inhibitor, PUR may be estimated by the following equations:

$$PUR = PUR_{max} \times \frac{S}{S + K_s} \times \frac{K_{iFNA}}{S_{FNA} + K_{iFNA}} \quad (5.17)$$

in the case of FNA and:

$$PUR = PUR_{max} \times \frac{S}{S \left(1 + \frac{S_{FA}}{K_{iFA}}\right) + K_s} \quad (5.18)$$

in the case of FA, where S: the concentration of PO₄-P in the medium, K_s: the half-saturation constant for PO₄-P, S_{FNA}&S_{FA}: the concentrations of FNA and FA respectively, K_{iFNA}&K_{iFA}: the inhibition constants for FNA and FA respectively.

Based on the results of the experiments described in section 5.4.1 in which the simultaneous effect of FNA and FA was investigated, it is likely that under the effect of both inhibitors, PUR may be estimated as:

$$PUR = PUR_{max} \times \frac{K_{iFNA}}{S_{FNA} + K_{iFNA}} \times \frac{S}{S \left(1 + \frac{S_{FA}}{K_{iFA}}\right) + K_s} \quad (5.19)$$

For an acclimatized biomass, a good estimate for the inhibition constants based on the experiments described in sections 5.2.1.2 and 5.3.1.1 are: K_{iFNA}=1.5 µg/L and K_{iFA}=10mg/L. As mentioned, the experiments presented in the previous section that investigated the dual effect of FNA and FA, commenced prior to the achievement of steady state conditions in the SBR in order to test the mechanism of simultaneous inhibition on PUR regardless of the degree of acclimation to either inhibitor. As a result, eq 5.19 may not accurately describe PUR inhibition for the experiments conducted under non-acclimatized conditions. Instead, the empirical model (eq. 5.19) was evaluated for the experiments conducted after day 85 of operation, where a steady performance had been reached and the biomass was well-acclimatized to the presence of both FA and FNA. A total of 4 experiments were conducted after this time. The combined nitrite and ammonium concentrations along with the respective FNA and FA concentrations, the pH and the degree of inhibition observed for each experiment are shown in Table 5.9.

Table 5.9. Conditions of batch experiments for acclimatized biomass

#	pH	NO ₂ -N	NH ₄ -N	HNO ₂ -N (mg/L)	NH ₃ -N (mg/L)	Inhibition (%)
1	7.3	25	700	3.21×10 ⁻³	5.48	82%
2	7.3	50	250	6.43×10 ⁻³	2.10	87%
3	7.5	20	250	1.67×10 ⁻³	2.87	68%
4	7.7	120	250	6.48×10 ⁻³	4.19	89%

According to the empirical model (eq. 5.19), the inhibition of PUR may be estimated as:

$$Inhibition(\%) = \left(1 - \frac{K_{iFNA}}{S_{FNA} + K_{iFNA}} \times \frac{S}{S \left(1 + \frac{S_{FA}}{K_{iFA}} \right) + K_S} \right) \times 100\% \quad (5.20)$$

For each experiment, the predicted inhibition for the associated FNA and FA concentrations was calculated using a K_{iFNA} of 1.5 $\mu\text{g/L}$ and a K_{iFA} of 10 mg/L which best describe an acclimated biomass (sections 5.2.2.3 and 5.3.1.2). A K_S of 4.5 mg/L was used which is considered a good estimate, although the significantly high $\text{PO}_4\text{-P}$ concentrations of the experiments ($>80 \text{ mg/L}$) deemed it of lesser importance.

The results of the simulation are compared to the inhibition of PUR observed in the experiments and presented in Figure 5.55. As shown, the simple model was successful in estimating the combined inhibitory effect of FNA and FA on PUR to a very satisfactory degree.

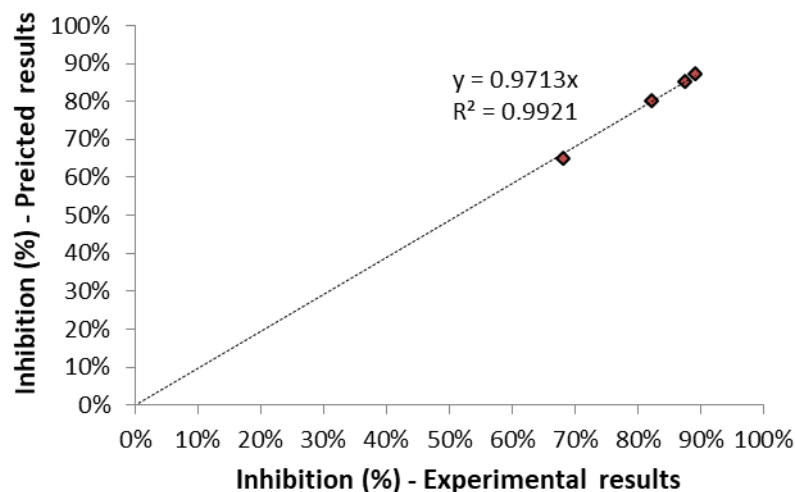


Figure 5.55. Comparison of simulated and experimental inhibition for various FNA and FA combinations.

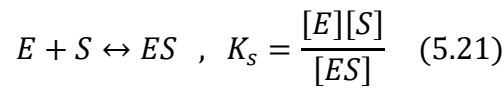
As mentioned, the exact inhibitive mechanism of FNA on PAOs has not been well evidenced yet although it has been reported that its negative effect most likely concerns the proper function of the *ppk* enzyme. The effect of FNA on aerobic PUR was found to be best described by a non-competitive inhibition model indicating that perhaps FNA is capable of binding equally well to both the *ppk* enzyme and the enzyme-substrate complex. As previously stated, in non-competitive inhibition it is assumed that both bindings occur at a site distinct from the active binding site that is being occupied by the substrate (allosteric site). The binding of FNA to the allosteric site results in a conformational change to the active site of the enzyme thus resulting in the decrease of product formation, while the affinity of the enzyme for phosphates (substrate) is practically unaffected as FNA does not compete with phosphates for the active site. Aerobic PUR inhibition by FA on the other hand was found to be best described by an uncompetitive model. According to the general principles of uncompetitive inhibition, the inhibitor binds only to the enzyme-substrate complex (ES) rather than directly to the free enzyme (E). It does not

interfere with the binding of substrate (S) to the active site but prevents the dissociation of the enzyme-substrate complex. The exclusivity of the compound's binding to the ES complex, may be due to a conformational change of the enzyme upon substrate binding, which creates or modifies a neomorphic pocket for inhibitor interactions. As the inhibitory effect of FA on PAOs has only recently come to light, information regarding the exact mechanism of the process is nonexistent as of this point.

5.4.2.1 Examination of an enzyme kinetic model (model 1) to describe the combined effect of FNA and FA on PUR

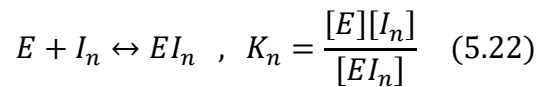
While the exact mechanisms of the effects of FNA and FA on PAOs are not clear, an attempt to model their combined effect on PUR may be made by following the general principles of non-competitive and uncompetitive inhibition. The model described in this section is derived from the work of Park and Bae (2009) on the combined effect of FNA and FA on AOB and NOB.

The formation of the enzyme-substrate complex may be described by the following reaction:

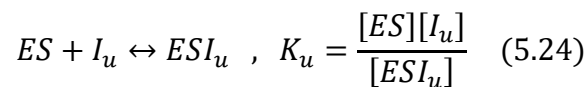
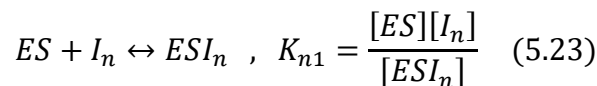


where: [E]= unoccupied enzyme concentration per unit biomass, [S]= concentration of substrate (PO₄-P) and [ES]= enzyme-substrate complex concentration per unit biomass.

The attachment of a non-competitive inhibitor to the allosteric site of the enzyme may be described as:



where: [In]= concentration of non-competitive inhibitor, [EI_n]= concentration of enzyme sites occupied by inhibitor per unit biomass. The binding of a non-competitive and an uncompetitive inhibitor to the enzyme-substrate complex may be described by the following reactions:



where: [I_u]= concentration of uncompetitive inhibitor, [ESI_n],[ESI_u]= enzyme-substrate complex occupied by either inhibitor concentration per unit biomass.

By the definition of non-competitive inhibition: K_n=K_{n1}. Therefore, from equations (5.21) and (5.22):

$$[EI_n] = \frac{[E][I_n]}{K_n} = \frac{K_s[ES]}{[S]} \frac{[I_n]}{K_n} \quad (5.25)$$

The total concentration of enzyme sites is:

$$[E_t] = [E] + [ES] + [EI_n] + [ESI_n] + [ESI_u] \quad (5.26)$$

By rearranging equations (5.21),(5.23) and (5.25):

$$[E] = \frac{K_s[ES]}{[S]} \quad (5.27), \quad [ESI_n] = \frac{[ES][I_n]}{K_n} \quad (5.28), \quad [ESI_u] = \frac{[ES][I_u]}{K_u} \quad (5.29)$$

By applying equations (5.25), (5.27), (5.28) and (5.29) to equation (5.26) and rearranging for [ES]:

$$[ES] = \frac{[E_t][S]}{K_s \left(1 + \frac{[I_n]}{K_n}\right) + [S] \left(1 + \frac{[I_n]}{K_n} + \frac{I_u}{K_u}\right)} \quad (5.30)$$

By definition:

$$-\frac{d[S]}{dt} = q = k_2[ES] \quad (5.31)$$

$$q_{max} = k_2[E_t] \quad (5.32)$$

Therefore:

$$q = \frac{q_{max}[S]}{K_s \left(1 + \frac{[I_n]}{K_n}\right) + [S] \left(1 + \frac{[I_n]}{K_n} + \frac{I_u}{K_u}\right)} \quad (5.33)$$

In the case of PUR inhibition by FNA and FA:

$$PUR = \frac{PUR_{max}[S]}{K_s \left(1 + \frac{[S_{FNA}]}{K_{iFNA}}\right) + [S] \left(1 + \frac{[S_{FNA}]}{K_{iFNA}} + \frac{[S_{FA}]}{K_{FA}}\right)} \quad (5.34)$$

According to equation 5.34, the degree of PUR inhibition by a combination of FNA and FA may be estimated as:

$$Inhibition(\%) = \left(1 - \frac{[S]}{K_s \left(1 + \frac{[S_{FNA}]}{K_{iFNA}}\right) + [S] \left(1 + \frac{[S_{FNA}]}{K_{iFNA}} + \frac{[S_{FA}]}{K_{FA}}\right)}\right) \times 100\% \quad (5.35)$$

For each experiment, the predicted inhibition for the associated FNA and FA concentrations was calculated using a K_{iFNA} of 1.5 $\mu\text{g/L}$ and a K_{iFA} of 10 mg/L similarly to the empirical model (equation 5.19). The predicted inhibitions are compared to the experimental results alongside to the results of the empirical model and are presented in Figure 5.56 and Figure 5.57 . While the enzyme kinetic inhibition model does provide some agreement with the experimental data, it appears that the empirical model provides more satisfactory results.

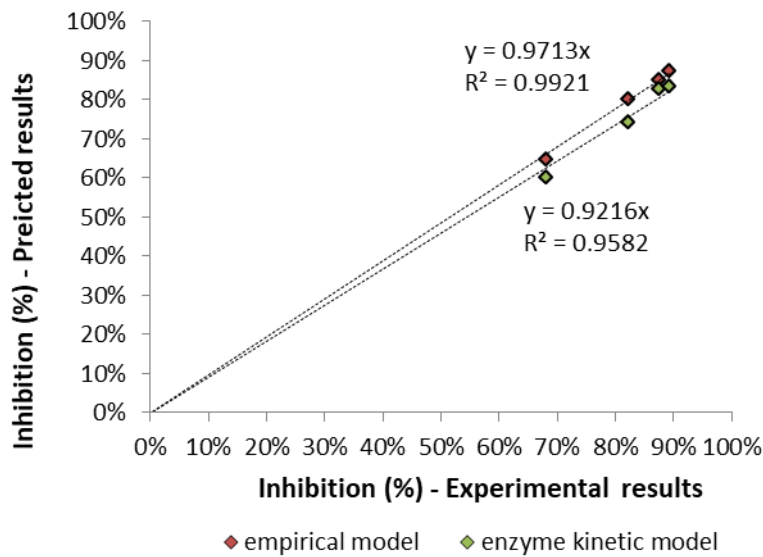


Figure 5.56. Comparison of simulated and experimental inhibition for various FNA and FA combinations (empirical vs enzyme kinetic model).

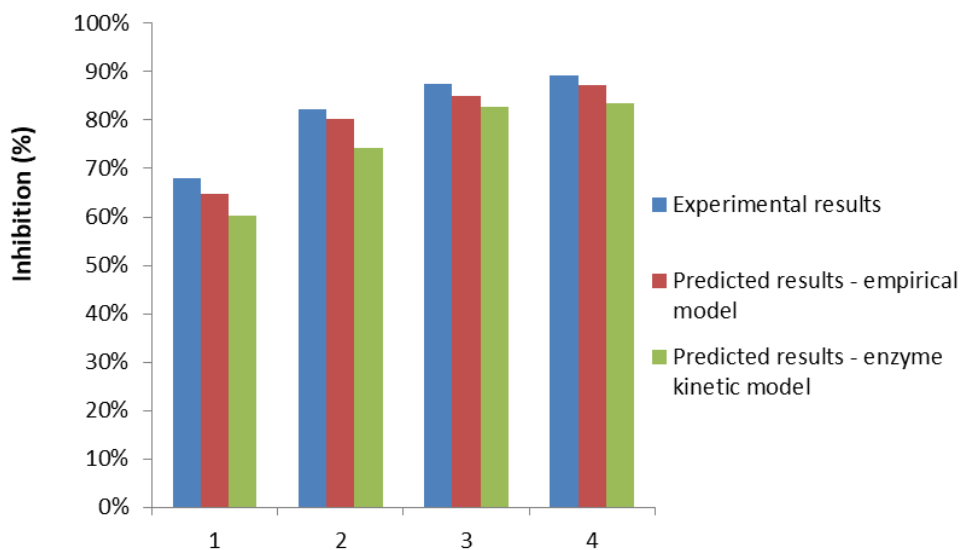


Figure 5.57. Comparison of simulated and experimental inhibition for various FNA and FA combinations

5.4.2.2 Examination of a modified enzyme kinetic model (model 2) to describe the combined effect of FNA and FA on PUR

While model 1 could be considered satisfactory in describing combined inhibition on PUR, there is a certain aspect that should be addressed. According to the methodology applied in the case of model 1, it is assumed that a non-competitive inhibitor may not bind to an enzyme-substrate complex that is already occupied by an uncompetitive inhibitor and vice-versa. This would mean that the attachment of one inhibitor causes a conformational change to the complex that disallows the binding of the other. However it might be possible that FNA has the affinity to bind to an enzyme-substrate complex that is already occupied by FA and vice-versa. In this case, the reactions may be described as:

$$ESI_n + I_u \leftrightarrow ESI_n I_u, \quad K_{u1} = \frac{[ESI_n][I_u]}{[ESI_n I_u]} \quad (5.36a)$$

$$ESI_u + I_n \leftrightarrow ESI_u I_n, \quad K_{n2} = \frac{[ESI_u][I_n]}{[ESI_u I_n]} \quad (5.36b)$$

Assuming that the attachment of one inhibitor doesn't affect the binding of the other:

$$K_{n2}=K_{n1}=K_n, \quad K_{u1}=K_u, \quad [ESI_u I_n]=[ESI_n I_u]$$

$$(5.36a)/(5.36b) \xrightarrow{(5.23)/(5.24)} [ESI_u I_n] = \frac{[ES][I_n][I_u]}{K_n K_u} \quad (5.37)$$

In this case, the total concentration of enzyme sites is:

$$[E_t] = [E] + [ES] + [EI_n] + [ESI_n] + [ESI_u] + [ESI_u I_n] \quad (5.38)$$

By applying equations (5.25), (5.27), (5.28), (5.29) and (5.37) to equation (5.38) and rearranging for [ES]:

$$[ES] = \frac{[E_t][S]}{K_s \left(1 + \frac{[I_n]}{K_n}\right) + [S] \left(1 + \frac{[I_n]}{K_n} + \frac{I_u}{K_u} + \frac{I_n I_u}{K_n K_u}\right)} \quad (5.39)$$

By applying equations (5.31) and (5.32) and adjusting for PUR and the inhibitors in question:

$$\begin{aligned} PUR &= \frac{PUR_{max}[S]}{K_s \left(1 + \frac{[S_{FNA}]}{K_{iFNA}}\right) + [S] \left(1 + \frac{[S_{FNA}]}{K_{iFNA}} + \frac{[S_{FA}]}{K_{FA}} + \frac{[S_{FNA}][S_{FA}]}{K_{iFNA}K_{iFA}}\right)} \Rightarrow \\ &\Rightarrow PUR \\ &= PUR_{max} \frac{K_{iFNA}[S]}{K_s(K_{iFNA} + [S_{FNA}]) + [S] \left(K_{iFNA} + [S_{FNA}] + \frac{[S_{FA}]}{K_{FA}}(K_{iFNA} + [S_{FNA}])\right)} \Rightarrow \\ &\Rightarrow PUR = PUR_{max} \times \frac{K_{iFNA}}{S_{FNA} + K_{iFNA}} \times \frac{S}{S \left(1 + \frac{S_{FA}}{K_{iFA}}\right) + K_s} \quad (5.19) \end{aligned}$$

which is the same equation referred to as the empirical model in the previous sections. As was presented in Figures 5.56 and 5.57, model 2 provides a more satisfactory description of the combined effect of FNA and FA compared to model 1. This would suggest that FNA or FA may bind to a complex that is already occupied by the other inhibitor, resulting in an increased degree of inhibition. This is because of the increased availability of complexes for either inhibitor. As inhibitors attach and detach to the complexes, a complex that is occupied by both inhibitors would still be rendered inactive if one of them were to detach. As more complexes are available for either inhibitor to bind, the probability of a complex being occupied by at least one is increased, resulting in a more severe overall inhibition. The implications of this behavior may also concern the combined effect of FNA and FA on AOB, NOB, as well as other microorganisms.

While model 2 appears to describe combined inhibition to a very satisfactory degree, there are still some limitations. For instance, it is assumed that, in the case of non-competitive inhibition, the occupation of 50% of the enzyme sites ($[E]+[ES]$) also inhibits the process by 50% ($K_n=K_{iFNA}$). Similarly, in the case of uncompetitive inhibition, the assumption is that the occupation of 50% of the enzyme-substrate complexes ($[ES]$), translates to 50% inhibition ($K_u=K_{iFA}$). This would suggest that as long as an enzyme or enzyme substrate complex is occupied, it is incapable of yielding products. In reality, it is possible that an enzyme substrate complex that is occupied by an inhibitor may still yield products but at a reduced rate. In other words, the process is governed not only by $[ES]$ but also by $[ESI_n]$ and $[ESI_u]$, to a lesser extent. In the case of a single inhibitor this is not problematic in terms of modelling, as the adopted K_i would still directly correlate to the percentage of occupied sites. When both inhibitors are involved however, since the occupied complexes may yield products at different rates, the process is complex and may not be described accurately without knowledge of the energies involved. The complexity increases considering that the dual presence of FNA and FA may have a cumulatively effect on the enzyme, meaning that $[ESI_nI_u]$ complexes could provide products at a more reduced rate than the complexes occupied by a single inhibitor. This may explain the slightly higher inhibition observed in the experiments compared to the model's prediction. Despite these limitations, from a practical standpoint, the combined effect of FNA and FA on PUR may be described by model 2 to a very satisfactory degree.

5.4.3 Implications for full-scale applications according to the unified inhibition model

With the use of the combined inhibition model (eq. 5.19), the combined effect of all combinations of FNA concentrations (up to 20 $\mu\text{g/L}$) and FA concentrations (up to 40 mg/L) on PUR was predicted and is presented in Figure 5.58.

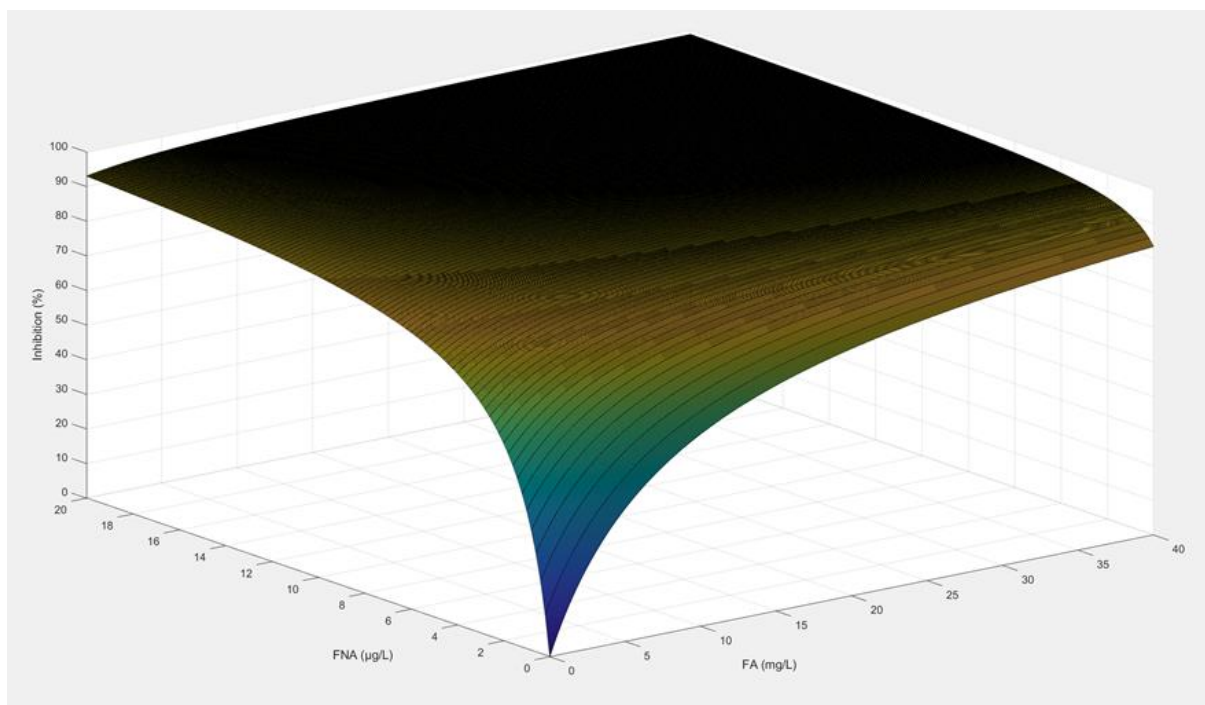
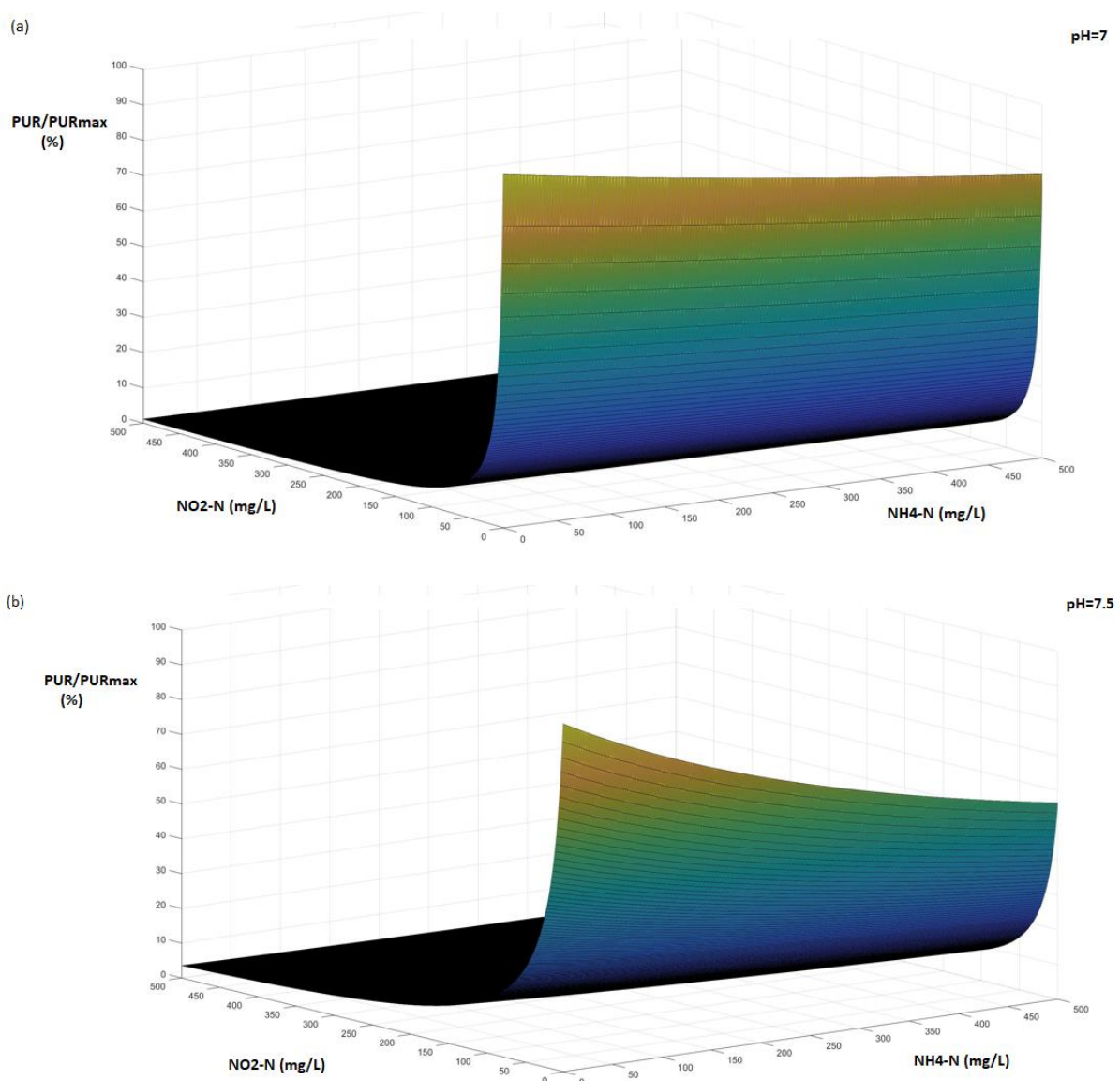


Figure 5.58. PUR inhibition under the combined presence of FNA and FA

It has been demonstrated that pH is of significant importance in regard to PAO activity as it dictates the percentage of nitrite in the form of FNA and that of ammonium in the form of FA. Figure 5.59 presents the combined effect of nitrite and ammonium on PAOs for various pH, as predicted by model 2. For a clearer image, PAO activity is represented by PUR/PUR_{max} (or: 1-Inhibition) which represents the fraction of their inhibited PUR to their uninhibited capacity to remove phosphorus. The simulation was done for ammonium and nitrite concentrations up to 500 mg N/L which may likely occur in high nitrogen treatment systems. As shown, at low pH, the activity of PAOs is almost completely dictated by the concentration of nitrite and is practically unaffected by the ammonium concentrations of this range. As pH rises, the effect of ammonium becomes more significant while the effect of nitrite decreases. At $pH=8.2$ the effect of nitrite comes to an equilibrium with that of ammonium and PAO activity appears to be greater in general. At the pH of 8.5, PAOs are inhibited to a greater extent by ammonium than by nitrite.



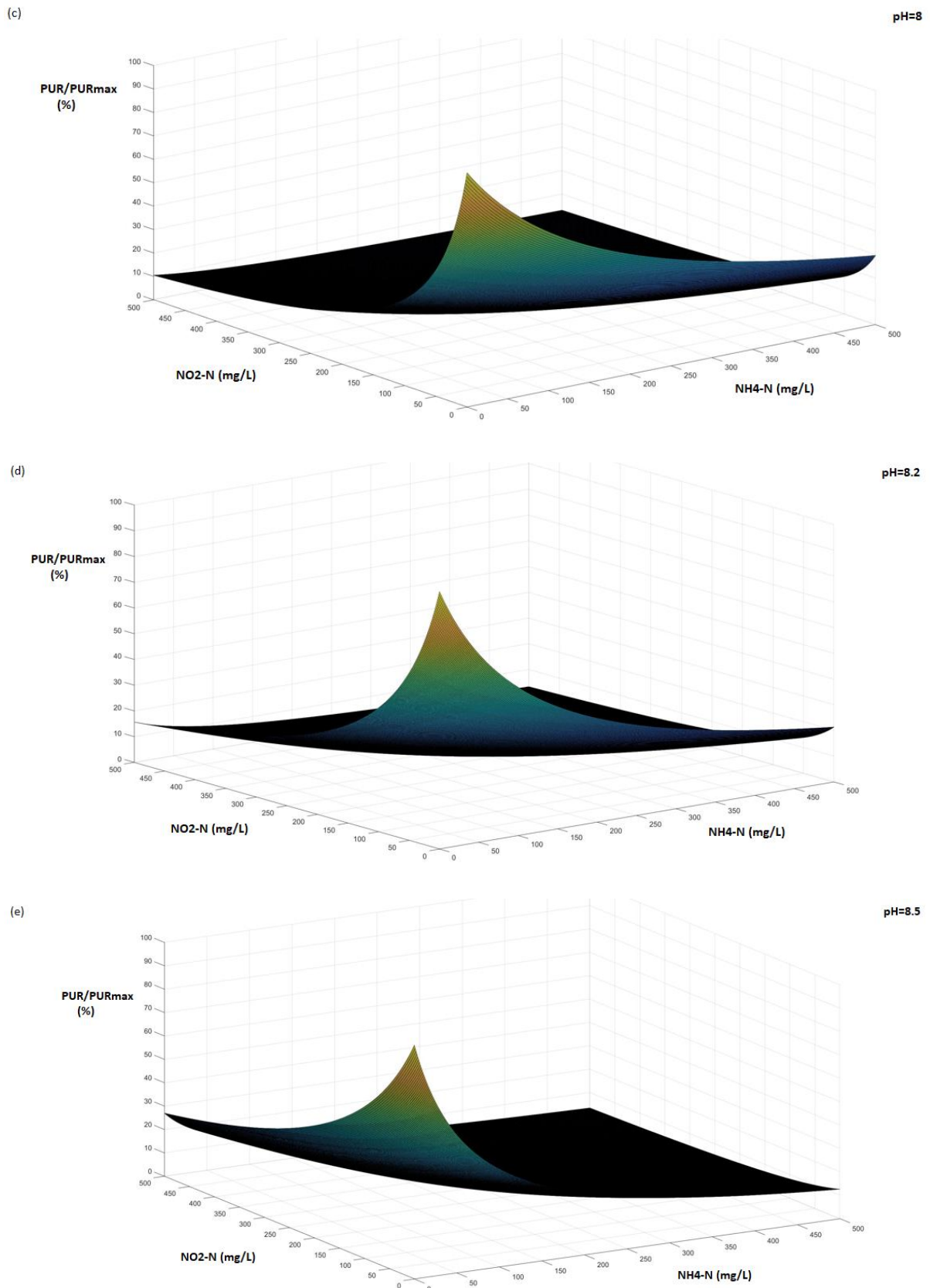


Figure 5.59. PAO activity under the combined effect of nitrite and ammonium at the pH of 7 (a), 7.5 (b), 8 (c), 8.2 (e) and 8.5 (d).

While Figure 5.59 is useful in providing some insight into the dual inhibition of PAOs by nitrite and ammonium, a perspective of the combined inhibition with regard to the processes of nitrification and denitrification is of greater value. To this end, a mathematical simulation model based on the combined inhibition model was developed to predict PAO inhibition during nitrification and denitrification for various nitrogen loadings. In each simulation, an initial ammonium concentration was steadily converted to nitrite at a pace of 0.1 mg N/L. At each step, the concentrations of FNA and FA were calculated with respect to $\text{NH}_4\text{-N}$, $\text{NO}_2\text{-N}$, temperature and pH. Then, the combined inhibition of FNA and FA on PUR was calculated for pH values of 6.5 up to 8.5 at a pace of 0.005 and locked the pH value that resulted in minimum inhibition. This way, the simulation would predict PUR inhibition throughout nitrification under optimum pH conditions. Once the ammonium had been completely depleted, the nitrite concentration was steadily reduced at a pace of 0.1 mg N/L to represent denitrification, with the degree of inhibition being calculated at each step. Since, in the absence of ammonium, there is no limit for optimum pH, the pH of 8.5 was chosen as the maximum value.

Figure 5.60 displays the results of the simulations for the initial NH_4 concentrations of 100, 200, 400 and 800 mg N/L at $T=20^\circ\text{C}$ and optimum pH (<8.5). The conversion of ammonium to nitrite during nitrification and from nitrite to nitrogen gas during denitrification is expressed as a fraction of the processes' completion for a better comparison of the different nitrogen loadings and to also be independent of specific nitrification/denitrification rates. This way, the optimum pH displayed in the diagram is the same for every nitrogen load.

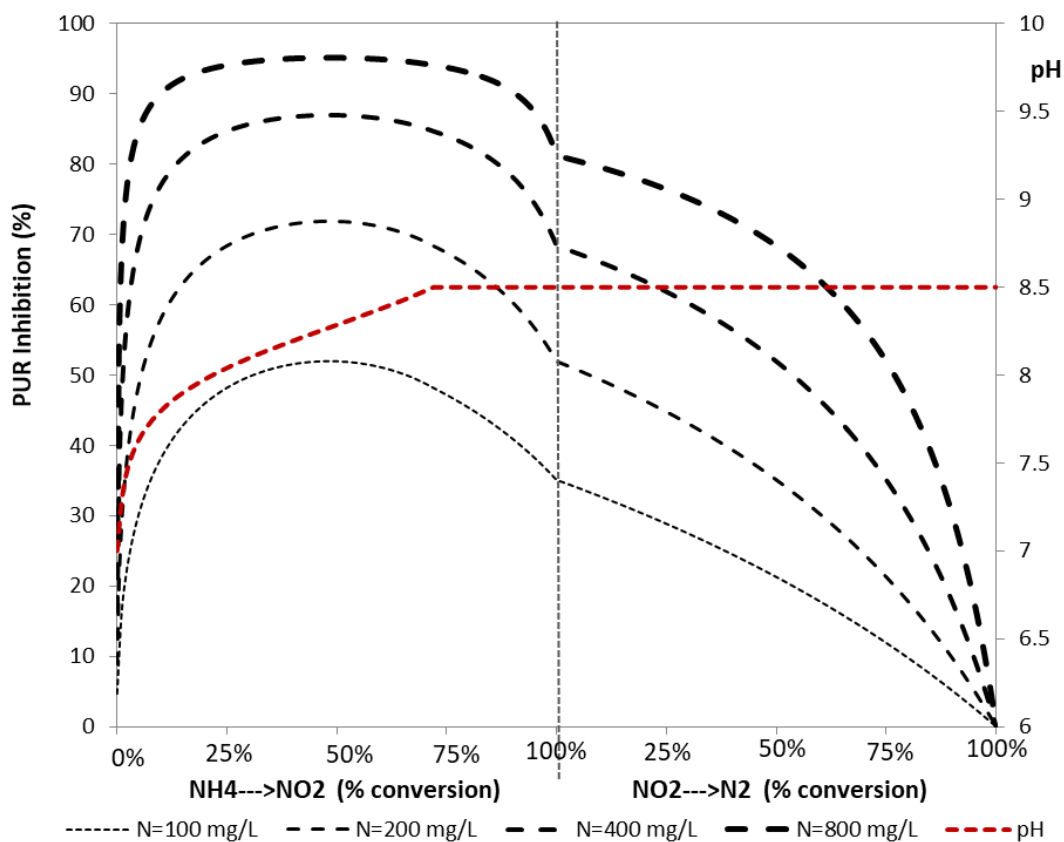


Figure 5.60. Simulated PUR inhibition during nitrification and denitrification under different ammonium loads at $T=20^\circ\text{C}$ and optimum pH

The optimum pH for EBPR is shown to rise above 8 relatively early during nitrification (upon 25% completion) and becomes greater as nitrification progresses. As pH naturally drops during nitrification, operating EBPR under optimum pH would be a costly and possibly impractical option. As shown, even under optimum conditions, PUR would be significantly inhibited even for the lowest nitrogen loading of the simulated scenarios. During denitrification, the overall inhibition appears less significant although it would require a high pH value from the start of the process. Since pH rises naturally during denitrification, EBPR may be assisted. It is also worth noting that during the very early stages of nitrification, PAOs may benefit from a pH that is considerably lower than that of what would be expected from a reject-water treatment facility (owing to the generally high pH of sludge liquors and the high pH at the end of the denitrification stage). In view of the above, one might conclude that PAOs benefit from a pH variation that directly opposes the natural variation of pH during the nitrification/denitrification processes.

Assuming that nitrification and denitrification occur at a steady rate (which is plausible for the greater part of the process), the overall inhibition of PAOs may be calculated by the areas under the formed curves of each scenario. The overall inhibition of PAOs under the aerobic and anoxic conditions of the simulation is presented in Figure 5.61. As shown, the overall aerobic inhibition of PAOs for the lowest ammonium load tested is just above 45%. This would suggest that the growth of PAOs under aerobic conditions is almost halved, raising concerns about their sustainability under these conditions, especially when considering the threat of a more resilient GAO culture. The growth of PAOs under anoxic conditions seems less threatened, with the overall PUR inhibition standing at 20%. It should be noted, however, that PAOs remove phosphorus at a significantly slower rate under anoxic conditions (approximately 40% of the aerobic PUR). Therefore, the benefits from the better conditions during denitrification are not as important both in terms of PAO sustainability and in P-removal.

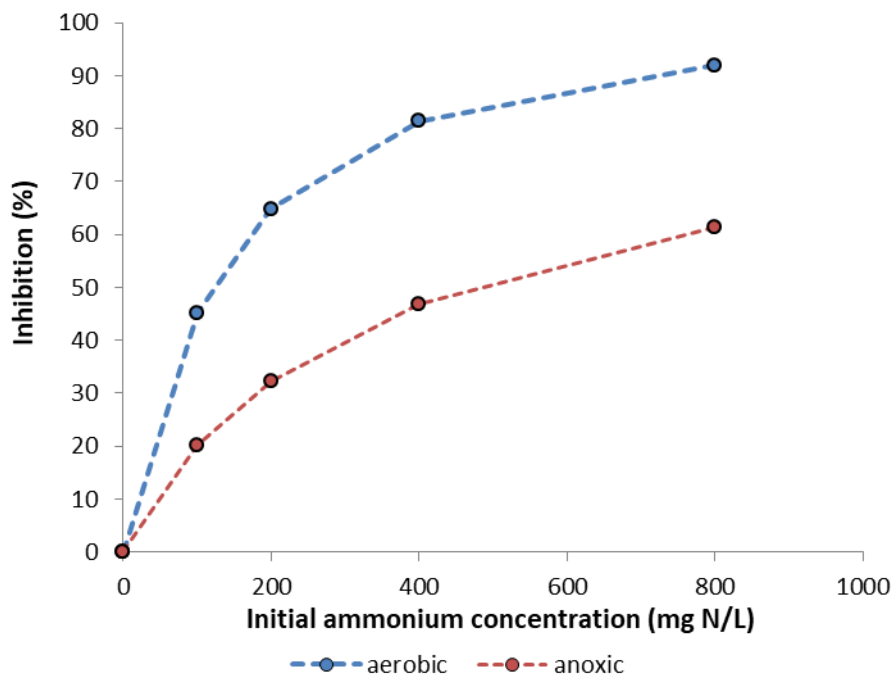


Figure 5.61. Overall inhibition of PAOs under aerobic and anoxic conditions for various initial $\text{NH}_4\text{-N}$ concentrations at optimum pH.

Overall, it would appear that EBPR is at the very least challenging under nitrification/denitrification conditions. Even under optimum pH control, the sustainability of PAOs is questionable for nitrogen concentrations as low as 100 mg/L (or 0.1 kg NH₄-N/m³ per cycle). The main questions concerning the viability of coupling EBPR with nitrification/denitrification are the following:

- While EBPR may be feasible for low ammonium loadings, would this prevent NOB shunt and cancel the benefits of the short-cut nitrification/denitrification process?
- As the natural pH variation during denitrification is hostile to the activities of PAOs, what can be done to minimize the need for pH control?
- While PAOs may be able to persevere under high nitrogen conditions, can their sustainability under such conditions be threatened by a more resilient GAO population?

These concerns are addressed in section 5.7.

5.5 Assessing the inhibitory effect of FNA and FA on GAO activity

As demonstrated through sections 5.2-5.4, both FNA and FA have been found to inhibit PAO activity. As such, the development of PAOs in systems under high nitrogen loading that utilize the nitrification/denitrification pathway may be severely diminished. The adaptation of a high SRT could allow the maintenance of an adequate PAO population under these conditions for phosphorus removal, but likely at the expense of partially allowing full nitrification to occur since it would also allow the presence of a greater NOB population. However, this may not be the case, as the growth of GAOs, the main antagonist group of PAOs, under these conditions may be affected to a lesser extent. If this were so, the differential growth of GAOs would ultimately lead to the wash-out of PAOs from the system. Therefore, determination of the viability of EBPR in such systems should not only consider the effect of FNA and FA on PAOs, but also their respective effect on GAOs whose growth may prove to be the bottleneck of EBPR in many cases.

In order to investigate the effect of FNA and FA on GAOs, an SBR was set up aiming to develop a highly GAO-enriched biomass, unacclimatized to FNA and FA. Upon achievement, the biomass fuelled a series of experiments focusing on the effect of FNA and FA on the growth rate of GAOs. The operation of the SBR and the experiments conducted are analysed in the following subsections.

5.5.1 Performance of the experimental system

5.5.1.1 Start-up period

During the start-up period the SBR operated on 4 daily cycles each consisting of a 1 h anaerobic phase, a 3 h aerobic phase and a 1.5 h endogenous phase. Settling and decanting occurred once per day over a 2 hour period due to technical limitations mentioned in the materials and methods section.

Feed consisted of a concentrated mixture of acetate and ammonium that was introduced at the beginning of each anaerobic phase. The volume of each dose was 250 mL. Before decanting, the SBR contained 10.5 L of liquor. Following the removal of 5.5 L of effluent, 5.5 L of water was added to the SBR bringing the mixed liquor's volume to 10.5 L. Under mixing conditions, 1 L of

mixed liquor was removed in order to achieve an SRT of 10 days. Thus, with the daily addition of 1 L of the concentrated feed, the SBR's working volume averaged at 10 L simulating an HRT of 2 days.

In order to prevent the growth of PAOs, the concentration of phosphorus in the SBR was routinely monitored and kept below 1 mg/L with the occasional addition of a potassium phosphate solution to provide for the growth of GAOs. A thiourea solution was added daily following the refilling of the SBR as to maintain a concentration of 20 mg/L for the suppression of both AOB and NOB. The addition of a carbon source at the beginning of the anaerobic phase would provide GAOs with an advantage over common heterotrophic organisms, giving them priority in the utilization of COD. During the aerobic phase, the sufficient DO concentrations (>3 mg/L) would allow GAOs to develop by oxidizing their stored PHAs, while residual acetate would be rapidly removed by other heterotrophs. With the cease of aeration, the SBR remained without the addition of a carbon source for 1.5 h for the endogenous removal of the dissolved oxygen prior to the following anaerobic phase. Over time, by the end of the anaerobic phase less and less acetate would remain available to be oxidized by common heterotrophs, leading to the development of a practically pure GAO culture.

The daily dose of COD was 7 g/d, regulated with respect to the aerobic SRT (≈ 5 d) in order to achieve a biomass concentration of around 2,000 mg VSS/L. The daily dose of ammonium was 300 mg N/d in order to ensure an adequate source of nitrogen for biomass growth. Ammonium concentrations in the effluent were monitored on a daily basis and the daily dosage was modified in order to maintain effluent concentrations lower than 10 NH₄-N mg/L to prevent accumulation of ammonium in the SBR.

5.5.1.2 Steady-state operation

The SBR was successful in developing a highly GAO-enriched biomass over the course of approximately 90 days after which a stable operation was observed. The pH of the reactor ranged from 7.5 to 8.2 throughout operation, while temperature was kept constant at 20 ± 2 °C. Due to the suppression of AOB and NOB by thiourea, nitrite concentrations in the SBR did not exceed 0.5 mg NO₂-N/L, while nitrate was non-detected. Figure 5.62 displays the typical variation of COD in the SBR during the first daily cycle. As shown, the vast majority of acetate is taken up anaerobically, leaving approximately 15 mg/L to be readily oxidized during aeration. This, along with the fact that no phosphorus was released anaerobically or was taken up during aeration, which is indicative of PAO activity, demonstrates the presence of a strong GAO population. The strong presence of GAOs was also verified by FISH analysis (Figure 5.63). As expected, the *Competibacter spp.* that possesses a high affinity for acetate dominated the biomass composition. Quantitative analysis of composite FISH images revealed that *Competibacter* made up for more than 90% of the total biomass. Therefore experiments regarding the effect of nitrite or ammonium on the biomass developed here may provide accurate information on their effect on GAOs.

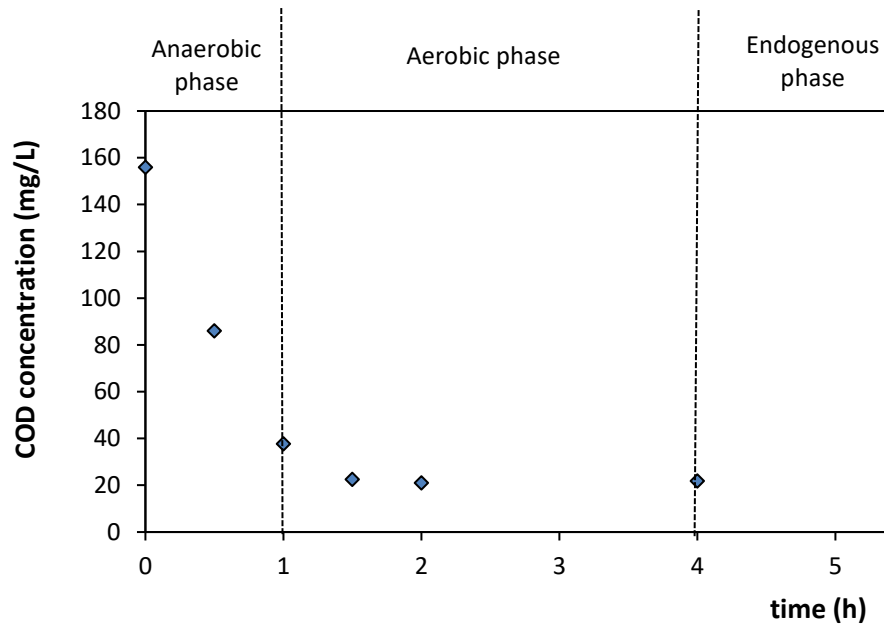


Figure 5.62. Typical variation of COD in the SBR during the first daily cycle.

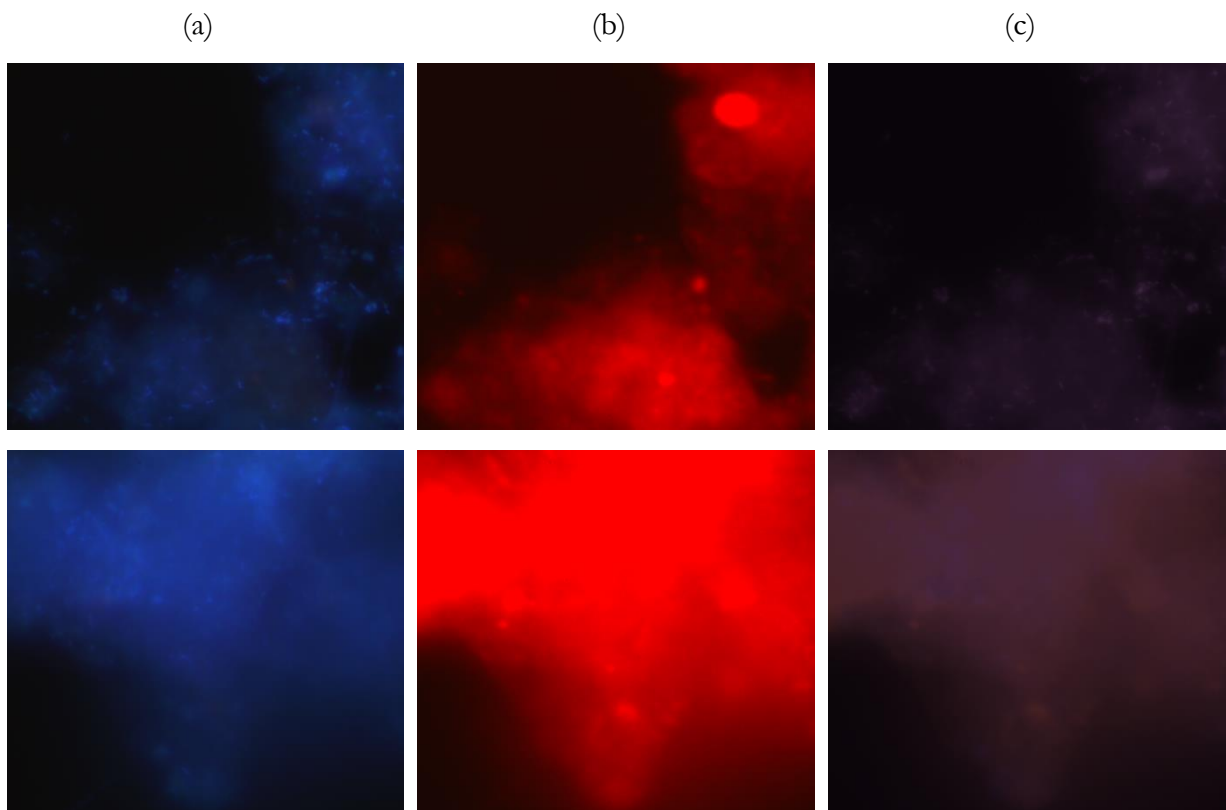


Figure 5.63. In situ identification of GAOs using Cy-3 labeled GAOMIX. All microorganisms stained with DAPI presented in blue (column a), GAOs depicted in red (column b), composite images in purple (column c).

5.5.2 Experimental assessment of the effect of FNA on GAO activity

Having established a highly GAO enriched sludge, a series of batch experiments was conducted in order to investigate the effect of FNA on the maximum growth rate of GAOs. In each experiment, approximately 450 mL of biomass was retrieved from the SBR and divided equally into 3 containers, each with a working volume of 1 L. Water was added to each container bringing the volume of the diluted sludge to 500 mL, after which an appropriate amount of acetate, in the form of a sodium acetate solution, ammonium, in the form of an ammonium chloride solution and phosphorus, in the form of a potassium phosphate solution were added. The sludge was then further diluted up to a volume of 1 L and kept under stirring conditions. The pH of each reactor was set to the desired value and kept constant throughout the experiment. The targeted initial concentrations of each parameter are presented in Table 5.10.

Table 5.10. Initial concentrations of main parameters in each reactor

VSS (mg/L)	300
COD (mg/L)	3000
NH₄-N (mg/L)	300
PO₄-P (mg/L)	50

As described in detail in the Materials and Methods Section, the high F:M ratio of 10 along with the abundance of nutrients would provide maximum growth conditions (Stasinakis et al., 2003; Noutsopoulos, 2002). In this respect, the initial concentration of ammonium was chosen to be at 10% of the initial COD and phosphorus at just above 1.5%, which would correspond to the typical stoichiometric demands for microbial growth.

In each experiment, one of the reactors served as a control, while an appropriate amount of nitrite, in the form of a sodium nitrite solution was added to the other reactors in order to achieve the targeted nitrite concentration that was to be examined. The reactors were aerated over a period of 26 hours under constant pH and temperature (25°C). The VSS of each reactor were measured on an hourly basis, while samples were routinely retrieved and analyzed for nitrite to ensure a constant concentration.

In total, 4 experiments were conducted at the pH of 7, and the nitrite concentrations examined were 20, 40, 60 and 120 mg NO₂-N/L. The respective FNA concentrations with regard to pH and temperature were 4, 8.5, 13 and 27 µg HNO₂N/L. In each experiment the slopes for VSS concentration evolution during the exponential growth phase were calculated, determining the net growth rates (μ_{max-b}) in each reactor. The growth rate of the control reactor was then compared to that of the reactors containing nitrite, establishing a degree of inhibition for each nitrite concentration. The methodology for determining the inhibitory effect of nitrite on the growth of GAOs is analysed in the following typical experiment.

Figure 5.64 and Figure 5.65 display the experimental results for the growth of GAOs under the nitrite concentration of 40 mg NO₂-N/L. More specifically, Figure 5.64 shows the variation of VSS concentration in the control reactor throughout the course of the experiment. During the first 8-10 hours of the experiment practically no growth was observed as the biomass was getting

acclimated to the new conditions (lag phase). Following this, the biomass grew exponentially over time (exponential phase) and would generally reach a peak towards the end of the experiment (stationary phase). As growth in the reactors containing nitrite was diminished, biomass growth did not reach the stationary phase in these cases.

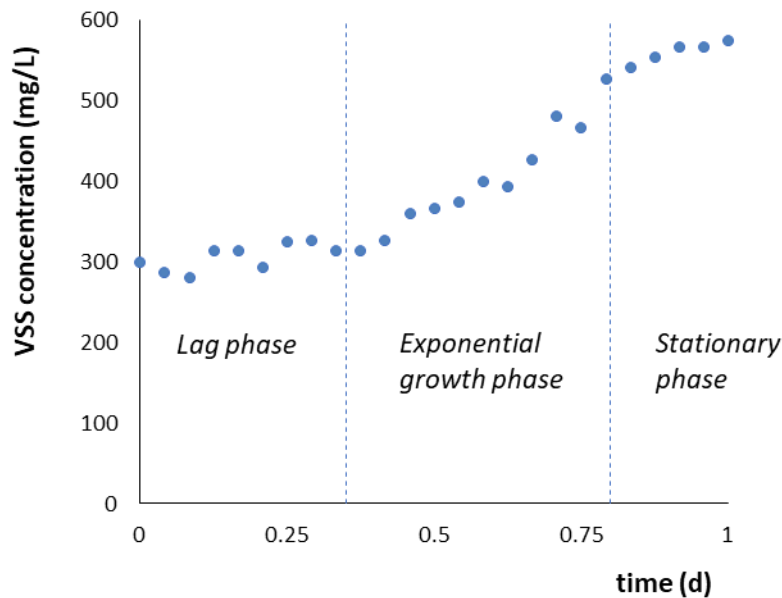


Figure 5.64. Typical example of VSS evolution in control reactor.

Microbial growth during the exponential phase may be described as:

$$\frac{dX}{dt} = (\mu_{max} - b) \times X \quad \Rightarrow$$

$$\Rightarrow X = X_0 \times e^{(\mu_{max}-b)t} \quad (5.38)$$

where X is the concentration of VSS.

Figure 5.65 displays the variation of VSS during the exponential growth phase in all reactors. In accordance with equation (5.38), the net growth of the biomass in each reactor may be determined by the exponent of the exponential trend line for VSS. Therefore, the net growth rate of GAOs in the control reactor was found to be 1.14 d^{-1} , while the net growth rate under the presence of $40 \text{ mg NO}_2\text{-N/L}$ averaged at 0.65 d^{-1} . Consequently, it was determined that the specific nitrite concentration inhibits the net growth of GAOs by approximately 43%. Following the same methodology, the inhibition in GAOs maximum growth rate at all tested nitrite concentrations were calculated and the results are presented in Figure 5.66.

In order to examine any possible effect of pH on the inhibitory function of FNA on GAOs growth, additional experiments based on the experimental protocol already detailed were performed at the pH of 8 for nitrite concentrations equal to 35, 70 and $140 \text{ mg NO}_2\text{-N/L}$. The respective FNA concentrations with regard to pH and temperature were 0.8, 1.6, and $3.1 \text{ } \mu\text{g HNO}_2\text{N/L}$. The results of the additional experiments are also included in Figure 5.66.

As evidenced in Figure 5.66 the increase of nitrite concentration resulted in an increase of the inhibition which also seems to be amplified at the pH of 7. Definitely the nitrite-fna chemistry rules the inhibitive effect recorded with the lower pH values supporting higher FNA values.

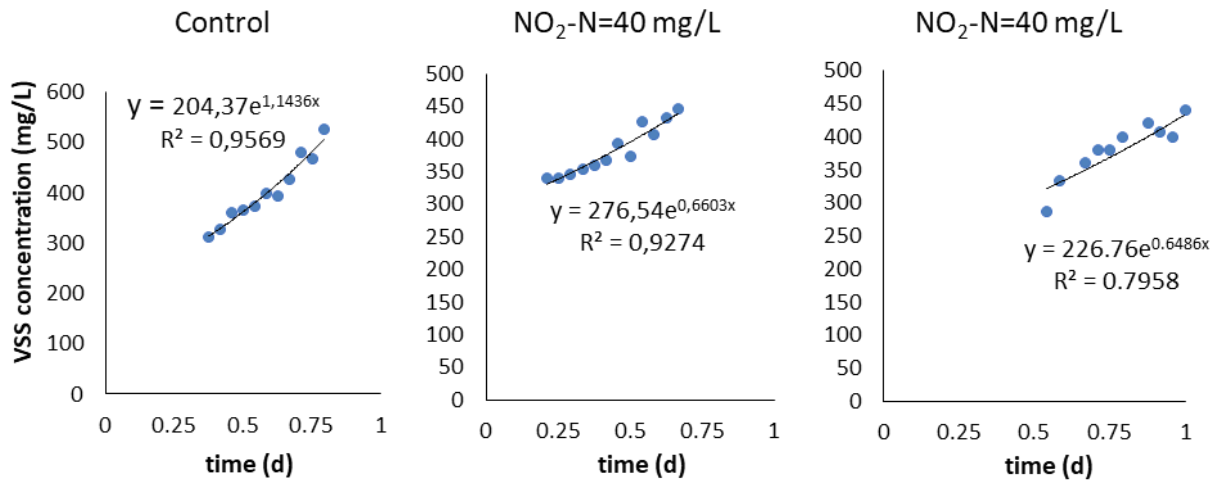


Figure 5.65. Determination of the net growth rates of GAOs in each reactor

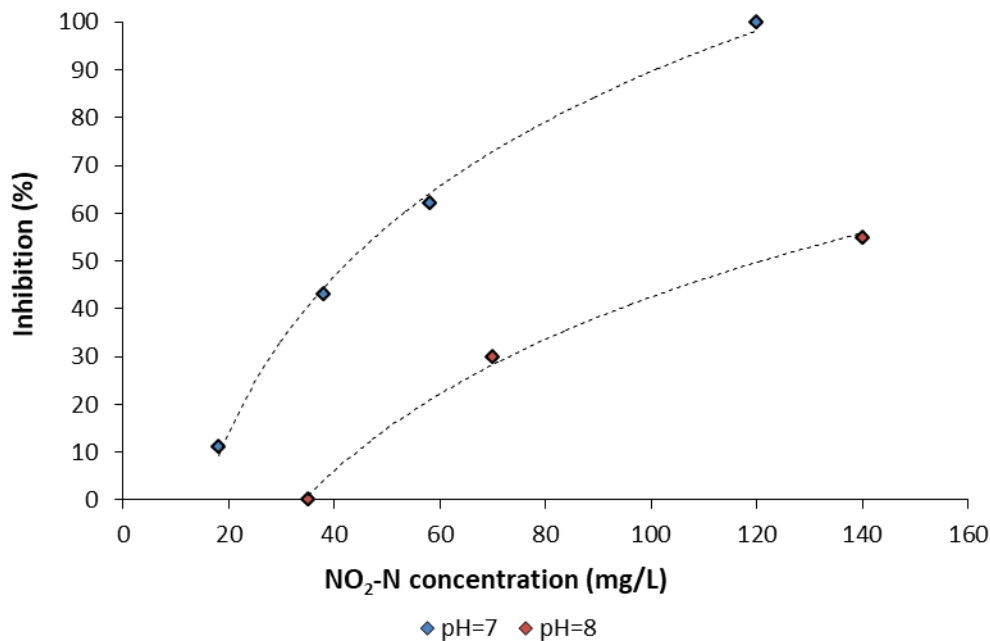


Figure 5.66. Inhibition of GAO growth with regard to nitrite nitrogen concentration.

Figure 5.67 displays a comparison of the inhibitory effect of FNA on PAOs, as established in section 5.2.1 and GAOs (as calculated here). Interestingly enough, the increase of pH from 7 to 8 resulted in significantly higher inhibition of GAOs growth. Evidently, an FNA concentration of 4 $\mu\text{g HNO}_2\text{-N/L}$ emerge an inhibition of 11% at the pH of 7, while an FNA concentration of 3.1 $\mu\text{g HNO}_2\text{-N/L}$ produced an inhibition of 55% at the pH of 8. Therefore, it is anticipated that FNA, although the primary, is not the exclusive parameter affecting the GAOs growth. The adverse effect of high pH values on GAOs activities has also be documented by Filipe et al.

(2001) and Lopez-Vazquez et al. (2009). As postulated by the authors the rise in pH at 8 results in a higher energy demand for the uptake of carbon by GAOs, leading to a greater consumption of stored glycogen. Similar pH-dependence of FNA effect has also been reported by Stein and Arp (1998) for AOB activity. The authors provide experimental evidence highlighting that in the presence of high nitrite concentrations the effect on ammonia oxidizing activity gradually increases with the increase of pH from 7 to 8, thus concluding that the interactions between nitrite and pH should be more complex than the ones being described by the traditional nitrite chemistry. It needs to be underlined that the maximum net growth rate measured at control experiments at both pH values of 7 and 8 were almost identical ($1.13 \pm 0.02 \text{ d}^{-1}$ at the pH of 7 and $1.10 \pm 0.06 \text{ d}^{-1}$ at the pH of 8) thus highlighting that the effect of pH in the absence of nitrite is practically minimal.

Based on the results, it is evidenced that for a pH of 7, an FNA concentration around $10 \mu\text{g HNO}_2\text{-N/L}$ halves GAOs growth, while complete growth inhibition takes place at FNA concentration around $27 \mu\text{g HNO}_2\text{-N/L}$. These concentrations are almost identical to the ones reported by Ganda et al. (2016). The authors present experimental results showing that GAOs growth was inhibited by 50% at an FNA concentration of $10 \mu\text{g HNO}_2\text{-N/L}$, while microorganisms' activity ceased at an FNA concentration of $25 \mu\text{g HNO}_2\text{-N/L}$. The authors (Ganda et al., 2016) further report that the acetate uptake rate by GAOs was decreased by 50% at an FNA concentration of $7.5 \mu\text{g HNO}_2\text{-N/L}$ while the maximum inhibition measured was 70% for an FNA value as high as $80 \mu\text{g HNO}_2\text{-N/L}$. It should be mentioned that the aforementioned study was performed for various pH values between 6.5-8 but the FNA concentrations of the experiments at the pH of 8 were very low ($<1.8 \mu\text{g HNO}_2\text{-N/L}$). Furthermore, the study was conducted without having performed control tests at every pH value examined. Lower values than the ones of the present study have been reported by Ye et al. (2010) who presented half and complete inhibition at FNA concentrations of $1.5 \mu\text{g HNO}_2\text{-N/L}$ and $7.1 \mu\text{g HNO}_2\text{-N/L}$ respectively. According to the authors at the highest FNA content glycogen production decreased by 40%, while PHA consumption was inhibited by 50%. Again, the experiments were performed at pH values between 6.5 and 8 but the experiments targeted to the pH of 8 were conducted with rather low FNA content. In any case according to the results, an FNA concentration of $1.88 \mu\text{g HNO}_2\text{-N/L}$ at the pH of 8 caused an inhibition around 60%, very close to the value of the present study for an FNA content of $3 \mu\text{g HNO}_2\text{-N/L}$. It should be emphasized though, that the experimental protocol followed by the authors of the previous studies was completely different from the one of the present study. We assess the effect of FNA on GAOs activity by direct measurement of the maximum specific growth rate, while in the other studies this was implicitly accounted by monitoring the ammonium nitrogen utilization rate of biomass.

Figure 5.67 also highlights GAO's increased resilience to FNA compared to PAOs at least for the pH of 7; for instance, for the pH of 7, the concentration of $4 \mu\text{g HNO}_2\text{-N/L}$ was found to inhibit GAOs by just above 10% and PAOs by approximately 75%. As such, the presence of FNA may strongly influence the PAO-GAO competition in the favour of GAOs. This might not be valid when pH rises to values around 8 where both PAOs and GAOs seem to be comparably affected by FNA. Therefore, it is anticipated that controlling the pH in an EBPR system treating wastewater with low C/N content might be a promising strategy towards the competition of PAOs and GAOs.

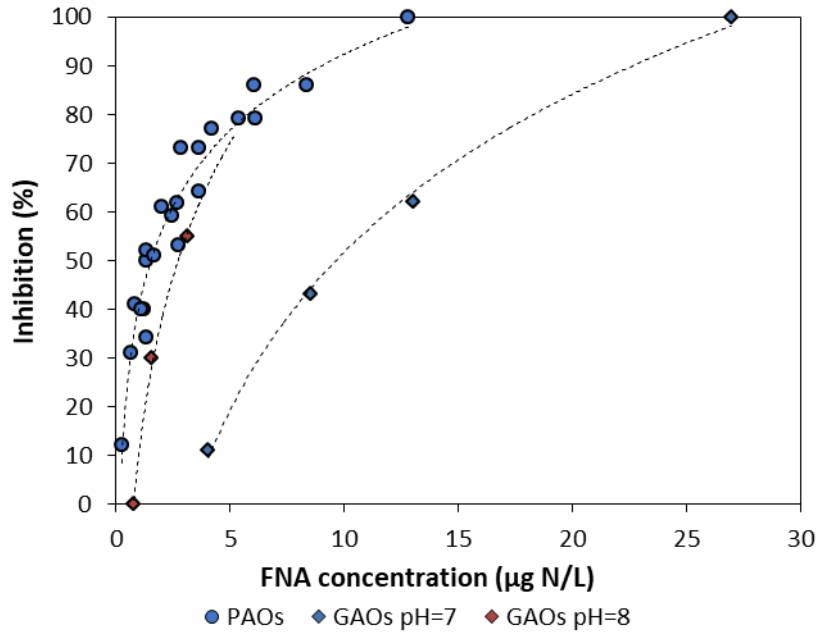


Figure 5.67. Comparison of the effect of FNA on the aerobic PUR of PAOs and the growth of GAOs.

5.5.3 Mathematical modelling of the inhibitory effect of FNA on GAO activity

The exact inhibitive effect of FNA on GAOs activities has not been well understood yet. Few studies report rather controversial hypotheses on FNA effect on GAOs. Some reports refer to the decrease of the VFAs uptake rate during the anaerobic processes (Ye et al., 2013), while others report on its negative impact on both anabolic and catabolic processes (i.e. PHA degradation, glycogen production, bacterial growth) (Ye et al., 2010; Ganda et al., 2016). However, the exact inhibitive mechanisms have not been studied yet nor the type of inhibition.

Most studies as of today have proposed the non-competitive inhibition function to best describe FNA effect on several groups of microorganisms. Based on the results of the present study, it was evidenced that PAOs aerobic activity both in aerobic and anoxic conditions was affected by FNA according to a non-competitive inhibition model. Accordingly, several studies report the non-competitive mode of inhibition as the optimum function to describe the FNA effect on AOBs and anammox bacteria (Wett and Rauch, 2003; Van Hulle et al., 2007; Jones et al., 2007; Park and Bae 2009; Jimenez et al., 2012; Pujol et al., 2014).

Equation (5.1) has been widely proposed to simulate non-competitive inhibition kinetics inhibition as already be analyzed.

$$\mu = \mu_{max} \frac{K_{iFNA}}{S_{FNA} + K_{iFNA}} \quad (5.1)$$

where K_{iFNA} is the inhibition constant corresponding to the FNA concentration that inhibits GAOs growth rate by 50%, S_{FNA} is the FNA concentration in the tank, μ is the relative growth rate and μ_{max} is the non-inhibited maximum growth rate of GAOs (practically refers to the growth rate measured at the control system).

The value of K_{iFNA} was calculated by performing best fit analysis to the experimental data in order to obtain the least sum of square errors (SSE). However, both in the case of pH of 7 and 8 no single K_{iFNA} value to establish a satisfactory correlation between experimental and simulated data could be obtained. This was due to the pH-related FNA inhibition of the maximum specific growth rate of GAOs which is clearly illustrated in Figure 5.67. Therefore, separate K_{iFNA} values rather than a common one were calculated for each pH. Based on these results, the K_{iFNA} is equal to 9.2 $\mu\text{g HNO}_2\text{-N/L}$ for the pH of 7, while this value drops to 3 $\mu\text{g HNO}_2\text{-N/L}$ for the pH of 8 due to the significant lower GAOs resilience at the increase pH conditions.

The ability of equation 5.1 to provide a satisfactory simulation of FNA inhibition on GAOs activity was tested against the Andrew's inhibition model (Andrews, 1968, equation 5.4), the Hill-type model (Prinz, 2010, equation 5.11) and the model proposed by Zhou et al. (2007) to describe FNA effect on anoxic PUR (equation 5.5):

$$\mu = \mu_{max} \frac{S_{FNA}}{K_S + S_{FNA} + \frac{S_{FNA}^2}{K_{iFNA}}} \quad (5.4)$$

$$\mu = \mu_{max} \frac{K_{iFNA}^n}{S_{FNA}^n + K_{iFNA}^n} \quad (5.11)$$

$$\mu = \mu_{max} \frac{S_{FNA}}{K_S + S_{FNA}} e^{\alpha S_{FNA}} \quad (5.5)$$

where S_{FNA}^* is the critical FNA concentration in the mixed liquor at which growth is completely inhibited, K_s is the affinity coefficient constant, α is a constant and n is the Hill coefficient representing the number of bound ligands.

The aforementioned methodology was applied separately for the experiments conducted at a pH of 7 and 8. The Nash-Sutcliffe efficiency coefficient (NSE) and the percent bias (PBIAS) were used as statistic indices to evaluate models' performances as proposed by Moriasi et al. (2007). Performance criteria used to accept each model's predictivity were $NSE > 0.8$ and PBIAS within $\pm 20\%$.

By adopting an FNA inhibition constant of 9.2 $\mu\text{g HNO}_2\text{-N/L}$ and 3 $\mu\text{g HNO}_2\text{-N/L}$ for the pH of 7 and 8 respectively (calculated for the simple non-competitive inhibition model) (eq. 5.1), the optimum fitting of the dose-response Hill-type model (equation 5.11) was achieved for a Hill coefficient value of 2.45 and 2 for the pH of 7 and 8 respectively, thus indicating positively cooperative binding at both cases. Both Andrews's and Zhou's models (equations 5.4, 5.5) were applied by using a K_s value of 0.031 $\mu\text{g/L}$ as proposed by Zhou et al. (2007), while in Andrews's model, best fit analysis resulted in K_{iFNA} values identical to the ones calculated for the simple non-competitive inhibition model. The statistics of the four inhibition models examined for each pH are presented in Table 5.11.

Table 5.11. Statistic indices for the FNA inhibition models examined

Statistical Index	Simple non-competitive	Andrews (1968)	Hill-type (Printz, 2010)	Zhou et al., (2007)
SSE (pH=7)	1066	1081	118	440
NSE (pH=7)	0.74	0.74	0.97	0.89
PBIAS (pH=7)	1.90%	1.65%	-2.21%	0.32%
SSE (pH=8)	465	577	118	378
NSE (pH=8)	0.69	0.62	0.92	0.75
PBIAS (pH=8)	-25.18%	-29.26%	5.37%	-13.95%

Based on the results it is evidenced that the simple non-competitive model cannot provide for a satisfactory simulation of FNA inhibition on GAOs activity. On the contrary, the dose-response Hill-type model, described by equation 5.11, presents sufficient statistics and is able to simulate the inhibition process very effectively for both pH values examined.

The variation of the Hill coefficient with pH (in the range between 7 and 8) can be approximated by the following exponential function:

$$n = 10.142 \cdot e^{-0.203 \cdot pH} \quad (5.40)$$

By incorporating equation (5.40) into the conventional dose-response model of equation (5.11), the following expression was resulted:

$$\mu = \mu_{max} \frac{K_{iFNA}^{10.142 \cdot e^{-0.203 \cdot pH}}}{S_{FNA}^{10.142 \cdot e^{-0.203 \cdot pH}} + K_{iFNA}^{10.142 \cdot e^{-0.203 \cdot pH}}} \quad (5.41)$$

Figure 5.68 illustrates the comparison between the experimental data and the simulation results by adopting equation (5.41) for all experiments (pH=7 and 8).

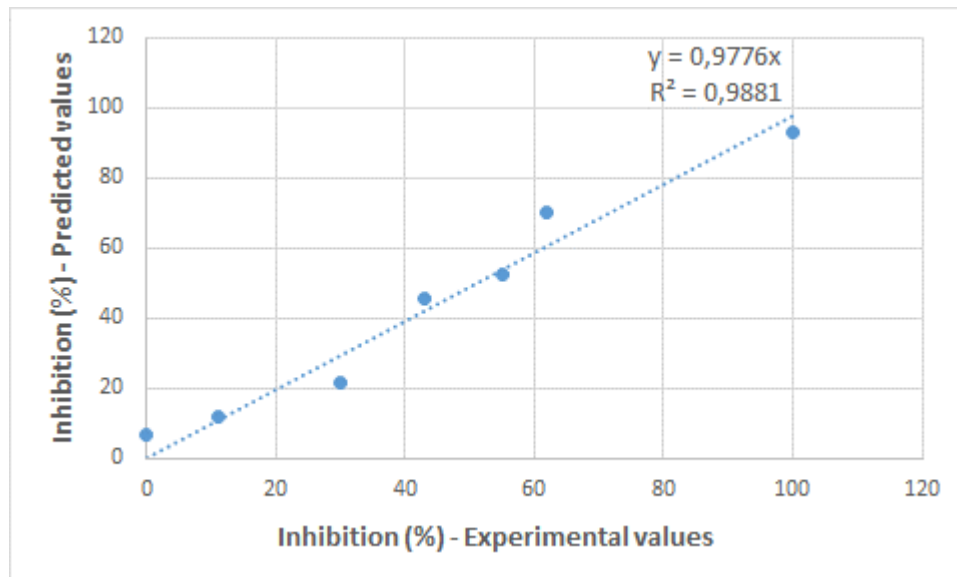


Figure 5.68. Comparison of experimental and simulated values for FNA inhibition in GAOs growth

As evidenced in Figure 5.68 equation 5.41 can be effectively adopted to simulate the FNA effect on GAO growth kinetics.

5.5.4 Experimental assessment of the effect of FA on GAO activity

Following the series of experiments investigating the effect of FNA on the aerobic growth of GAOs, an additional experimental series was carried out in order to examine the possible inhibitory effect of FA on GAOs. In this experiment, approximately 600 mL of sludge was retrieved from the SBR and divided equally into 4 containers, each with a working volume of 1 L. Similarly to the experiments regarding the effect of FNA, acetate, ammonium and phosphorus were added and the sludge was diluted up to a volume of 1 L in order to obtain the initial concentrations presented in Table 5.10. The pH for two of the reactors was set to 7, while the pH of the other reactors was set to 8 and kept stable throughout the duration of the experiment. The temperature of all reactors was kept stable at 25 ± 1 throughout the experiment. As the initial ammonium concentration in each reactor was 300 mg N/L the initial concentrations of FA could be calculated as 1.63 mg N/L for the reactors at the pH of 7 and 16.13 mg N/L for the reactors at the pH of 8. The reactors were aerated over a period of 26 hours under and the VSS of each reactor were analyzed on an hourly basis.

The net growth rates of GAOs in each reactor were established according to the methodology described in section 5.5.2 and compared in Figure 5.69. The net growth rates averaged at $1.13 \pm 0.02 \text{ d}^{-1}$ at the pH of 7 and at $1.10 \pm 0.06 \text{ d}^{-1}$ at the pH of 8. This would indicate that FA has a negligible effect on the growth of GAOs as growth under the concentration of 16.13 mg $\text{NH}_3\text{-N/L}$ was practically the same as it was under almost a tenth of this concentration. To put things into perspective, FA concentrations of this magnitude have been found to inhibit PAOs by more than 50%. As such, in addition to FNA, the presence of FA may strongly influence the PAO-GAO competition in the favour of GAOs. This finding is also supported by the experimental

results of Zheng et al. (2013) who report that FA concentrations to the order of 18 mgN/L can significantly influence the microbial consortium of an EBPR system in favour to GAOs.

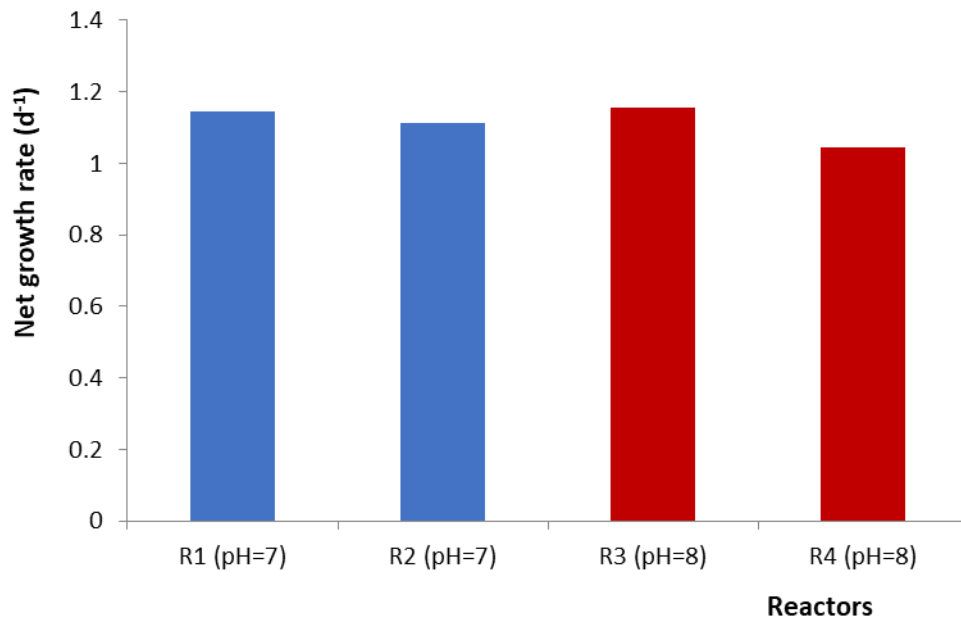


Figure 5.69. Comparison of the net growth rates of GAOs under the FA concentration of 1.7 mg NH₃-N (pH=7) and under the FA concentration of 16.1 mg NH₃-N (pH=8)

5.5.5 Investigating the effect of FA on the anaerobic activity of GAOs

Parallel to the series of experiments investigating the effects of nitrite and ammonium on the growth of GAOs, a number of additional experiments were conducted focusing on the effect of FA on the anaerobic processes of GAOs, specifically the COD uptake rate.

Initially two series of batch experiments were conducted. The first investigated the effect of 140 mg NH₄-N/L at the pH of 8.5 (20.84 mg NH₃-N/L), while the second assessed the effect of the ammonium concentration of 270 mg N/L at the pH of 8.5 (39.62 mg NH₃-N/L) on the anaerobic uptake rate. In each series, sludge was retrieved from the SBR and divided equally into 3 containers, each with a working volume of 0.5 L. The pH of each reactor was set to 8.5 ± 0.05 and kept constant for the duration of the experiment. Each reactor was fed with readily biodegradable organic carbon, in the form of a sodium acetate solution, in order to obtain an initial COD concentration of 100 mg/L. One of the bioreactors served as a control, while the other two reactors were fed with an equal amount of ammonium, in the form of an ammonium chloride solution to obtain the desired ammonium concentration that was to be investigated. The reactors were maintained under anaerobic conditions for a period of 1 hour in which the uptake of COD was studied.

The FA concentration of 20.84 mg N/L was found to have practically no effect on the anaerobic uptake of COD with the control performing at a rate of 51.53 mg COD/g VSS h, while the reactors under the presence of FA performed at 51.74 and 50.06 mg COD/g VSS h. The FA concentration of 39.62 mg N/L on the other hand was found to inhibit the anaerobic uptake of COD by approximately 53%. The control performed at a rate of 33.25 mg COD/g VSS h, while the reactors under the presence of FA performed at 15.79 and 15.55 mg COD/g VSS h.

An additional experiment series was conducted, investigating the effect of the ammonium concentrations of 100, 200 and 300 mg N/L at the pH of 8.5 on the COD uptake rate of GAOs. The corresponding FA concentrations were 15.55, 30 and 46.12 mg NH₃-N/L. In this experiment however, following the setting of pH and the addition of ammonium chloride, the reactors were kept stirring under anaerobic conditions for a time period of 1.5 h prior to the addition of sodium acetate. The targeted initial COD concentration for this experiment was 200 mg/L. The reactors were then maintained under anaerobic conditions for a period of 1.5 hour in which the uptake of COD was studied. The experiment was replicated to ensure repeatability.

The results of this experiment are presented in Figure 5.70. As shown, with the exception of the reactor containing the highest FA concentration, all other reactors performed similarly throughout the experiment. While there is an apparent lag in the uptake of COD during the first 30 minutes of the experiment for all reactors, this lag period appears to be slightly extended in the case of the reactor containing 300 mg NH₄-N/L. Ultimately however, by the completion of the experiment, in all reactors practically the same amount of acetate was removed. The COD uptake rates over the 1.5 h anaerobic period are presented in Table 5.12. It would appear that under these conditions, ammonium has a negligible effect on the anaerobic uptake of COD by GAOs. However, as it was noticed in the first batch experiments, an ammonium shock load may have a brief negative effect on the anaerobic processes of GAOs which require some time to recover. The recovery time may be extended for greater FA concentrations as shown in Figure 5.70. It is worth noting that PAOs appear to be affected by FA shock-loads to a greater extent than GAOs, as demonstrated in section 5.3.3.

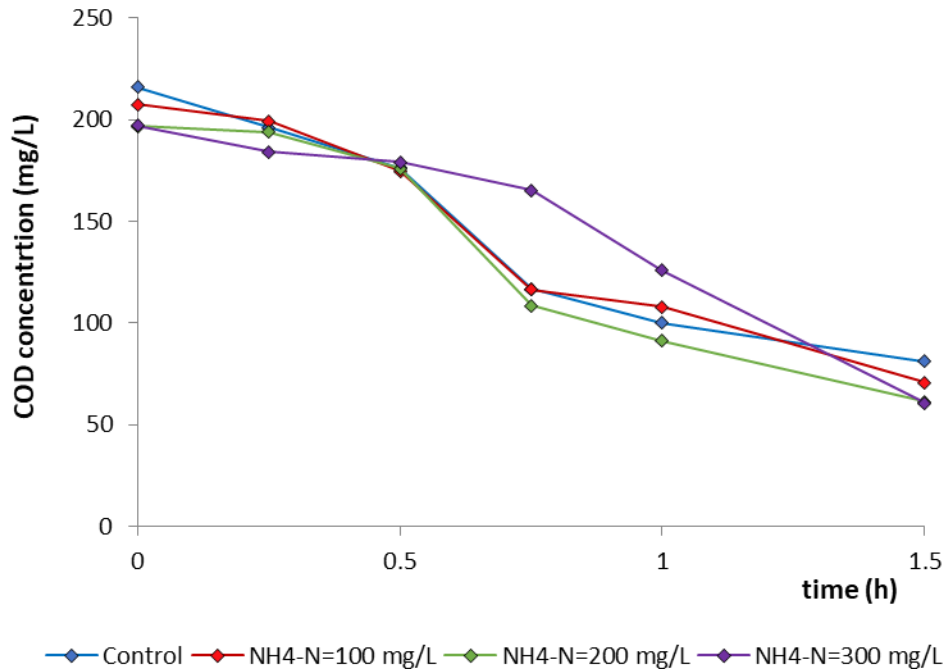


Figure 5.70. The effect of ammonium on the COD uptake of GAOs

Table 5.12. COD uptake rates of all reactors

Reactor:	Control (NH ₄ -N=5 mg/L)	NH ₄ -N=100 mg/L	NH ₄ -N=200 mg/L	NH ₄ -N=300 mg/L
COD uptake rate (mg COD/g VSS h):	90	91.1	90.2	90.8

5.6 Evaluating alternative operational strategies for promoting EBPR

5.6.1 Investigating the role of the carbon source in the PAO-GAO competition

It is understood that the viability of EBPR in high nitrogen loading systems depends not only on the tolerance of PAOs to FNA and FA but also on the resilience of the competitive GAO community to these inhibitors. As mentioned, GAOs can take up VFAs under anaerobic conditions and store them intracellularly as PHAs similarly to PAOs. Unlike PAOs, however, they do not possess polyphosphate chains and the energy required for the reception and storage of VFAs is provided via the hydrolysis of intracellular glycogen followed by glycolysis of the produced glucose. The most prominent GAOs are the Gammaproteobacterial *Candidatus Competibacter* and the Alphaproteobacterial *Defluviicoccus vanus* (Oehmen et al., 2007; Oehmen et al., 2010; Shen and Zhou, 2016). A key difference between these two groups is their preference in carbon. *Competibacter* have a high affinity for acetate, while being practically incapable of utilizing propionate. On the opposite, *Defluviicoccus vanus* have a higher affinity for propionate but are reportedly capable of taking up acetate at a similar rate to *Competibacter*.

Table 5.13 presents a comparison of the anaerobic acetate and propionate uptake rates reported in the literature for various PAO and GAO species. As shown, PAOs appear capable of taking up both VFAs at practically the same rate. *Competibacter* appear to have an affinity for acetate that is similar to that of PAOs but a severely limited affinity for propionate. Although the preference for propionate of *Defluviicoccus vanus* and Alphaproteobacterial GAOs in general is clear, the extent of their capacity to take up acetate is questionable. While the acetate uptake rate of *Defluviicoccus vanus* is reportedly identical to that of *Competibacter*, in systems that utilize an anaerobic/aerobic configuration with acetate as the sole carbon source the main GAO species that prevails appears to be *Competibacter* and the *Defluviicoccus*-related organisms are either not detected or present only in low abundance (<1%) (Oehmen et al., 2005). As such, the type of substrate strongly influences the competition between the different PAO and GAO populations.

As the type of carbon source plays a key role in controlling population dynamics for the effective implementation of EBPR, many studies have investigated its influence on the PAO-GAO competition and proposed various strategies. The types and effectiveness of these strategies vary in the literature and often contradict each other. In addition, while the use of acetate, propionate or a mixture of both and their influence on the EBPR-related microbial communities has been discussed extensively, their effectiveness in promoting EBPR under conditions where PAOs and GAOs are inhibited to a different extent (by FA and/or FNA) has not been thoroughly

investigated. For instance, an effective strategy based on the utilization of acetate may prove to be most ineffective under these conditions due to the strong tolerance of *Competibacter* to FNA.

Table 5.13. Comparison of anaerobic acetate and propionate uptake rates by PAOs and GAOs

Carbon source	Organisms (Reference)	r_s (C-mol/C-mol · h)
Acetate	PAOs (<i>Accumulibacter</i>) (Filipe et al., 2001)	0.19
	GAOs (Filipe et al., 2001)	0.24
	<i>Competibacter</i> (Zeng et al., 2003)	0.17
	<i>Defluviicoccus Vanus</i> (Dai et al., 2007)	0.17
	Alphaproteobacterial GAOs (Oehmen et al., 2005)	0.08
Propionate	PAOs (<i>Accumulibacter</i>) (Oehmen et al., 2005)	0.18
	<i>Competibacter</i> (Oehmen et al., 2004)	0.01
	<i>Defluviicoccus Vanus</i> (Dai et al., 2007)	0.25
	Alphaproteobacterial GAOs (Oehmen et al., 2006)	0.18

In order to further investigate the role of the carbon source in the implementation of EBPR in nitrification/denitrification systems, an SBR was set-up and operated over 3 different periods for the following combinations of feed:

- Acetate as the sole carbon source
- Mixture of acetate and propionate (50%-50%)
- Regular rotation of acetate and propionate as the sole carbon source

With the exception of the type of organic substrate, the SBRs' configuration was the same for each investigation and is detailed in the following subsection.

5.6.1.1 Performance of the experimental system

The SBR operated on 3 daily cycles each consisting of a 1.5 h anaerobic phase, a 3.5 h aerobic phase and a 2.5 h anoxic phase. Settling and decanting occurred once per day over a 1.5 h period due to technical limitations mentioned in the materials and methods section. Feed consisted of a concentrated mixture of VFAs, ammonium and phosphorus that was introduced at the beginning of each anaerobic and each anoxic phase. The volume of each dose was 200 mL. Prior to decanting, the SBR contained 10.6 L of liquor. Following the removal of 5.6 L of effluent, 5.2 L of water was added to the SBR bringing the mixed liquor's volume to 10.2 L. Under mixing conditions, 0.8 L of mixed liquor was removed in order to achieve an SRT of 8 d. Thus, with the daily addition of 1.2 L of the concentrated feed, the SBR's working volume averaged at 10 L simulating an HRT of 2 d.

The addition of a carbon source at the beginning of the anaerobic phase would provide PAOs with an advantage over common heterotrophic organisms, giving them priority in the utilization of COD. During the aerobic phase, the sufficient DO concentrations (>3 mg/L) would allow PAOs to develop by oxidizing their stored PHAs, while residual acetate would be rapidly removed by other heterotrophs. Following the cease of aeration, feed was reintroduced to the SBR in order to allow the rapid removal of nitrate and nitrite that was produced during the aerobic phase via denitrification prior to the next anaerobic phase.

The daily dose of COD was gradually increased from 5 g/d to 8.5 g/d over a period of approximately 20 days. The dose of 8.5 g COD/d was regulated in order to achieve a biomass concentration of around 2,500 mg VSS/L. The daily dose of ammonium was gradually increased from 0.6 to 1.8 g $\text{NH}_4\text{-N}$ /d over a period of approximately 20 days, similarly to the dose of COD. The dose was regulated in order to allow the gradual increase of nitrite concentrations in the SBR. This would be achieved by the partial suppression of NOB due to the relatively low aerobic retention time (3.5 d). Ammonium concentrations in the effluent were monitored on a daily basis and the daily dosage was modified in order to maintain effluent concentrations lower than 30 $\text{NH}_4\text{-N}$ mg/L to prevent accumulation of ammonium in the SBR. The daily dose of phosphorus was 200 mg $\text{PO}_4\text{-P}$ /d, a dose much greater than the stoichiometric demand for growth of common heterotrophs in order to selectively promote the growth of PAOs. This dosage would also compensate for the phosphorus that is removed via chemical precipitation, allowing the availability of an adequate phosphorus source to be taken up by PAOs throughout the aerobic phase.

5.6.1.2 Acetate as the sole carbon source

The SBR was successful in developing PAOs that displayed notable activity as early as 10 days from the commencement of operation. MLVSS averaged at $2,500 \pm 300$ mg/L, while MLSS averaged at $2,800 \pm 300$ mg/L. The biomass concentration that was maintained in the SBR is a direct result of the chosen COD loading rate and SRT. The high MLVSS to MLSS ratio of approximately 90% is due to the use of synthetic wastewater that contained little to no solids. The pH ranged from 7 to 8.2, while temperature was controlled at $20 \pm 2^\circ\text{C}$. Following decanting and re-filling of the SBR, pH would drop to 7.5 and would remain unchanged during the following anaerobic period.

In order to properly evaluate the biomass' capacity to remove phosphorus without the interference of precipitation phenomena, regular ex-situ experiments were conducted on sludge retrieved from the SBR under controlled pH. Following feed, 500 mL of sludge was extracted and placed into a container of similar working volume and left stirring under anaerobic conditions for a period of 1 hour. Upon completion of this, the reactor was aerated for a period of up to 3 hours over which samples were retrieved every 30 minutes. Throughout the experiment pH was controlled at its initial value.

Figure 5.71 displays the performance of the biomass in terms of PUR throughout the duration of operation. As shown, the biomass displayed increasing capacity for phosphorus removal during the first 2 weeks of operation, reaching a PUR of 12.7 mg P/g VSS h by day 14. Following this period however, the performance of the biomass gradually declined and by day 32 no phosphorus removal was observed. The anaerobic P release rate along with the COD uptake rate

were also analysed throughout operation and are presented in Figure 5.72. While the P release rate seems to follow the variation of the aerobic PUR as would be expected, the COD uptake rate remained at a high value (~ 40 mg COD/g VSS h) following the decline of PUR and P-release. This is most likely indicative of the proliferation of GAOs in the biomass. It is therefore plausible that the deterioration of EBPR observed here was due to the prevalence of GAOs and the wash-out of PAOs from the system.

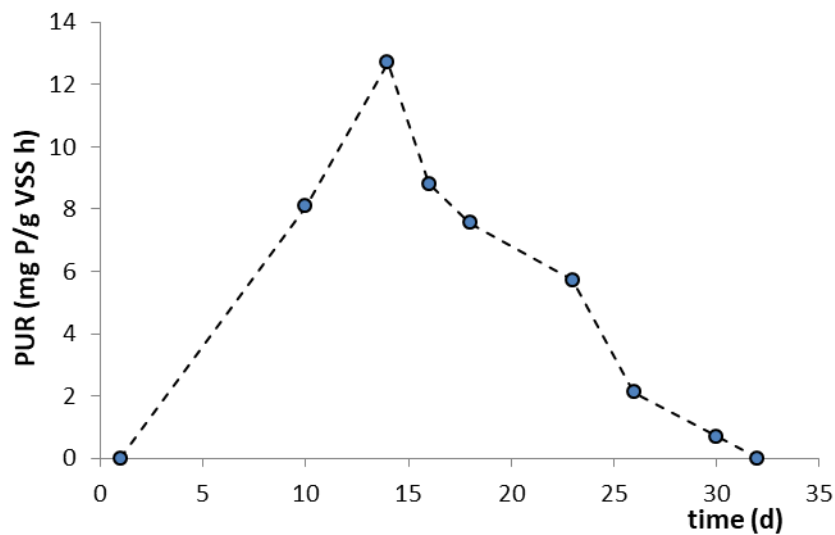


Figure 5.71. Variation of aerobic PUR throughout operation

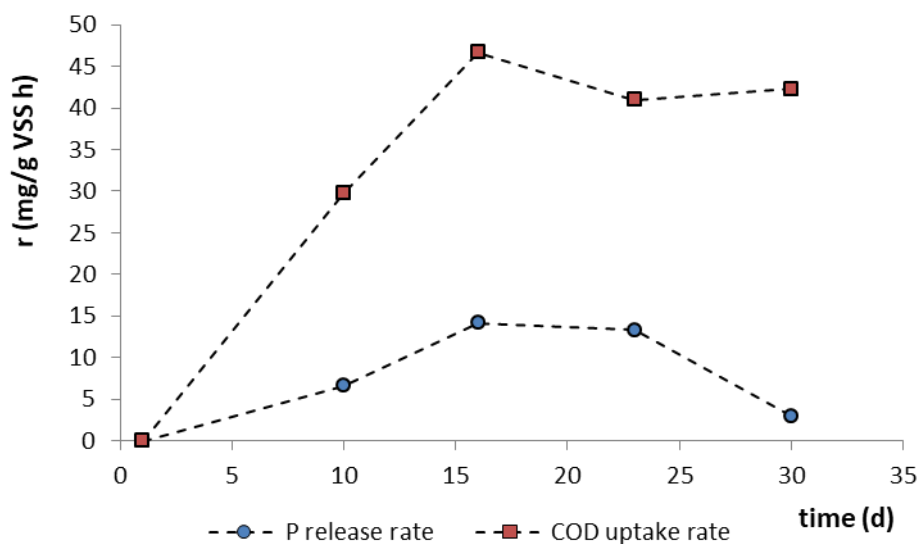


Figure 5.72. Variation of the anaerobic phosphorus release rate and COD uptake rate throughout operation

The SBR was also successful in partially shunting NOB activity. Over time as the nitrogen loading increased, so did the $\text{NO}_2\text{-N}/\text{NO}_3\text{-N}$ ratio in the SBR during aeration. Figure 5.73 displays the variation of NO_2 and total NO_x concentration in the SBR at the end of the aerobic phase throughout operation. As shown, by day 18 nitrite concentrations throughout operation

had stabilized at around 11 ± 1 mg N/L by the end of aeration. Figure 5.74 presents the variation of nitrite and total NO_x throughout the first daily cycle of day 18. The nitrite and nitrate produced during aeration were rapidly removed in the subsequent anoxic phase, ensuring strict anaerobic conditions for the start of the next cycle.

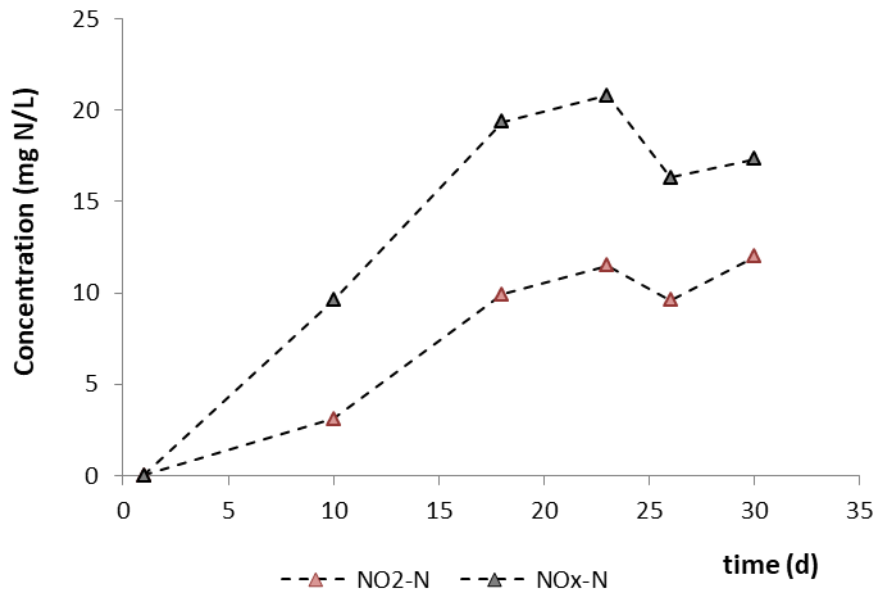


Figure 5.73. NO₂ and total No_x concentrations at the end of the aerobic phase over time.

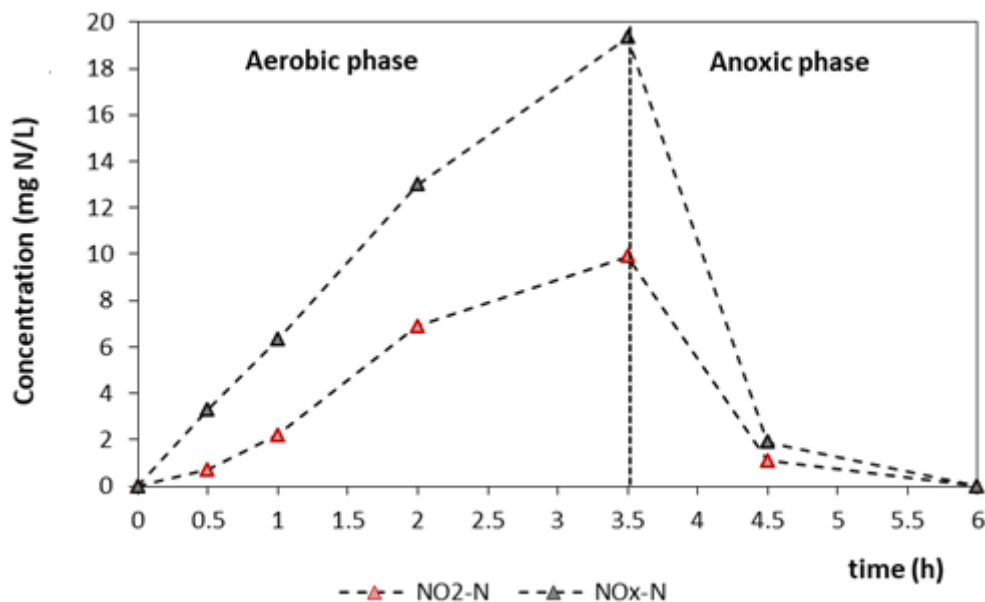


Figure 5.74. Variation of NO₂ and total NO_x concentrations during the aerobic and anoxic phase of the first daily cycle (day 18).

In accordance to Figure 5.74, the concentration of FNA throughout the aerobic phase was calculated with regard to the concentration of nitrite, temperature and pH. The variation of pH and FNA are presented in Figure 5.75. During the first 30 minutes of aeration there is an

increase in pH that may be attributed to carbon stripping due to the intensity of aeration. As more DO becomes available nitrification intensifies, leading to a drop in pH. Following this, pH rises again due to carbon stripping and is mostly stable for the remainder of the aerobic phase. Throughout most of the aerobic phase, the concentration of FNA is greater than $0.2 \mu\text{g HNO}_2\text{-N/L}$ with an observed maximum of $0.5 \mu\text{g HNO}_2\text{-N/L}$, a concentration that has been found to inhibit aerobic PUR by approximately 25%. Therefore, it is likely that the FNA content of the SBR during the aerobic steps may have contributed to the deterioration of EBPR. The fact that the highest observed FNA concentration appears relatively early during aeration mostly due to the lowering of pH, would support this as the performance of PAOs would possibly be affected for most of the aerobic phase. In addition, as demonstrated in section 5.5, acetotrophic GAOs (specifically *Competibacter*) appear to have a significantly stronger tolerance to FNA at low pH than PAOs. It is therefore likely that FNA influenced the PAO-GAO competition in the favour of GAOs.

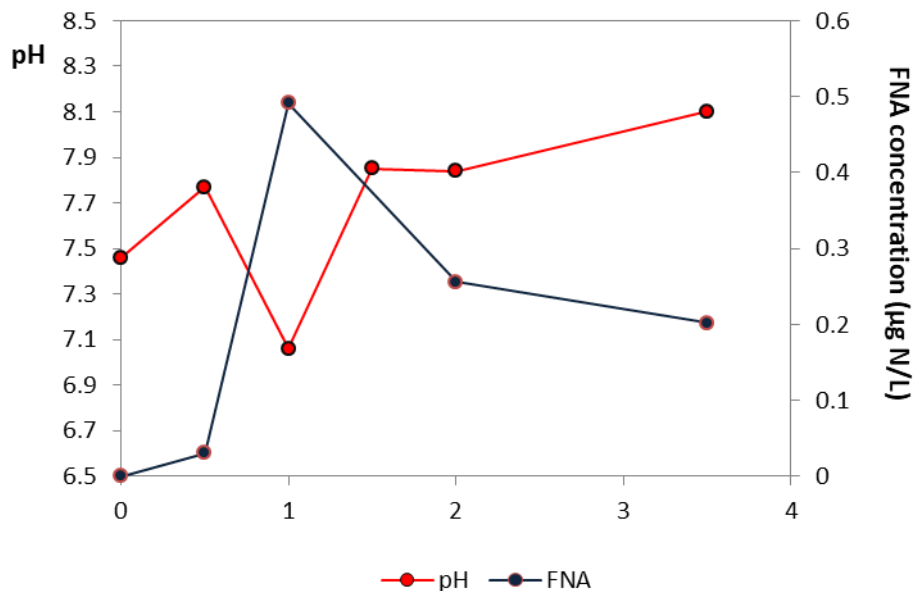


Figure 5.75. Variation of pH and the concentration of FNA during the aerobic phase of the first daily cycle (day 18).

Based on the performance of the SBR, it may be concluded that the use of acetate as a sole carbon source in systems where FNA concentrations as low as $0.5 \mu\text{g HNO}_2\text{-N/L}$ are produced, is not a viable strategy for the implementation of EBPR as it promotes the proliferation of GAOs. The extent of FNAs' influence on the PAO-GAO competition for acetate is further investigated in section 5.6.2.

5.6.1.3 Mixture of acetate and propionate (50%-50% Hac-HPr)

As *Competibacter* appear to be a strong competitor of PAOs in the uptake of acetate, several studies have suggested that propionate may be a more suitable substrate than acetate for enhancing phosphorus removal in EBPR systems. Oehmen et al. (2006) also suggested that propionate can provide PAOs with a competitive advantage even when the propionate fraction of the influent is relatively low and reported the achievement of good EBPR with the use of a combined feed of acetate and propionate (75-25% Hac-HPr). In order to examine the

effectiveness of this strategy in conditions where FNA is present, after the completion of the former investigation on the use of acetate, the SBR was reset and provided with a fresh seed-sludge. The carbon source of the feed in this investigation was a mixture of acetate and propionate at a COD ratio of 1:1.

The SBR was successful in developing PAOs that displayed notable activity as early as 8 days from the commencement of operation. Similarly to the previous investigation, MLVSS averaged at $2,500 \pm 300$ mg/L, while MLSS averaged at $2,800 \pm 300$ mg/L. The pH ranged from 7.3 to 8.2 and temperature was controlled at $20 \pm 2^\circ\text{C}$. Following decanting and re-filling of the SBR, pH dropped to 7.5 ± 1 and remain unchanged during the following anaerobic period.

In order to properly evaluate the biomass' capacity to remove phosphorus without the interference of precipitation phenomena, regular ex-situ experiments were conducted on sludge retrieved from the SBR under controlled pH. Following feed, 500 mL of sludge was extracted and placed into a container of similar working volume and left stirring under anaerobic conditions for a period of 1 hour. Following this, the reactor was aerated for a period of up to 3 hours over which samples were retrieved every 30 minutes. Throughout the experiment pH was controlled at its initial value.

Figure 5.76 displays the performance of the biomass in terms of PUR throughout the duration of operation. The performance was very similar to the one observed when only acetate was used. As shown, the biomass displayed increasing capacity for phosphorus removal during the first 2 weeks of operation, reaching a PUR of 11.5 mg P/g VSS h by day 13. Following this period however, the performance of the biomass gradually declined and by day 39 no phosphorus removal was observed. While the fraction of propionate in the feed slightly extended the performance of EBPR compared to the previous strategy, there was no significant benefit.

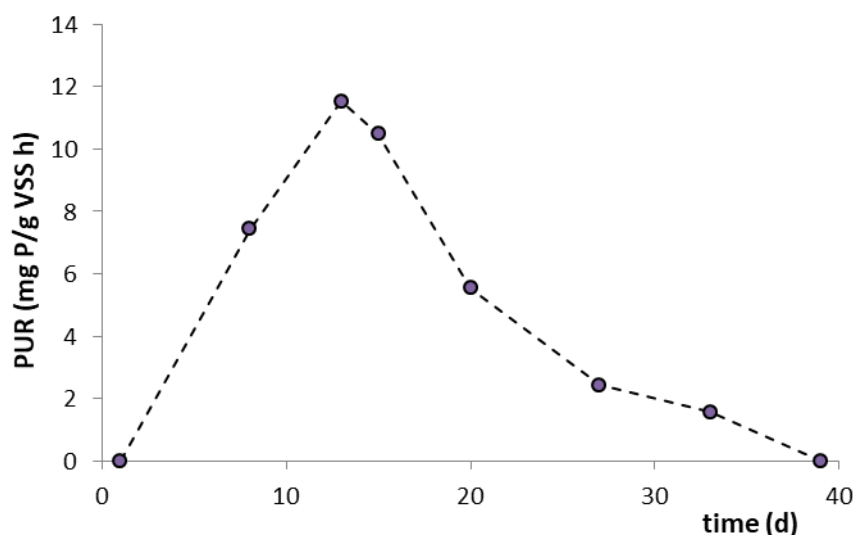


Figure 5.76. Variation of aerobic PUR throughout operation

The SBR configuration was once again successful in partially shunting NOB activity. Figure 5.77 displays the variation of NO_2 and total NO_x concentration in the SBR at the end of the aerobic

phase throughout operation. Figure 5.78 presents the variation of nitrite and total NO_x throughout the first daily cycle of day 20, after which nitrite concentrations in the SBR were consistent over time. The nitrite and nitrate produced during aeration were rapidly removed in the subsequent anoxic phase, ensuring strict anaerobic conditions for the start of the next cycle.

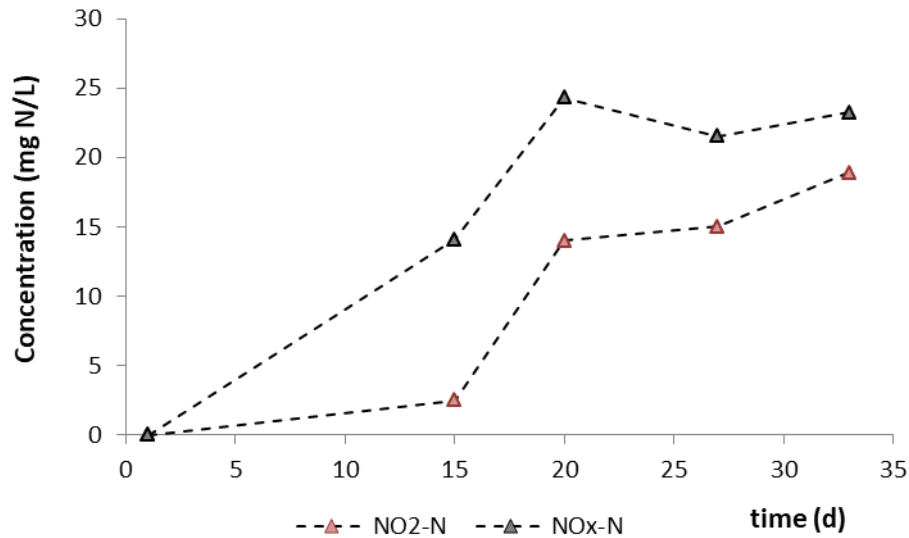


Figure 5.77. NO₂ and total NO_x concentrations at the end of the aerobic phase over time.

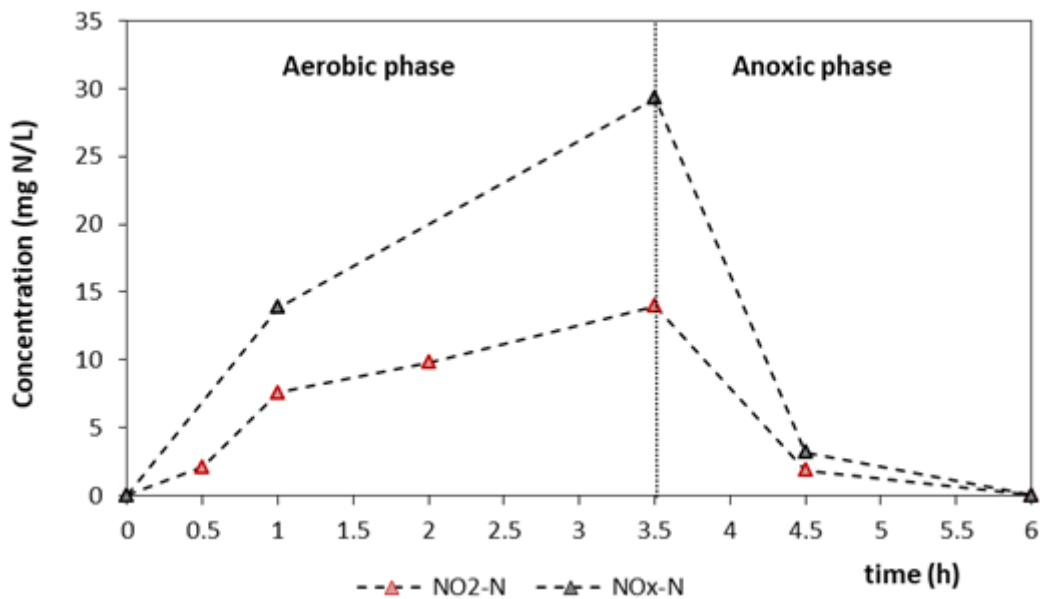


Figure 5.78. Variation of NO₂ and total NO_x concentrations during the aerobic and anoxic phase of the first daily cycle (day 20).

The respective concentrations of FNA throughout the aerobic phase were calculated with regard to the concentration of nitrite, temperature and pH and are presented in Figure 5.79 along with the variation of pH. While there is an initial increase in pH due to carbon stripping, it is followed by a drop in pH due to nitrification. Throughout most of the aerobic phase, the concentration of FNA is greater than 0.2 $\mu\text{g HNO}_2\text{-N/L}$ with an observed maximum at 0.5 $\mu\text{g HNO}_2\text{-N/L}$, after 2 hours of aeration. As such, the variation of FNA during the aerobic phase is comparable to

that observed in the previous investigation on acetate as the sole carbon source. It is therefore possible that FNA may have inhibited the growth of PAOs while having little effect on both *Competibacter* and the alphaproteobacterial GAO species present, leading to the wash-out of PAOs from the system.

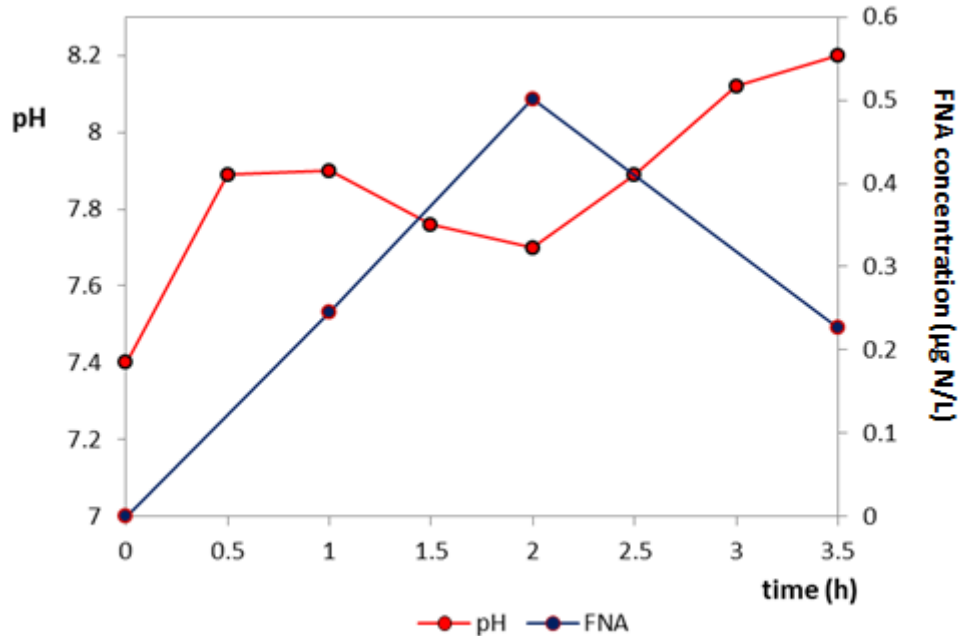


Figure 5.79. Variation of pH and the concentration of FNA during the aerobic phase of the first daily cycle (day 20).

Based on the performance of the SBR, it appears that the fraction of propionate in the feed did not improve EBPR as could be expected. This may be due to the suppression of PAOs by FNA. As *Competibacter* have demonstrated a high tolerance to FNA, it is possible that the alphaproteobacterial GAOs that have a high affinity for propionate are characterized by a similar resilience. Therefore, in systems where FNA concentrations as low as 0.5 µg HNO₂-N/L are produced, it is likely that the use of a mixture of acetate and propionate in the feed would result in the development of both GAO groups at the expense of PAOs. As such, it is likely not a viable strategy for the implementation of EBPR in these conditions.

5.6.1.4 Rotation of propionate and acetate as the sole carbon source

Following the completion of the former investigation on the use of a mixture of acetate and propionate in the feed, the SBR was reset and provided with a fresh seed-sludge. This time the strategy employed was based on the regular rotation between propionate and acetate as the sole type of carbon in the feed. As mentioned, PAOs are reportedly capable of taking up both acetate and propionate at similar rates. As such, a change in the type of VFA of the feed would likely have little effect on them. *Competibacter* on the other hand have a high affinity for acetate but are practically incapable of utilizing propionate. Therefore, if a significant *Competibacter* population were to be developed with the use of acetate, the change of the substrate to propionate would result in their suppression and ultimately their wash-out from the system. During this period, the

use of propionate would enhance the growth of the alphaproteobacterial GAOs that possess a high affinity for it. This may be combated with the switch back to acetate once the *Competibacter* population has diminished to provide the advantage back to PAOs. Therefore, the regular shift in the substrate type could possibly combat both GAO groups.

Due to the alphaproteobacterial GAOs having some affinity for acetate that is not entirely clear, the rotation of the substrate type was not regulated in regard to the SRT but was based on the observed performance of the SBR. When the biomass displayed a declining PUR that dropped below 2-3 mg P/g VSS h, the switch was made.

The SBR was successful in developing PAOs that displayed notable activity as early as 7 days from the commencement of operation. MLVSS averaged at $2,700 \pm 300$ mg/L, while MLSS averaged at $3,000 \pm 300$ mg/L. The pH ranged from 7.2 to 8.2 while temperature was controlled at $20 \pm 2^\circ\text{C}$. Following decanting and re-filling of the SBR, pH dropped to 7.5 ± 1 and remained unchanged during the following anaerobic period.

In order to properly evaluate the biomass' capacity to remove phosphorus without the interference of precipitation phenomena, regular ex-situ experiments were conducted on sludge retrieved from the SBR under controlled pH. Following feed, 500 mL of sludge was extracted and placed into a container of similar working volume and left stirring under anaerobic conditions for a period of 1 hour. Following this, the reactor was aerated for a period of up to 3 hours over which samples were retrieved every 30 minutes. Throughout the experiment pH was controlled at its initial value.

Figure 5.80 displays the performance of the biomass in terms of PUR throughout the duration of operation. The initial type of substrate in the feed was propionate as this could provide additional information regarding its use as the sole carbon source. As shown, phosphorus removal rose steadily during the first 24 days of operation, reaching a maximum PUR of 7.7 mg P/g VSS h on day. It would appear that PAOs develop at a slower rate with propionate than with acetate which would be in agreement with other studies (Oehmen et al., 2010). However, over the following days PUR declined, dropping to 2.8 mg P/g VSS h by day 35. This could be due to the development of alphaproteobacterial GAOs in the SBR. At this point the substrate was changed to acetate.

The change of the carbon type was successful in the renewal of phosphorus removal and within 8 days, a PUR of 9.4 mg P/g VSS h was recorded. This rise in PUR is a direct result of the increased growth of PAOs likely due to the fact that they can compete more effectively for acetate in the absence of *Competibacter*. However, PUR began to decline once again, likely due to the development of GAOs. On day 58, the biomass' PUR had dropped to 0.9 mg P/g VSS h and the change was made to propionate.

Within a week the PUR of the biomass had risen to 2.8 mg P/g VSS h indicating that the change of carbon was successful in renewing PAO activity due to the suppression of *Competibacter*. On day 69, PUR reached a peak of 3.9 mg P/g VSS h before declining again to 2.6 mg P/g VSS h over the following 4 days. By this point, propionate had been used as a substrate over the past 17 days (a period of just over $2 \times \text{SRT}$). It was therefore likely that the *Competibacter*. population had

diminished significantly during this time and considering the new decline in P-removal, the shift was made back to acetate.

Just two days after the change of substrate, a PUR of 8.6 mg P/g VSS h was recorded indicating that the change of substrate to acetate provided PAOs with a significant advantage over the alphaproteobacterial GAOs that had developed due to their higher affinity for the substrate. This also verified the decline of the *Competibacter* population due to the use of propionate. This good performance in P-removal however was short-lived as PUR declined over the following days, dropping to 0.81 mg P/g VSS h by day 92 (after 17 days of acetate use). At this point the carbon type was changed back to propionate.

The change of substrate resulted in a slight renewal of the biomass' capacity to remove phosphorus, reaching a PUR of 2.2 mg P/g VSS h by day 102. By day 110 however PUR had once more dropped below 1 mg P/g VSS h. In view of the above, it is anticipated that while the regular rotation of the substrate type prolonged the longevity of the PAO population in the SBR, each change of the carbon source had diminishing returns over time.

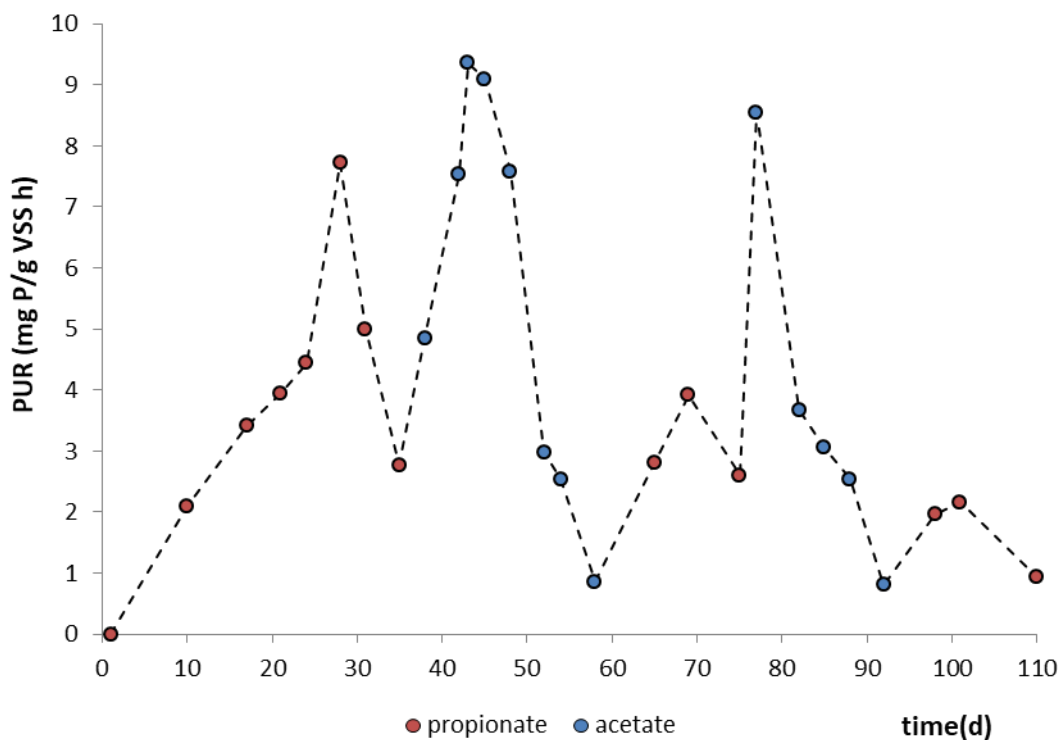


Figure 5.80. Variation of aerobic PUR throughout operation

Similarly to the operations described in sections 5.6.1.2 and 5.6.1.3, the SBR configuration was once again successful in partially shunting NOB activity. Figure 5.81 displays the variation of NO₂ and total NO_x concentration in the SBR at the end of the aerobic phase throughout operation. Figure 5.82 presents the variation of nitrite and total NO_x throughout the first daily cycle of day 21, when increased nitrite concentrations in the SBR were starting to be observed. The nitrite and nitrate produced during aeration were rapidly removed in the subsequent anoxic phase, ensuring strict anaerobic conditions for the start of the next cycle.

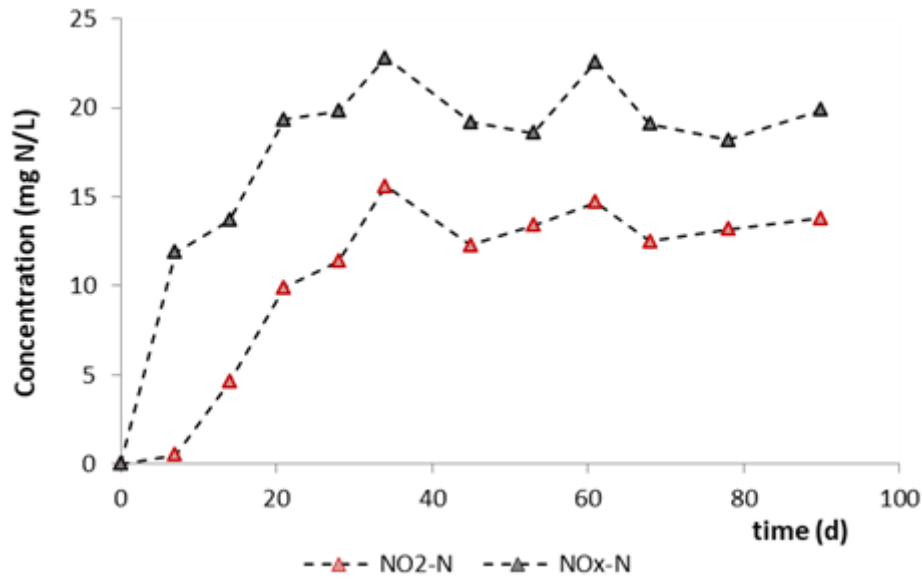


Figure 5.81. NO₂ and total NO_x concentrations at the end of the aerobic phase over time.

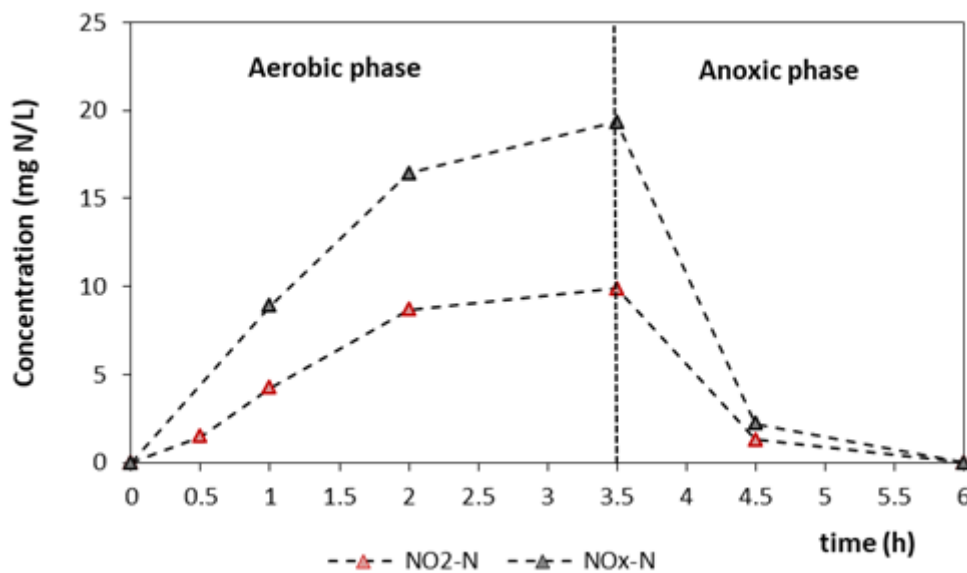


Figure 5.82. Variation of NO₂ and total NO_x concentrations during the aerobic and anoxic phase of the first daily cycle (day 21).

In accordance to Figure 5.83, the concentration of FNA throughout the aerobic phase was calculated with regard to the concentration of nitrite, temperature and pH. Due to nitrification, there is a drop in pH during the first hour of aeration after which it is raised due to carbon stripping. Throughout most of the aerobic phase, the concentration of FNA is greater than 0.2 $\mu\text{g HNO}_2\text{-N/L}$ with an observed maximum of 0.5 $\mu\text{g HNO}_2\text{-N/L}$, similarly to the observed FNA concentrations of sections 5.6.1.2 and 5.6.1.3. It is therefore likely that the FNA content of the SBR during aeration may have inhibited the growth of PAOs while possibly having little effect on the GAO populations present during each step. This could counter possible advantages of PAOs in the uptake of VFAs. For instance, following a period where propionate is used as the carbon source resulting in the wash-out of the *Competibacter spp.* and the promotion of

alphaproteobacterial GAO growth, the change of the substrate type to acetate should result in an advantage for PAOs due to their higher affinity for the specific VFA. If however their processes are inhibited, the alphaproteobacterial GAO population that has developed may prove capable of competing with PAOs for acetate, meaning that the regular rotation of the carbon source, while effective for the suppression of *Competibacter* may not be effective in the suppression of alphaproteobacterial GAOs. This would explain the diminishing returns in PUR for every substrate change over time as a large portion of the alphaproteobacterial group is maintained when acetate is used.

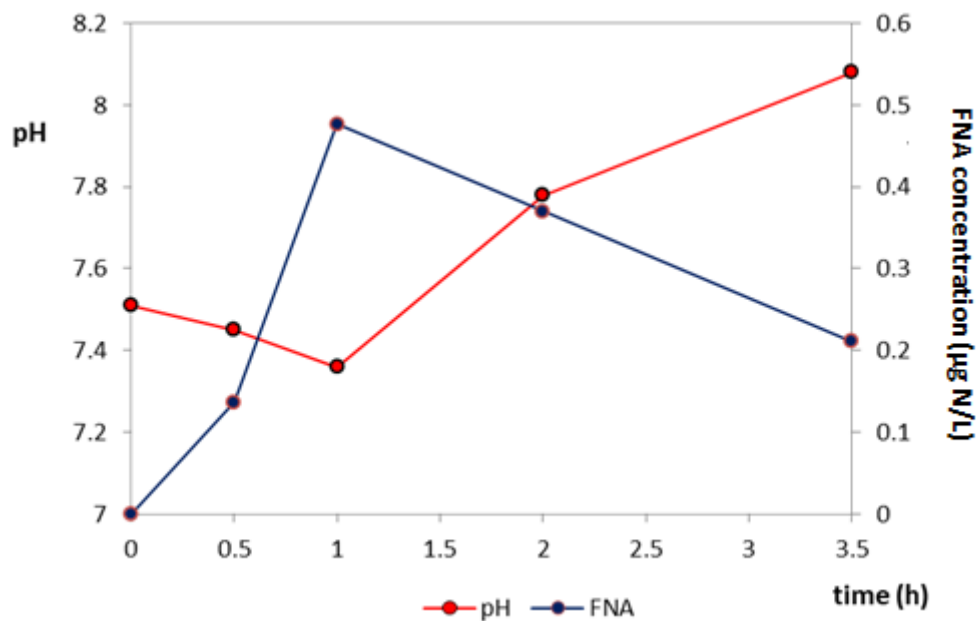


Figure 5.83. Variation of pH and the concentration of FNA during the aerobic phase of the first daily cycle (day 21).

Based on the performance of the SBR, it appears that the change of substrate from propionate to acetate benefited phosphorus removal to a greater extent than when the change was made from acetate to propionate. This is most likely due to the higher affinity of PAOs for acetate when *Competibacter* are not present. In order to further examine the immediate effect of substrate change, 2 batch experiments were performed, the results of which are presented in the following subsections.

5.6.2 Evaluating the influence of nitrite in the PAO-GAO competition

Based on the performances of the SBR for the configurations discussed in section 5.6.1, it is apparent that none of the feeding strategies were ultimately successful in establishing stable EBPR for the specific operating conditions and nitrogen loading. When either acetate, propionate or a mixture of both was used as the carbon source, the system was initially successful in developing PAOs, displaying rising PURs over time. However, once greater nitrite concentrations (that would accumulate to over 10 mg N/L) began prevailing during aeration, owing to NOB shunt that accompanied the increase of nitrogen loading, PUR began to

deteriorate over time. The regular rotation between acetate and propionate as the carbon type helped prolong EBPR though PAOs were again ultimately washed-out of the system.

As already mentioned, under the operating conditions of each feeding strategy with regard to pH and nitrite concentration during aeration, FNA concentrations of up to $0.5 \mu\text{g HNO}_2\text{-N/L}$ were produced. According to the experimental results of section 5.2.1 and 5.5.2, this FNA concentration inhibits the aerobic PUR of PAOs by approximately 25%, while having practically no effect on GAOs. It is therefore likely that the presence of FNA influenced the PAO-GAO competition in the favour of GAOs whose proliferation lead to EBPR failure.

In order to examine the extent of the effect that FNA had on the shift in the biomass towards the proliferation of GAOs, the SBR was reset and provided with a new seed sludge. The system's configuration remained as described in section 5.6.1.1 with acetate as the only type of carbon in the feed. This time however ammonium loading was kept at $0.06 \text{ g NH}_4\text{-N/m}^3 \text{ d}$ throughout operation. Ammonium concentrations in the effluent were monitored on a daily basis and the daily dosage was modified in order to maintain effluent concentrations lower than $10 \text{ NH}_4\text{-N mg/L}$ to prevent accumulation of ammonium in the SBR. With this, nitrite (and therefore FNA) concentrations in the SBR could be expected to be significantly lower than the ones observed throughout the operation of the system described in section 5.6.1.2.

The SBR was successful in the development of PAOs with noticeable phosphorus removal observed as early as 10 days into operation. By day 30 the system had reached a steady operation in regard to nitrification and denitrification. The variation of nitrite and nitrate throughout a typical cycle from this point on is shown in Figure 5.84. As expected, due to the low ammonium loading, total $\text{NO}_x\text{-N}$ concentrations were relatively low (less than 4.5 mg/L by the end of the aerobic phase) with $\text{NO}_2\text{-N}$ accounting for a small fraction of the total amount.

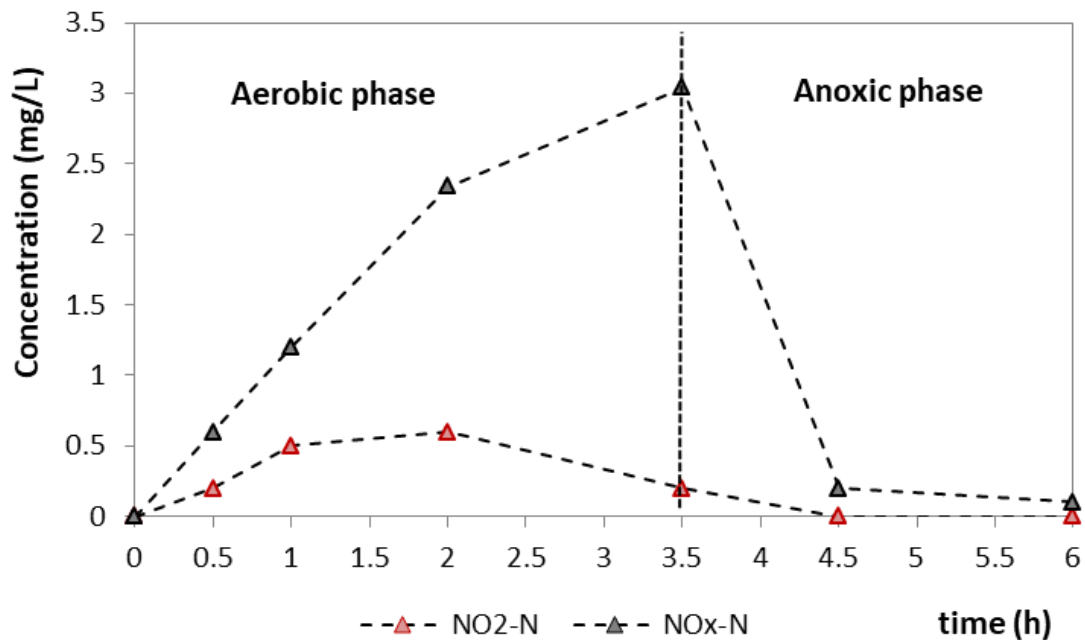


Figure 5.84. Variation of NO_2 and total NO_x concentrations throughout a typical cycle.

During the aerobic phase, pH raised rapidly due to carbon stripping from 7.5 to 8.1 within the first hour of aeration, reaching just below 8.2 by the end of aeration. In the subsequent anoxic phase, pH would remain mostly unaffected, with only an insignificant rise being observed during the first 10-15 minutes due to denitrification. Figure 5.85 displays the variation of pH throughout a typical aerobic cycle along with the associated FNA concentrations calculated with regard to nitrite. Due to the relatively high pH and low nitrite concentrations, FNA concentrations in the SBR were significantly low (less than $0.012 \mu\text{g N/L}$) and would likely have no effect on the activities of PAOs.

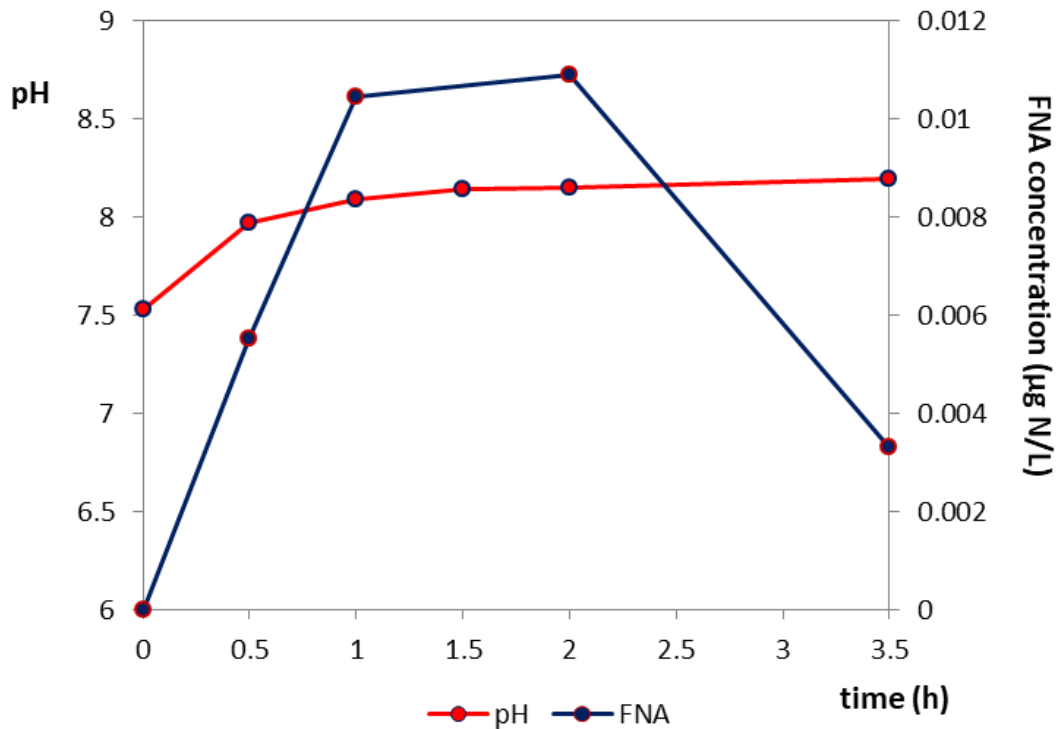


Figure 5.85. Variation of pH and the concentration of FNA during the aerobic phase of the first daily cycle.

Figure 5.86 shows the variation of aerobic PUR as recorded during the first daily cycle over time. As shown, phosphorus removal increased steadily over the first days of operation, reaching a peak on day 22. Following that, PUR declined slowly over the following 45 days, after which a rapid decline was observed. By day 88, phosphorus removal had ceased, indicating that PAOs had been washed out of the SBR.

The anaerobic P-release and COD uptake rates were also monitored throughout operation and are displayed in Figure 5.87. Anaerobic P-release decreased steadily over time, similarly to aerobic PUR while the anaerobic uptake of acetate remained practically unaffected. This is indicative of changes in the populations of the biomass and specifically of the proliferation of GAOs over PAOs. The PAO/GAO population dynamics may be monitored by the evolution of anaerobic $P_{\text{released}}/\text{COD}_{\text{uptake}}$ ratio which clearly indicates a steady shift in the biomass in the favour of GAOs. This shift is likely the result of the use of acetate as the source of carbon, which as discussed previously has been shown to favour the growth of *Competibacter* over

Accumulibacter. The abundance of the *Competibacter spp.* in the SBR was also verified by FISH analysis (Figure 5.88) which also revealed a negligible PAO population (<1%).

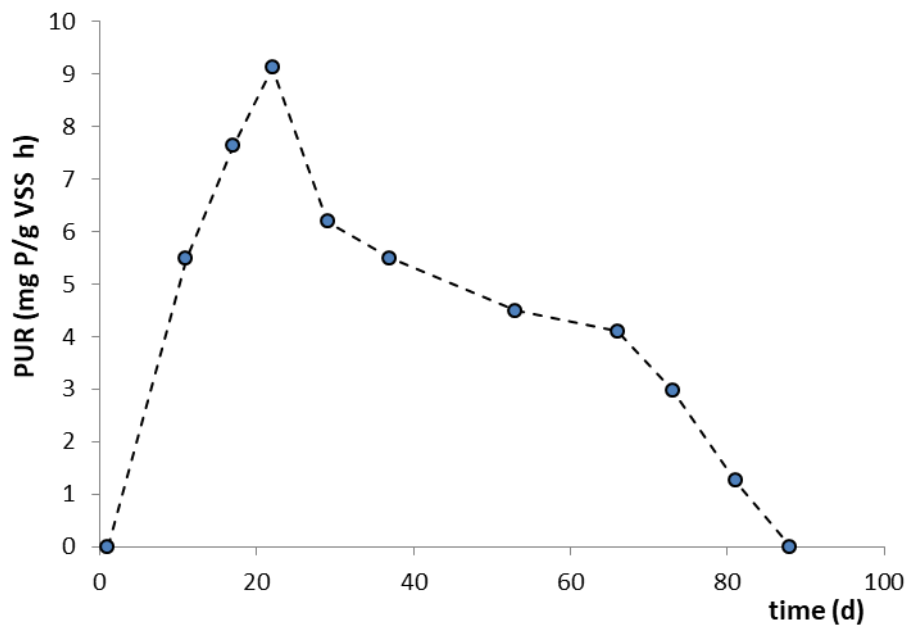


Figure 5.86. Variation of aerobic PUR throughout operation

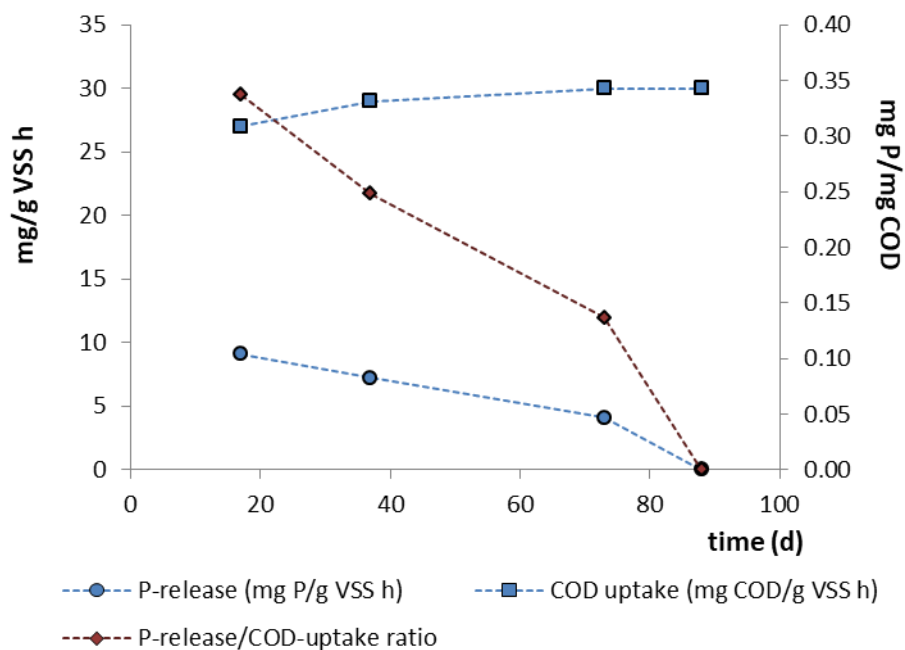


Figure 5.87. Variation of the anaerobic phosphorus release and COD uptake rates throughout operation.

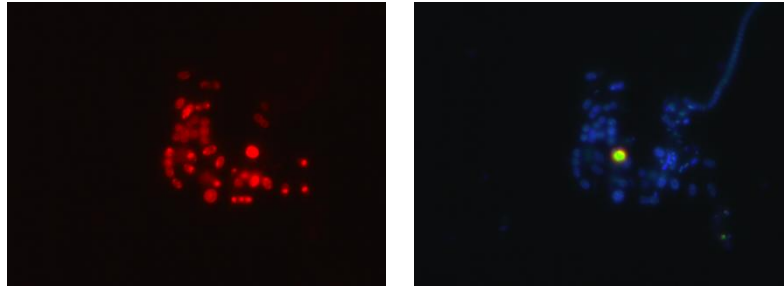


Figure 5.88. In situ identification of GAOs using Cy-3 labelled GAOMIX (GAOs depicted in red, all microorganisms stained with DAPI presented in blue) on day 88 of operation.

Figure 5.89 presents a comparison of the SBR's performance with that described in section 5.6.1.2. As is evident, the absence of FNA helped prolong the longevity of EBPR although GAOs ultimately prevailed in the SBR. This would suggest that the use of acetate as the form of carbon should be avoided since PAOs appear incapable of competing with acetotrophic GAOs. The presence of FNA hastened the shift in the biomass in the favour of GAOs, as the growth of PAOs was inhibited.

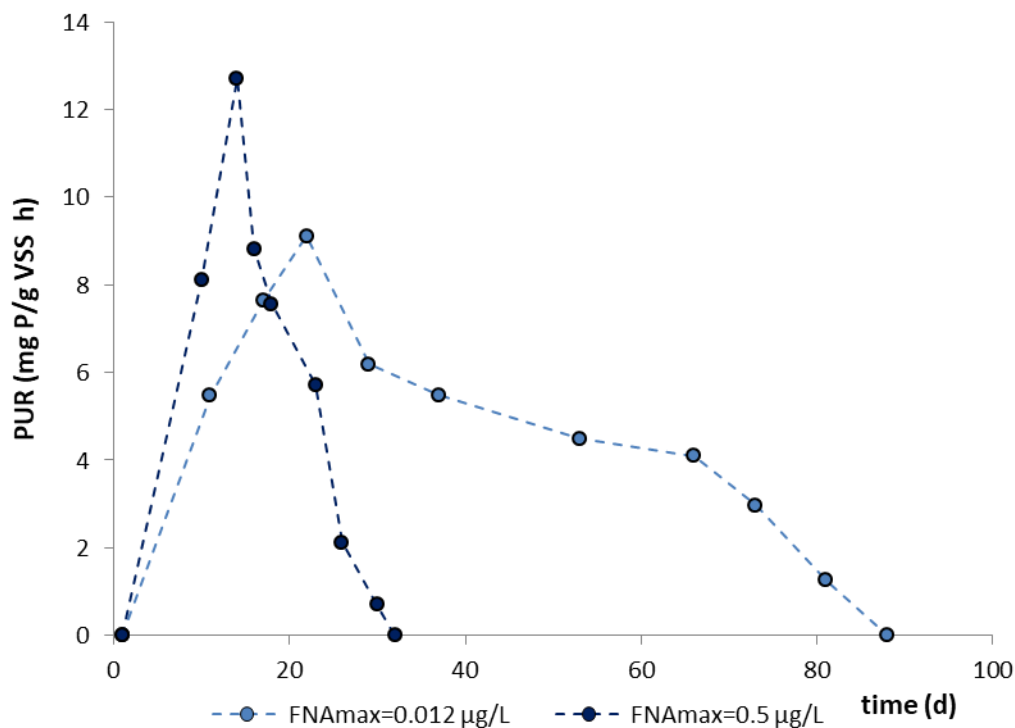


Figure 5.89. Comparison of the SBR's performance with that observed under higher FNA accumulations

5.6.3 Optimizing EBPR via the selection of PAOs through the denitritation pathway with propionate as the sole carbon source

As evidenced, the configurations employed and described in sections 5.6.1 and 5.6.2 were unsuccessful in providing favourable conditions for the sustainability of EBPR. While all

configurations were initially successful in developing PAOs, their population was eventually washed out by the growth of antagonistic GAO populations. Their wash-out from the SBR was hastened when significant nitrite concentrations began to accumulate in the SBR, owing to the associated presence of FNA.

The growth of PAOs throughout an operation cycle may be adequately described by the following equation:

$$\begin{aligned} \Delta X_{PAOs} = & \int_0^{\theta_{aer}} \left(\mu_{max-aer} \times \frac{[PHAs]}{K_{PHAs_aer} + [PHAs]} \times \frac{[P]}{K_P + [P]} \times \frac{[DO]}{K_{DO} + [DO]} \dots \right. \\ & \left. \times (1 - inh_{FA+FNA}) \times X_{PAOs} \right) dt \\ + & \int_0^{\theta_{anox}} \left(\mu_{max-denitritation} \times \frac{PHAs}{K_{PHAs_anox} + PHAs} \times \frac{[P]}{K_P + [P]} \times \frac{[NO_2]}{K_{NO_2} + [NO_2]} \dots \right. \\ & \left. \times (1 - inh_{FA+FNA}) \times X_{PAOs} \right) dt \\ + & \int_0^{\theta_{anox}} \left(\mu_{max-denitratation} \times \frac{PHAs}{K_{PHAs_anox} + PHAs} \times \frac{[P]}{K_P + [P]} \times \frac{[NO_3]}{K_{NO_3} + [NO_3]} \dots \right. \\ & \left. \times (1 - inh_{FA+FNA}) \times X_{PAOs} \right) dt \quad (5.42) \end{aligned}$$

In order for PAOs to proliferate over GAOs:

$$\Delta X_{PAOs} > \Delta X_{GAOs}$$

In order to satisfy this requirement, the following strategies may be employed:

- Prioritization of the anaerobic uptake of COD by PAOs. This may be achieved by employing one of the strategies discussed in section 5.3.3, namely: either employing a relatively low anaerobic retention time (45-60 min) when VFAs are the carbon source, or longer anaerobic retention times for slowly degradable carbon sources. The slow addition of the feed over a prolonged time period, when VFAs are the carbon source, may also benefit PAOs, as they have been shown to persevere over GAOs in conditions of substrate scarcity.
- Providing adequate phosphorus concentrations throughout the cycle. The availability of phosphorus is a prerequisite for the development of PAOs. The sustain of PAOs under steady state conditions requires:

$$P_{released}(X_{PAOs}) + P_{feed} - P_c - P_s = P_{uptake}(X_{PAOs} + \Delta X_{PAOs})$$

for each cycle, where: $P_{released}$ is the phosphorus released anaerobically by PAOs, P_{feed} is the phosphorus of the feed, P_c is the phosphorus that is removed via precipitation, P_s is the phosphorus that is utilized for microbial synthesis, P_{uptake} is the phosphorus taken up by PAOs and ΔX_{PAOs} is the increase in PAOs during a cycle. In full scale applications, this relation will determine the required SRT for the sustenance of the required PAO

population needed for the effective removal of phosphorus. However, as the objective of the SBR in this study is the growth of PAOs and not general phosphorus removal, which may be achieved by natural chemical precipitation as well, in this case a significant portion of phosphorus that is removed by other means ($P_c + P_s$) needs to be replenished in order to sustain PAOs. Essentially, phosphorus in the feed must be regulated so:

$$P_{feed} = P_{uptake}(\Delta X_{PAOs}) + P_c + P_s$$

- Selection of the antagonistic GAO group and employment of specific strategies against them: As mentioned, GAOs may be divided into 2 main subgroups: the strictly acetotrophic group (*Competibacter spp.*) and the propionate favouring alphaproteobacterial group (mainly *Defluvicoccus vanus spp.*). The selection of a specific subgroup via choice of carbon source may provide PAOs with a handicap in their antagonism, as one group may be less resilient to FNA or FA than the other, have a slower growth rate, or other limitations. In general, *Competibacter* have been reported to thrive over PAOs even in conditions of low FNA and FA accumulations, for which they have displayed a strong tolerance (as demonstrated in section 5.5). Alphaproteobacterial GAOs on the other hand are seen as a more balanced opponent for PAOs in the absence of FNA and FA. While their tolerance to these inhibitors has not been documented yet, the results of section 5.6.1.4 would indicate that they are favoured in conditions where FNA concentrations as low as 0.5 µg N/L accumulate. However, it has been reported that *Defluvicoccus vanus* does not have the capacity to utilize nitrite as an electron acceptor when propionate is the carbon source. It is therefore possible that, by providing PAOs a priority in denitrification, their net-growth may surpass that of their antagonists even under inhibiting conditions. In other words, the second term of equation (5.41):

$$\int_0^{\theta_{anox}} \left(\mu_{max-denitrification} \times \frac{PHAs}{K_{PHAs_{anox}} + PHAs} \frac{[NO_2]}{K_{NO_2} + [NO_2]} \dots \right. \\ \left. \times (1 - inh_{FA+FNA}) \times X_{PAOs} \right) dt$$

should be increased. In order to achieve this, sufficient nitrite must be made available to PAOs along with a sufficient anoxic retention time. In addition, since ordinary heterotrophic organisms (OHOs) reduce nitrite at a much faster rate than PAOs, it may be necessary to limit their action at least for some fraction of the phase, or completely if nitrite concentrations are generally low. This may be achieved by either postponing the addition of carbon during the anoxic phase in order to give PAOs priority over denitrification, or by regulating the carbon dosage so as to rapidly remove a portion of nitrite (by OHOs), leaving the residual concentration to be reduced by PAOs. The second option would also provide PAOs with a more favourable denitrification period, due to lower FNA concentration. In aid of the above, it is required that PAOs still possess an abundant PHA storage, meaning that the prior aerobic phase should not be prolonged. Reducing the aerobic retention time in favour of the anoxic retention time (which would be required since PAOs have a lower denitrification time) would also further promote NOB shunt, making more nitrite available.

Based on the above strategies, the SBR was reset with a new configuration focusing on the promotion of PAO growth via the denitrification pathway with the use of propionate as the sole carbon source. During the start-up period the NLR was gradually increased up to $0.1 \text{ kg N/m}^3 \text{ d}$ at which it remained for the first phase of operation. The NLR was then increased to $0.15 \text{ kg N/m}^3 \text{ d}$ for the second phase of operation. During the third phase of operation, the NLR remained at $0.15 \text{ kg N/m}^3 \text{ d}$ but pH was controlled at the low value of 6.5 in order to evaluate the sustainability of PAOs under increased FNA concentrations. The SBR's performance for all operation phases is presented in the following subsections.

5.6.3.1 Performance of the experimental system

The configuration examined in this section is similar to the one that was presented in section 5.2.2.1, in which information regarding the start-up period may be found.

5.6.3.1.1 First phase of operation (vNLR=0.1 kg N/m³ d)

After the 60-day start-up period, the SBR achieved steady state conditions and demonstrated significant PAO activity. During operation, pH ranged from 7.5 to 8.5 and SBR temperature was maintained at $20 \pm 2^\circ\text{C}$. VSS and TSS averaged at $3,000 \pm 500 \text{ mg/L}$ and at $3,300 \pm 500 \text{ mg/L}$, respectively. The SBR's configuration was successful in developing a highly PAO-enriched biomass as confirmed by FISH analyses and high PURs that were observed throughout operation.

Figure 5.90 displays the variation of phosphorus and COD throughout a typical SBR cycle. During the anaerobic phase, propionate was taken up by PAOs at an average rate of $17.6 \text{ mg COD/g VSS h}$, while P was released at an average rate of approximately 12 mg P/g VSS h . At the beginning of the aerobic phase, $\text{PO}_4\text{-P}$ averaged at $70 \pm 10 \text{ mg/L}$. During aeration, phosphorus was rapidly removed at an average PUR of 12 mg P/g VSS h , while nitrite and nitrate concentrations accumulated up to $18 \pm 3 \text{ mg N/L}$ and $4.5 \pm 1 \text{ mg N/L}$ respectively at the end of this phase. The abundance of nitrite over nitrate was due to the suppression of NOB that was achieved mainly by the low aerobic SRT. The concentration of ammonium was reduced from $24 \pm 2 \text{ mg N/L}$ to $2 \pm 1 \text{ mg N/L}$ during aeration due to nitrification/nitritation and its utilization for microbial synthesis. With the cease of aeration, nitrite was reduced by PAOs at an average rate of 3.1 mg N/g VSS h . However, the biomass's capacity for anoxic P-removal could not be evaluated in the conditions of the SBR since most of the phosphorus was removed during the aerobic phase. The variation of ammonium, nitrite and nitrate during a typical cycle is presented in Figure 5.91. Accordingly, Figure 5.92 displays the variation of pH and DO during the aerobic phase of a typical cycle. In order to prevent a rapid increase in pH due to carbon stripping, the intensity of aeration was kept within limits, resulting in lower concentrations at the start of the aerobic phase where oxygen demand was higher. Consequently, the concentration of DO during the first hour of aeration was below optimum values for nitritation and phosphorus removal.

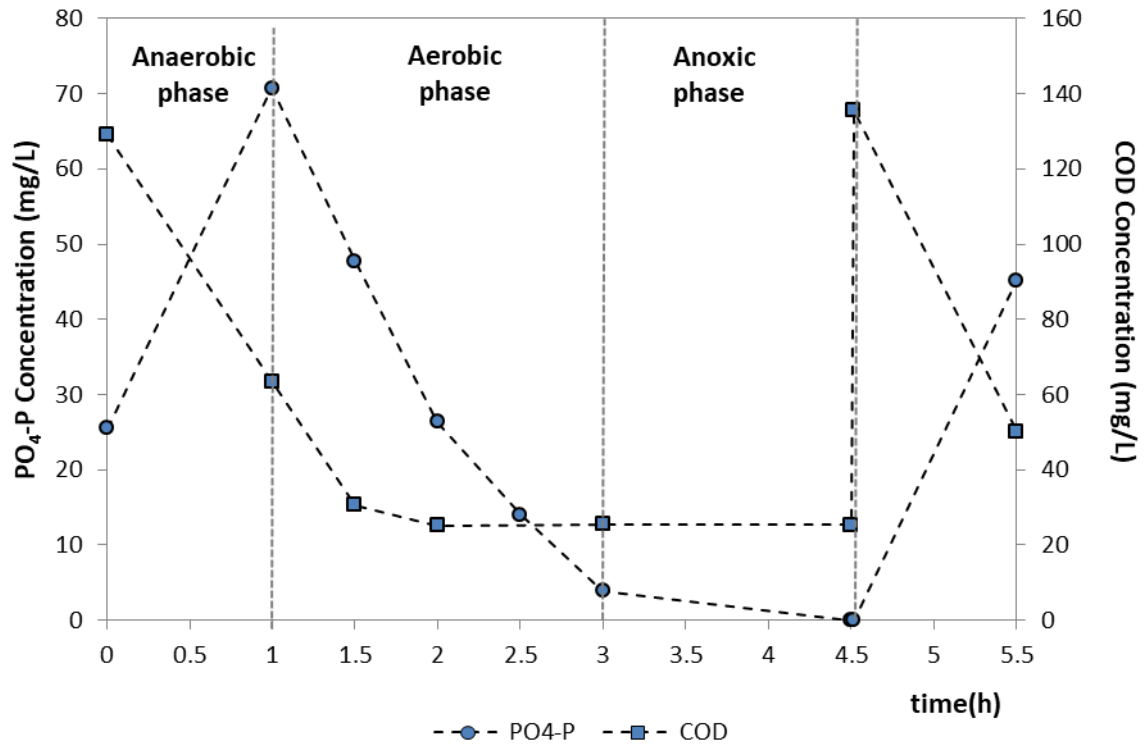


Figure 5.90. Variation of phosphorus and COD throughout a typical SBR cycle.

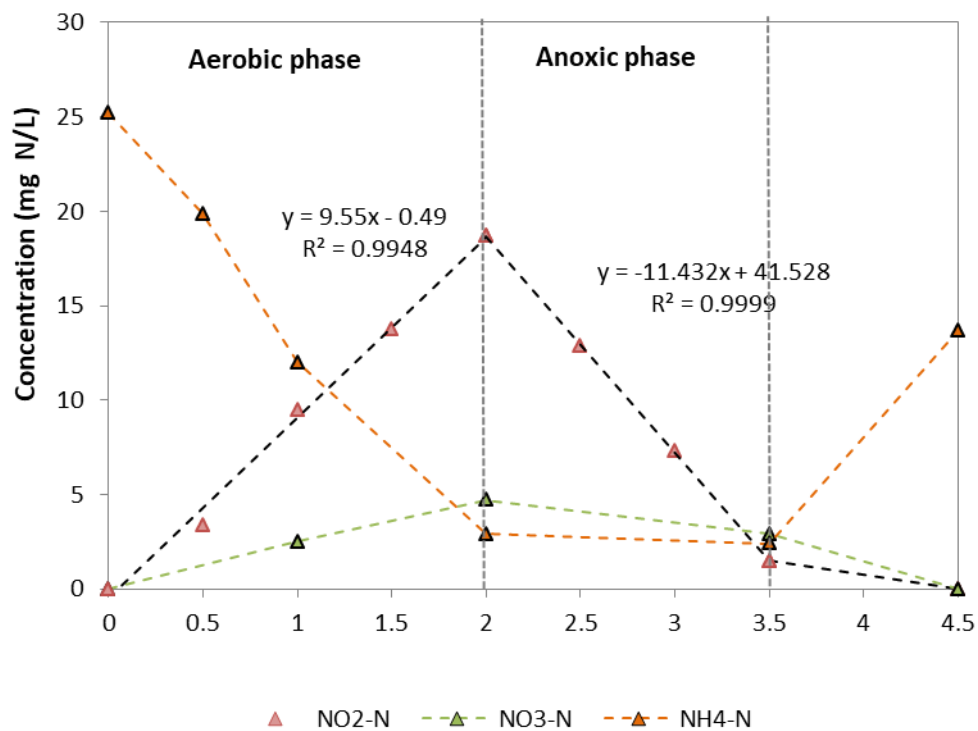


Figure 5.91. Variation of ammonium, nitrite and nitrate throughout the aerobic and anoxic phase of a typical SBR cycle.

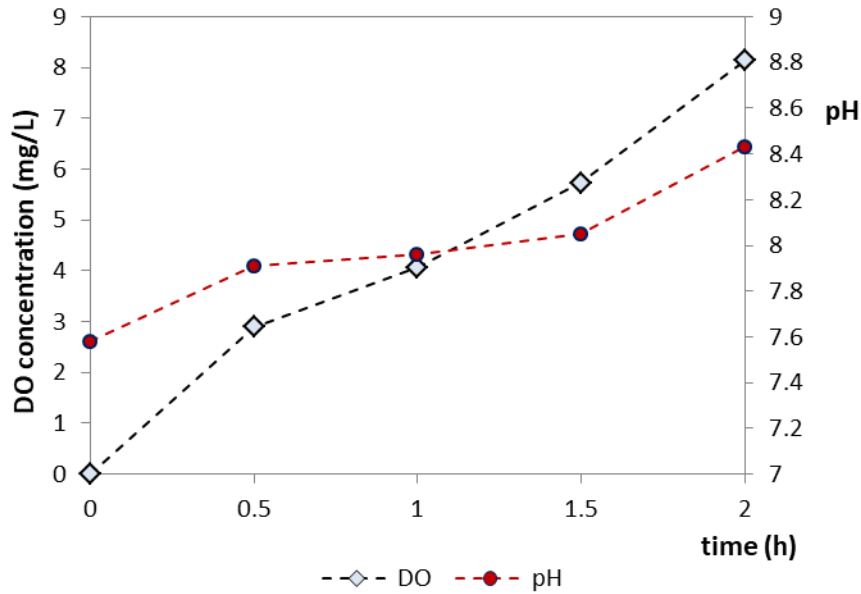


Figure 5.92. Variation of DO and pH throughout the aerobic phase of a typical SBR cycle.

Figure 5.93 displays the variation of FNA throughout the aerobic and anoxic phase along with its predicted inhibitory effect on PUR according to the inhibition model that was developed in section 5.4. FNA would accumulate to just below $0.35 \mu\text{g N/L}$, a concentration that has been found to inhibit PUR by approximately 20%. The overall inhibition of PAOs throughout the cycle may be roughly estimated by calculating the area under the formed inhibition curve. According to this, the overall inhibition during aeration is approximately 12%, while the overall inhibition during denitritation is just over 4%. As such, conditions in the SBR allowed the growth of PAOs under limited inhibition. This, along with the designated denitritation phase for PAOs, ensured their prevalence over GAOs and the stability of EBPR.

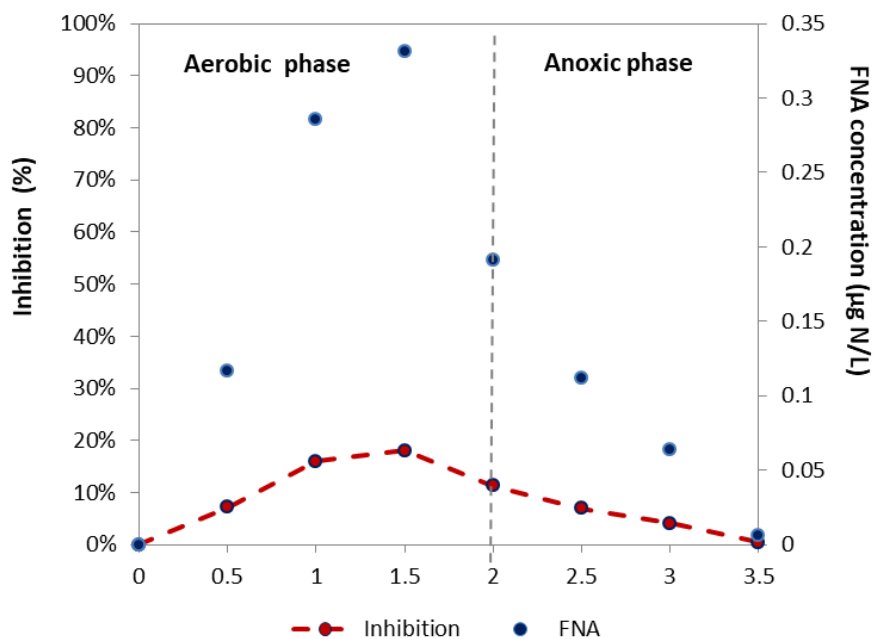


Figure 5.93. Variation of FNA and the degree of inhibition throughout a typical SBR cycle

The SBR's configuration was successful in developing a highly PAO-enriched biomass, which was documented by FISH analysis (Figure 5.94). Quantification of a total of 52 pairs of FISH images (16 pairs for each duplicate of 2 separate samples) showed *Accumulibacter* (the main PAO species), to account for approximately 50% of the total microbial community. In addition, neither *Competibacter* nor *Deffluvicoccus vanus* (the main alphaproteobacterial GAO species) were shown to have a substantial presence in the biomass (<2% of the total microbial population), indicating that the system's configuration was effective in their suppression.

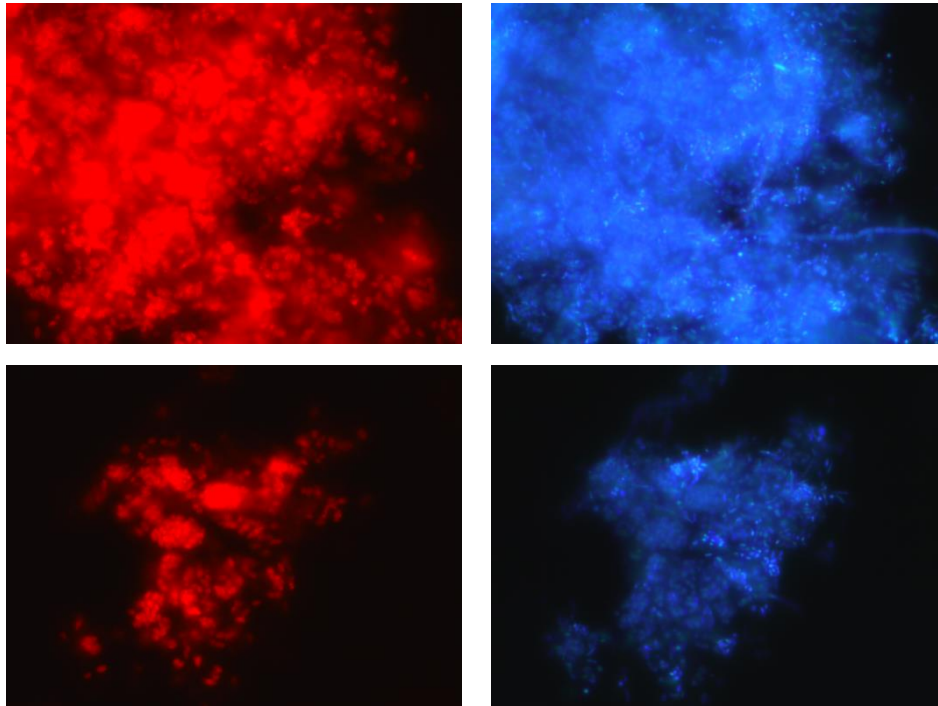


Figure 5.94. In situ identification of PAOs using Cy-3 labelled PAOMIX (PAOs depicted in red, all microorganisms stained with DAPI presented in blue).

As demonstrated, the SBR displayed good EBPR performance throughout operation. However, the biomass's potential for P-removal could not be observed in in-situ conditions. This is due to the relatively low DO concentration throughout the first hour of aeration (within which, most of the phosphorus is removed) along with the inhibitory effect of FNA that is present. In addition, the change in pH could influence water chemistry and precipitation/dissolution reactions involving phosphorus. As such, the biomass's capacity for P-removal was examined in regular ex-situ batch experiments, both under aerobic and under anoxic conditions.

In each experiment, 1 L of sludge was extracted from the SBR (prior to feed) and was divided equally into 2 containers each with a working volume of 500 mL. The pH of each reactor was set to 8 and kept constant throughout the duration of the experiment. Each reactor was fed with readily biodegradable organic carbon, in the form of a sodium acetate solution, in order to establish a starting COD content of 100 mg/L and was stirred for 1 h under anaerobic conditions. The first reactor was used for the examination of P-removal under aerobic conditions, while the second reactor was used for the examination of P-removal via denitrification. Following the anaerobic period, the first reactor was aerated for a period of 2 h. DO concentrations exceeded 7 mg/L within 5 minutes of aeration while nitrite concentrations did

not exceed 5 mg N/L throughout the experiment due to the low initial ammonium concentration. The associated FNA concentrations due to the high pH, would have a negligible effect on PAOs. The second reactor received a nitrite concentration of 10 mg NO₂-N/L with the addition of an appropriate volume of a sodium nitrite solution and was kept constant at 8 ± 2 mg N/L throughout the experiment with regular sodium nitrite addition. The anoxic PUR was determined for a 2.5 h period.

Throughout operation, the aerobic PUR averaged at 25 ± 4 mg P/g VSS h, while the anoxic PUR averaged at 10 ± 3 mg P/g VSS h. The anoxic/aerobic PUR ratio appeared relatively steady throughout operation with anoxic PUR being observed to occur at approximately 40% of the aerobic PUR. The occasional use of propionate as the carbon source in these experiments instead of acetate, did not affect aerobic and anoxic PUR, as well as the anaerobic release of phosphorus, in agreement with the observations of section 5.6.1.4.1. By accounting for the total volume of nitrite added to the anoxic reactor, an average denitritation rate of 8 ± 1 mg N/g VSS h may be determined. However, this rate concerns not only PAOs, but also endogenous denitritation by common heterotrophs. The anaerobic release of P occurred at a rate of 23 ± 6 mg P/g VSS h, that was accompanied by an average COD uptake rate of 44 ± 12 mg COD/g VSS h. This would correspond to a P_{release}/COD_{uptake} ratio of approximately 0.5. As GAOs were not detected by FISH analysis, the entire amount of COD may be attributed solely to PAOs. Since PAOs were found to account for approximately 50% of the population, the following rates may be determined for PAOs (Table 5.14):

Table 5.14. Determined metabolic rates of PAOs

Aerobic PUR _{max} :	50 mg P/g VSS _{PAOs} h
Anoxic PUR _{max} :	20 mg P/g VSS _{PAOs} h
Anoxic/Aerobic PUR ratio:	0.4
Anaerobic P-release rate:	46 mg P/g VSS _{PAOs} h
Anaerobic COD-uptake rate:	88 mg P/g VSS _{PAOs} h
P _{release} /COD _{uptake} ratio:	0.5

The parameters of Table 5.14 may effectively be used in mathematical simulations of EBPR with regard to the PAO population. For the simulation of a similar configuration, the anaerobic P-release rate of 12 mg P/g VSS h along with the aerobic PUR of 12 mg P/g VSS h × (1-Inh), where Inh is the degree of inhibition according to the inhibition model of section 5.4, that were observed in the SBR, may be used for a simplified simulation that focuses on PUR inhibition.

5.6.3.1.2 **Second phase of operation (vNLR=0.15 kg N/m³ d)**

Following the successful performance of the SBR at the NLR of 0.1 kg N/m³ d, the concentration of ammonium in the feed was gradually increased over a period of 14 days, raising the NLR to 0.15 kg N/m³ d. During this time, the dosage of COD was also gradually raised from 8 to 9 g/d to compensate for the increased demand in denitritation. The SBR was maintained under the new NLR conditions for a further 14 days during which a steady state had been achieved.

The SBR's performance under the new NLR is presented in Figure 5.95 and Figure 5.96. As expected, nitrite concentrations during aeration increased, accumulating to over 25 mg N/L by the end of the aerobic phase. Approximately half of the nitrite produced was removed by PAOs over the subsequent 1.5 h anoxic phase, with the rest being removed by PAOs along with OHOs in the follow-up 1 h phase. The abundance of PAOs was still evident, as phosphorus continued to be removed at a high yet considerably diminished rate, displaying an aerobic PUR of 6 mg P/g VSS h (approximately half of that observed in the SBR under the NLR of 0.1 kg N/m³ d). Due to the reduced removal of phosphorus during the aerobic phase, P-removal was also observed in the SBR during the subsequent anoxic phase at a rate of 3.2 mg P/g VSS h.

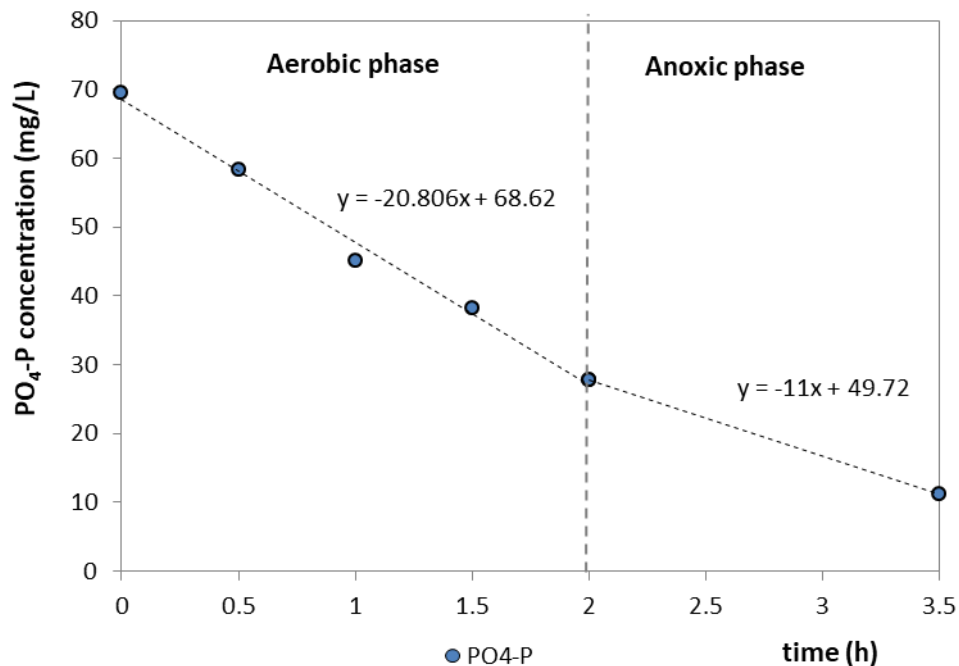


Figure 5.95. Variation of phosphorus in the SBR during the first daily cycle.

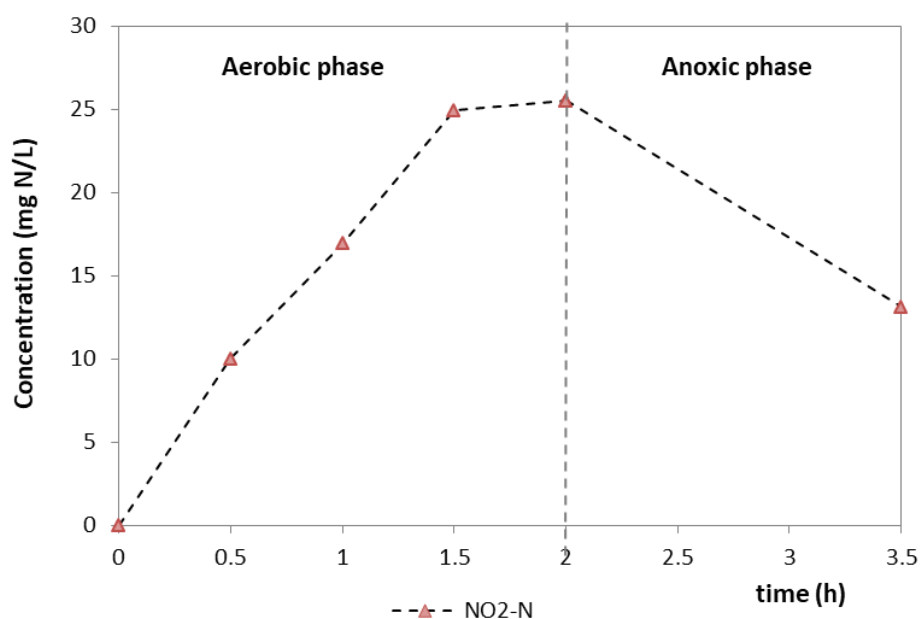


Figure 5.96. Variation of nitrite in the SBR during the first daily cycle.

Figure 5.97 displays the variation of FNA throughout the aerobic and anoxic phase along with its predicted inhibitory effect on PUR. Due to the increased nitrification, which in addition to greater nitrite concentrations also resulted in a variation of pH at lower values, FNA reached concentrations up to $1 \mu\text{g N/L}$, a concentration that has been found to inhibit PUR by 40%. A rough estimate of the overall inhibition of PAOs, based on calculation of the area under the formed curve, would be 28% during aeration and 13% during denitritation.

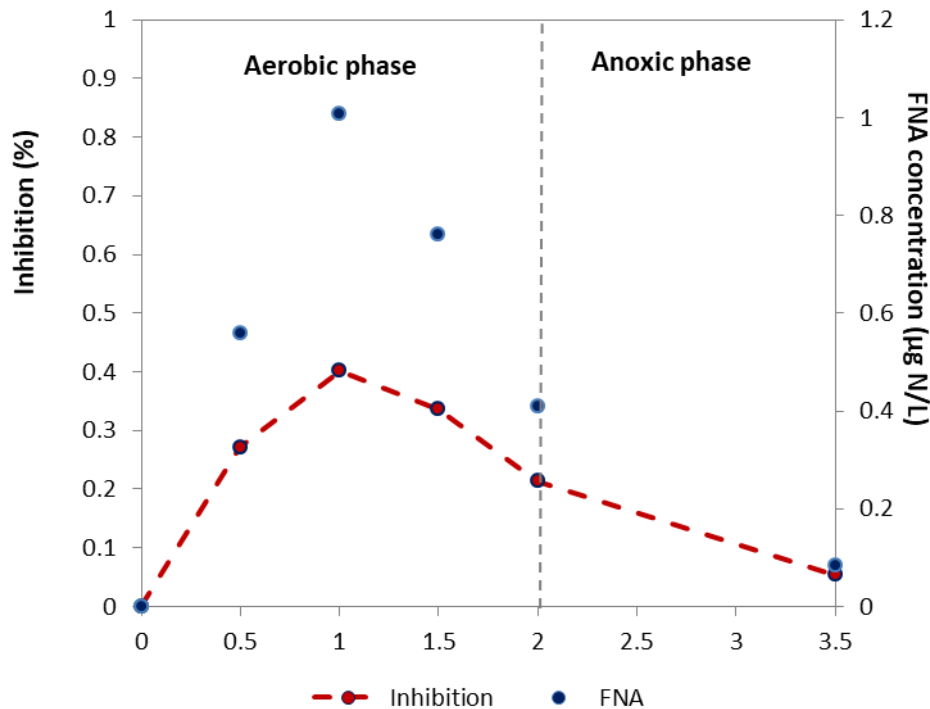


Figure 5.97. Variation of FNA and the degree of inhibition throughout a typical SBR cycle

For a comparison with the system's performance during the first operation phase ($\text{NLR}=0.1 \text{ kg N/m}^3 \text{ d}$), it should be acknowledged that this degree of inhibition observed concerns not only the performance of the present PAO population, but also the reduced PAO community due to inhibition of their growth. For instance, considering the PUR of 6 mg P/g VSS h observed in the SBR, it may be estimated that in the absence of inhibitors, the biomass may perform at $6/(1-0.28)=8.3 \text{ mg P/g VSS h}$ under aerobic conditions. If the inhibitive conditions during the first period of operation were to be considered negligible, then comparison of the aerobic PURs from each period would reveal that the PAO population has been reduced by 30%, which is a reasonable deduction considering the new conditions.

In general, if EBPR under a specific configuration and the absence of inhibitors is performed at a steady PUR, then in the presence of inhibitors, the system should be expected to perform at less than $\text{PUR} \times (1 - \text{Inh})^2$, where *Inh* is the degree of the overall inhibition due to FA and FNA. This is due to both the diminished PAO population, and their stunted performance under the new conditions.

5.6.3.1.3 Third phase of operation (vNLR=0.15 kg N/m³ d – low pH)

During this phase, NLR remained the same but the system performed at a lower pH. The objective was to determine the sustainability of PAOs under high FNA accumulations without the need of increasing nitrogen loading. To achieve this, the HRT was increased to 10 days (by decanting 1 L of effluent every day, which was just enough for the 1 L of feed that would enter daily) in order to limit the renewal of the medium's alkalinity. With this, the effect of carbon stripping during aeration was minimal and the pH levels gradually dropped over a period of 7 days, reaching a value of 6.5 that would remain practically constant throughout each cycle. Following this, the SBR was operated under this constant pH for a period of 10 days, after which an evaluation of the system's performance was performed.

The SBR's performance under these conditions is presented in Figure 5.98 and Figure 5.99. The system's capacity to remove phosphorus had completely deteriorated, with negligible phosphorus removal being observed during the aerobic phase. As shown, neither nitrite nor phosphorus was removed during the anoxic period reserved for PAOs, indicating a complete absence of the community. Instead, nitrite rose slightly, most likely as a result of some denitrification.

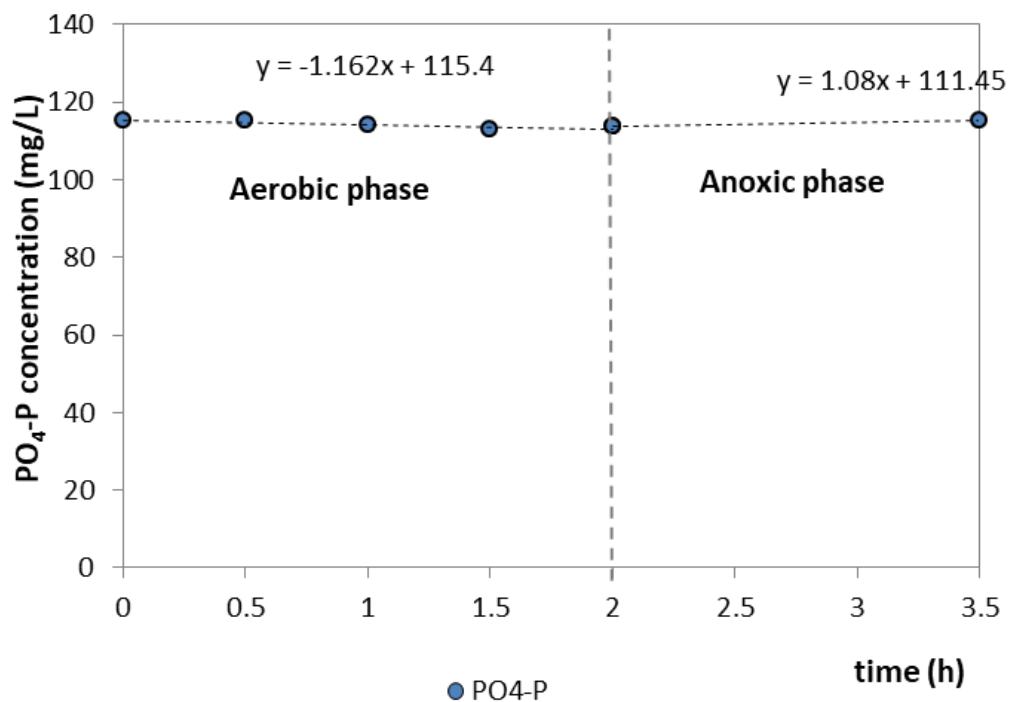


Figure 5.98. Variation of phosphorus in the SBR during the first daily cycle.

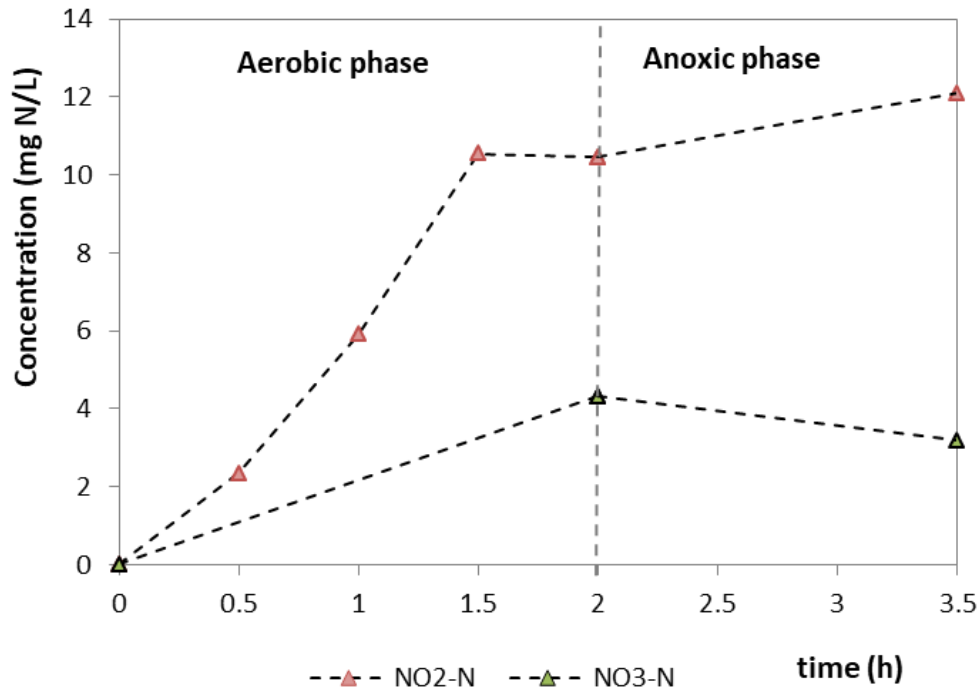


Figure 5.99. Variation of nitrite and nitrate in the SBR during the first daily cycle.

Figure 5.100 displays the variation of FNA throughout the aerobic and anoxic phase along with its predicted inhibitory effect on PUR. Due to the low pH value of 6.5, FNA concentrations increased significantly in the SBR along with the production of nitrite, reaching $8.2 \mu\text{g HNO}_2\text{-N/L}$. A rough estimate of the overall inhibition of PAOs, by calculation of the area under the formed curve, would be 64% during aeration and 80% during anoxic conditions.

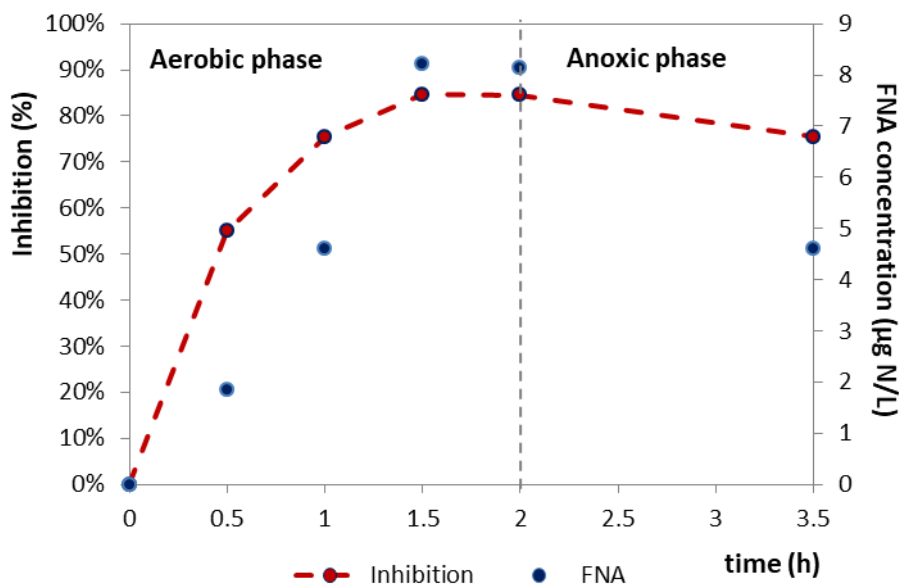


Figure 5.100. Variation of FNA and the degree of inhibition throughout a typical SBR cycle

The FNA concentrations that accumulated in the SBR were sufficient for the complete wash-out of PAOs. Interestingly, no COD appeared to be removed during the anaerobic phase, indicating that the wash-out of PAOs was not due to a proliferation of GAOs, but a direct result of the inhibitory conditions. This was confirmed by FISH analysis which revealed a negligible percentage (<5%) of *Accumulibacter*, but also *Deffluviococcus vanus*. The results of this operation phase clearly demonstrate the importance of pH control for the establishment of EBPR in low C/N treatment systems.

5.7 Optimizing EBPR in low C/N systems with nitrogen removal via nitrite

As demonstrated throughout chapter 5, the application of EBPR alongside nitrification/denitrification appears challenging at the least. Section 5.2 presented the inhibitory effect of nitrite on the aerobic and anoxic PUR of PAOs and confirmed that FNA is the actual inhibitor of these processes, while also determining the mode of inhibition as non-competitive. FNA appears to inhibit both processes to a similar extent for which a K_i of 1.5 $\mu\text{g HNO}_2\text{-N/L}$ has been determined. As such, pH heavily influences the degree of inhibition, since significantly more nitrite is in the form of FNA at lower pH values. For instance, the concentration of a mere 10 mg $\text{NO}_2\text{-N/L}$ at the pH of 7 would significantly inhibit PAOs (by approximately 50%), while at the pH of 8, PAOs would be inhibited to a much lesser extent (by only 10%). Therefore, the control of pH at high values may be beneficiary to PAOs as it would limit the abundance of FNA (and consequently the degree of inhibition).

While the control of pH at high values would seem like a viable strategy, section 5.3 demonstrated that PAOs are also inhibited by FA which becomes more abundant at higher pH values. As such, the high ammonium concentrations that are typical of high nitrogen loading treatment systems could severely limit the potential of raising pH to favour PAOs. FA was found to inhibit PAOs practically to the same degree under aerobic and anoxic conditions. The mode of inhibition was determined as uncompetitive with a K_i of approximately 8 mg $\text{NH}_3\text{-N/L}$.

The combined inhibition of FNA and FA, presented in section 5.4, showed that the simultaneous presence of nitrite and ammonium (a characteristic of nitrification/denitrification systems) could severely inhibit EBPR with pH being of significant importance. As ammonium is converted to nitrite through nitrification, the optimum pH for PAOs rises. A combined inhibition model was developed and validated by the experimental data which may be used not only to determine the combined inhibition of EBPR for a given set of parameters, but also to predict the optimum variation of pH throughout the process which would limit the degree of inhibition. The effective control of pH throughout the nitrification and denitrification processes with regard to the nitrogen load may prove a viable strategy to limit PAO inhibition and allow EBPR.

While the performance of PAOs under the aforementioned inhibitory conditions is challenged, their sustainability in such systems should also come into question as they may prove to be incapable of competing with GAOs under such circumstances. Section 5.5 demonstrated that acetotrophic GAOs (namely *Competibacter*) possess a higher tolerance to FNA than PAOs, particularly at low pH values. In addition, this GAO group appears to be unaffected by FA, meaning that while the control of pH at high values could lessen the effect of FNA in their

antagonism with PAOs, it would provide them with an advantage in terms of FA inhibition. Section 5.6.2 demonstrated that acetotrophic GAOs may also prevail over PAOs in conditions of negligible FNA and FA accumulations. As such, the use of acetate as a carbon source in such systems should be considered an unviable option. The use of propionate did not appear to provide PAOs with an advantage over the alphaproteobacterial GAO group. However, when PAOs were given priority over ordinary heterotrophic organisms (OHOs) in denitrification, the biomass displayed excellent EBPR activity, while GAOs were not detected. This is most likely due to the fact that alphaproteobacterial GAOs (specifically the main organism: *Defluviicoccus vanus*) are reportedly incapable of utilizing nitrite when propionate is the carbon source. Therefore, while the growth of PAOs may be inhibited to a greater extent than that of GAOs during aerobic conditions, their growth via denitrification may compensate and allow their proliferation over GAOs. In regard to this, it may be concluded that the use of propionate could elevate the net-growth of PAOs over GAOs, providing that adequate denitrification retention times are made available for PAOs.

In light of the above, two strategies emerge for the assistance of EBPR:

- Appropriate pH control. This strategy focuses on lessening the combined inhibition by ammonium and nitrite by controlling FNA and FA concentrations. This strategy may be applied by controlling pH throughout the process as to provide minimum inhibition for PAOs. In practice, controlling pH to its optimum (for EBPR) variation may be unviable due to the associated costs of chemicals and monitoring/automation equipment. However, the application of a clever configuration centred on altering aeration with denitrification could bring the variation of pH closer to its optimum values, providing favourable conditions with limited chemical addition.
- Promoting denitrification by PAOs with propionate: This strategy focuses on providing PAOs with an advantage over GAOs. It may be achieved by allowing the growth of PAOs via denitrification, ensuring an overall greater net-growth than that of GAOs. In order for this strategy to be effective, the anoxic growth of PAOs must compensate for the stunted growth during aerobic conditions in which GAOs may develop faster. As such, adequate anoxic retention times must be made available to PAOs that would most likely require the partial exclusion of OHOs for the utilization of nitrite.

In this section, the potential for EBPR in nitrification/denitrification systems is evaluated via a set of simulations for a theoretical full-scale configuration, based on the laboratory configuration discussed in section 5.6.4. The series of simulations was carried out through a developed coded program, that utilized data from an existing pilot SBR that was operated at the WWTP of Psytalia for the side-treatment of reject-water. While the side-stream pilot system did not employ EBPR by including an anaerobic phase, the nitrification and denitrification rates along with the variation of pH throughout its operation, could be considered comparable with those of the theoretical configuration, with respect to the vNLR.

Description of the existing pilot plant / acquisition of data:

The pilot SBR operated at an $vNLR$ of 0.31 ± 0.08 kg N/m³ d. The SRT was 10 d and the concentration of VSS averaged at 4,600 mg/L. The system performed at 5 daily cycles, each consisting of 4 hours of alteration between aerobic and anoxic conditions (2 h aeration – 0.5 h denitrification - 1 h aeration – 0.5 h denitrification) and 1 h for settling and decanting. The variations of NH₄-N and NO₂-N during a typical cycle are presented in Figure 5.101, while the variation of pH is presented in Figure 5.102). The ammonium concentration at the beginning of the cycle is 159 mg N/L. Over the first aeration period, it is reduced to 92 mg N/L due to nitrification (producing 68 mg NO₂-N/L in the process – 7.4 mg N/g VSS h) and its utilization for microbial synthesis. During the subsequent anoxic period, ammonium remains constant while nitrite is reduced at a rate of 22.6 mg N/g VSS h, reaching 16 mg N/L at the start of the next aeration phase. Over the following hour, nitrification resumes at an increased rate of 14.35 mg N/g VSS h, resulting in the accumulation of 82 mg NO₂-N/L before being reduced during the follow-up anoxic phase at a rate of 30.9 mg N/g VSS h.

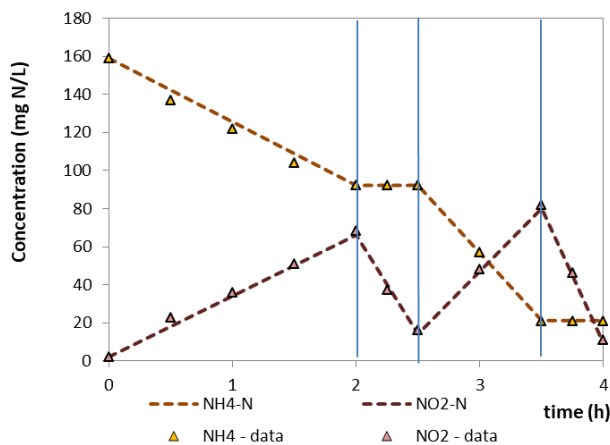


Figure 5.101. Variations of NH₄-N and NO₂-N during a typical cycle of the pilot SBR.

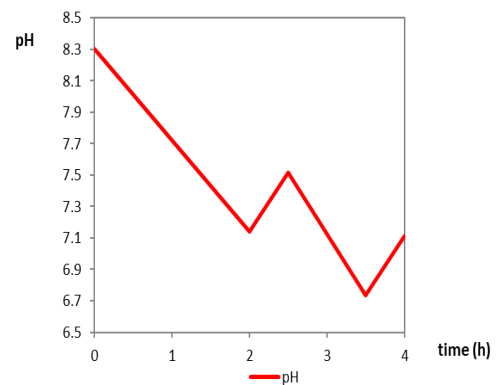


Figure 5.102. Variation of pH during a typical cycle of the pilot SBR.

The theoretical configuration was accepted to operate with the same reactor volume as the existing SBR at a similar VSS concentration. The inclusion of an anaerobic phase would require appropriate alteration of the operational cycles, reducing them to 4 per day (slightly increasing the aerobic/anoxic duration of each cycle). With this, the nitrogen concentrations after loading for each $vNLR$ were appropriately established.

The nitrification and denitrification rates along with the variation of pH with regard to nitrification or denitrification were coded into the mathematical simulation which predicted the combined inhibition of PAOs throughout the processes based on the inhibition model discussed in section 5.4. In short, the program simulated a typical cycle of operation where the ammonium concentration was reduced during the aerobic phase at the rate derived from the experimental data with a step of 0.5 min. In each step, nitrite was also increased according to the observed nitrification rate, while the concentrations of FNA and FA were calculated with regard to pH and temperature, along with the predicted degree of inhibition.

5.7.1 Simulation of an optimized system for EBPR

In this simulation, the viability of EBPR coupled with nitrification/denitrification is evaluated for a theoretical configuration that focuses on promoting the sustainability of PAOs, for vNLRs of 0.1 up to 0.3 kg N/m³ d. The theoretical configuration is based on the operation of 4 daily cycles, each consisting of a 1 h anaerobic phase, a 4.5 h period of altering between aerobic and anoxic conditions, and 0.5 h for settling and decanting. The duration of the aerobic and anoxic phase is altered appropriately for each vNLR with longer aeration times being demanded for higher vNLRs. The systems configuration along with the process for estimating the inhibition of PAOs is presented for the vNLR of 0.2 kg N/m³ d in the following section.

5.7.1.1 Exemplary simulation for the vNLR of 0.2 kg N/m³ d

System configuration:

- Anaerobic phase (60 min): The inclusion of an anaerobic phase in which a soluble carbon source can be taken up by PAOs is an axiomatic demand for EBPR. It is generally accepted that a retention time of 45-90 minutes is adequate for the uptake of readily available VFAs by PAOs, while the adoption of a relatively low retention time may also provide an antagonistic advantage against GAOs. The carbon source in this scenario is propionate, as the configuration relies on the proliferation of PAOs over GAOs via promotion of the denitrification pathway with propionate as the sole carbon source.
- First aerobic phase (70 min): The nitrification rate and AUR for this phase are adopted from the data from the existing pilot plant, as the ammonium loading is comparable to this scenario. The duration of aeration is chosen with regard to the vNLR of the scenario, as to achieve the required nitrification. Nitrite is predicted to accumulate to 35 mg N/L, based on the nitrification rate of the scenario.
- First anoxic phase (50min): With the cease of aeration, a specific dosage of propionate is introduced for the removal of the remaining DO and a portion of nitrite. The dose is regulated for the removal of just over 20 mg NO₂-N/L by mostly OHOs, lowering the concentration of nitrite to around 14 mg N/L. The denitrification rate for this stage is adopted from the data of the existing pilot plant. After the depletion of the added carbon, nitrite is then removed only by PAOs and by OHOs endogenous respiration at 40% of the initial rate and accounting for inhibition by FA&FNA. The reduced rate is based on the denitrification rates of PAOs that have been observed under negligible inhibitory conditions (section 5.2). As such, the denitrification rate by PAOs is $9 \times (1-\text{Inh})$ mg N/g VSS h. Due to the rapid removal of a significant portion of nitrite by OHOs, PAOs are able to reduce nitrite at lower FNA concentrations. The required dosage of COD may be estimated between 2.5 and 3.5 mg COD/g NO₂-N to be removed.
- Second aerobic phase (70 min): Similar to the first aeration phase. Nitrite is predicted to accumulate to just below 50 mg N/L.
- Second anoxic phase (80 min): Similar to the first anoxic phase. The COD dosage is increased, as more nitrite needs to be removed. PAOs are provided a greater anoxic period in which they may reduce nitrite at a high pH and a low ammonium background.

- Settling and decanting (30 min): An added bonus of EBPR is that the PAO enriched sludge possesses excellent settling qualities. This allows settling and decanting to be carried out over a short duration of time.

Figure 5.103 displays the predicted variation of ammonium and nitrite throughout the cycle

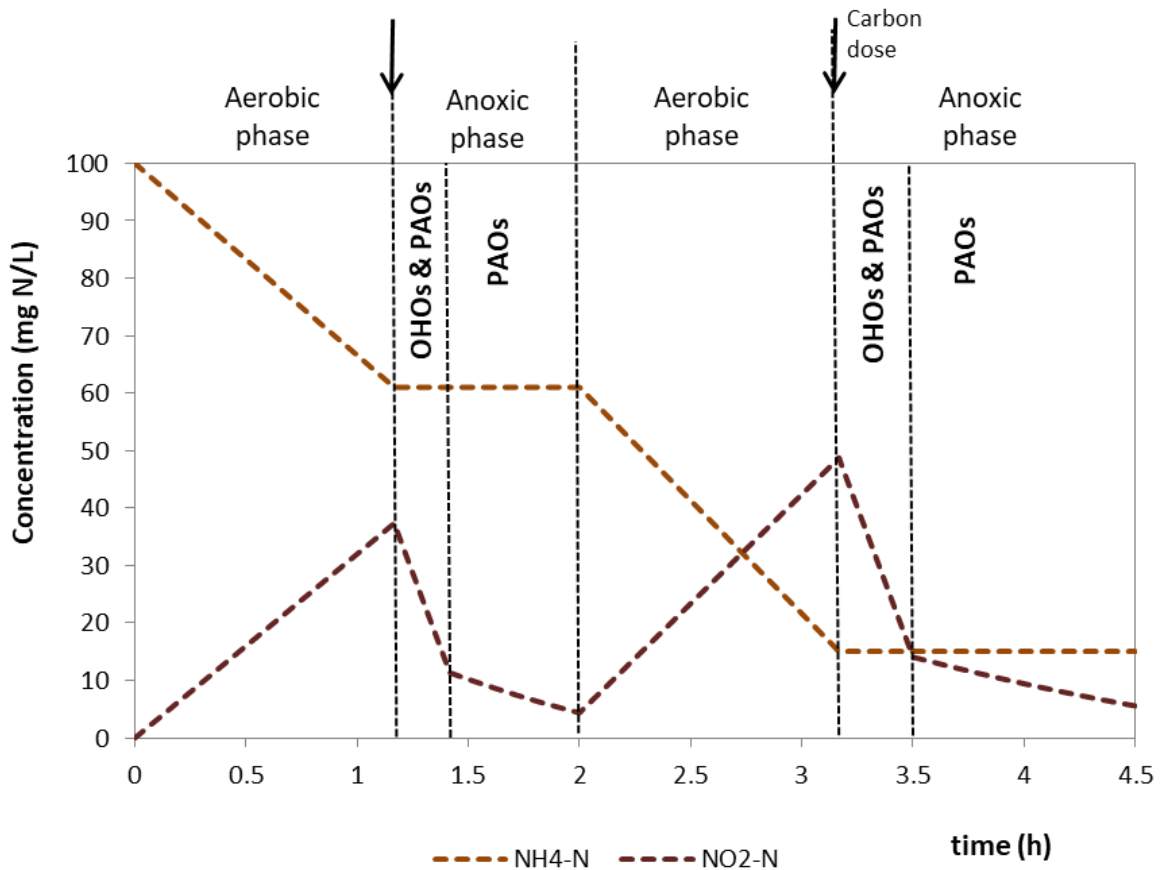


Figure 5.103. Variation of NH₄-N and NO₂-N according to the simulation setting

The simulation was performed for 2 scenarios of pH variation; one where pH was left uncontrolled and one where pH was controlled at optimum values for EBPR, according to the unified inhibition model. Figure 5.104 presents the variation of pH throughout the cycle for both scenarios. The rise of pH during denitrification by PAOs was predicted in relation to the fraction of the denitrification rates.

Figure 5.105 presents the inhibition of PUR throughout the process for the 2 scenarios. By calculating the areas under the formed curves, it is revealed that the process is inhibited by 40% if pH is left uncontrolled and by 33% if pH is controlled to the extent of reaching its optimum variation. The inhibition of PUR during each phase for both scenarios is presented in Figure 5.106. The control of pH to its optimum variation does not appear to provide a very significant benefit to the sustainability of PAOs. This is due to the design of the configuration with the appropriate alternation between aerobic and anoxic conditions, bringing the pH range closer to its optimum variation. Therefore, control of pH may be considered unnecessary for successful EBPR. However, an attractive option could be to control pH during the second aerobic period.

This would not only provide better conditions for PAOs, but also result in a high pH of the effluent which would increase natural precipitation of phosphorus as an added bonus.

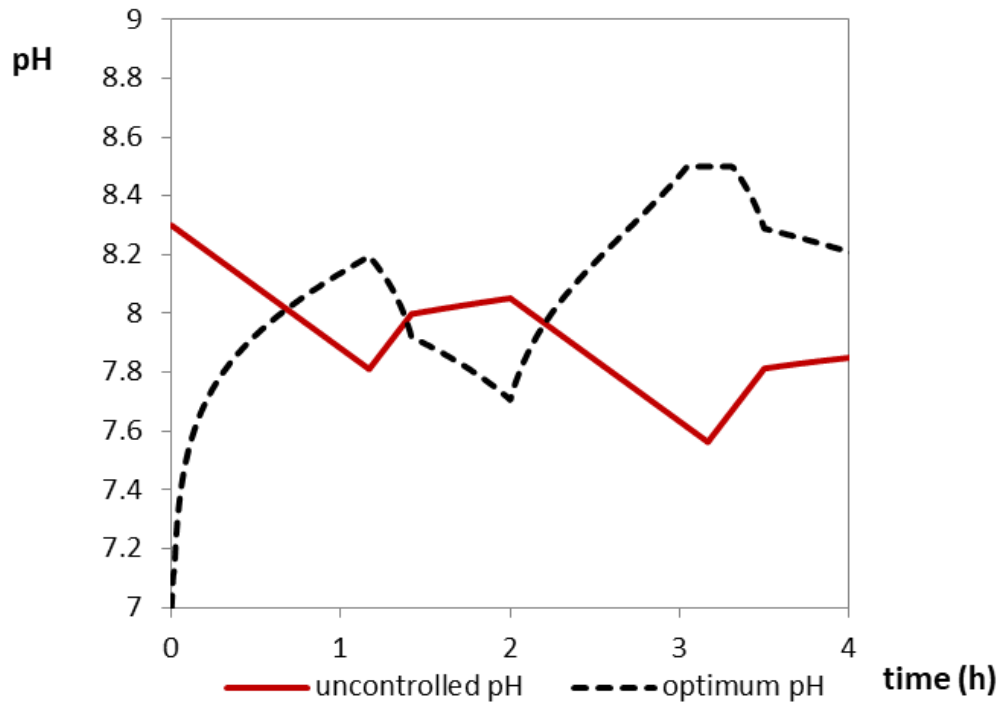


Figure 5.104. Variation of pH throughout the cycle for the scenarios of the simulation.

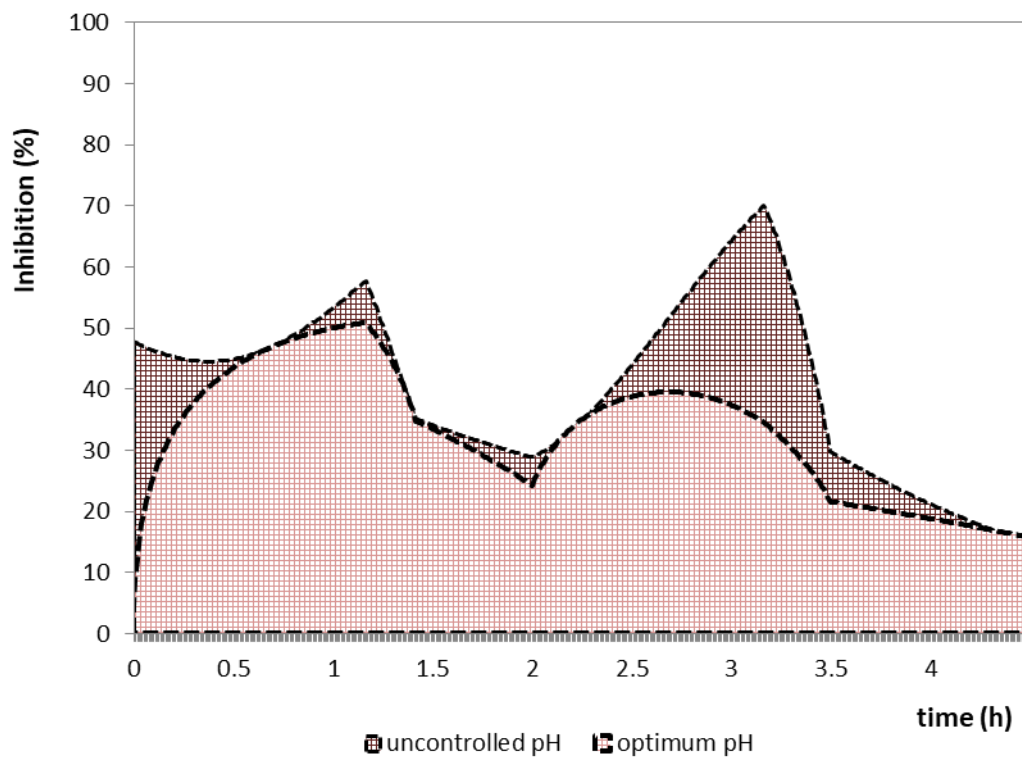


Figure 5.105. PUR inhibition throughout an SBR cycle for each scenario

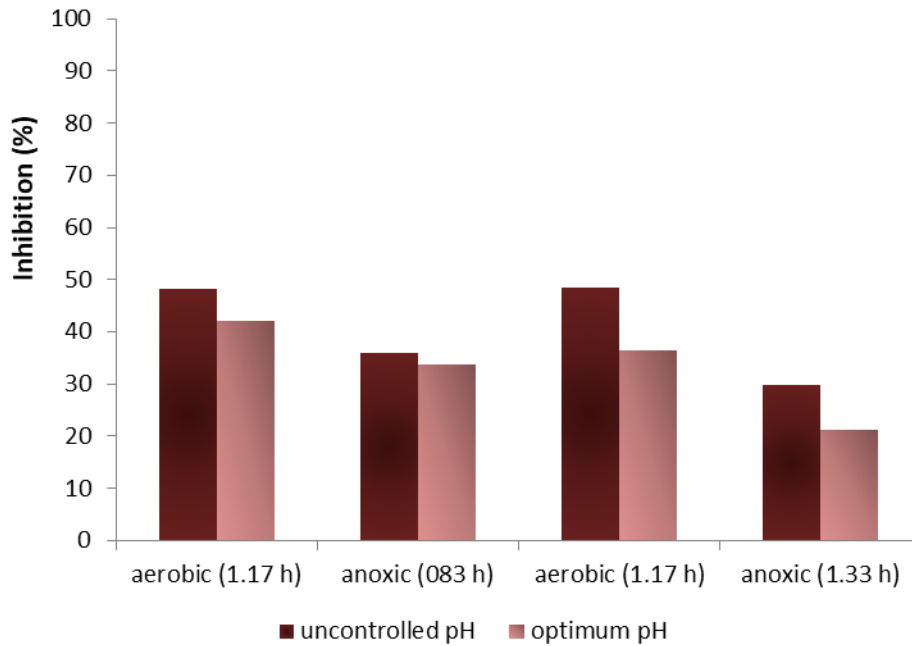


Figure 5.106. PUR inhibition during each phase for each scenario

Based on the results of the simulation, the application of this or a similar configuration may prove effective in achieving EBPR for moderate to high nitrogen loading systems. If pH were to be left uncontrolled, the process would be inhibited by 40%. The configuration employed is somewhat similar to the one applied in section 5.6.4 in terms of anaerobic, aerobic and anoxic SRTs. As such, it is possible that a biomass developed under these conditions may contain up to 60% of PAO population that was developed in the laboratory setting. However, since the inhibitory conditions are more severe during the aerobic phase (48% compared to 33% in the anoxic phase), a more conservative estimate would be at 50%. This would mean that, in the absence of inhibitors, the biomass could perform with an aerobic PUR of 6 mg P/g VSS h, and an anoxic PUR of 2.5 mg P/g VSS h (based on the aerobic PUR of 12 mg P/g VSS h that was observed under laboratory conditions – section 5.6.3.4 and assuming an anoxic PUR at 40% of the aerobic PUR). In the conditions of the scenario, aerobic PUR will be inhibited by 48% during both phases, while anoxic PUR will be inhibited by 36% during the first phase and by 29% during the second phase. Therefore, the uptake of phosphorus per cycle could be calculated at: 10 mg P/g VSS/cycle. Phosphorus release during the anaerobic phase may be estimated at 6 mg P/g VSS/cycle (from 12 mg P/g VSS h observed in lab scale conditions), which would mean a net removal of 4 mg P/g VSS/cycle. Assuming a VSS concentration of 3,000 mg/L, then the net removal of 12 mg P/L/cycle may be achieved with EBPR. Therefore, for the specific vNLR, influents with a N/P ratio higher than 8.3 may be treated effectively without the need of pH control.

According to the simulation, the configuration employed would likely be successful in the removal of phosphorus. However, certain criteria need to be satisfied:

1. The achievement of NOB shunt. Due to the relatively low ammonium concentrations throughout operation, it may be questioned if the nitrification/denitrification pathway can be achieved, since significant FA concentrations are required to suppress NOB. In this

configuration, the suppression of NOB is achieved by a combination of maintaining a relatively high pH (and consequently high FA concentrations), and a low aerobic SRT (39% of the total SRT). The SBR configuration described in section 5.7.1, was successful in suppressing NOB with ammonium concentrations around 160 mg N/L at the start of each cycle. Considering that the FA concentrations throughout operation were lower (due to lower pH) and that the aerobic SRT was 6.25 days, it is most likely that the wash-out of NOB will be achieved.

2. The minimization of the need for pH control. As mentioned PAOs seem to benefit from a pH variation that is contrary to the natural variation in nitrification/denitrification systems. However, the appropriate alteration between aerobic and anoxic conditions, in addition to preventing great accumulation of nitrite and FNA, ensured more favourable pH conditions for the growth of PAOs. Based on the results of the simulation, the need for pH control may be unnecessary.
3. The proliferation of PAOs over GAOs. The development of GAOs may be considered the bottleneck of EBPR and their suppression is of vital importance. In this configuration, the suppression of GAOs is achieved by promoting the denitrification pathway with propionate as the sole carbon source. As such, GAOs may not develop during the anoxic phase. Due to the relatively low aerobic retention time (52% of the total effective SRT) and the prolonged anoxic retention time (48% of the total effective SRT), it is likely that the net-growth of PAOs will be greater than that of GAOs, even under inhibitory conditions that may have no effect on GAOs.

Other considerations:

- As the aerobic retention time is relatively low, the SRT applied may need to be prolonged to support the growth of AOB and ensure good nitrification performance. The SRT should be sufficient for the growth of AOB but not allow the growth of NOB. This should take into consideration the inhibition of NOB due to FA. Park and Bae (2009) reported a K_{iFA} of 0.644 mg N/L for NOB. Based on this, the inhibition of NOB in regard to the variation of ammonium and pH for this scenario is shown in Figure 5.107. As is evident, NOB are inhibited significantly under the conditions of the scenario. Area calculation reveals that NOB are inhibited by 88% and 66% during the first and second aeration period respectively, if pH is left uncontrolled, whereas under the optimum variation of pH for EBPR, they are inhibited by 85% and 83% respectively. The greater suppression of NOB that is observed with pH control during the second aeration period, may give a further incentive for controlling pH during this phase, in addition to the benefits previously mentioned. The hostile conditions for NOB growth may allow their suppression at a high SRT, which could boost nitrification conditions, while also allowing a greater PAO population. However, it is possible that acclimatized NOB may possess a higher tolerance to FA, meaning that a lower SRT would be required for their wash-out.

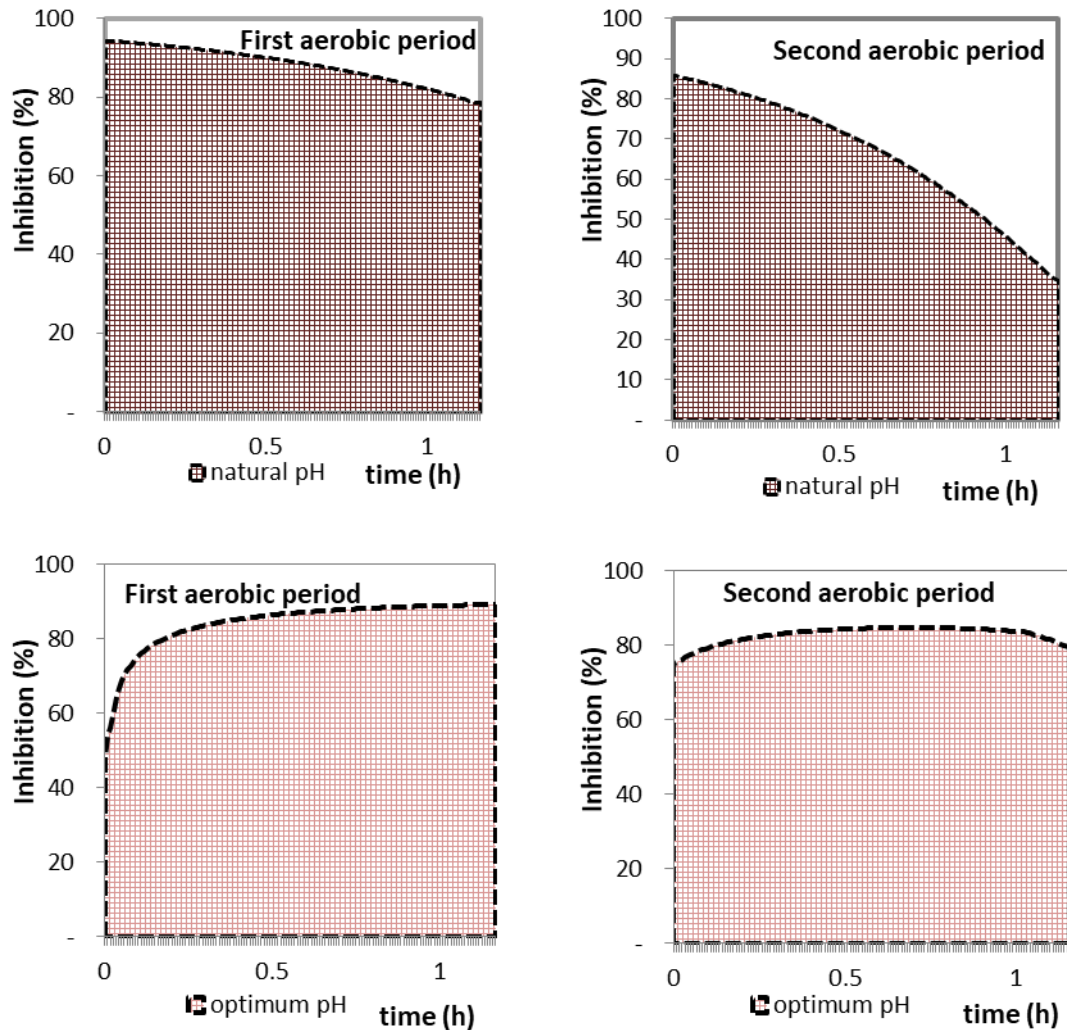


Figure 5.107. NOB inhibition during the aeration phases of the scenario

- The rapid denitritation of the nitrite portion reduced by OHOs would require a sufficient heterotrophic population. The required nitrite to be removed by heterotrophs according to the configuration of this scenario is approximately 220 mg NO₂-N/L d. Assuming a 2.5 mg COD/NO₂-N ratio and a biomass yield of Y=0.6, then the growth of OHOs under anoxic conditions would be 330 mg VSS/L d. This, with respect to the SRT and the decay rate of OHOs, would likely allow the sustenance of the desired heterotrophic population solely via the anoxic pathway and without the need for carbon addition in the aerobic phase.

Based on the above, it may be concluded that a configuration similar to the one examined in this section could achieve effective EBPR alongside short-cut nitrification for a vNLR equal to 0.2 kg N/m³ d. It should be noted that the viability of EBPR was examined based on the aerobic PUR of 12 mg P/g VSS h that was observed during the operation of the system described in section 5.6.4.2. While the configurations are similar in regard to the cycles and retention times, the laboratory SBR operated with a relatively low DO during the aerobic period for which PUR was determined, due to the limitations mentioned. The same biomass

was capable of performing at a maximum PUR of 25 mg P/g VSS h. As such, by optimizing aeration in a full-scale application, it is possible that higher PURs could be achieved than the ones estimated in this analysis. In addition, P-removal via denitrification was estimated to occur at 40% of the aerobic PUR. However, since this ratio concerns maximum PURs, the anoxic PURs would likely be greater than the ones estimated for this analysis. Therefore, the evaluation of EBPR potential in this analysis may be considered a conservative approach and it is possible that effective EBPR could also be achieved for greater vNLRs.

5.7.1.2 Results of the simulations

The overall aerobic and anoxic inhibition of PAOs for each vNLR is presented in Figure 5.108, Figure 5.109 and Figure 5.110.

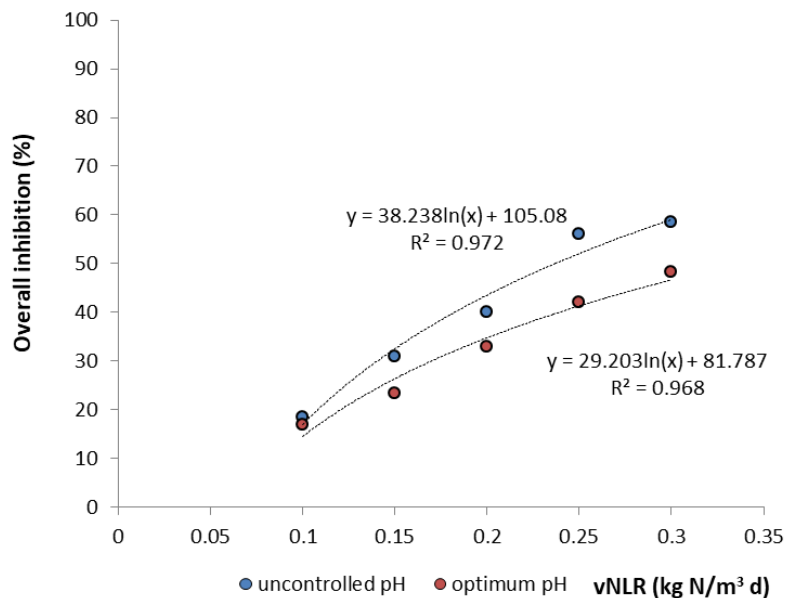


Figure 5.108. Overall inhibition of PAOs in regard to vNLR

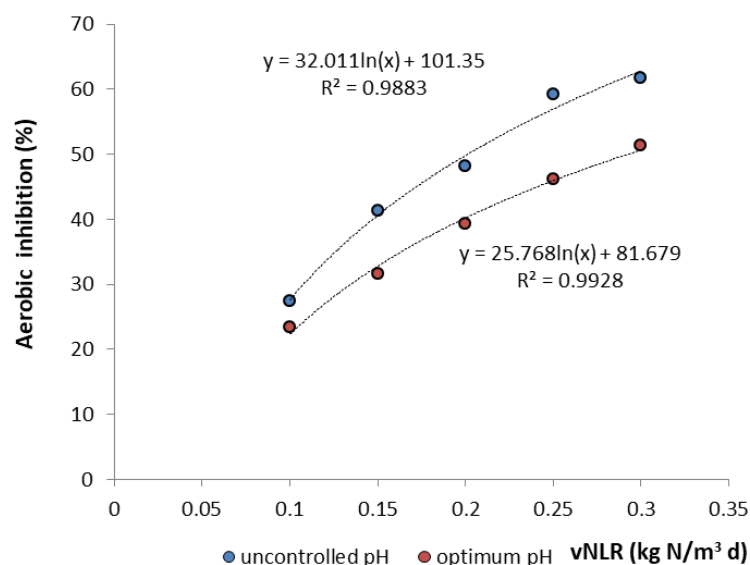


Figure 5.109. Overall aerobic inhibition of PAOs in regard to vNLR

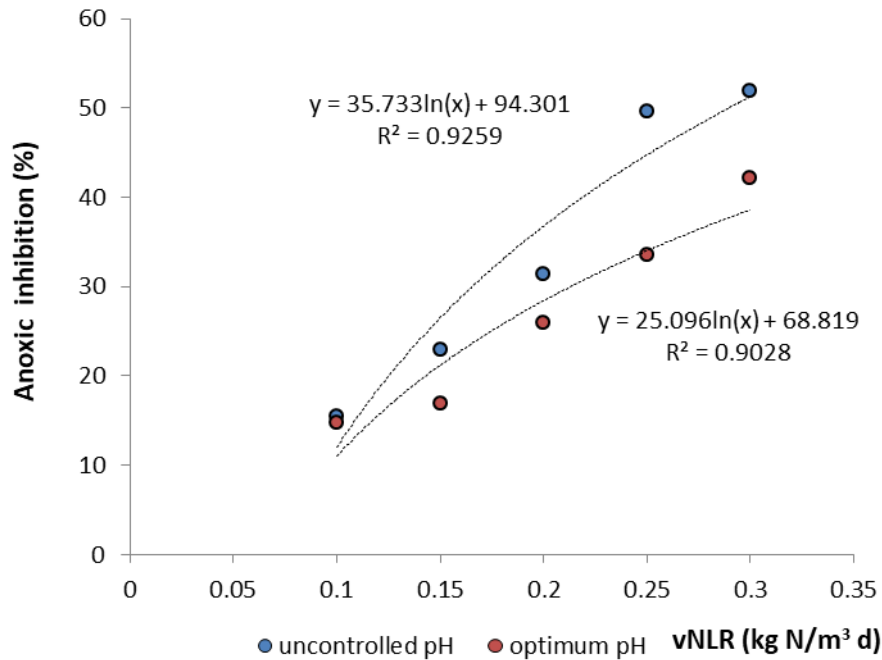


Figure 5.110. Overall anoxic inhibition of PAOs in regard to vNLR

In all cases, the control of pH to its optimum variation had a beneficiary effect on PAOs as would be expected, although to a lesser extent for the lower vNLRs. Inhibition is generally higher during the aerobic phase, as a significant portion of nitrite is rapidly reduced by OHOs early in the anoxic phase. Based on the results of the simulations, one could conclude that the SBR configuration is capable of handling vNLRs up to 0.3 kg N/m³ d. However, it should be noted that higher vNLRs demand greater aerobic retention times which would be obtained at the expense of the anoxic retention time designated for PAOs. As such, the overall inhibition of PAOs would be greater and the main strategy for their proliferation over GAOs could be compromised.

In general, adopting a vNLR of 0.2 kg N/m³ d would seem like the most reliable option for EBPR as it would require limited pH control and ensure the sustainability of PAOs against GAOs. While EBPR could be achieved for greater vNLRs (with 0.3 kg N/m³ d likely being the limit), the required increase of the aerobic retention time along with the decrease of the available denitrification time for PAOs, would likely allow the growth of GAOs which could jeopardize the process.

Chapter 6: Conclusions and recommendations

This final chapter presents the main conclusions of the present thesis. In addition to presenting the main findings of the experimental investigation, that were discussed in chapter 5, this chapter also addresses the main concerns regarding the feasibility of simultaneous EBPR and nitrification/denitrification, based on these findings, and makes several suggestions for the effective application of such treatment systems. In addition, specific aspects of the problem that require further study are recommended.

6.1 Main conclusions

- Both nitrite, in the form of free nitrous acid, and ammonium, as free ammonia, were found to inhibit PAO activity. As such, the successful implementation of EBPR in high nitrogen loading systems based on short-cut nitrification/denitrification appears challenging at the least.
- PAOs that were unacclimatized to nitrite (<0.1 mg $\text{NO}_2\text{-N/L}$, $\text{FNA} = 0$) were found to be severely inhibited by FNA, with aerobic PUR being inhibited by more than 90% at an FNA concentration of 0.14 $\mu\text{g HNO}_2\text{-N/L}$ (6 mg $\text{NO}_2\text{-N/L}$ at the pH of 8). A PAO-enriched biomass that was developed under conditions of higher nitrite accumulations (which corresponded to FNA accumulations of up to 0.08 $\mu\text{g HNO}_2\text{-N/L}$) displayed a practically identical tolerance to FNA, to that of a PAO-enriched biomass that was developed under conditions of FNA accumulations that would reach 0.35 $\mu\text{g HNO}_2\text{-N/L}$. In addition, the degree of tolerance displayed by both biomasses appear more consistent with those which has been reported in the literature for an acclimated biomass. As such, it is likely that PAOs are acclimatized to FNA at concentrations as low as 0.08 $\mu\text{g HNO}_2\text{-N/L}$.
- In the case of a PAO-enriched biomass acclimatized to nitrite, PUR was found to be inhibited by 50% at the FNA concentration of 1.5 $\mu\text{g HNO}_2\text{-N/L}$ and by 100% at the FNA concentration of just over 13 $\mu\text{g HNO}_2\text{-N/L}$. The corresponding nitrite concentrations are 10 and 50 mg $\text{NO}_2\text{-N/L}$ at the pH of 7, and 100 and 500 mg $\text{NO}_2\text{-N/L}$ at the pH of 8. This demonstrates the importance of pH for EBPR under conditions of high nitrite accumulations. As the accumulation of nitrite during nitrification is accompanied by a biochemical drop of pH, conditions for PAOs become rapidly worse over the duration of the process. This may be combated by controlling pH at high values in order to minimize the effect of nitrite.
- Anoxic PUR (via denitrification) was found to be inhibited by FNA to an almost identical degree as aerobic PUR. The extensive study conducted may settle contradictory reports in the literature regarding the resilience of either pathway to the inhibitor. The fact that PUR appears to be inhibited by FNA to the same degree regardless of the electron acceptor (oxygen, nitrite) may help provide some insight for the investigation of the exact mechanism of FNA-induced inhibition of PAOs.

- While anoxic P-removal appears just as tolerant to FNA as aerobic P-removal, conditions for PAOs during denitrification continuously improve over the duration of the process, as nitrite is removed alongside a biochemical increase of pH.
- PUR inhibition by FNA, both under aerobic and anoxic conditions, was determined to be best described by a non-competitive inhibition model with an inhibition constant of $K_{iFNA}=1.5 \mu\text{g N/L}$. The non-competitive mode of inhibition for FNA has been established in the literature for the processes of AOB and NOB, and the evidence provided by the present work regarding the non-competitive nature of FNA inhibition on PAOs, provides further information for a more comprehensive understanding of FNA as an inhibitor and its effect on various microbial processes. The non-competitive inhibition model for PUR inhibition may be used to accurately determine the performance of PAOs under various nitrite concentrations and pH variations and assess the capacity for phosphorus removal under different operating conditions scenarios.
- Ammonium was also found to inhibit PUR, with FA (a known inhibitor) appearing to be the actual inhibitor of the process. Aerobic PUR was found to be inhibited by 50% at the FA concentration of 8 mg NH_3/L , and by over 90% at FA concentrations greater than 30 mg NH_3/L . Anoxic PUR was found to be inhibited by FA to a similar degree as aerobic PUR, indicating that PUR inhibition by FA is independent of the electron acceptor.
- As the percentage of ammonium in the form of FA increases logarithmically with pH, PAO inhibition by ammonium becomes significantly more severe at high pH values. This raises certain concerns regarding the application of EBPR in the side-stream treatment of ammonium-rich reject water from the sludge treatment processes, which are typically characterized by a high pH.
- PUR inhibition by FA was determined to be best described by an uncompetitive inhibition model with a K_{iFA} in the range of 8-10 mg N/L. This mode of inhibition for FA has also been established in the literature for the processes of AOB and NOB. In the case of anoxic PUR inhibition, the inhibition model proposed by Levenspiel gave the most satisfactory fit with the experimental data. The uncompetitive inhibition model for PUR inhibition may be used to accurately determine the performance of PAOs under various ammonium concentrations and pH variations.
- Both aerobic and anoxic PUR were found to be inhibited by FNA to the same degree regardless of the carbon source (acetate/propionate). The same observation was made for PUR inhibition by FA. This would indicate that FNA and FA directly affect the PPK enzyme of PAOs, which is responsible for synthesis of intracellular polyphosphate chains and not indirectly by affecting hydrolysis of their stored PHAs for the required energy (PHBs in the case of acetate/PHVs in the case of propionate).
- The severity of PUR inhibition by either nitrite or ammonium is strongly dependent on pH which controls the respective forms of FNA and FA. In terms of nitrogen, nitrite is the strongest inhibitor when pH is below approximately 8.2, whereas ammonium is the more severe inhibitor at pH above this value.

- The simultaneous presence of FA and FNA has a much more adverse effect on PAOs compared to exposure to a single inhibitor. If PUR is inhibited by a given FNA concentration by I_{FNA} (%) and by a given FA concentration by I_{FA} (%), then the overall inhibition of PUR by both inhibitors may be estimated as $I_{\text{total}}(\%) = 100\% - (1 - I_{\text{FNA}})(1 - I_{\text{FA}})$.
- An enzymatic inhibition model was developed to describe the simultaneous effect of FNA and FA on PUR, based on the separate inhibition models previously established for FNA and FA. This combined inhibition model gave very satisfactory predictions when FNA and FA were assumed to be capable of binding to the same enzyme-substrate complex, and less accurate predictions when FNA and FA were assumed to be incapable of binding to the same complex. This observation may provide some insight for the exact mechanisms of FA and FNA inhibition on PAOs and possibly the nature of FNA and FA as inhibitors in general. The methodology applied in this approach may also be used in future studies regarding combined inhibition for various enzymatic processes.
- The combined inhibition model may be used to predict the performance of PAOs under a specific set of conditions (NH_4 concentration, NO_2 concentration, pH, temperature) but also provide an optimum pH for P-removal, depending on the distribution of nitrogen between the forms of ammonium and nitrite. As such, the combined inhibition model may provide optimum pH variations for the processes of nitrification and denitrification, minimizing PAO inhibition.
- FNA was also found to inhibit GAOs, although generally to a lesser extent than PAOs. Interestingly, the effect of FNA on GAO growth appears to be pH dependant, with FNA affecting GAOs significantly more at higher pH. At the pH of 7, the growth of GAOs was determined to be inhibited by 50% and 100% under the effect of 10 and 25 $\mu\text{g HNO}_2\text{-N/L}$ respectively, while at the pH of 8, GAO growth was halved by an FNA concentration of approximately 3 $\mu\text{g HNO}_2\text{-N/L}$. The reasons for the differentia regarding FNA tolerance at different pH is not clear as of this point, although it is likely related to the role of pH in the enzymatic performances of GAOs. In comparison to PAOs, GAOs appear to have a significantly higher tolerance to FNA at low pH (7), while at relatively high pH (8), the resilience of the microbial communities to the inhibitor are considered comparable. As such, a high pH may benefit PAOs, not only by reducing FNA content, but also by minimizing the antagonism of GAOs.
- The inhibitory effect of FNA on the growth of GAOs was determined to be best described by the Hill-type model, with a $K_{i\text{FNA}}$ of 9.2 and 3 $\mu\text{g HNO}_2\text{-N/L}$ for the pH of 7 and 8 respectively, and a Hill coefficient value of 2.45 and 2 for the pH of 7 and 8 respectively.
- Investigation of the effect of FA on the growth of GAOs revealed that GAOs were practically unaffected by the inhibitor, up to a concentration of 16.3 mg $\text{NH}_3\text{-N/L}$ (the highest concentration studied). This concentration on the other hand, has been found to inhibit PAOs by approximately 50%. As such, high FA concentrations which are prevalent in high nitrogen loading systems may provide an antagonistic advantage to GAOs. This would also counter the benefit of operating at a high pH as to favor PAOs in regard to FNA tolerance.

- Several feeding strategies that have been applied successfully for the suppression of GAOs and the proliferation of PAOs, were examined in situ under nitrification/denitrification conditions, during which FNA would accumulate up to 0.5 $\mu\text{g N/L}$. These included the use of propionate as the sole carbon source, the use of a mixture of acetate and propionate, and the regular alteration between acetate and propionate as a single carbon source. The investigation showed that these strategies proved unsuccessful in preventing the eventual wash-out of PAOs and the proliferation of GAOs, most likely due to FNA-induced PAO inhibition.
- The promotion of PAOs via the denitrification pathway with the use of propionate as the sole carbon source, proved a most effective strategy for the suppression of GAOs and the achievement of stable EBPR. The strategy relies on providing PAOs with priority in the utilization of nitrite over ordinary heterotrophic organisms (OHOs), during the anoxic phase. As all GAO subgroups are reportedly incapable of reducing nitrite with stored propionate (as PHVs), PAOs are given a significant advantage and GAOs are ultimately washed out even in conditions of FNA accumulations. At a vNLR of 0.1 $\text{kg N/m}^3 \text{ d}$, *Accumulibacter* (most PAOs) accounted for 50% of the total microbial community, whereas populations for *Competibacter* and *Deftluviococcus vanus* (the main GAO groups) were significantly low (<5%). The biomass displayed a capacity for excellent P-removal both under aerobic and anoxic conditions, performing at an average PUR of 25 mg P/g VSS h under aerobic conditions and 10 mg P/g VSS h under anoxic conditions (via denitrification).
- Based on the observations on the highly PAO-enriched biomass, anoxic P-removal appears to be slower than aerobic P-removal which would be in agreement with other studies, as well as theoretical redox potential related estimates. In the case of denitrification, anoxic P-removal was observed to occur at 40% of the aerobic PUR. From a practical standpoint, this would highlight that PAO inhibition under aerobic conditions is of more importance compared to the more favourable anoxic conditions, as there is greater potential for P-removal.
- The denitrification rate of PAOs was observed to be significantly slower than the denitrification rates that have been reported for OHOs. Similarly to PUR, the denitrification rate of PAOs is influenced by the concentration of nitrite which dictates the concentration of FNA with respect to pH. In conditions of minimum FNA influence, where the biomass performed at an anoxic PUR of 10 mg P/g VSS h , the corresponding denitrification rate was approximately 10 mg N/g VSS h (giving a $N_{\text{removed}}/P_{\text{removed}}$ ratio of 1). The slower denitrification rates of PAOs mean that their prioritization over OHOs in nitrite reduction, would require greater anoxic retention times at the expense of the aerobic retention time and consequently, greater reactor volumes.
- An increase of the vNLR from 0.1 to 0.15 $\text{kg N/m}^3 \text{ d}$ resulted in the biomass performing at half its previous capacity for P-removal. The overall inhibition of PAOs under the new conditions was estimated with the use of the combined inhibition model to be just under 30%. The observed performance was due to the diminished PAO population in the biomass as a result of inhibited growth but also the inhibited performance of PAOs under the new conditions. As FNA and FA affect both the growth and performance of PAOs, a PAO-enriched biomass performing under a specific set of conditions (in the absence of FA and

FNA) at a specific PUR, may be expected to perform roughly at $PUR \times (1 - Inh)^2$, where Inh is the overall inhibition. A much more accurate prediction may be provided via dynamic mathematical simulations of the exact configuration, using the combined inhibition model to establish the PAO population and its performance.

- A series of mathematical simulations was carried out in order to evaluate the potential for EBPR coupled with nitrification/denitrification in high nitrogen loading systems. The theoretical configuration that was examined was optimized with regard to: i) the alteration of aerobic and anoxic conditions, as to prevent accumulation of nitrite and retain pH at relatively high values, ii) providing PAOs an exclusive denitrification period (as to employ the aforementioned GAO suppression strategy), following removal of a significant portion of nitrite by providing OHOs a regulated carbon dose, and iii) the quality of the treated effluent. The viability of EBPR was evaluated for different vNLRs, from 0.1 to 0.3 kg N/m³ d, with special consideration to: a) the overall inhibition of PAOs under the conditions of each scenario, both in terms of population maintenance and performance, b) the adequacy of the GAO suppression strategy in each scenario, c) the need for pH control as to minimize PAO inhibition and d) the effective achievement of NOB shunt. Based on the results of the simulations and their evaluation, it was concluded that a vNLR of 0.2 kg N/m³ d could allow sufficient and relatively safe EBPR without the need for pH control. It is possible that EBPR could be achieved for higher vNLR's, although this would require pH manipulation which is costly, while it is uncertain as to what extent it may influence the PAO-GAO competition in the favour of GAOs. Regardless, the successful application of EBPR for vNLR's above 0.3 kg N/m³ d seems highly unlikely, as the inhibitory conditions alone would severely compromise PAO sustainability.
- While the application of EBPR in nitrification/denitrification systems is challenging, it may be achieved by employing a series of strategies that have been discussed in this work. However, EBPR under such conditions will always demand greater reactor volumes, as there is a relatively low limit to the vNLR that can be handled compared to when it is excluded. Another possible downside is that, based on the principal GAO-suppression strategy, effective EBPR under these conditions would likely require a significant amount of propionate to be made available. As the use of industrial sodium propionate would more than likely be considered economically unfeasible, propionate would need to be supplied by other means, such as via fermentation of primary sludge, and by certain available propionate-rich industrial and agricultural by-products which in most cases would require some level of processing.
- In WWTPs, the choice between applying EBPR to the side-stream treatment of reject water or allowing phosphorus to return to the main treatment stream, should firstly consider the main-stream's capacity for effective phosphorus removal. If phosphorus removal is adequate, side-stream EBPR treatment of reject water should not be considered, as contrary to treatment for ammonium, there is no particular benefit for its removal at this stage. Insufficiency of the main-stream to biologically remove phosphorus is ultimately due to low VFA content of the wastewater. In this case, supplementation with an external carbon source could develop and maintain the required PAO population. Since reject water contains some biodegradable COD and its treatment via nitrification/denitrification likely requires the addition

of an external carbon source due to the low C/N ratio that characterizes it, the option of incorporating EBPR at this stage in order to allow simultaneous P and N removal by the same carbon source is a legitimate one. However, unless the external feed is substantial in propionate as to promote the proliferation of PAOs via the denitrification pathway, EBPR implementation will likely be unsuccessful and at the cost of limiting the potential vNLR of the treatment process. Therefore, it is likely that side-stream EBPR treatment may only be viable and beneficiary when there is an availability of propionate as the external carbon source.

6.2 Recommendations for future research

- PAO-GAO competition: As the proliferation of GAOs may be considered the bottleneck of EBPR, strategies for their suppression and the selection of PAOs are of significant importance. Investigation of the role of VFAs in the PAO-GAO competition, such as butyrate, could provide further information and viable strategies for the proliferation of PAOs in inhibitive conditions.
- Acid digesters: As discussed, the availability of propionate may be a key consideration for the application of side-stream EBPR. As such, the development and optimization of processes designed for its production, particularly within the WWTP, is of significant interest. A promising source of propionate is primary sludge fermentation, which yields significant amounts of VFAs which may be utilized in the side-stream treatment of reject water. Optimization of this process could yield more propionate, both in quantity and as a fraction of the total VFAs that are produced. For instance, operation of this unit at a high temperature and an appropriate SRT, which would allow more rapid sludge fermentation, could also allow the presence of acetotrophic methanogens which would reduce the acetate content of the yielded VFAs.
- FNA and FA inhibition on GAOs: As of this point, the limited research that has been conducted on the tolerance of GAOs to inhibitors such as FNA and FA, concerns the acetotrophic *Competibacter* species. Information regarding the effect of FNA and FA on the propionate-fed Alphaproteobacterial GAO community would be valuable for assessing the PAO/GAO competition in high nitrogen loading systems.
- Mechanism of FNA and FA inhibition on PAOs: While the effect of FNA and FA on PAOs has been extensively researched in this work with regard to the performance of PAOs and the feasibility of EBPR under inhibitive conditions, the exact mechanisms of PAO inhibition on an enzymatic scale are not clear as of this point. Further research on the microbial mechanisms involved would provide a greater understanding of the observed behavior of PAOs and could expand our knowledge on the complexities of EBPR and the nature of FNA and FA as inhibitors, in general.
- Strategies for the combined application of nitrification/denitrification and EBPR: To date, EBPR has not been applied successfully alongside nitrification/denitrification in the side-stream treatment of reject water. The strategies and suggested configuration for such an application, discussed in section 5.7, appear promising and may be applied at a pilot-scale. The implementation of these strategies at a pilot-scale treatment facility may reveal new

challenges regarding the application of effective EBPR in side-stream reject water treatment, but also new potential for the environmentally friendly, cost-effective removal of nutrients in WWTPs.

References

- Acevedo, B., Camiña, C., Corona, J.E., Borrás, L., Barat, R., 2015. The metabolic versatility of PAOs as an opportunity to obtain a highly P-enriched stream for further P-recovery. *Chem. Eng. J.* 270, 459–467. <https://doi.org/10.1016/j.cej.2015.02.063>
- Acevedo, B., Murgui, M., Borrás, L., Barat, R., 2017. New insights in the metabolic behaviour of PAO under negligible poly-P reserves. *Chem. Eng. J.* 311, 82–90. <https://doi.org/10.1016/j.cej.2016.11.073>
- Acevedo, B., Oehmen, A., Carvalho, G., Seco, A., Borrás, L., Barat, R., 2012. Metabolic shift of polyphosphate-accumulating organisms with different levels of polyphosphate storage. *Water Res.* 46, 1889–1900. <https://doi.org/10.1016/j.watres.2012.01.003>
- Ahn, Y.-H., 2006. Sustainable nitrogen elimination biotechnologies: A review. *Process Biochem.* 41, 1709–1721. <https://doi.org/10.1016/j.procbio.2006.03.033>
- Altundoğan, H.S., Tümen, F., 2002. Removal of phosphates from aqueous solutions by using bauxite. I: Effect of pH on the adsorption of various phosphates: Removal of phosphates from aqueous solutions. *J. Chem. Technol. Biotechnol.* 77, 77–85. <https://doi.org/10.1002/jctb.525>
- Amann, R.I., 1995. Fluorescently labelled, rRNA-targeted oligonucleotide probes in the study of microbial ecology. *Mol. Ecol.* 4, 543–554. <https://doi.org/10.1111/j.1365-294X.1995.tb00255.x>
- Andrés, E., Araya, F., Vera, I., Pozo, G., Vidal, G., 2018. Phosphate removal using zeolite in treatment wetlands under different oxidation-reduction potentials. *Ecol. Eng.* 117, 18–27. <https://doi.org/10.1016/j.ecoleng.2018.03.008>
- Andrews, J.F., 1968. A mathematical model for the continuous culture of microorganisms utilizing inhibitory substrates. *Biotechnol. Bioeng.* 10, 707–723. <https://doi.org/10.1002/bit.260100602>
- Arias, M., Da Silva-Carballal, J., García-Río, L., Mejuto, J., Núñez, A., 2006. Retention of phosphorus by iron and aluminum-oxides-coated quartz particles. *J. Colloid Interface Sci.* 295, 65–70. <https://doi.org/10.1016/j.jcis.2005.08.001>
- Aslan, S., Dahab, M., 2008. Nitritation and denitritation of ammonium-rich wastewater using fluidized-bed biofilm reactors. *J. Hazard. Mater.* 156, 56–63. <https://doi.org/10.1016/j.jhazmat.2007.11.112>
- Barat, R., van Loosdrecht, M.C.M., 2006. Potential phosphorus recovery in a WWTP with the BCFS® process: Interactions with the biological process. *Water Res.* 40, 3507–3516. <https://doi.org/10.1016/j.watres.2006.08.006>
- Barnard, J.L., 1976. A review of Biological Phosphorus Removal in the Activated Sludge Process. *Water SA* 2, 135-144.
- Battistoni, P., Paci, B., Fatone, F., Pavan, P., 2006. Phosphorus Removal from Anaerobic Supernatants: Start-Up and Steady-State Conditions of a Fluidized Bed Reactor Full-Scale Plant. *Ind. Eng. Chem. Res.* 45, 663–669. <https://doi.org/10.1021/ie050796g>
- Blackall, L.L., Crocetti, G.R., Saunders, A.M., Bond, P.L., 2002. A review and update of the microbiology of enhanced biological phosphorus removal in wastewater treatment plants. *Antonie Van Leeuwenhoek* 81, 681–691. <https://doi.org/10.1023/A:1020538429009>

- Brdjanovic, D., van Loosdrecht, M.C.M., Hooijmans, C.M., Mino, T., Alaerts, G.J., Heijnen, J.J., 1998. Effect of polyphosphate limitation on the anaerobic metabolism of phosphorus-accumulating microorganisms. *Appl. Microbiol. Biotechnol.* 50, 273–276. <https://doi.org/10.1007/s002530051289>
- Bunce, J.T., Ndam, E., Ofiteru, I.D., Moore, A., Graham, D.W., 2018. A Review of Phosphorus Removal Technologies and Their Applicability to Small-Scale Domestic Wastewater Treatment Systems. *Front. Environ. Sci.* 6, 8. <https://doi.org/10.3389/fenvs.2018.00008>
- Burow, L.C., Kong, Y., Nielsen, J.L., Blackall, L.L., Nielsen, P.H., 2007. Abundance and ecophysiology of *DeFluviicoccus* spp., glycogen-accumulating organisms in full-scale wastewater treatment processes. *Microbiology* 153, 178–185. <https://doi.org/10.1099/mic.0.2006/001032-0>
- Camejo, P.Y., Owen, B.R., Martirano, J., Ma, J., Kapoor, V., Santo Domingo, J., McMahon, K.D., Noguera, D.R., 2016. Candidatus *Accumulibacter phosphatis* clades enriched under cyclic anaerobic and microaerobic conditions simultaneously use different electron acceptors. *Water Res.* 102, 125–137. <https://doi.org/10.1016/j.watres.2016.06.033>
- Carrillo, V., Fuentes, B., Gómez, G., Vidal, G., 2020. Characterization and recovery of phosphorus from wastewater by combined technologies. *Rev. Environ. Sci. Biotechnol.* 19, 389–418. <https://doi.org/10.1007/s11157-020-09533-1>
- Carvalho, M., Oehmen, A., Carvalho, G., Reis, M.A.M., 2014a. The effect of substrate competition on the metabolism of polyphosphate accumulating organisms (PAOs). *Water Res.* 64, 149–159. <https://doi.org/10.1016/j.watres.2014.07.004>
- Carvalho, M., Oehmen, A., Carvalho, G., Reis, M.A.M., 2014b. Survival strategies of polyphosphate accumulating organisms and glycogen accumulating organisms under conditions of low organic loading. *Bioresour. Technol.* 172, 290–296. <https://doi.org/10.1016/j.biortech.2014.09.059>
- Carvalho, G., Lemos, P.C., Oehmen, A., Reis, M.A.M., 2007. Denitrifying phosphorus removal: Linking the process performance with the microbial community structure. *Water Res.* 41, 4383–4396. <https://doi.org/10.1016/j.watres.2007.06.065>
- Chaïm De Mulder, 2016. Impact of intrinsic and extrinsic parameters on the oxygen kinetic parameters of Ammonia and Nitrite Oxidizing Bacteria. <https://doi.org/10.13140/RG.2.2.11347.17444>
- Comeau, Y., Hall, K., Hancock, R., Oldham, W., 1986. Biochemical model for enhanced biological phosphorus removal. *Water Res.* 20, 1511–1521. [https://doi.org/10.1016/0043-1354\(86\)90115-6](https://doi.org/10.1016/0043-1354(86)90115-6)
- Comeau, Y., Oldham, W.K., Hall, K.J., 1987. Dynamics of carbon reserves in biological dephosphatation of wastewater. *Biological Phosphate Removal from Wastewaters*. Elsevier, pp. 39–55. <https://doi.org/10.1016/B978-0-08-035592-4.50010-9>
- Crocetti, G.R., Banfield, J.F., Keller, J., Bond, P.L., Blackall, L.L., 2002. Glycogen-accumulating organisms in laboratory-scale and full-scale wastewater treatment processes b bThe GenBank accession numbers for the sequences reported in this paper are given in Methods. *Microbiology* 148, 3353–3364. <https://doi.org/10.1099/00221287-148-11-3353>
- Crocetti, G.R., Hugenholtz, P., Bond, P.L., Schuler, A., Keller, J., Jenkins, D., Blackall, L.L., 2000. Identification of Polyphosphate-Accumulating Organisms and Design of 16S rRNA-Directed Probes for Their Detection and Quantitation. *Appl. Environ. Microbiol.* 66, 1175–1182. <https://doi.org/10.1128/AEM.66.3.1175-1182.2000>

- D. N. Moriasi, J. G. Arnold, M. W. Van Liew, R. L. Bingner, R. D. Harmel, T. L. Veith, 2007. Model Evaluation Guidelines for Systematic Quantification of Accuracy in Watershed Simulations. *Trans. ASABE* 50, 885–900. <https://doi.org/10.13031/2013.23153>
- Dai, X., Hu, C., Zhang, D., Dai, L., Duan, N., 2017. Impact of a high ammonia-ammonium-pH system on methane-producing archaea and sulfate-reducing bacteria in mesophilic anaerobic digestion. *Bioresour. Technol.* 245, 598–605. <https://doi.org/10.1016/j.biortech.2017.08.208>
- Dai, Y., Lambert, L., Yuan, Z., Keller, J., 2008. Microstructure of copolymers of polyhydroxyalkanoates produced by glycogen accumulating organisms with acetate as the sole carbon source. *Process Biochem.* 43, 968–977. <https://doi.org/10.1016/j.procbio.2008.04.023>
- Dai, Y., Yuan, Z., Wang, X., Oehmen, A., Keller, J., 2007. Anaerobic metabolism of *Defluviococcus vanus* related glycogen accumulating organisms (GAOs) with acetate and propionate as carbon sources. *Water Res.* 41, 1885–1896. <https://doi.org/10.1016/j.watres.2007.01.045>
- Daigger, G.T., Waltrip, G.D., Romm, E.D., Morales L.M. Morales, 1988. Enhanced Secondary Treatment Incorporating Biological Nutrient Removal. *Water Pollution Control Federation* 60, 1833–42.
- Eisenthal, R., Cornish-Bowden, A., 1974. The direct linear plot. A new graphical procedure for estimating enzyme kinetic parameters. *Biochem. J.* 139, 715–720. <https://doi.org/10.1042/bj1390715>
- Ferreira, T.B., Carrondo, M.J.T., Alves, P.M., 2007. Effect of ammonia production on intracellular pH: Consequent effect on adenovirus vector production. *J. Biotechnol.* 129, 433–438. <https://doi.org/10.1016/j.jbiotec.2007.01.010>
- Filipe, Carlos D. M., Daigger, G.T., Grady, C.P.L., 2001a. Stoichiometry and kinetics of acetate uptake under anaerobic conditions by an enriched culture of phosphorus-accumulating organisms at different pHs. *Biotechnol. Bioeng.* 76, 32–43. <https://doi.org/10.1002/bit.1023>
- Filipe, Carlos D. M., Daigger, G.T., Grady, C.P.L., 2001b. A metabolic model for acetate uptake under anaerobic conditions by glycogen accumulating organisms: Stoichiometry, kinetics, and the effect of pH. *Biotechnol. Bioeng.* 76, 17–31. <https://doi.org/10.1002/bit.1022>
- Filipe, Carlos D.M., Daigger, G.T., Grady, C.P.L., 2001. Effects of pH on the Rates of Aerobic Metabolism of Phosphate-Accumulating and Glycogen-Accumulating Organisms. *Water Environ. Res.* 73, 213–222. <https://doi.org/10.2175/106143001X139191>
- Flowers, J.J., He, S., Yilmaz, S., Noguera, D.R., McMahon, K.D., 2009. Denitrification capabilities of two biological phosphorus removal sludges dominated by different ‘*Candidatus Accumulibacter*’ clades. *Environ. Microbiol. Rep.* 1, 583–588. <https://doi.org/10.1111/j.1758-2229.2009.00090.x>
- Ganda, L., Zhou, Y., Lim, C.-P., Liu, Y., Ng, W.J., 2016. Free nitrous acid inhibition on carbon storage microorganisms: Accumulated inhibitory effects and recoverability. *Chem. Eng. J.* 287, 285–291. <https://doi.org/10.1016/j.cej.2015.11.027>
- Ge, H., Batstone, D.J., Keller, J., 2015. Biological phosphorus removal from abattoir wastewater at very short sludge ages mediated by novel PAO clade Comamonadaceae. *Water Res.* 69, 173–182. <https://doi.org/10.1016/j.watres.2014.11.026>

- Gerber, A., De Villiers, R. H., Mostert, E. S., & Van Riet, C. J. J., 1987. The phenomenon of simultaneous phosphate uptake and release, and its importance in biological nutrient removal. *Biological phosphate removal from wastewaters* (pp. 123-134). Pergamon.
- Gu, S., Fu, B., Ahn, J.-W., Fang, B., 2021. Mechanism for phosphorus removal from wastewater with fly ash of municipal solid waste incineration, Seoul, Korea. *J. Clean. Prod.* 280, 124430. <https://doi.org/10.1016/j.jclepro.2020.124430>
- Guerrero, J., Guisasola, A., Baeza, J.A., 2011. The nature of the carbon source rules the competition between PAO and denitrifiers in systems for simultaneous biological nitrogen and phosphorus removal. *Water Res.* 45, 4793–4802. <https://doi.org/10.1016/j.watres.2011.06.019>
- Guisasola, A., Qurie, M., Vargas, M. del M., Casas, C., Baeza, J.A., 2009. Failure of an enriched nitrite-DPAO population to use nitrate as an electron acceptor. *Process Biochem.* 44, 689–695. <https://doi.org/10.1016/j.procbio.2009.02.017>
- Gustavsson, D.J.I, Syd, V.A., Malmo, S., 2010. Biological sludge liquor treatment at municipal wastewater treatment plants-a review. *Vatten* 66, 179-192.
- He, S., McMahon, K.D., 2011. Microbiology of ‘*Candidatus Accumulibacter*’ in activated sludge: Microbiology of ‘*Candidatus Accumulibacter*.’ *Microb. Biotechnol.* 4, 603–619. <https://doi.org/10.1111/j.1751-7915.2011.00248.x>
- Hesselmann, R., 2000. Anaerobic metabolism of bacteria performing enhanced biological phosphate removal. *Water Res.* 34, 3487–3494. [https://doi.org/10.1016/S0043-1354\(00\)00092-0](https://doi.org/10.1016/S0043-1354(00)00092-0)
- Hinsinger, P., 2001. Bioavailability of soil inorganic P in the rhizosphere as affected by root-induced chemical changes: A review. *Plant Soil* 237, 173–195. <https://doi.org/10.1023/A:1013351617532>
- Hruschka, H., 1980. Waste treatment by precipitation with lime - a cost and efficiency analysis. *Prog. Water Tech*, 12, 383-393.
- Hu, J.Y., Ong, S.L., Ng, W.J., Lu, F., Fan, X.J., 2003. A new method for characterizing denitrifying phosphorus removal bacteria by using three different types of electron acceptors. *Water Res.* 37, 3463–3471. [https://doi.org/10.1016/S0043-1354\(03\)00205-7](https://doi.org/10.1016/S0043-1354(03)00205-7)
- Izadi, Parnian, Izadi, Parin, Eldyasti, A., 2020. Design, operation and technology configurations for enhanced biological phosphorus removal (EBPR) process: a review. *Rev. Environ. Sci. Biotechnol.* 19, 561–593. <https://doi.org/10.1007/s11157-020-09538-w>
- Jiang, H., Yang, P., Wang, Z., Ren, S., Qiu, J., Liang, H., Peng, Y., Li, X., Zhang, Q., 2021. Novel insights into overcoming nitrite oxidation bacteria acclimatization problem in treatment of high-ammonia wastewater through partial nitrification. *Bioresour. Technol.* 336, 125254. <https://doi.org/10.1016/j.biortech.2021.125254>
- Jiménez, E., Giménez, J.B., Seco, A., Ferrer, J., Serralta, J., 2012. Effect of pH, substrate and free nitrous acid concentrations on ammonium oxidation rate. *Bioresour. Technol.* 124, 478–484. <https://doi.org/10.1016/j.biortech.2012.07.079>
- Johansson, P., 1994. SIPHOR a kinetic model for simulation of biological phosphate removal. Ph.D. thesis, Lund University, Sweden.
- Jones, R.M., Dold, P.L., Takács, I., Chapman, K., Wett, B., Murthy, S., Shaughnessy, M.O., 2007. Simulation for operation and control of reject water treatment processes. *Proc. Water Environ. Fed.* 2007, 4357–4372. <https://doi.org/10.2175/193864707787974599>

- Kapagiannidis, A.G., Zafiriadis, I., Aivasidis, A., 2013. Comparison between aerobic and anoxic metabolism of denitrifying-EBPR sludge: effect of biomass poly-hydroxyalkanoates content. *New Biotechnol.* 30, 227–237. <https://doi.org/10.1016/j.nbt.2012.05.022>
- Keasling, J.D., Van Dien, S.J., Trelstad, P., Renninger, N., McMahon, K., 2000. Application of polyphosphate metabolism to environmental and biotechnological problems. *Biochem. Biokhimiia* 65, 324–331.
- Kong, Y., Ong, S.L., Ng, W.J., Liu, W.-T., 2002. Diversity and distribution of a deeply branched novel proteobacterial group found in anaerobic-aerobic activated sludge processes: A novel gamma-proteobacterial group in activated sludge. *Environ. Microbiol.* 4, 753–757. <https://doi.org/10.1046/j.1462-2920.2002.00357.x>
- Kong, Y., Xia, Y., Nielsen, J.L., Nielsen, P.H., 2006. Ecophysiology of a group of uncultured Gammaproteobacterial glycogen-accumulating organisms in full-scale enhanced biological phosphorus removal wastewater treatment plants. *Environ. Microbiol.* 8, 479–489. <https://doi.org/10.1111/j.1462-2920.2005.00914.x>
- Kroiss, H., Rechberger, H., Egle, L., 2011. Phosphorus in Water Quality and Waste Management, in: Kumar, S. (Ed.), *Integrated Waste Management - Volume II*. InTech. <https://doi.org/10.5772/18482>
- Lee, H., Yun, Z., 2014. Comparison of biochemical characteristics between PAO and DPAO sludges. *J. Environ. Sci.* 26, 1340–1347. [https://doi.org/10.1016/S1001-0742\(13\)60609-9](https://doi.org/10.1016/S1001-0742(13)60609-9)
- Levenspiel, O., 1980. The monod equation: A revisit and a generalization to product inhibition situations. *Biotechnol. Bioeng.* 22, 1671–1687. <https://doi.org/10.1002/bit.260220810>
- Levin, G.V., Shapiro, J., 1965. Metabolic Uptake of Phosphorus by Wastewater Organisms. *Water Pollution Control Federation* 37, 800–821
- Li, Y., Nan, X., Li, D., Wang, L., Xu, R., Li, Q., 2021. Advances in the treatment of phosphorus-containing wastewater. *IOP Conf. Ser. Earth Environ. Sci.* 647, 012163. <https://doi.org/10.1088/1755-1315/647/1/012163>
- Li, Y., Rahman, S.M., Li, G., Fowle, W., Nielsen, P.H., Gu, A.Z., 2019. The Composition and Implications of Polyphosphate-Metal in Enhanced Biological Phosphorus Removal Systems. *Environ. Sci. Technol.* 53, 1536–1544. <https://doi.org/10.1021/acs.est.8b06827>
- Liu, Y., Ngo, H.H., Guo, W., Peng, L., Wang, D., Ni, B., 2019. The roles of free ammonia (FA) in biological wastewater treatment processes: A review. *Environ. Int.* 123, 10–19. <https://doi.org/10.1016/j.envint.2018.11.039>
- Lopez-Vazquez, C.M., Hooijmans, C.M., Brdjanovic, D., Gijzen, H.J., van Loosdrecht, M.C.M., 2009a. Temperature effects on glycogen accumulating organisms. *Water Res.* 43, 2852–2864. <https://doi.org/10.1016/j.watres.2009.03.038>
- Lopez-Vazquez, C.M., Oehmen, A., Hooijmans, C.M., Brdjanovic, D., Gijzen, H.J., Yuan, Z., van Loosdrecht, M.C.M., 2009b. Modeling the PAO–GAO competition: Effects of carbon source, pH and temperature. *Water Res.* 43, 450–462. <https://doi.org/10.1016/j.watres.2008.10.032>
- Lopez-Vazquez, C.M., Song, Y.-I., Hooijmans, C.M., Brdjanovic, D., Moussa, M.S., Gijzen, H.J., van Loosdrecht, M.C.M., 2008. Temperature effects on the aerobic metabolism of glycogen-accumulating organisms. *Biotechnol. Bioeng.* 101, 295–306. <https://doi.org/10.1002/bit.21892>

- Lopez-Vazquez, C.M., Song, Y.-I., Hooijmans, C.M., Brdjanovic, D., Moussa, M.S., Gijzen, H.J., van Loosdrecht, M.M.C., 2007. Short-term temperature effects on the anaerobic metabolism of glycogen accumulating organisms. *Biotechnol. Bioeng.* 97, 483–495. <https://doi.org/10.1002/bit.21302>
- Lopez-Vazquez, C.M., 2009. The competition between polyphosphate-accumulating organisms and glycogen-accumulating organisms: temperature effects and modeling. [s.n.], S.I.
- Mamais D., 1991. The effects of Temperature and Mean Cell Residence Time on Enhanced Biological Phosphorus Removal by Activated Sludge. Ph.D. Dissertation, University of California, Berkeley, CA, USA.
- Martin, B.D., Parsons, S.A., Jefferson, B., 2009. Removal and recovery of phosphate from municipal wastewaters using a polymeric anion exchanger bound with hydrated ferric oxide nanoparticles. *Water Sci. Technol.* 60, 2637–2645. <https://doi.org/10.2166/wst.2009.686>
- Martín, H.G., Ivanova, N., Kunin, V., Warnecke, F., Barry, K.W., McHardy, A.C., Yeates, C., He, S., Salamov, A.A., Szeto, E., Dalin, E., Putnam, N.H., Shapiro, H.J., Pangilinan, J.L., Rigoutsos, I., Kyrpides, N.C., Blackall, L.L., McMahon, K.D., Hugenholtz, P., 2006. Metagenomic analysis of two enhanced biological phosphorus removal (EBPR) sludge communities. *Nat. Biotechnol.* 24, 1263–1269. <https://doi.org/10.1038/nbt1247>
- McIlroy, S., Seviour, R.J., 2009. Elucidating further phylogenetic diversity among the *Defluviicoccus*-related glycogen-accumulating organisms in activated sludge. *Environ. Microbiol. Rep.* 1, 563–568. <https://doi.org/10.1111/j.1758-2229.2009.00082.x>
- Metcalf & Eddy, 2003. *Wastewater Engineering: Treatment and Reuse*. 4th Edition, McGraw-Hill, New York..
- Meyer, R.L., Saunders, A.M., Blackall, L.L., 2006. Putative glycogen-accumulating organisms belonging to the Alphaproteobacteria identified through rRNA-based stable isotope probing. *Microbiology* 152, 419–429. <https://doi.org/10.1099/mic.0.28445-0>
- Mino, T., Satoh, H., Matsuo, T., 1994. Metabolisms of Different Bacterial Populations in Enhanced Biological Phosphate Removal Processes. *Water Sci. Technol.* 29, 67–70. <https://doi.org/10.2166/wst.1994.0309>
- Mino, T., van Loosdrecht, M.C.M., Heijnen, J.J., 1998. Microbiology and biochemistry of the enhanced biological phosphate removal process. *Water Res.* 32, 3193–3207. [https://doi.org/10.1016/S0043-1354\(98\)00129-8](https://doi.org/10.1016/S0043-1354(98)00129-8)
- Morse, G., Brett, S., Guy, J., Lester, J., 1998. Review: Phosphorus removal and recovery technologies. *Sci. Total Environ.* 212, 69–81. [https://doi.org/10.1016/S0048-9697\(97\)00332-X](https://doi.org/10.1016/S0048-9697(97)00332-X)
- Nielsen, P.H., McIlroy, S.J., Albertsen, M., Nierychlo, M., 2019. Re-evaluating the microbiology of the enhanced biological phosphorus removal process. *Curr. Opin. Biotechnol.* 57, 111–118. <https://doi.org/10.1016/j.copbio.2019.03.008>
- Noutsopoulos, C., 2002. Impact of alternative treatment schemes on the settling characteristics of nutrient removal activated sludge systems. PhD Thesis, National Technical University of Athens, Greece
- Noutsopoulos, C., Mamais, D., Stataris, E., Lerias, E., Malamis, S., Andreadakis, A., 2018. Reject water characterization and treatment through short-cut nitrification/denitrification: assessing the effect of temperature and type of substrate: Reject water characterization

- and treatment via nitrification/denitrification. *J. Chem. Technol. Biotechnol.* 93, 3638–3647. <https://doi.org/10.1002/jctb.5745>
- Oehmen, A., Carvalho, G., Lopez-Vazquez, C.M., van Loosdrecht, M.C.M., Reis, M.A.M., 2010a. Incorporating microbial ecology into the metabolic modelling of polyphosphate accumulating organisms and glycogen accumulating organisms. *Water Res.* 44, 4992–5004. <https://doi.org/10.1016/j.watres.2010.06.071>
- Oehmen, A., Keller-Lehmann, B., Zeng, R.J., Yuan, Z., Keller, J., 2005a. Optimisation of poly- β -hydroxyalkanoate analysis using gas chromatography for enhanced biological phosphorus removal systems. *J. Chromatogr. A* 1070, 131–136. <https://doi.org/10.1016/j.chroma.2005.02.020>
- Oehmen, A., Lemos, P., Carvalho, G., Yuan, Z., Keller, J., Blackall, L., Reis, M., 2007. Advances in enhanced biological phosphorus removal: From micro to macro scale. *Water Res.* 41, 2271–2300. <https://doi.org/10.1016/j.watres.2007.02.030>
- Oehmen, A., Lopez-Vazquez, C.M., Carvalho, G., Reis, M.A.M., van Loosdrecht, M.C.M., 2010b. Modelling the population dynamics and metabolic diversity of organisms relevant in anaerobic/anoxic/aerobic enhanced biological phosphorus removal processes. *Water Res.* 44, 4473–4486. <https://doi.org/10.1016/j.watres.2010.06.017>
- Oehmen, A., Saunders, A.M., Vives, M.T., Yuan, Z., Keller, J., 2006. Competition between polyphosphate and glycogen accumulating organisms in enhanced biological phosphorus removal systems with acetate and propionate as carbon sources. *J. Biotechnol.* 123, 22–32. <https://doi.org/10.1016/j.jbiotec.2005.10.009>
- Oehmen, A., Teresa Vives, M., Lu, H., Yuan, Z., Keller, J., 2005b. The effect of pH on the competition between polyphosphate-accumulating organisms and glycogen-accumulating organisms. *Water Res.* 39, 3727–3737. <https://doi.org/10.1016/j.watres.2005.06.031>
- Oehmen, A., Yuan, Z., Blackall, L.L., Keller, J., 2005c. Comparison of acetate and propionate uptake by polyphosphate accumulating organisms and glycogen accumulating organisms. *Biotechnol. Bioeng.* 91, 162–168. <https://doi.org/10.1002/bit.20500>
- Oehmen, A., Yuan, Z., Blackall, L.L., Keller, J., 2004. Short-term effects of carbon source on the competition of polyphosphate accumulating organisms and glycogen accumulating organisms. *Water Sci. Technol. J. Int. Assoc. Water Pollut. Res.* 50, 139–144.
- Ong, Y.H., Chua, A.S.M., Fukushima, T., Ngoh, G.C., Shoji, T., Michinaka, A., 2014. High-temperature EBPR process: The performance, analysis of PAOs and GAOs and the fine-scale population study of Candidatus “*Accumulibacter phosphatis*.” *Water Res.* 64, 102–112. <https://doi.org/10.1016/j.watres.2014.06.038>
- Panswad, T., Doungchai, A., Anotai, J., 2003. Temperature effect on microbial community of enhanced biological phosphorus removal system. *Water Res.* 37, 409–415. [https://doi.org/10.1016/S0043-1354\(02\)00286-5](https://doi.org/10.1016/S0043-1354(02)00286-5)
- Park, S., Bae, W., 2009a. Modeling kinetics of ammonium oxidation and nitrite oxidation under simultaneous inhibition by free ammonia and free nitrous acid. *Process Biochem.* 44, 631–640. <https://doi.org/10.1016/j.procbio.2009.02.002>
- Park, S., Bae, W., 2009b. Modeling kinetics of ammonium oxidation and nitrite oxidation under simultaneous inhibition by free ammonia and free nitrous acid. *Process Biochem.* 44, 631–640. <https://doi.org/10.1016/j.procbio.2009.02.002>
- Petriglieri, F., Petersen, J.F., Peces, M., Nierychlo, M., Hansen, K., Baastrand, C.E., Nielsen, U.G., Reitzel, K., Nielsen, P.H., 2022. Quantification of Biologically and Chemically

- Bound Phosphorus in Activated Sludge from Full-Scale Plants with Biological P-Removal. *Environ. Sci. Technol.* 56, 5132–5140. <https://doi.org/10.1021/acs.est.1c02642>
- Philips, S., Laanbroek, H.J., Verstraete, W., 2002. Origin, causes and effects of increased nitrite concentrations in aquatic environments. *Rev. Environ. Sci. Biotechnol.* 1, 115–141. <https://doi.org/10.1023/A:1020892826575>
- Pijuan, M., Casas, C., Baeza, J.A., 2009. Polyhydroxyalkanoate synthesis using different carbon sources by two enhanced biological phosphorus removal microbial communities. *Process Biochem.* 44, 97–105. <https://doi.org/10.1016/j.procbio.2008.09.017>
- Pijuan, M., Saunders, A.M., Guisasola, A., Baeza, J.A., Casas, C., Blackall, L.L., 2004. Enhanced biological phosphorus removal in a sequencing batch reactor using propionate as the sole carbon source. *Biotechnol. Bioeng.* 85, 56–67. <https://doi.org/10.1002/bit.10813>
- Pijuan, M., Ye, L., Yuan, Z., 2010. Free nitrous acid inhibition on the aerobic metabolism of poly-phosphate accumulating organisms. *Water Res.* 44, 6063–6072. <https://doi.org/10.1016/j.watres.2010.07.075>
- Prinz, H., 2010. Hill coefficients, dose–response curves and allosteric mechanisms. *J. Chem. Biol.* 3, 37–44. <https://doi.org/10.1007/s12154-009-0029-3>
- Puyol, D., Carvajal-Arroyo, J.M., Sierra-Alvarez, R., Field, J.A., 2014. Nitrite (not free nitrous acid) is the main inhibitor of the anammox process at common pH conditions. *Biotechnol. Lett.* 36, 547–551. <https://doi.org/10.1007/s10529-013-1397-x>
- Rajagopal, R., Massé, D.I., Singh, G., 2013. A critical review on inhibition of anaerobic digestion process by excess ammonia. *Bioresour. Technol.* 143, 632–641. <https://doi.org/10.1016/j.biortech.2013.06.030>
- Ramasahayam, S.K., Guzman, L., Gunawan, G., Viswanathan, T., 2014. A Comprehensive Review of Phosphorus Removal Technologies and Processes. *J. Macromol. Sci. Part A* 51, 538–545. <https://doi.org/10.1080/10601325.2014.906271>
- Randall, A.A., Liu, Y.-H., 2002. Polyhydroxyalkanoates form potentially a key aspect of aerobic phosphorus uptake in enhanced biological phosphorus removal. *Water Res.* 36, 3473–3478. [https://doi.org/10.1016/S0043-1354\(02\)00047-7](https://doi.org/10.1016/S0043-1354(02)00047-7)
- Ren, N., Kang, H., Wang, X., Li, N., 2011. Short-term effect of temperature variation on the competition between PAOs and GAOs during acclimation period of an EBPR system. *Front. Environ. Sci. Eng. China* 5, 277–282. <https://doi.org/10.1007/s11783-010-0226-x>
- Rubio-Rincón, F.J., Lopez-Vazquez, C.M., Welles, L., van Loosdrecht, M.C.M., Brdjanovic, D., 2017. Cooperation between *Candidatus Competibacter* and *Candidatus Accumulibacter* clade I, in denitrification and phosphate removal processes. *Water Res.* 120, 156–164. <https://doi.org/10.1016/j.watres.2017.05.001>
- Saito, T., Brdjanovic, D., van Loosdrecht, M.C.M., 2004. Effect of nitrite on phosphate uptake by phosphate accumulating organisms. *Water Res.* 38, 3760–3768. <https://doi.org/10.1016/j.watres.2004.05.023>
- Saunders, A.M., Oehmen, A., Blackall, L.L., Yuan, Z., Keller, J., 2003. The effect of GAOs (glycogen accumulating organisms) on anaerobic carbon requirements in full-scale Australian EBPR (enhanced biological phosphorus removal) plants. *Water Sci. Technol.* 47, 37–43. <https://doi.org/10.2166/wst.2003.0584>

- Sedlak, R. (Ed.), 1991. Phosphorus and nitrogen removal from municipal wastewater: principles and practice, 2nd ed. ed. Lewis Publishers, Chelsea, Mich.
- Sengupta, S., Pandit, A., 2011. Selective removal of phosphorus from wastewater combined with its recovery as a solid-phase fertilizer. *Water Res.* 45, 3318–3330. <https://doi.org/10.1016/j.watres.2011.03.044>
- Seviour, R.J., Mino, T., Onuki, M., 2003. The microbiology of biological phosphorus removal in activated sludge systems. *FEMS Microbiol. Rev.* 27, 99–127. [https://doi.org/10.1016/S0168-6445\(03\)00021-4](https://doi.org/10.1016/S0168-6445(03)00021-4)
- Shen, N., Zhou, Y., 2016. Enhanced biological phosphorus removal with different carbon sources. *Appl. Microbiol. Biotechnol.* 100, 4735–4745. <https://doi.org/10.1007/s00253-016-7518-4>
- Slater, F.R., Johnson, C.R., Blackall, L.L., Beiko, R.G., Bond, P.L., 2010. Monitoring associations between clade-level variation, overall community structure and ecosystem function in enhanced biological phosphorus removal (EBPR) systems using terminal-restriction fragment length polymorphism (T-RFLP). *Water Res.* 44, 4908–4923. <https://doi.org/10.1016/j.watres.2010.07.028>
- Song, W., Zheng, M.J., Li, H., Zheng, W., Guo, F., 2019. Profiling population-level diversity and dynamics of *Accumulibacter* via high throughput sequencing of *ppk1*. *Appl. Microbiol. Biotechnol.* 103, 9711–9722. <https://doi.org/10.1007/s00253-019-10183-9>
- Sperling, M. von, 2007. Wastewater characteristics, treatment and disposal, Biological wastewater treatment series. IWA Publ. [u.a.], London.
- Stasinakis, A.S., Mamais, D., Paraskevas, P.A., Lekkas, T.D., 2003. Evaluation of Different Methods for the Determination of Maximum Heterotrophic Growth Rates. *Water Environ. Res.* 75, 549–552. <https://doi.org/10.2175/106143003X141349>
- Stein, L.Y., Arp, D.J., 1998. Loss of Ammonia Monooxygenase Activity in *Nitrosomonas europaea* upon Exposure to Nitrite. *Appl. Environ. Microbiol.* 64, 4098–4102. <https://doi.org/10.1128/AEM.64.10.4098-4102.1998>
- Stokholm-Bjerregaard, M., McIlroy, S.J., Nierychlo, M., Karst, S.M., Albertsen, M., Nielsen, P.H., 2017. A Critical Assessment of the Microorganisms Proposed to be Important to Enhanced Biological Phosphorus Removal in Full-Scale Wastewater Treatment Systems. *Front. Microbiol.* 8, 718. <https://doi.org/10.3389/fmicb.2017.00718>
- Tarayre, C., Nguyen, H.-T., Brognaux, A., Delepierre, A., De Clercq, L., Charlier, R., Michels, E., Meers, E., Delvigne, F., 2016. Characterisation of Phosphate Accumulating Organisms and Techniques for Polyphosphate Detection: A Review. *Sensors* 16, 797. <https://doi.org/10.3390/s16060797>
- Tayà, C., Garlapati, V.K., Guisasola, A., Baeza, J.A., 2013. The selective role of nitrite in the PAO/GAO competition. *Chemosphere* 93, 612–618. <https://doi.org/10.1016/j.chemosphere.2013.06.006>
- Thistleton, J., Clark, T., Pearce, P., Parsons, S.A., 2001. Mechanisms of Chemical Phosphorus Removal. *Process Saf. Environ. Prot.* 79, 339–344. <https://doi.org/10.1205/095758201753373104>
- Tu, Y., Schuler, A.J., 2013. Low Acetate Concentrations Favor Polyphosphate-Accumulating Organisms over Glycogen-Accumulating Organisms in Enhanced Biological Phosphorus Removal from Wastewater. *Environ. Sci. Technol.* 47, 3816–3824. <https://doi.org/10.1021/es304846s>

- Ugurlu, A., 1998. Phosphorus removal by fly ash. *Environ. Int.* 24, 911–918. [https://doi.org/10.1016/S0160-4120\(98\)00079-8](https://doi.org/10.1016/S0160-4120(98)00079-8)
- Vadivelu, V.M., Keller, J., Yuan, Z., 2006. Effect of free ammonia and free nitrous acid concentration on the anabolic and catabolic processes of an enriched *Nitrosomonas* culture. *Biotechnol. Bioeng.* 95, 830–839. <https://doi.org/10.1002/bit.21018>
- Van Hulle, S.W., Volcke, E.I., Teruel, J.L., Donckels, B., van Loosdrecht, M.C., Vanrolleghem, P.A., 2007. Influence of temperature and pH on the kinetics of the Sharon nitrification process. *J. Chem. Technol. Biotechnol.* 82, 471–480. <https://doi.org/10.1002/jctb.1692>
- Vargas, M., Guisasola, A., Artigues, A., Casas, C., Baeza, J.A., 2011. Comparison of a nitrite-based anaerobic–anoxic EBPR system with propionate or acetate as electron donors. *Process Biochem.* 46, 714–720. <https://doi.org/10.1016/j.procbio.2010.11.018>
- Vargas, M., Yuan, Z., Pijuan, M., 2013. Effect of long-term starvation conditions on polyphosphate- and glycogen-accumulating organisms. *Bioresour. Technol.* 127, 126–131. <https://doi.org/10.1016/j.biortech.2012.09.117>
- Wang, D., Duan, Y., Yang, Q., Liu, Y., Ni, B.-J., Wang, Q., Zeng, G., Li, X., Yuan, Z., 2018. Free ammonia enhances dark fermentative hydrogen production from waste activated sludge. *Water Res.* 133, 272–281. <https://doi.org/10.1016/j.watres.2018.01.051>
- Wang, X., Zeng, R.J., Dai, Y., Peng, Y., Yuan, Z., 2008. The denitrification capability of cluster 1 *DeFluviicoccus vanus*-related glycogen-accumulating organisms. *Biotechnol. Bioeng.* 99, 1329–1336. <https://doi.org/10.1002/bit.21711>
- Wang, X., Zhao, J., Yu, D., Du, S., Yuan, M., Zhen, J., 2019. Evaluating the potential for sustaining mainstream anammox by endogenous partial denitrification and phosphorus removal for energy-efficient wastewater treatment. *Bioresour. Technol.* 284, 302–314. <https://doi.org/10.1016/j.biortech.2019.03.127>
- Wang, Y., Geng, J., Ren, Z., He, W., Xing, M., Wu, M., Chen, S., 2011. Effect of anaerobic reaction time on denitrifying phosphorus removal and N₂O production. *Bioresour. Technol.* 102, 5674–5684. <https://doi.org/10.1016/j.biortech.2011.02.080>
- Wang, Y., Jiang, F., Zhang, Z., Xing, M., Lu, Z., Wu, M., Yang, J., Peng, Y., 2010. The long-term effect of carbon source on the competition between polyphosphorus accumulating organisms and glycogen accumulating organism in a continuous plug-flow anaerobic/aerobic (A/O) process. *Bioresour. Technol.* 101, 98–104. <https://doi.org/10.1016/j.biortech.2009.07.085>
- Wang, Y., Zhou, S., Ye, L., Wang, H., Stephenson, T., Jiang, X., 2014. Nitrite survival and nitrous oxide production of denitrifying phosphorus removal sludges in long-term nitrite/nitrate-fed sequencing batch reactors. *Water Res.* 67, 33–45. <https://doi.org/10.1016/j.watres.2014.08.052>
- Wett, B., Rauch, W., 2003. The role of inorganic carbon limitation in biological nitrogen removal of extremely ammonia concentrated wastewater. *Water Res.* 37, 1100–1110. [https://doi.org/10.1016/S0043-1354\(02\)00440-2](https://doi.org/10.1016/S0043-1354(02)00440-2)
- Whang, L.-M., Park, J.K., 2006. Competition between Polyphosphate- and Glycogen-Accumulating Organisms in Enhanced-Biological-Phosphorus-Removal Systems: Effect of Temperature and Sludge Age. *Water Environ. Res.* 78, 4–11. <https://doi.org/10.2175/106143005X84459>
- Wilfert, P., Kumar, P.S., Korving, L., Witkamp, G.-J., van Loosdrecht, M.C.M., 2015. The Relevance of Phosphorus and Iron Chemistry to the Recovery of Phosphorus from

- Wastewater: A Review. *Environ. Sci. Technol.* 49, 9400–9414. <https://doi.org/10.1021/acs.est.5b00150>
- Wong, M.-T., Tan, F.M., Ng, W.J., Liu, W.-T., 2004. Identification and occurrence of tetrad-forming Alphaproteobacteria in anaerobic–aerobic activated sludge processes. *Microbiology* 150, 3741–3748. <https://doi.org/10.1099/mic.0.27291-0>
- Xia, W.-J., Guo, L.-X., Yu, L.-Q., Zhang, Q., Xiong, J.-R., Zhu, X.-Y., Wang, X.-C., Huang, B.-C., Jin, R.-C., 2021. Phosphorus removal from diluted wastewaters using a La/C nanocomposite-doped membrane with adsorption-filtration dual functions. *Chem. Eng. J.* 405, 126924. <https://doi.org/10.1016/j.cej.2020.126924>
- Xu, Q., Liu, X., Wang, D., Wu, Y., Wang, Q., Liu, Y., Li, X., An, H., Zhao, J., Chen, F., Zhong, Y., Yang, Q., Zeng, G., 2018. Free ammonia-based pretreatment enhances phosphorus release and recovery from waste activated sludge. *Chemosphere* 213, 276–284. <https://doi.org/10.1016/j.chemosphere.2018.09.048>
- Yang, G., Xu, Q., Wang, D., Tang, L., Xia, J., Wang, Q., Zeng, G., Yang, Q., Li, X., 2018. Free ammonia-based sludge treatment reduces sludge production in the wastewater treatment process. *Chemosphere* 205, 484–492. <https://doi.org/10.1016/j.chemosphere.2018.04.140>
- Ye, L., Pijuan, M., Yuan, Z., 2013. The effect of free nitrous acid on key anaerobic processes in enhanced biological phosphorus removal systems. *Bioresour. Technol.* 130, 382–389. <https://doi.org/10.1016/j.biortech.2012.11.127>
- Ye, L., Pijuan, M., Yuan, Z., 2010. The effect of free nitrous acid on the anabolic and catabolic processes of glycogen accumulating organisms. *Water Res.* 44, 2901–2909. <https://doi.org/10.1016/j.watres.2010.02.010>
- Yoshida, Y., Takahashi, K., Saito, T., Tanaka, K., 2006. The effect of nitrite on aerobic phosphate uptake and denitrifying activity of phosphate-accumulating organisms. *Water Sci. Technol.* 53, 21–27. <https://doi.org/10.2166/wst.2006.165>
- Zeng, W., Bai, X., Guo, Y., Li, N., Peng, Y., 2017. Interaction of “*Candidatus Accumulibacter*” and nitrifying bacteria to achieve energy-efficient denitrifying phosphorus removal via nitrite pathway from sewage. *Enzyme Microb. Technol.* 105, 1–8. <https://doi.org/10.1016/j.enzmictec.2017.06.005>
- Zeng, W., Li, B., Wang, X., Bai, X., Peng, Y., 2016a. Influence of nitrite accumulation on “*Candidatus Accumulibacter*” population structure and enhanced biological phosphorus removal from municipal wastewater. *Chemosphere* 144, 1018–1025. <https://doi.org/10.1016/j.chemosphere.2015.08.064>
- Zeng, W., Wang, A., Zhang, J., Zhang, L., Peng, Y., 2016b. Enhanced biological phosphate removal from wastewater and clade-level population dynamics of “*Candidatus Accumulibacter phosphatis*” under free nitrous acid inhibition: Linked with detoxication. *Chem. Eng. J.* 296, 234–242. <https://doi.org/10.1016/j.cej.2016.03.063>
- Zhao, D., Sengupta, A.K., 1998. Ultimate removal of phosphate from wastewater using a new class of polymeric ion exchangers. *Water Res.* 32, 1613–1625. [https://doi.org/10.1016/S0043-1354\(97\)00371-0](https://doi.org/10.1016/S0043-1354(97)00371-0)
- Zhao, J., Liu, Y., Wang, Y., Lian, Y., Wang, Q., Yang, Q., Wang, D., Xie, G.-J., Zeng, G., Sun, Y., Li, X., Ni, B.-J., 2018. Clarifying the Role of Free Ammonia in the Production of Short-Chain Fatty Acids from Waste Activated Sludge Anaerobic Fermentation. *ACS Sustain. Chem. Eng.* 6, 14104–14113. <https://doi.org/10.1021/acssuschemeng.8b02670>

- Zheng, X., Sun, P., Lou, J., Cai, J., Song, Y., Yu, S., Lu, X., 2013. Inhibition of free ammonia to the granule-based enhanced biological phosphorus removal system and the recoverability. *Bioresour. Technol.* 148, 343–351. <https://doi.org/10.1016/j.biortech.2013.08.100>
- Zhou, Y., Ganda, L., Lim, M., Yuan, Z., Kjelleberg, S., Ng, W.J., 2010. Free nitrous acid (FNA) inhibition on denitrifying poly-phosphate accumulating organisms (DPAOs). *Appl. Microbiol. Biotechnol.* 88, 359–369. <https://doi.org/10.1007/s00253-010-2780-3>
- Zhou, Y., Ganda, L., Lim, M., Yuan, Z., Ng, W.J., 2012. Response of poly-phosphate accumulating organisms to free nitrous acid inhibition under anoxic and aerobic conditions. *Bioresour. Technol.* 116, 340–347. <https://doi.org/10.1016/j.biortech.2012.03.111>
- Zhou, Y., Pijuan, M., Yuan, Z., 2007. Free nitrous acid inhibition on anoxic phosphorus uptake and denitrification by poly-phosphate accumulating organisms. *Biotechnol. Bioeng.* 98, 903–912. <https://doi.org/10.1002/bit.21458>
- Zhou, Y., Pijuan, M., Zeng, R.J., Yuan, Z., 2009. Involvement of the TCA cycle in the anaerobic metabolism of polyphosphate accumulating organisms (PAOs). *Water Res.* 43, 1330–1340. <https://doi.org/10.1016/j.watres.2008.12.008>
- Zielińska, M., Rusanowska, P., Jarzabek, J., Nielsen, J.L., 2016. Community dynamics of denitrifying bacteria in full-scale wastewater treatment plants. *Environ. Technol.* 37, 2358–2367. <https://doi.org/10.1080/09593330.2016.1150350>

